UNIVERSIDAD COMPLUTENSE DE MADRID

FACULTAD DE CIENCIAS QUÍMICAS
Departamento de Química Orgánica I

DEVELOPMENT OF NEW INHIBITORS OF THE ENZIME MONOACYLGLYCEROL LIPASE (MGL).

MEMORIA PARA OPTAR AL GRADO DE DOCTOR

PRESENTADA POR

José Antonio Cisneros Trigo

Bajo la dirección de las doctoras

María Luz López Rodríguez
Silvia Ortega Gutiérrez

Madrid, 2011

ISBN: 978-84-694-5118-2

UNIVERSIDAD COMPLUTENSE DE MADRID

FACULTAD DE CIENCIAS QUÍMICAS

Departamento de Química Orgánica I

DEVELOPMENT OF NEW INHIBITORS OF THE ENZYME MONOACYLGLYCEROL LIPASE (MGL)

PhD candidate

José Antonio Cisneros Trigo

Advisors:
Prof. Dr. María Luz López Rodríguez
Dr. Silvia Ortega Gutiérrez

MADRID, 2011

If I have ever made any valuable discoveries, it has been
owing more to patient attention, than to any other talent.
Isaac Newton (1642-1727)

A mi familia

De acuerdo con la Normativa de desarrollo del régimen relativo a elaboración, tribunal, defensa y evaluación de la Tesis Doctoral, del Real Decreto 1393/2007, de 29 de Octubre, (BOE 30 de Octubre de 2007) por el que se establece la ordenación de las enseñanzas universitarias oficiales de la Universidad Complutense de Madrid, y de acuerdo a lo dispuesto en sus artículos 4.1 y 4.2, la presente Tesis Doctoral se ha redactado en inglés previo visto bueno de los directores, autorización del Departamento así como autorización de la Comisión de Doctorado. Conforme a esta normativa se incluye adicionalmente un amplio resumen en español que consta de introducción, objetivos, resultados y discusión y conclusiones (véase sección S1-S27 al final de este manuscrito).

El presente trabajo ha sido realizado en el laboratorio de Química Médica del Departamento de Química Orgánica I de la Facultad de Ciencias Químicas de la Universidad Complutense de Madrid.

El tema ha sido propuesto y dirigido por la Catedrática Dra. Mª Luz López Rodríguez *y la* Dra. Silvia Ortega Gutiérrez*, a quienes deseo expresar mi más profundo agradecimiento por su acogida en este grupo de investigación, por sus continuas enseñanzas a lo largo de todo este tiempo, y muy especialmente, por todo el ánimo, apoyo y confianza depositada en este proyecto.*

Asimismo, quiero expresar mi agradecimiento:

Al Profesor Christopher J. Fowler, a la Dra. Emily Björklund y a la Dra. Séverine Vandevoorde (Universidad de Umeå, Suecia), así como al Profesor Nephi Stella (University of Washington, EEUU) por la realización de las pruebas biológicas.

Al Profesor Beat Lutz y la Dra. Krisztina Monory del Instituto de Química Fisiológica de la Universidad Johannes Gutenberg (Alemania) por su acogida y sus enseñanzas en los estudios de biología celular y molecular.

A la Dra. Ángeles Canales y a los Drs. Francisco Javier Medrano y Antonio Romero, del Centro de Investigaciones Biológicas (CSIC, Madrid) por la realización de los estudios de cinética enzimática.

Al Profesor Dr. Guillermo Orellana por su admisión en el Departamento de Química Orgánica I de la Universidad Complutense de Madrid. Asimismo, quiero agradecer a Soledad Martínez Real, secretaria del Departamento, su inestimable ayuda a lo largo de estos años.

A mis compañeros de laboratorio, con los que he compartido experiencias más allá del lugar de trabajo y que han hecho de este laboratorio quizá el mejor lugar de trabajo del mundo. A los que ya estaban aquí cuando llegué y que hicieron que me sintiera en el laboratorio como en mi propia casa: Bellinda, Ángel, Clèment, Tania, Rocío, Carlos y especialmente Marga. Muchas gracias por enseñarme tantas cosas desde el principio, por ayudarme tanto y por hacer que mis primeros momentos fueran tan agradables. A Mar, que llegó poco después que yo, por su ayuda, colaboración y apoyo. A Lidia, la que ha sido durante tanto tiempo mi compañera de vitrina y con la que tantos buenos momentos he pasado. A Dulce, a la que acompañaré al otro lado del Atlántico, por su buen humor. Muchas gracias. Por supuesto a Natalia, Violeta y muy especialmente a Inés, a las que intenté enseñar lo que sabía y que me han reportado tanta satisfacción por ello. A Marisa y Fátima, a las que también quiero recordar. Y aquéllos que han llegado posteriormente: Moisés, Henar, Jorge, Ana, Nono, Marta, Carolina, Javi, Paco y Dani que también me han apoyado. Y naturalmente, a Laura, con la que me une una estrecha amistad desde hace tanto tiempo. Finalmente, no quisiera olvidarme de mis compañeros de la Universidad Johannes Gutenberg, a los que tanto recurrí, tanto me enseñaron y tanta paciencia tuvieron: Frauke, Giacomo, Sabine, Nadine Kaiser,

Nadine Mersmann, Martin Häring, Martin Purrio, Stephan, Nina, Matthias, Andrea y muy especialmente a las técnicos que más me ayudaron: Claudia, Anisa y Danka. Muchas gracias a todos.

Y por último, a mis padres, sin cuya inestimable ayuda y ánimo nada de esto hubiera salido adelante. Muchas gracias por todo lo que habéis hecho por mí. A mis hermanas, por ser como sois. A mi familia y a aquéllos que les hubiera gustado estar en este momento pero que ya no están. Y por supuesto a mis amigos.

TABLE OF CONTENTS

REFERENCES, ABBREVIATIONS AND ACRONYMS

All the references have been placed at the bottom of the columns in which they are first cited, following the format of the *Journal of the American Chemical Society* printed version.

Throughout this manuscript, abbreviations and acronyms recommended by the American Chemical Society in the Organic Chemistry area (revised in the *Journal of Organic Chemistry* on January 2010; http://pubs.acs.org/paragonplus/submission/joceah/joceah_authguide.pdf) have been employed. In addition, those indicated below have also been used.

ABHD	α/β hydrolase domain
Abn-CBD	Abnormal cannabidiol
ABPP	Activity-based protein profiling
AC	Adenylyl cyclase
AEA	*N*-arachidonoylethanolamine (anandamide)
2-AG	2-Arachidonoylglycerol
BSA	Bovine serum albumin
CB	Cannabinoid
CBD	Cannabidiol
CBN	Cannabinol
p-CMB	*p*-chloromercuribenzoic acid
CNS	Central nervous system
COX	Cyclooxygenase
CREAE	Chronic relapsing experimental autoimmune encephalomyelitis
3D	Tridimensional
DAG	Diacylglycerol
DAGL	Diacylglycerol lipase
DMEM	Dulbecco's modified Eagle medium
dpm	Disintegrations per minute
ECS	Endogenous cannabinoid system
FAAH	Fatty acid amide hydrolase
FBS	Fetal bovine serum
Glu	Glutamate

cGMP	Cyclic guanosine monophosphate
GPCR	G protein coupled receptor
HEPES	4-(2-Hydroxyethyl)-1-piperazineethanesulfonic acid
HPRT	Hypoxanthine guanine phosphoribosyltransferase
H.S.	Heterocyclic subunit
HTS	High throughput screening
IC_{50}	Inhibitory concentration 50
IFN	Interferon
K_i	Affinity constant
2-LG	2-Linoleoylglycerol
LOX	Lipooxygenase
MAPK	Mitogen-activated protein kinase
MGL	Monoacylglycerol lipase
MS	Multiple sclerosis
MTT	3-(4,5-Dimethylthiazol-2-yl)-2,5-diphenyltetrazolium bromide
NAM	*N*-arachidonylmaleimide
NAPE	*N*-arachidonoyl phosphatidylethanolamine
NEM	*N*-ethylmaleimide
NO	Nitric oxide
2-OG	2-Oleoylglycerol
PBS	Phosphate buffered saline
PDB	Protein data bank
PEA	*N*-palmitoylethanolamine
PG	Prostaglandin
PL	Phospholipase
PPAR	Peroxisome proliferator-activated receptor
RT-PCR	Retrotranscriptase-polymerase chain reaction
s.e.m.	Standard error mean
STD	Saturation transfer difference
THC	(-)-Δ^9-Tetrahydrocannabinol
Tris-HCl	Tris(hidroxymethyl)aminomethane chlorhydrate
TRPV	Transient receptor potential vanilloid
UCM	Universidad Complutense de Madrid

1. INTRODUCTION

1.1. The endogenous cannabinoid system (ECS)

Cannabis sativa contains over 60 phytocannabinoids, at least three of which are bioactive: (-)-Δ^9-tetrahydrocannabinol (THC), cannabinol (CBN) and cannabidiol (CBD) due to their ability to interact with a class of receptors located in cell membranes called cannabinoid (CB) receptors. The best-known cannabinoid is THC, which is thought to mediate most of its psychotropic and addictive properties and to modify essential physiological processes by interacting with these CB receptors expressed by neurons and other cell types.[1] However, this substance also produces other non-psychotropic effects like analgesia, hypotension, inflammatory response and influence in sexual behavior.[1,2]

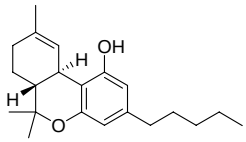

(-)-Δ^9-Tetrahydrocannabinol (THC)

The isolation of THC in 1964 by Mechoulam's group[3] represents the first step in the cannabinoid research and has its continuity with the description of its total synthesis.[4]

Recent evidences suggest that the antiinflammatory properties of *C. sativa* may be mediated by CBN and CBD. Therefore, these two non-psychotropic cannabinoids constitute promising lead compounds to develop cannabinoid-based antiinflammatory medicines. It is thought that CBN reduces inflammatory responses by interacting with CB receptors expressed by immune cells, while CBD reduces blood pressure and inflammation most likely by interacting with CB receptors expressed by neurons, vascular endothelial cells and immune cells.[5]

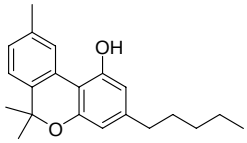

Cannabinol (CBN)

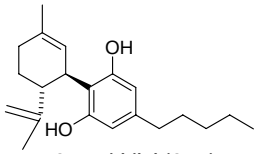

Cannabidiol (CBD)

Research in this field has focused on the elucidation of the molecular mechanisms mediating the action of cannabinoids in specific cell types. Towards this aim, a set of powerful pharmacological and genetic tools targeting the endogenous cannabinoid system (ECS) has been developed. They have enabled a better understanding of its involvement in physiological functions and pathological processes. The basic components of this signaling system are the CB receptors, their endogenous ligands (endocannabinoids), and the metabolic enzymes.[6]

To date, at least five different CB receptors have been identified. CB_1 and CB_2, which have been molecularly characterized; GPR55, which is thought to be an orphan receptor; and two other receptors which have been pharmacologically defined but remain to be identified at the molecular level.[7]

Both receptors, CB_1 and CB_2, are located in the cell plasma membrane and they belong to the seven transmembrane G protein coupled receptor (GPCR) superfamily. They affect signal transduction through the

---

[1] Howlett, A.C., Barth, F., Bonner, T.I., Cabral, G., Casellas, P., Devane, W.A., Felder, C.C., Herkenham, M., Mackie, K., Martin, B.R., Mechoulam, R., Pertwee, R.G. *Pharmacol. Rev.* 2002, *54*, 161.
[2] (a) Stella, N. *Proc. Natl. Acad. Sci. USA* 2001, *98*, 793. (b) Elmes, S.J.R., Winyard, L.A., Medhurst, S.J., Clayton, N.M., Wilson, A.W., Kendall, D.A., Chapman, V. *Pain* 2005, *118*, 327.
[3] Gaoni, Y., Mechoulam, R. *J. Am. Chem. Soc*. 1964, *86*, 1646.
[4] Mechoulam, R., Gaoni, Y. *J. Am. Chem. Soc*. 1965, *87*, 3273.
[5] (a) Malfait, A.M., Gallily, R., Sumariwalla, P.F., Malik, A.S., Andreakos, E., Mechoulam, R., Feldmann, M. *Proc. Natl. Acad. Sci. USA* 2000, *97*, 9561. (b) Kozela, E., Pietr, M., Juknat, A., Rimmerman, N., Levy, R., Vogel, Z. *J. Biol. Chem*. 2010, *285*, 1616.
[6] Di Marzo, V. *Pharmacol. Res*. 2009, *60*, 77.
[7] Stella, N. *Neuropharmacology* 2009, *56*, 244.

inhibition of the adenylyl cyclase (AC), ion channel regulation, activation of the mitogen-activated protein kinase (MAPK) pathway as well as the stimulation of the nitric oxide synthase.[1] They share 44% amino acid identity and display different pharmacological profiles and expression patterns.[8] The CB_1 receptor is constituted by 472 amino acids and is mainly expressed by neurons and at lower levels in other cell types in brain such as astrocytes, oligodendrocytes and stem cells.[1,8,9] In adult mammalian brain these receptors are principally located in the presynaptic zone, although they are also expressed in dendrites and soma. They are especially abundant in GABAergic neurons while they are between three and ten times less expressed in glutamatergic neurons.[10] They are coupled to $G_{i/o}$ proteins and modulate the activity of specific ion channels and second messengers. In this way, acute stimulation of neuronal CB_1 receptors for milliseconds to seconds inhibits presynaptic N-type channels, reducing neurotransmission.[11] Moreover, these receptors regulate effector proteins such as protein kinase A and extracellular regulated kinase (Erk),[12] modifying enzymatic activity and gene regulation. Additionally, CB_1 receptor has been reported to be expressed in other peripheral tissues such as pancreas and prostate.[13]

The CB_2 receptor was identified in 1993 and it is constituted by 360 aminoacids.[8] It is coupled to G_i proteins and it is expressed fundamentally in immune system cells (B cells, NK cells, macrophages and neutrophils).[14] It was originally considered to be expressed only in peripheral tissues,[15] however, recent evidence has pointed to a neuronal location in some regions of mammalian brain.[16] In addition, CB_2 immunoreactivity is increased under pathological conditions associated to neuroinflammation, including multiple sclerosis (MS), amyotrophic lateral sclerosis or Alzheimer's disease.[17]

Recent evidences suggest that the orphan receptor GPR55 might be a third CB receptor. However, more work is required to establish this receptor as a true component of the ECS.[18] Other subtype of CB receptor that inhibits glutamatergic transmission in the hippocampus has been identified by several laboratories using CB_1 knockout mouse brain tissue. This unique receptor does not control AC activity[19] and it is stimulated by the cannabinoid agonists WIN552122 and CP55940, and antagonized by micromolar concentrations of SR141716A. The last group of CB receptors identified to date is constituted by the abnormal-cannabidiol (abn-CBD) receptors. These receptors were identified using a CB_1/CB_2 double

[8] (a) Matsuda, L.A., Lolait, S.J., Brownstein, M.J., Young, A.C., Bonner, T.I. *Nature* 1990, *346*, 561. (b) Munro, S., Thomas, K.L., Abu-Shaar, M. *Nature* 1993, *365*, 61.

[9] (a) Rodríguez, J.J., Mackie, K., Pickel, V.M. *J. Neurosci.* 2001, *21*, 823. (b) Molina-Holgado, E., Vela, J.M., Arévalo-Martín, A., Almazán, G., Molina-Holgado, F., Borrell, J., Guaza, C. *J. Neurosci.* 2002, *22*, 9742. (c) Aguado, T., Monory, K., Palazuelos, J., Stella, N., Cravatt, B.F., Lutz, B., Marsicano, G., Kokaia, Z., Guzmán, M., Galve-Roperh, I. *FASEB J.* 2005, *19*, 1704.

[10] (a) Kawamura, Y., Fukaya, M., Maejima, T., Yoshida, T., Miura, E., Watanabe, M., Ohnio-Shosaku, T., Kano, M. *J. Neurosci.* 2006, *26*, 2991. (b) Uchigashima, M., Narushima, M., Fukaya, M., Katona, I., Kano, M., Watanabe, M. *J. Neurosci.* 2007, *27*, 3663.

[11] Mackie, K., Lai, Y., Westenbroek, R., Mitchell, R. *J. Neurosci.* 1995, *15*, 6552.

[12] Chevaleyre, V., Heifets, B.D., Kaeser, P.S., Sudhof, T.C., Castillo, P.E. *Neuron* 2007, *54*, 801.

[13] (a) Juan-Picó, P., Fuentes, E., Bermúdez-Silva, F.J., Díaz-Molina, F.J., Ripoll, C., Rodríguez de Fonseca, F., Nadal, A. *Cell Calcium* 2006, *39*, 155. (b) Tokanovic, S., Malone, D.T., Ventura, S. *Br. J. Pharmacol.* 2007, *150*, 227.

[14] Cabral, G.A., Griffin-Thomas, L. *Expert. Rev. Mol. Med*. 2009, *11*, e3.

[15] Di Marzo, V., Bifulco, M., De Petrocellis, M. *Nat. Rev. Drug Discov*. 2004, *3*, 771.

[16] Van Sickle, M.D., Duncan, M., Kingsley, P.J., Mouihate, A., Urbani, P., Mackie, K., Stella, N., Makriyannis, A., Piomelli, D., Davison, J.S., Marnett, L.J., Di Marzo, V., Pittman, Q.J., Patel, K.D., Sharkey, K.A. *Science* 2005, *310*, 329.

[17] (a) Yiangou, Y., Facer, P., Durrenberger, P., Chessell, I.P., Naylor, A., Bountra, C., Banati, R., Anand, P. *BMC Neurol.* 2006, *6*, 12. (b) Ruiz-Valdepeñas, L., Benito, C., Tolón, R.M., Martínez-Orgado, J.A., Romero, J. *Exp. Neurol.* 2010, *224*, 66.

[18] (a) Godlewski, G., Offertáler, L., Wagner, J.A., Kunos, G. *Prostaglandins Other Lipid Mediat*. 2009, *89*, 105. (b) Ross, R.A. *Trends Pharmacol. Sci.* 2009, *30*, 156. (c) Nevalainen, T., Irving, A.J. *Curr. Top. Med. Chem*. 2010, *10*, 799.

[19] (a) Hoffman, A.F., Macgill, A.M., Smith, D., Oz, M., Lupica, C.R. *Eur. J. Neurosci*. 2005, *22*, 2387. (b) Monory, K., Tzavara, E.T., Lexime, J., Ledent, C., Parmentier, M., Borsodi, A., Hanoune, J. *Biochem. Biophys. Res. Commun*. 2002, *292*, 231.

knockout, and are expressed by endothelial cells of blood vessels. They are activated by abn-CBD and antagonized by CBD and O-1918. They are coupled to $G_{i/o}$ proteins increasing cGMP production and regulating blood pressure.[20] These receptors are also expressed in microglia.[21]

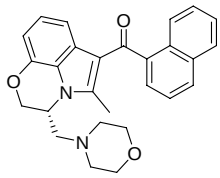

WIN552122

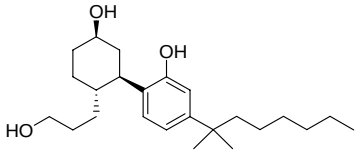

CP55940

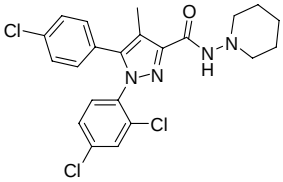

SR141716A

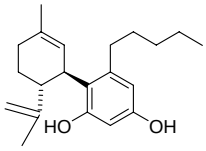

abn-CBD

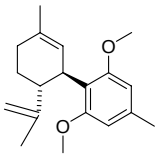

O-1918

The existence of these CB receptors and their associated biological effects suggested the presence of endogenous ligands which specifically interact with them, so a great effort has been devoted to identify and characterize these substances. In this way, in 1992, Mechoulam's group identified the first endocannabinoid, *N*-arachidonoylethanolamine, also called anandamide (AEA), which binds to CB_1 receptors with high affinity.[22] It is considered a *bona fide* endocannabinoid because (i) it is produced by cells in an activity-dependent manner, (ii) it activates a cannabinoid receptor, and (iii) it undergoes regulated deactivation. Although AEA is generally believed to be synthesized from a *N*-arachidonoyl phosphatidylethanolamine (NAPE) precursor in a calcium-dependent manner by a NAPE phospholipase D (NAPE PLD) enzyme,[23] however, alternative AEA biosynthesis pathways have been also recently reported.[24]

AEA exerts its effects in the synapsis, from where it is transported to the cytosol through a reuptake process,[25] in order to be hydrolyzed into arachidonic acid and ethanolamine (Figure 1, page 6). This step is primarily mediated by fatty acid amide hydrolase (FAAH),[26] although additional pathways also exist. They involve several different enzymes such as cyclooxygenase-2 (COX-2),[27] lipooxygenases (LOXs), such as LOX-12 and-15,[28] or the cytochrome P450.[29] A

[20] Begg, M., Mo, F.-M, Offertáler, L., Bátkai, S., Pacher, P., Razdan, R.K., Lovinger, D.M., Kunos, G. *J. Biol. Chem.* 2003, *278*, 46188.
[21] Franklin, A., Stella, N. *Eur. J. Pharmacol.* 2003, *474*, 195.

[22] Devane, W.A., Hanus, L., Breuer, A., Pertwee, R.G., Stevenson, L.A., Griffin, G., Gibson, D., Mandelbaum, A., Etinger, A., Mechoulam, R. *Science* 1992, *258*, 1946.
[23] (a) Okamoto, Y., Morishita, J., Tsuboi, K., Tonai, T., Ueda, N. *J. Biol. Chem*. 2004, *279*, 5298. (b) Simon, G.M., Cravatt, B.F. *J. Biol. Chem*. 2008, *283,* 9341.
[24] Ahn, K., McKinney, M.K., Cravatt, B.F. *Chem. Rev*. 2008, *108*, 1687.
[25] Piomelli, D. *Prostaglandins Other Lipid Mediat*. 2005, *77*, 223.
[26] (a) Cravatt, B.F., Demarest, K., Patricelli, M.P., Bracey, M.H., Giang, D.K., Martin, B.R., Lichtman, A.H. *Proc. Natl. Acad. Sci. USA* 2001, *98*, 9371. (b) Cravatt, B.F., Giang, D.K., Mayfield, S.P., Boger, D.L., Lerner, R.A., Gilula, N.B. *Nature* 1996, *384*, 83.
[27] Kim, J., Alger, B.E. *Nat. Neurosci*. 2004, 7, 697.
[28] Starowicz, K., Nigam, S., Di Marzo, V. *Pharmacol. Ther*. 2007, *114*, 13.
[29] Snider, N.T., Kornilov, A.M., Kent, U.M., Hollenberg, P.F. *J. Pharmacol. Exp. Ther*. 2007, *321*, 590.

large amount of data about FAAH, the main enzyme responsible of AEA hydrolysis, is available such as its crystal structure and the chemical platform required for its selective inhibition.[30]

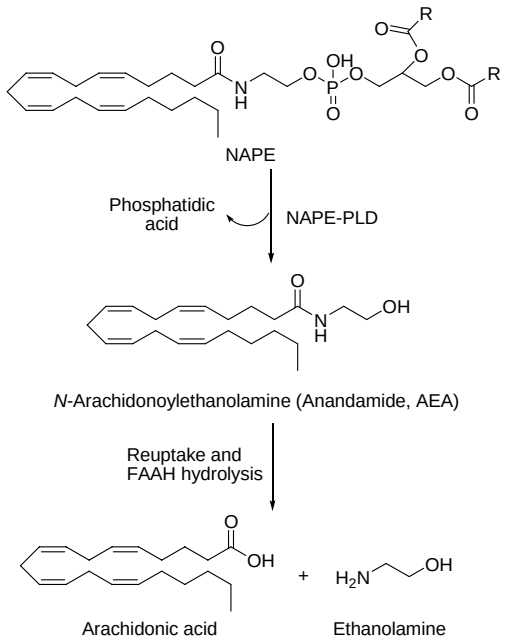

Figure 1. Biosynthesis and degradation of AEA

In 1995, two laboratories simultaneously identified a second endogenous ligand, 2-arachidonoylglycerol (2-AG), which is around hundred times more abundant in brain than AEA.[31] Like AEA, 2-AG is believed to be stored in the membrane as its phospholipid precursor. 2-AG is synthesized from diacylglycerol (DAG) by diacylglycerol lipase (DAGL) in a calcium dependent fashion. This process also involves the action of phospholipases because DAG can be produced either from the hydrolysis of phosphatidylinositol by phospholipase C-β (PLC-β) or from the hydrolysis of phosphatidic acid.[32] Two *sn*-1-selective DAGLs have been cloned and identified as responsible of 2-AG synthesis, DAGL-α and DAGL-β (Figure 2), being therefore essential in endocannabinoid signaling in the brain.[33] However, alternative pathways for 2-AG synthesis have been reported as well.[34]

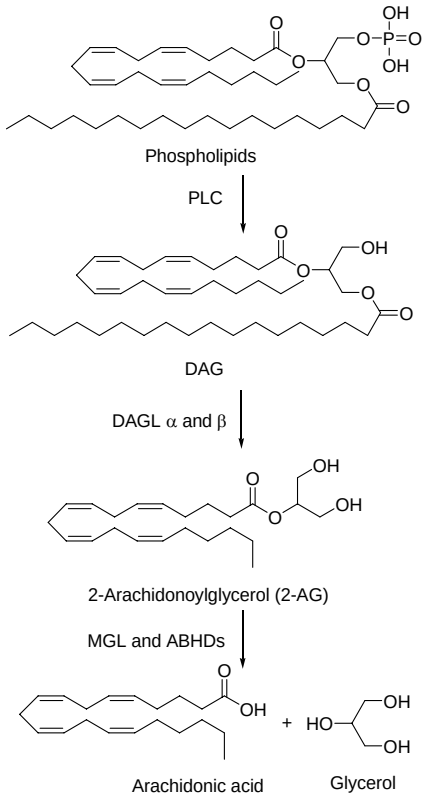

Figure 2. Biosynthesis and degradation of 2-AG

[30] McKinney, M.K., Cravatt, B.F. *Annu. Rev. Biochem.* 2005, *74*, 411.

[31] (a) Mechoulam, R., Ben-Shabat, S., Hanus, L., Ligumsky, M., Kaminski, N.E., Schatz, A.R., Gopher, A., Almog, S., Martin, B.R., Compton, D.R., Pertwee, R.G., Griffin, G., Bayewitch, M., Barg, J., Vogel, Z. *Biochem. Pharmacol.* 1995, *50*, 83. (b) Sugiura, T., Kondo, S., Sukagawa, A., Nakane, S., Shinoda, A., Itoh, K., Yamashita, A., Waku, K. *Biochem. Biophys. Res. Commun*. 1995, *215*, 89.

[32] (a) Stella, N., Schweitzer, P., Piomelli, D. *Nature* 1997, 388, 773. (b) Bisogno, T., Melck, D., De Petrocellis, L., Di Marzo, V. *J. Neurochem.* 1999, *72*, 2113.

[33] (a) Bisogno, T., Howell, F., Williams, G., Minassi, A., Cascio, M.G., Ligresti, A., Matias, I., Schiano-Moriello, A., Paul, P., Williams, E.F., Gangadharan, U., Hobbs, C., Di Marzo, V., Doherty, P. *J. Cell Biol*. 2003, *163*, 463. (b) Gao, Y., Vasilyev, D.V., Goncalves, M.B., Howell, F.V., Hobbs, C., Reisenberg, M., Shen, R., Zhang, M.Y., Strassle, B.W., Lu, P., Mark, L., Piesla, M.J., Deng, K., Kouranova, E.V., Ring, R.H., Whiteside, G.T., Bates, B., Walsh, F.S., Williams, G., Pangalos, M.N., Samad, T.A., Doherty, P. *J. Neurosci*. 2010, *30*, 2017. (c) Tanimura, A., Yamazaki, M., Hashimotodani, Y., Uchigashima, M., Kawata, S., Abe, M., Kita, Y., Hashimoto, K., Shimizu, T., Watanabe, M., Sakimura, K., Kano, M. *Neuron* 2010, *65*, 320.

[34] Sugiura, T., Kishimoto, S., Oka, S., Gokoh, M. *Prog. Lipid Res*. 2006, *45*, 405.

Unlike AEA, 2-AG binds to CB_1 and CB_2 receptors as a full agonist but with lower affinity.[34] Moreover, 2-AG has been found to act as a full agonist at abn-CBD receptors.[21]

2-AG is produced in postsynaptic cells, released in the synaptic cleft and subsequently internalized in the cytoplasm of the presynaptic cell through either passive diffusion or carrier-mediated transport. The inactivation of this endocannabinoid can be carried out through three mechanisms: (i) hydrolysis to arachidonic acid and glycerol, (ii) oxidation to a series of oxygenated derivatives and (iii) anabolic metabolism.[35] Among them, 2-AG hydrolysis constitutes the main mechanism, and it is carried out by a series of serine hydrolases, being the enzyme monoacylglycerol lipase (MGL) the primary enzyme mediating this process.

Besides these two main endocannabinoids it has been proposed the existence of at least another three:[36] (i) virodhamine, which selectively activates CB_2 receptors, (ii) 2-arachidyl glyceryl ether (noladin ether), which is a partial agonist selective for CB_1 receptors, and (iii) *N*-palmitoylethanolamine (PEA).[37]

While the physiological role as endocannabinoids of virodhamine and noladin ether has been questioned, the importance of PEA is increasingly gaining attention since it exerts anti-inflammatory activity via direct activation of peroxisome proliferator-activated receptor-α (PPAR-α)[38] and possibly GPR55[39] or via enhancement of AEA actions at CB_1, transient receptor potential vanilloid type 1 (TRPV-1) or PPAR-γ receptors.[40]

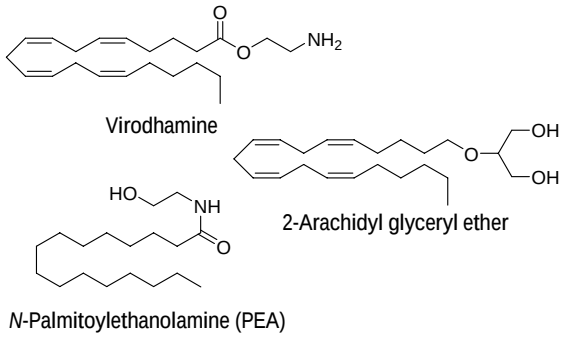

All these components including receptors, endogenous ligands and enzymes responsible of their biosynthesis and degradation constitute the ECS (Figure 3, page 8).

However, the potential exploitation of CB receptors as therapeutic targets is not easy, with two main problems to be resolved: (i) the psychotropic effects associated to CB receptor activation, and (ii) the broad expression of this system, so that any exogen intervention could modify the response in an undesirable manner. These problems could be resolved by tightly regulation of the biosynthesis-degradation machinery of endocannabinoids, which would avoid the undesirable psychotropic effects as well as the general activation of the system. In this way, a great effort has been carried out in the last years in the study of the degradation routes of AEA and 2-AG in order to selectively achieve high concentration of endocannabinoids at the adecuate place at the right time. Until recently, AEA and the enzyme responsible of its deactivation, FAAH, have constituted the major focus of research, but nowadays increasing evidence points out the prominent role of 2-AG in the regulation of different functions.

[35] Astarita, G., Geaga, J., Ahmed, F., Piomelli, D. *Int. Rev. Neurobiol*. 2009, *85*, 35.
[36] Petrosino, S., Ligresti, A., Di Marzo, V. *Curr. Opin. Chem. Biol*. 2009, *13*, 309.
[37] (a) Hanus, L., Abu-Lafi, S., Fride, E., Breuer, A., Vogel, Z., Shalev, D.E., Kustanovich I., Mechoulam, R. *Proc. Natl. Acad. Sci. USA* 2001, *98*, 3662. (b) Porter, A.C., Sauer, J.M., Knierman, M.D., Becker, G.W., Berna, M.J., Bao, J., Nomikos, G.G., Carter, P., Bymaster, F.P., Leese, A.B., Felder, C.C. *J. Pharmacol. Exp. Ther*. 2002, *301*, 1020. (c) Mackie, K., Stella, N. *AAPS J*. 2006, *8*, E298.
[38] LoVerme, J., La Rana, G., Russo, R., Calignano, A, Piomelli, D. *Life Sci*. 2005, *77*, 1685.
[39] Ryberg, E., Larsson, N., Sjögren, S., Hjorth, S., Hermansson, N.O., Leonova, J., Elebring, T., Nilsson, K., Drmota, T., Greasley, P.J. *Br. J. Pharmacol*. 2007 ,*152*, 1092.
[40] Costa, B., Comelli, F., Bettoni, I., Colleoni, M., Giagnoni, G. *Pain* 2008, *139*, 541.

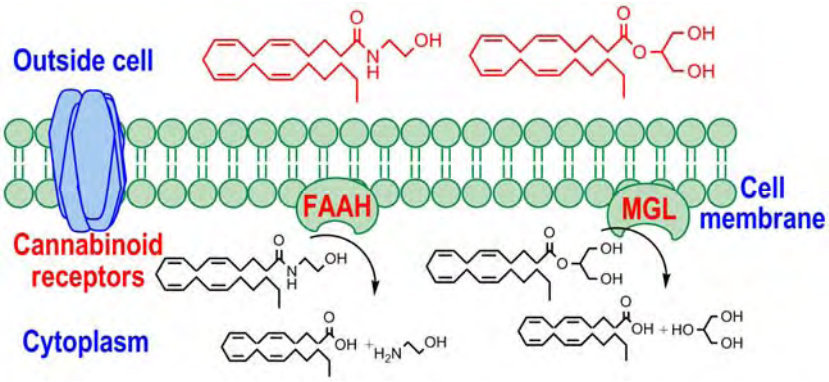

Figure 3. Endogenous Cannabinoid System (ECS)

As such, increase of endogenous levels of AEA has demonstrated therapeutic relevance for the treatment of nociception, neuronal damage, inflammation and neurodegenerative-associated motor symptoms.[41] In particular, inhibitors of FAAH represent promising candidates for the pharmacological treatment of pain and anxiety.[42] These advances have been possible due to a deep basic knowledge of FAAH, which have been molecularly characterized,[26] its tridimensional (3D) structure has been solved,[43] knockout and transgenic mouse models have been generated[26,44] and structure-activity relationship (SAR) studies have been reported.[45] All these endeavors have culminated in the development of compounds able to inhibit FAAH in a potent and selective manner.[46]

Respect to the 2-AG, this endocannabinoid is present in higher concentrations in brain than AEA, it behaves as a full agonist at both CB receptors (as opposed to the partial character of AEA) and it is involved in the regulation of an important number of physiological events including regulation of neurotransmission, inflammatory and immune processes.[47] All these facts represent a solid start point for a pharmacological intervention aimed at increasing the endogenous levels of 2-AG. At the beginning it was suggested the possibility that FAAH was the responsible of degradation of 2-AG. In fact, this enzyme hydrolyzes 2-AG at a higher rate than AEA *in vitro*,[48] although later experiments in FAAH knockout mouse models ruled out the possibility that this protein was the responsible of the *in vivo* deactivation of 2-AG.[49] Several lines of evidence

[41] (a) Massa, F., Marsicano, G., Hermann, H., Cannich, A., Monory, K., Cravatt, B.F., Ferri, G.L., Sibaev, A., Storr, M., Lutz, B. *J. Clin. Invest*. 2004, *113*, 1202. (b) Lichtman, A.H., Shelton, C.C., Advani, T., Cravatt, B.F. *Pain* 2004, *109*, 319. (c) Ortega-Gutiérrez, S., Molina-Holgado, E., Arévalo-Martín, A., Correa, F., Viso, A., López-Rodríguez, M.L., Di Marzo, V., Guaza, C. *FASEB J.* 2005, *19*, 1338. (d) Marsicano, G., Goodenough, S., Monory, K., Hermann, H., Eder, M., Cannich, A., Azad, S.C., Cascio, M.G., Ortega-Gutiérrez, S., van der Stelt, M., López-Rodriguez, M.L., Casanova, E., Schütz, G., Zieglgänsberger, W., Di Marzo, V., Behl, C., Lutz, B. *Science*. 2003, *302*, 84.

[42] Ahn, K., Johnson, D.S., Mileni, M., Beidler, D., Long, J.Z., McKinney, M.K., Weerapana, E., Sadagopan, N., Liimatta, M., Smith, S.E., Lazerwith, S., Stiff, C., Kamtekar, S., Bhattacharya, K., Zhang, Y., Swaney, S., Van Becelaere, K., Stevens, R.C., Cravatt, B.F. *Chem. Biol*. 2009, *16*, 411.

[43] Bracey, M.H., Hanson, M.A., Masuda, K.R., Stevens, R.C., Cravatt, B.F. *Science* 2002, *298*, 1793.

[44] Cravatt, B.F., Saghatelian, A., Hawkins E.G., Clement, A.B., Bracey, M.H., Lichtman, A.H. *Proc. Natl. Acad. Sci. USA* 2004, *101*, 10821.

[45] Boger, D.L., Sato, H., Lerner, A.E., Hedrick, M.P., Fecik, R.A., Miyauchi, H., Wilkie, G.D., Austin, B.J., Patricelli, M.P., Cravatt, B.F. *Proc. Natl. Acad. Sci. USA* 2000, *97*, 5044.

[46] (a) Alexander, J.P., Cravatt, B.F. *Chem. Biol*. 2005, *12*, 1179. (b) Mileni, M., Garfunkle, J., Ezzili, C., Kimball, F.S., Cravatt, B.F., Stevens, R.C., Boger, D.L. *J. Med. Chem*. 2010, *53*, 230.

[47] Sugiura, T. *Biofactors* 2009, *35*, 88.

[48] Patricelli, M.P., Cravatt, B.F. *Biochemistry* 1999, *38*, 14125.

[49] Lichtman, A.H., Hawkins, E.G., Griffin, G., Cravatt, B.F. *J. Pharmacol. Exp. Ther*. 2002, *302*, 73.

suggest that MGL is the primary enzyme responsible for hydrolyzing 2-AG in the nervous system, (i) recombinant expression of MGL reduces receptor-dependent 2-AG accumulation in cortical neurons, (ii) immunodepletion of MGL decreases 2-AG hydrolysis activity in rat brain tissue by 50% and (iii) activity-based protein profiling (ABPP) allowed assignment of 85% of the total 2-AG hydrolysis in the brain to MGL, being mainly localized in membrane fractions but also detected in soluble cytosolic fractions. The remaining activity is due to the activities of α/β hydrolase domain-6 (ABHD-6) and α/β hydrolase domain-12 (ABHD-12) enzymes. Less of 1% can be appointed to FAAH, hormone-sensitive lipase and neuropathy target esterase.[50]

Although the therapeutic potential of MGL inhibitors is still unclear and the availability of a knockout model was elusive until recently,[51] however, the development of selective and potent inhibitors could help to elucidate the potential of MGL as a therapeutic target[52] in the same way it has been possible with FAAH.

1.2. Structural and catalytic features of MGL

Historically, lipolytic enzymes have attracted an enormous attention. They are physiologically relevant metabolic enzymes, responsible for the hydrolysis of the dietary triacylglycerides as well as for the lipolysis of adipose tissue acylglycerols.[53] Moreover, from a different perspective, they have an impressive biotechnological potential as biocatalysts because of their excellent capabilities to carry out regio-, stereo- and enantiospecific reactions.[54] Lipolytic enzymes are widely expressed throughout animals, plants and microorganisms and include different subclasses such as carboxylesterases (EC 3.1.1.1), which hydrolize esters of short to medium-chain carboxylic acids ($C \leq 12$), and lipases (EC 3.1.1.3) which display maximum activity towards water-insoluble long-chain ($C > 12$) acylglycerides. Monoacylglycerol lipase or monoglyceride lipase (MGL, EC 3.1.1.23) has been characterized as the enzyme that catalyses the hydrolysis of monoglycerides, with a preference for this type of substrates versus di- or triglycerides, to fatty acid and glycerol.[55] The first mammalian MGL molecularly characterized was cloned from a mouse adipocyte cDNA library.[56] This enzyme showed some of the typical features of a true MGL activity such as practically complete lack of activity against diglycerides, triglycerides or cholesterol ester substrates. Therefore, when it was clear that FAAH was not responsible for the 2-AG inactivation and a 2-AG hydrolyzing activity, distinct from FAAH, was partially purified from porcine brain,[57] MGL emerged as the most logical candidate. Soon after, a rat brain MGL was cloned by homology[50] and a MGL activity described in rat cerebellar membranes.[58]

[50] (a) Dinh, T.P., Carpenter, D., Leslie, F.M., Freund, T.F., Katona, I., Sensi, S.L., Kathuria, S., Piomelli, D. *Proc. Natl. Acad. Sci. USA*. 2002, *99*, 10819. (b) Dinh, T.P., Kathuria, S., Piomelli, D. *Mol. Pharmacol*. 2004, *66*, 1260. (c) Blankman, J.L., Simon, G.M., Cravatt, B.F. *Chem. Biol*. 2007, *14*, 1347.

[51] Schlosburg, J.E., Blankman, J.L., Long, J.Z., Nomura, D.K., Pan, B., Kinsey, S.G., Nguyen, P.T., Ramesh, D., Booker, L., Burston, J.J., Thomas, E.A., Selley, D.E., Sim-Selley, L.J., Liu, Q.S., Lichtman, A.H., Cravatt, B.F. *Nat. Neurosci*. 2010, *13*, 1113.

[52] Viso, A., Cisneros, J.A., Ortega-Gutiérrez, S. *Curr. Top. Med. Chem*. 2008, *8*, 231.

[53] Lengsfeld, H., Beaumier-Gallon, G., Chahinian, G., De Caro, A., Verger, R., Laugier, R., Carrièrre, F. Physiology of gastrointestinal lipolysis and therapeutical uses of lipases and digestive lipase inhibitors. In *Lipases and Phospholipases in Drug Development*, Müller, G., Petry, S., Eds, Wiley VCH: Weinheim, 2004, pp195-229.

[54] Jaeger, K.E., Eggert, T. *Curr. Opin. Biotechnol*. 2002, *13*, 390.

[55] (a) Tornqvist, H., Belfrage, P. *J. Biol. Chem*. 1976, *251*, 813. (b) Fredrikson, G., Tornqvist, H., Belfrage, P. *Biochim. Biophys. Acta* 1986, *876*, 288.

[56] Karlsson, M., Contreras, J.A., Hellman, U., Tornqvist, H., Holm, C. *J. Biol. Chem*. 1997, *272*, 27218.

[57] Goparaju, S. K., Ueda, N., Taniguchi, K., Yamamoto, S. *Biochem. Pharmacol.* 1999, *57*, 417.

[58] Saario, S.M., Savinainen, J.R., Laitinen, J.T., Järvinen, T., Niemi, R. *Biochem. Pharmacol.* 2004, *67*, 1381.

1.2.1. Structural features of MGL

The primary structure of the proposed rat brain MGL consists of 303 amino acids, with a molecular weight of 33.4 KDa and a sequence identity of 92% when aligned with the mouse adipocyte MGL.[50] This high homology has allowed to assign the catalytic triad which has been confirmed by mutagenesis studies in the adipocyte MGL and it is conserved in the brain MGL. Mechanistically, the enzyme belongs to the serine hydrolase family characterized by the presence of the classical catalytic triad formed by serine (S122), aspartic (D239) and histidine (H269) residues that form the active site. Besides, it also possesses a second lipase motif, the histidine-glycine (HG) dipeptide, element found in many lipases between 70 and 100 residues N-terminal of the catalytic serine. Sequence homology with other known proteins revealed a distant relation with various microbial enzymes such as haloperoxidases, esterases and lysophospholipases.[52]

The rational design of inhibitors relies on the structural and mechanistic knowledge of the enzyme of interest. The 3D structure of human MGL (hMGL) has been elucidated very recently.[59,60] The crystallized hMGL is constituted by 303 amino acids with two molecules in the asymmetric unit (Figure 4).

The structure of the protein has been reported either as a dimer[59] or a monomer.[60] In the first case, the two monomers are in contact by a surface of 884 Å^2, which would represent only the 7% of the surface of the monomer. In support of this idea, MGL was found as a dimer in mass spectrometry and no peak corresponding to the monomeric protein was found after gel filtration chromatography.[59] However, in the other study,[60] MGL was found to be a monomer.

Figure 4. Global fold of hMGL (PDB ID: 3HJU)

As it was predicted, MGL has the main structural features of the α/β hydrolases, being very similar to bacterial α/β hydrolases. The structurally conserved central β-sheet is constituted by seven parallel and one antiparalell strand surrounded by six α helices. This so-called α/β hydrolase fold (Figure 5) has been identified in many other distantly or closely related enzymes including a variety of hydrolases and dehalogenases from diverse origins ranging from prokaryotes to eukaryotes. A cap domain is located over the active site and the β-sheet. Below this cap is the catalytic triad which is constituted by the residues serine (S122), aspartic (D239) and histidine (H269),[59,60] consistently with previous reports based on mutagenesis studies.

The nucleophilic serine is located in the highly conserved sequence Gly-X-Ser-X-Gly between helix α3 (A3) and strand β5, where X represents any amino acid. This pentapeptide also constitutes one of the most strictly conserved features of the α/β hydrolase enzymes, the so-called "nucleophilic elbow". This structural element is a sharp γ turn that makes the nucleophilic residue lies in an unfavourable region of the Ramachandran plot. Therefore, it is needed for the optimal positioning of the nucleophile to allow easy

[59] Labar, G., Bauvois, C., Borel, F., Ferrer, J.L., Wouters, J., Lambert, D.M. *ChemBioChem* 2010, *11*, 218.
[60] Bertrand, T., Augé, F., Houtmann, J., Rak, A., Vallée, F., Mikol, V., Berne, P.F., Michot, N., Cheuret, D., Hoornaert, C., Mathieu, M. *J. Mol. Biol*. 2010, *396*, 663.

access of the substrate. The position of the catalytic serine at the end of the sharp turn allows the histidine to approach on one side and the substrate to gain access on the other.[61] Forming this γ turn imposes steric restrictions that require a small side chain at positions –2 and +2 with respect to the serine. This explains the presence of the evolutionary conserved pentapeptide (Gly-X-Ser-X-Gly) with two glycines at the –2 and +2 positions.[62]

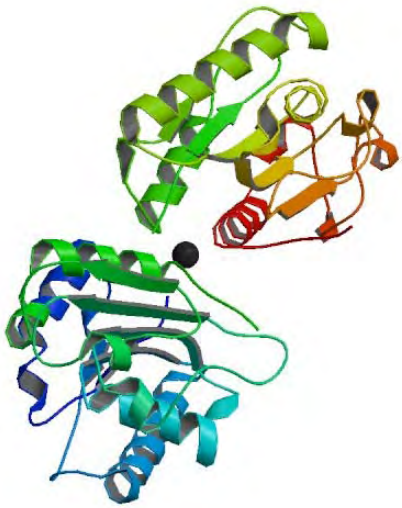

Figure 5. The α/β hydrolase fold (PDB ID: 1I6W)

Other important structural module is the lid domain, which is composed of two large loops surrounding helix A4 (residues 156-190; Figure 4). An equivalent domain was found in the structure of rat FAAH and is described as a putative membrane-interacting region of the protein.[43] In the case of MGL, this helix is amphipatic with its hydrophobic side oriented towards the membrane, which could suggest the same role as for FAAH.[60] Additionally, this fragment is believed to be flexible since this helix participates in the crystalline packing and there are different conformations. This lid is located at the entrance of a large occluded tunnel that ends near the catalytic S122. Hence, although the entrance of the pocket is solvent-exposed, the catalytic triad is buried at the bottom of the pocket. The tunnel is occluded at its end but with a broad exit to the solvent region at its top. Close to the end of the tunnel is a narrow hole which connects the catalytic triad region with the solvent region. Actually, it has been hypothesized that 2-AG is extracted from the lipid membrane, process that is mainly allowed by the flexibility of the α/β fold core. This process, known as interfacial activation, is responsible for the increased enzyme activity when acting at the lipid-water interface of micellar substrates and it was experimentally demonstrated for the first time for porcine pancreatic lipase.[63] This increase in the enzyme activity is believed to be triggered by structural rearrangements of the lid making catalytic residues accessible to substrates.

The topology of the tunnel, a large hydrophobic segment ending in a polar bottom is in agreement with this hypothesis and with the structure of the endogenous ligand, 2-AG, that contains a long aliphatic chain and a polar head that is cleaved by the catalytic triad. Indeed, L148, A164, L176, I179, L205, V207, I211, L213, L214, V217 and L241 side chains are properly located to interact with the arachidonoyl moiety of the substrate. The proximal area of the catalytic triad presents a more hydrophilic character and therefore delimits a polar cavity that accommodates the polar glycerol head of 2-AG.

On the other hand, MGL has been reported to hydrolyze 1(3)-AG and 2-AG at similar rates,[58] and docking models help to understand this lack of selectivity. The long hydrophobic chain is stacked along the left part of the binding pocket, while the reactive carbonyl is H-bonded to A61. The polar head is kept in place by means of three hydrogen bonds that block both

[61] Kim, K.K., Song, H.K., Shin, D.H., Hwang, K.Y., Suh, S.W. *Structure* 1997, *5*, 173.
[62] Schrag, J.D., Cygler, M. *Methods Enzymol.* 1997, *284*, 85.
[63] Sarda, L., Desnuelle, P. *Biochim. Biophys. Acta* 1958, *30*, 513.

terminal hydroxyl groups. The distance from the oxygen of the catalytic serine to the reactive carbonyl is 3.2 and 3.0 Å for 2-AG and 1(3)-AG respectively, which are ideal distances for the reaction to take place.[60]

1.2.2. Catalytic mechanism

The kinetics of lipolytic enzymes can be considered as a two-phase process that includes a first binding step followed by hydrolysis of the substrate. As a general feature of lipases, they can hydrolize monomeric substrate molecules, but only after binding to the interface conversion of aggregated substrate can take place. This initial binding step of the lipase to the substrate interface, followed by binding of a single substrate molecule in the active site of the enzyme and catalytic turnover, results in complex kinetics as compared to the situation where both enzyme and substrate are water soluble.

Once the substrate reaches the active site, its ester bond is hydrolysed in a mechanism similar to that of serine proteases. Catalysis is initiated by nucleophilic attack of the serine hydroxyl on the susceptible carbonyl carbon of the substrate (Figure 6). This attack is facilitated by a general acid-base mechanism in which the serine is activated by a hydrogen bond in relay with histidine and aspartate or glutamate.

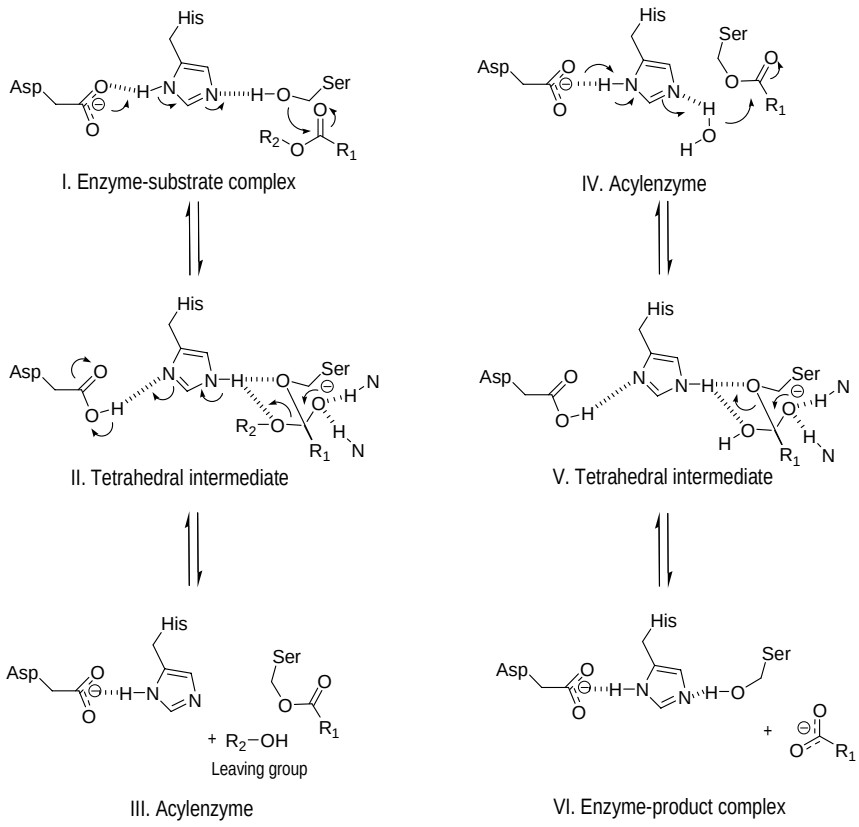

Figure 6. MGL catalytic mechanism

Afterwards, a tetrahedral acyl-enzyme is formed, which is stabilized by the "oxyanion hole". In general, the "oxyanion hole" is not preformed but it is created by the opening of the lid and the exposure of a substrate-binding pocket. Collapse of the tetrahedral adduct in the forward direction involves expulsion of the leaving group (corresponding to the alcohol moiety) and generation of a second acyl-enzyme complex. Finally, the deacylation step involves the attack of a water molecule at the active site similarly activated as a more effective nucleophile due to the proton shuttling of the charge-relay system (Figure 6). The released glycerol might diffuse toward a narrow hole located at the same level of the catalytic triad, while arachidonic acid could diffuse back to the top of tunnel and exit of the protein.

The effect of some inhibitors or activators on MGL activity can give clues about the residues important for activity. In this context, as expected from a serine hydrolase, MGL activity can be inhibited by general inhibitors such as fluorophosphonates, sulfonylfluorides and trifluoromethylketones,[52] reagents that inactivate the catalytic serine.

MGL can also be inhibited by *N*-ethylmaleimide (NEM), $HgCl_2$ and *p*-chloromercuribenzoic acid (*p*-CMB), effects that can be reversed in presence of dithiothreitol.[55,64] These findings point out the functional importance of one or several free sulfhydryl groups. Sometimes the presence of reactive sulfhydryl groups indicates the existence of a reversible modulatory mechanism by *S*-nitrosylation characterized by sensitivity to nitric oxide (NO).[65] However, MGL activity seems unaffected by diverse NO donors such as *S*-nitrosoglutathione, *S*-nitrosocysteine or sodium nitroprusside, which likely indicates that MGL activity is not regulated by NO.[66]

1.2.3. Catalytic specificity

The close homology between MGL and the widely studied family of lipases has facilitated the analysis of MGL structure and its catalytic mechanism. However, MGL also presents some unique features that clearly differentiate it from other lipases. One of these aspects is its substrate specificity. MGL hydrolyses 2-monooleoylglycerol at the same rate as 1(3)-monooleoylglycerol with an apparent K_M at 21 ºC and pH 7.4 for both substrates of 0.2 mM although it seems to prefer 2-arachidonoylglycerol to its corresponding 1(3)-regioisomer. The optimum pH is 7.0-8.0. MGL does not show appreciable activity against diglycerides, triglycerides, cholesterol esters or lysophosphatidylcholine.

Besides oleoyl- and arachidonoyl- fatty acid chains, MGL is able to hydrolyze other monoesters with different fatty acid chains such as octanoyl-, lauroyl-, palmitoyl-, stearoyl- or linoleoylglycerol.[67] In addition, MGL preferentially hydrolyses 2-[^{3}H]-AG and 2-[^{3}H]-oleolylglycerol (2-[^{3}H]-OG) than labelled AEA, PEA or *N*-oleoylethanolamine which is consistent with a better recognition of 2-monoglycerides.[68]

1.3. MGL inhibitors

Considering the extensive involvement of the ECS in an ample number of physiological functions and its impact on numerous pathologies, MGL has been proposed as a possible therapeutic target. However, to fully establish this potential, its validation is still needed. This process frequently relies on the development of solid and systematic SAR studies that provide potent and selective inhibitors of MGL. These compounds will

[64] Sakurada, T., Noma, A. *J. Biochem. (Tokyo)* 1981, *90*, 1413.
[65] Stamler, J.S., Lamas, S., Fang, F.C. *Cell* 2001, *106*, 675.
[66] Saario, S.M., Salo, O.M.H., Nevalainen, T., Poso, A., Laitinen, J.T., Järvinen, T., Niemi, R. *Chem. Biol.* 2005, *12*, 649.

[67] (a) Okazaki, O., Sagawa, N., Okita, J.R., Bleasdale, J.E., MacDonald, P.C., Johnston, J.M. *J. Biol. Chem*. 1981, *256*, 7316. (b) Prescott, S.M. Majerus, P.W. *J. Biol. Chem*. 1983, *258*, 764.
[68] Dinh, T.P., Freund, T.F., Piomelli, D. *Chem. Phys. Lipids* 2002, *121*, 149.

serve as powerful tools for examining the effects of increasing endogenous 2-AG in the regulation of ECS.

Nonetheless, and due to the recent characterization of MGL and the complexity of ECS, some of such studies are still to be developed. The structural requirements involved in the recognition and/or hydrolysis by MGL still remain unclear and only few potent and selective MGL inhibitors have been described so far. They fall into three broad categories: i) general serine hydrolase inhibitors, ii) endogenous substrate analogs and iii) other structures.

1.3.1. General serine hydrolase inhibitors

Since mechanistically MGL is a serine hydrolase, the first wide group of inhibitors are the general serine-hydrolase inhibitors. This series of mechanistically based inhibitors binds in an either reversible or irreversible covalent manner to the nucleophilic serine disrupting its catalytic activity. Chemically, we can distinguish three main reactive groups: fluorophosphonates, trifluoromethylketones and sulfonylfluorides. As the most representative compound within each of these classes we can mention methyl arachidonylfluorophosphonate (MAFP), arachidonyltrifluoromethylketone (ATFMK) and phenylmethylsulfonylfluoride (PMSF).

All these compounds are not new to the ECS field, since they are old known FAAH inhibitors. Considering the similarity of the mechanism and the structure of the substrate between MGL and FAAH, it is clear that one of the first aspects to consider when identifying potential MGL inhibitors is the selectivity between the two hydrolytic enzymes FAAH and MGL.

In general, those serine hydrolase inhibitors that were previously shown to block FAAH, also inhibit MGL activity although in a less potent manner, with IC_{50} values in the low micromolar range [IC_{50} (MAFP) = 0.8 μM; IC_{50} (ATFMK) = 2.5 μM; IC_{50} (PMSF) = 155 μM].[68] Even hexadecylsulfonylfluoride (HDSF, also referred to as AM374) a potent inhibitor of FAAH (IC_{50} = 10.2 nM) showed only a moderate activity towards MGL (IC_{50} = 6.2 μM).[52]

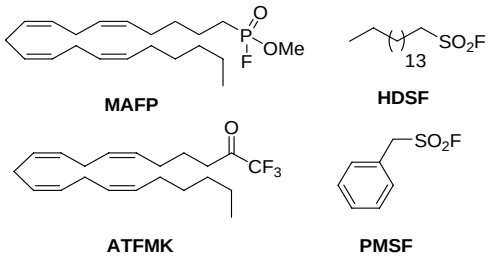

Extending this mechanistic approach but trying to gain some selectivity towards MGL *vs* other serine hydrolases, especially FAAH, a series of compounds with modifications in the side chain that bears the reactive group has been developed. In this regard, in addition to ATFMK, oleyl- and palmityltrifluoromethylketones have been studied [IC_{50} (MAGL) = 1.0 and 7.8 μM respectively], but they are still more potent inhibitors of FAAH (IC_{50} = 0.076 and 0.073 μM, respectively).[69]

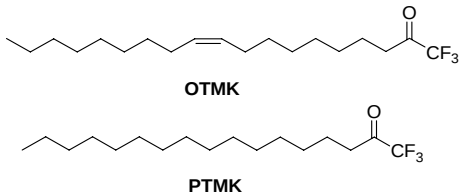

Further modification of the trifluoromethylketone moiety with the introduction of a sulfide (R-S-) group in the β position, structural motif known to inhibit esterases, has been also analysed in a brief SAR study aimed at the search of new antitumor agents acting as MGL inhibitors.[70]

[69] Ghafouri, N., Gunnar, T., Razdan, R.K., Mahadevan, A., Pertwee, R.G., Martin, B.R., Fowler, C.J. *Br. J. Pharmacol.* 2004, *143*, 774.
[70] Nithipatikom, K., Endsley, M.P., Isbell, M.A., Wheelock, C.E., Hammock, B.D., Campbell, W.B. *Biochem. Biophys. Res. Commun.* 2005, *332*, 1028.

Replacing the trifluoromethylketone with a different reactive moiety, a series of phosphonate esters of oleic acid has been recently screened for its ability to inhibit MGL. Nevertheless, none of the analysed compounds exerted a remarkable inhibition towards MGL, being UP101 the most potent compound, with an IC_{50} value of 3.2 μM and largely non-selective upon the rest of targets studied, including FAAH, DAGL α and CB_1 and CB_2 receptors.[71]

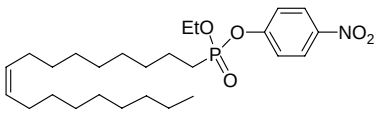

UP101

1.3.2. Arachidonoylglycerol analogs

A series of analogs of 2-AG (see page 6) have been examined for their ability to inhibit cytosolic MGL activity.[69] With respect to the fatty acid chain, the experimental data reveal that both isomers 2-AG and 1-AG are equipotent in disrupting MGL activity (IC_{50} = 13 and 17 μM, respectively). Shorter homologues, such as 2-OG and 2-linoleoylglycerol (2-LG), retain the values of affinity for MGL but show diminished selectivity towards FAAH. Branching and introduction of a hydroxyl group at the end of the chain, as in O-2204, maintains the affinity towards MGL (IC_{50} = 14 μM) while gaining a slight affinity towards FAAH (IC_{50} = 35 μM). In the linker, replacement of the ester group of 2-AG by an amide group leads to weaker inhibitors of MGL, while introduction of the urea moiety produces an almost complete loss of inhibition.

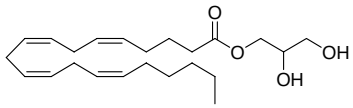

1-AG

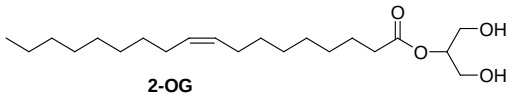

2-OG

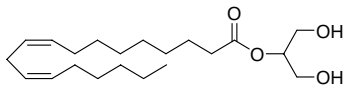

2-LG

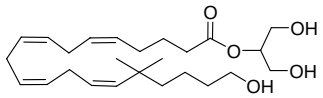

O-2204

Finally, the effect of modifications in the glycerol part was also examined. Thus, substitution of the glyceryl moiety by a thienylmethyl group (CAY10402, page 16) abolishes MGL activity while keeping a low FAAH inhibitory potency. Within this category also fall a couple of old known compounds, *N*-(4-hydroxy-2-methylphenyl)arachidonamide (VDM11) and *N*-(4-hydroxyphenyl)arachidonamide (AM404, page 16).

Originally proposed as AEA uptake inhibitors, they are also FAAH inhibitors.[72] Therefore, they were also tested as MGL inhibitors.[73] This work reveals that AM404 and its analog VDM11 inhibited the metabolism of AEA by rat brain FAAH equipotently (IC_{50} = 2.1 and 2.6 μM respectively) and to a lesser extent the degradation of 2-OG by cytosolic MGL (IC_{50} = 21 and 20 μM respectively).

[71] Bisogno, T., Cascio, M.G., Saha, B., Mahadevan A., Urbani, P., Minassi, A., Appendino, G., Saturnino, C., Martin, B., Razdan, R., Di Marzo, V. *Biochem. Biophys. Acta* 2006, *1761*, 205.

[72] Ortega-Gutiérrez, S. *Curr. Drug Targets CNS Neurol. Disord.* 2005, *4*, 697.

[73] Vandevoorde, S., Fowler, C.J. *Br. J. Pharmacol.* 2005, *145*, 885.

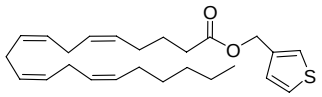

CAY10402

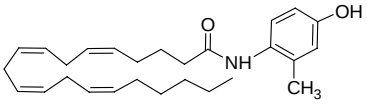

VDM11

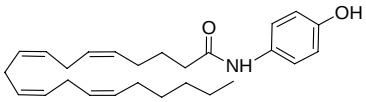

AM404

Since 1-AG shows comparable potency to 2-AG as MGL inhibitor but it is more stable in biological media, a group of 1-AG analogs have been examined as MGL inhibitors.[74] This structural study included variations in length and number of unsaturations of the fatty acid chains. The main conclusions of this study indicate that for cytosolic MGL the number of unsaturations does not significantly affect the activity with IC_{50} values between 4.5 and 21 μM. However, a decay of inhibition is observed for the monounsaturated compounds and a total loss of activity for the fully saturated C-20 analog of 1-AG. In contrast, shorter fully saturated compounds such as 1-palmitoylglycerol (C-16) and 1-myristoylglycerol (C-14) inhibit MGL (IC_{50} values of 12 and 32 μM, respectively).

Regarding selectivity, most of the compounds in this series inhibit FAAH activity with similar values (IC_{50} = 5.7-23 μM) and as previously observed for MGL, the fully saturated 1-AG analog does not inhibit FAAH activity. In a further attempt to improve the pharmacological profiles of the compounds, additional structural modifications on the fatty acid chain have been examined.[75] In this series of inhibitors, the arachidonoyl side chain of 1-AG has been replaced by cyclooxygenated chains related to prostaglandins (PG) including PGD_2-1G, PGE_2-1G and $PGF_{2\alpha}$-1G.

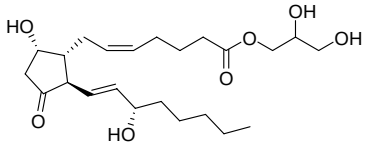

PGD_2-1G

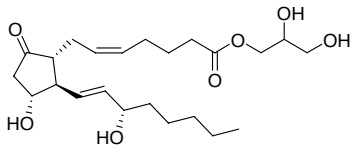

PGE_2-1G

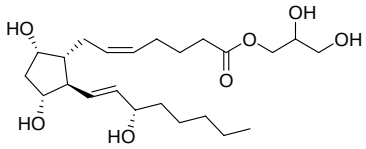

$PGF_{2\alpha}$-1G

However, these compounds showed a very weak effect upon MGL, inhibiting only about the 24-37% of MGL activity at 100 μM of compound. Similarly, the cyclooxygenated analogs of arachidonoylserinol (PGD_2-serinolamide), AEA (PGD_2-ethanolamide) and arachidonic acid (PGD_2) lack of any significant effect on MGL activity.

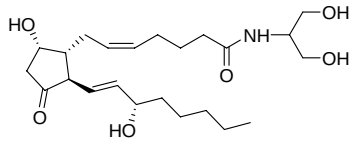

PGD_2-serinolamide

[74] Vandevoorde, S., Saha, B., Mahadevan, A., Razdan, R.K., Pertwee, R.G., Martin, B.R., Fowler, C.J. *Biochem. Biophys. Res. Commun.* 2005, *337*, 104.

[75] Fowler, C.J., Tiger, G. *Biochem. Pharmacol.* 2005, *69*, 1241.

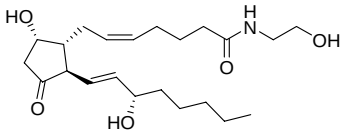

PGD_2-ethanolamide

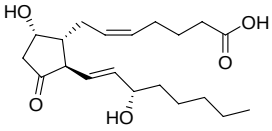

PGD_2

1.3.3. De novo inhibitors

The use of high throughput screening (HTS) techniques has enabled the discovery of MGL inhibitors whose structure do not resemble any endogenous cannabinoid. URB602 was described as the first moderate MGL inhibitor with selectivity vs FAAH [IC_{50} (MGL) = 28-75 μM depending on the source of enzyme].[76]

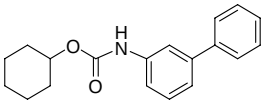

URB602

Recently, JZL184 has been reported as a novel MGL inhibitor.[77] This 4-nitrophenylcarbamate was identified through ABPP techniques as a highly selective and long-lasting MGL inhibitor. On systemic administration, it leads to increased 2-AG levels by around eight times in the brain and CB_1 receptor-mediated hypoalgesic, hypotermic, and locomotor-supressant effects in mice.

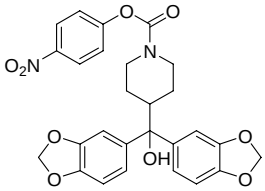

JZL184

This covalent inhibitor exhibits an IC_{50} for MGL of 8 nM, being 4 μM for FAAH. It irreversibly inhibits MGL via carbamoylation of the enzyme's serine nucleophile, maintaining good selectivity for this enzyme across a wide range of central and peripheral tissues. Moreover, it does not inhibit other 40 related serine hydrolases in the mouse brain membrane proteome and does not interact with other components of the ECS such as CB receptors and DAGL-α and –β enzymes.

1.3.4. Inhibitors targeting the essential sulfhydryl group(s) of MGL

Early data on MGL already pointed out the relevance of free thiol groups for the adequate performance of the enzyme based on the inhibitory ability of some general thiol modifiying agents such as *p*-CMB, $HgCl_2$ and NEM (IC_{50} values of 72, 42 and 53 μM, respectively).[55] These data are consistent with the presence of free thiol groups at or close to the catalytic site of the enzyme. Based on this, Saario's laboratory envisioned a rational approach to the development of MGL inhibitors taking advantage of this feature. They designed several maleimide analogs with groups of different size and lipophilicity attached to the nitrogen atom.[66] Maleimide analogs behave as Michael acceptors towards thiol residues of the catalytic site, binding irreversibly to the enzyme. Their SAR study indicates a higher potency of inhibition when lipophilicity and bulkiness of the group attached to nitrogen is increased, resulting in an optimal IC_{50} value when this group is an arachidonyl side chain (*N*-arachidonylmaleimide, NAM, IC_{50} = 140 nM).

[76] Hohmann, A.G., Suplita, R.L., Bolton, N.M., Neely, M.H., Fegley, D., Mangieri, R., Krey, J.F., Walker, J.M., Holmes, P.V., Crystal, J.D., Duranti, A., Tontini, A., Mor, M., Tarzia, G., Piomelli, D. *Nature* 2005, *435*, 1108.

[77] (a) Long, J.Z., Li, W., Booker, L., Burston, J.J., Kinsey, S.G., Schlosburg, J.E., Pavón, F.J., Serrano, A.M., Selley, D.E., Parsons, L.H., Lichtman, A.H., Cravatt, B.F. *Nat. Chem. Biol.* 2009, *5*, 37. (b) Long, J.Z., Nomura, D.K., Cravatt, B.F. *Chem. Biol.* 2009, *16*, 744.

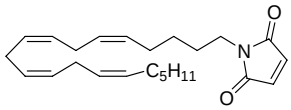

***N*-Arachidonylmaleimide (NAM)**

This trend suggests that the maleimide-sensitive site is located in a hydrophobic region that is likely to be close to the 2-AG binding pocket. Although this study reveals that NAM covalently interacts with C242, more recent studies[78] also observed an effect over C201. The residue 242 is buried in the active site, close to the catalytic serine, and the inhibitory effect upon covalent binding to this residue could be explained by a steric clash between the inhibitor and the natural ligand. On the other hand, C201 is located near the catalytic site, in a loop connecting α5 (A5) and α6 (A6) helices. It constitutes a good candidate for MGL activity regulation because it is accessible from the inside of the catalytic side, being located in the vicinity of the putative exit hole. In this work, SAR and computational studies are combined to characterize the role of cysteine residues and to identify a new class of MGL inhibitors based on the isothiazolone core. They report that the substitution of the *n*-octyl group of octhilinone [IC_{50} (MGL) = 88 nM] with a lipophilic group such as oleoyl chain exhibits the highest inhibitory potency in rat recombinant MGL (IC_{50} = 43 nM). This family of compounds inhibits MGL through a partially reversible mechanism that involves a specific interaction with C208.[78]

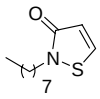

Octhilinone

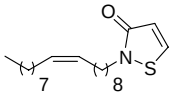

2-[(9*Z*)-octadec-9-enyl]isothiazol-3(2*H*)-one

Recently, through screening of a commercial chemical library, two terpenoids, pristimerin and euphol, have been reported to inhibit MGL with high potency (IC_{50} = 93 and 315 nM respectively).[79] These compounds act as reversible inhibitors and it is suggested that they occupy a common hydrophobic pocket located within the α-helical lid domain of the protein, and each reversibly interacts with one of the two cysteine residues 201 and 208 adjacent to the lid domain.

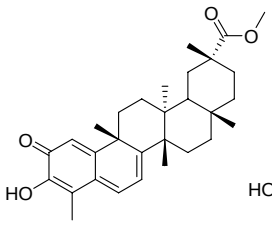

Pristimerin

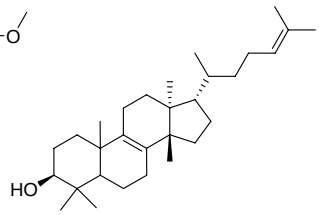

Euphol

1.3.5. Dual MGL/FAAH inhibitors

Pharmacological studies have reported that selective FAAH and MGL inhibitors produce an intriguing subset of the behavioural effects observed with CB_1 direct agonists, such as analgesia in multiple acute and chronic pain models.[80] Selective inhibition of MGL produces CB_1-dependent hypomotility, while FAAH inhibitors have proved inactive in models of drug abuse. These data indicate that selective blockade of FAAH or MGL can dissociate some of the beneficial and undesirable effects of CB_1 activation. In this field, recently, the carbamate JZL195 has been recently described as a dual inhibitor of FAAH/MGL (IC_{50} = 2 and 4 nM, respectively).[81]

[78] King, A.R., Lodola, A., Carmi, C., Fu, J., Mor, M., Piomelli, D. *Br. J. Pharmacol*. 2009, *157*, 974.

[79] King, A.R., Dotsey, E.Y., Lodola, A., Jung, K.M., Ghomian, A., Qiu, Y., Fu, J., Mor, M., Piomelli, D. *Chem. Biol*. 2009, *16*, 1045.

[80] Long, J.Z., Nomura, D.K., Vann, R.E., Walentiny, D.M., Booker, L., Jin, X., Burston, J.J., Sim-Selley, L.J., Lichtman, A.H., Wiley, J.L., Cravatt, B.F. *Proc. Natl. Acad. Sci. USA* 2009, *106*, 20270.

[81] Long, J.Z., Jin, X., Adibekian, A., Li, W., Cravatt, B.F. *J. Med. Chem*. 2010, *53*, 1830.

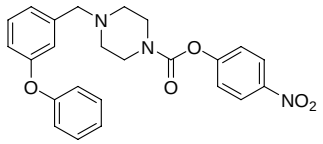

JZL195

This inhibitor shows broad activity in the tetrad test for CB_1 agonism, causing analgesia, hypomotility and catalepsy. Comparison of JZL195 to specific FAAH and MGL inhibitors identifies behavioural processes that are regulated by a single endocannabinoid pathway and, interestingly, those where disruption of both FAAH and MGL produces additive effects that are reversed by a CB_1 antagonist.

1.4. Therapeutic applications of MGL-targeting compounds

In the last years several studies have demonstrated the key physiological roles of 2-AG. Accordingly, the design and synthesis of compounds able to inhibit MGL could offer new perspectives in the understanding and treatment of several disorders. Some of the most promising applications are discussed below.

1.4.1. Neuroprotection and neurodegenerative diseases

Different studies suggest that endocannabinoids are neuroprotective in different *in vivo* and *in vitro* models. They can protect neurons from hypoxic injury, and may represent endogenous neuroprotective molecules in cerebral ischemia.[82] Additionally, levels of endogenous 2-AG were found significantly elevated in the closed head injury model in mice and 2-AG administration produced significant reduction of brain oedema and infarct volume, better clinical recovery, and reduced hippocampal cell death.[83] The protection induced by 2-AG has been attributed to CB_1 activation, since this effect was attenuated by the CB_1 selective antagonist SR141716A and was absent in CB_1(-/-) mice. This mechanism could involve inhibition of intracellular inflammatory signaling pathways.[84] Furthermore, the relation between 2-AG and epilepsy has also received attention, and it has been hypothesized that 2-AG inhibits the depolarization-induced increase in intracellular calcium in NG108-15 cells thereby modulating several neural functions in this cell type.[85] Hence, 2-AG could prevent the excessive excitability that takes place in epilepsy.

Another interesting aspect is the possible implication of 2-AG in neurodegenerative diseases, such as MS. For instance, in areas associated with nerve damage in the MS model of chronic relapsing experimental autoimmune encephalomyelitis (CREAE), increased levels of AEA and 2-AG were detected, suggesting a protective role of these endocannabinoids. In a different animal model of MS, experimental autoimmune encephalomyelitis (EAE), AEA and 2-AG levels were found to be decreased in motor related brain regions (striatum, midbrain).[86] Witting et al.[87] showed that in EAE the protective role of endocannabinoids can be disrupted by the action of interferon-γ (IFN-γ), thus providing additional support

[82] Degn, M., Lambertsen, K.L., Petersen, G., Meldgaard, M., Artmann, A., Clausen, B.H., Hansen, S.H., Finsen, B., Hansen, H.S., Lund, T.M. *J. Neurochem.* 2007, *103*, 1907.

[83] Shohami, E., Mechoulam, R. *Proc. Natl. Acad. Sci. USA* 2006, *103*, 6087.

[84] Panikashvili, D., Mechoulam, R., Beni, S.M., Alexandrovich, A., Shohami, E. *J. Cereb. Blood Flow Metab.* 2005, *25*, 477.

[85] Deshpande, L.S., Blair, R.E., Ziobro, J.M., Sombati, S., Martin, B.R., DeLorenzo, R.J. *Eur. J. Pharmacol.* 2007, *558*, 52.

[86] (a) Baker, D., Pryce, G., Croxford J.L., Brown, P., Pertwee, R.G., Makriyannis, A., Khanolkar, A., Layward, L., Fezza, F., Bisogno, T., Di Marzo, V. *FASEB J.* 2001, *15*, 300. (b) Cabranes, A., Venderova, K., de Lago, E., Fezza, F., Sanchez, A., Mestre, L., Valenti, M., Garcia-Merino, A., Ramos, J. A., Di Marzo, V., Fernandez-Ruiz, J. *Neurobiol. Dis.* 2005, *20*, 207.

[87] Witting, A., Chen, L., Cudaback, E., Striker, A., Walter, L., Rickman, B., Moller, T., Brosnan, C., Stella, N. *Proc. Natl. Acad. Sci. USA* 2006, *103*, 6362.

for the use of an endocannabinoid-based medicine to treat MS.

1.4.2. Feeding Behaviour

Marijuana and its major psychotropic component, THC, were found to stimulate appetite and to increase body weight in wasting syndromes. Additionally, endocannabinoids have been involved in the control of energy balance and food intake and their effects have been described as mainly CB_1–mediated, since they are antagonized by SR141716A.[88] They may also stimulate lipogenesis and fat accumulation.[89] Therefore, endocannabinoids add to the list of the numerous neurotransmitters and neuropeptides involved in the physiological control of appetite and satiety. Interestingly, the neurohormone leptin, which is the main regulator of the hypothalamic orexigenic and anoretic signals, exerts a negative control on the AEA and 2-AG levels. Considering the role played by endocannbinoids in the intricate network that regulates feed control, clearly the manipulation of their levels could offer useful approaches to the treatment of eating disorders as well as metabolic syndromes.[90]

1.4.3. Cancer

The endocannabinoid system is implicated in cancer because it plays a fundamental role in the control of the cell survival/death decision.[91] Although both endocannabinoids, AEA and 2-AG, have been found to inhibit proliferation of certain cancer cell lines, we will focus on the effects of the latter. 2-AG inhibits proliferation of human prostate cancer cell lines.[92] 2-AG has been also involved in cancer cell invasion. Blocking the 2-AG metabolism increases endogenous 2-AG levels, which inhibit invasion of the androgen-independent prostate cancer cells PC-3 and DU-145.[93] These effects have been linked to CB_1 receptor activation. Because prostate cancer has become the most common cancer in men, identifying novel targets and new agents for its treatment has become an imperative issue.

The 2-AG-mediated inhibition of cell proliferation can take place in other types of cancer cell lines such as colorectal carcinomas and C6 glioma cells, and tumors like meningiomas show a massive enhancement in the levels of 2-monoacylglycerols including 2-AG.[94] Therefore, it has been suggested that endocannabinoids could act as endogenous anti-tumour mediators by stimulation of both CB and non-CB receptor-mediated mechanisms.

Supporting a more general role of 2-AG in tumoral processes, it has been recently reported the increased MGL activity in primary tumours and in cancer cell lines classified as highly aggressive.[95] These data indicate that MGL regulates a fatty acid network enriched in oncogenic signalling lipids that promotes cell migration, invasion, survival and *in vivo* tumour growth. Genetic or pharmacological blockade of

[88] Di Marzo, V., Matias, I. *Nat. Neurosci.* 2005, *8*, 585.
[89] Cota, D., Marsicano G., Tschöp, M., Grübler, Y., Flachskamm, C., Schubert, M., Auer, D., Yassouridis, A., Thöne-Reineke, C., Ortmann, S., Tomassoni, F., Cervino, C., Nisoli, E., Linthorst, A.C.E., Pasquali, R., Lutz, B., Stalla, G.K., Pagotto, U. *J. Clin. Invest.* 2003, *112*, 423.
[90] Bellocchio, L., Lafenêtre, P., Cannich, A., Cota, D., Puente, N., Grandes, P., Chaouloff, F., Piazza, P.V., Marsicano, G. *Nat. Neurosci*. 2010, *13*, 281.
[91] (a) López-Rodríguez, M.L., Viso, A., Ortega-Gutiérrez, S., Díaz-Laviada, I. *Mini Rev. Med. Chem*. 2005*, 5*, 97. (b) Pisanti, S., Bifulco, M. *Pharmacol. Res*. 2009, *60*, 107.
[92] Endsley, M.P., Aggarwal, N., Isbell, M.A., Wheelock, C.E., Hammock, B.D., Falck, J.R., Campbell, W.B., Nithipatikom, K. *Int. J. Cancer*. 2007, *121*, 984.
[93] Nithipatikom, K., Endsley, M.P., Isbell, M.A., Falck, J.R., Iwamoto,Y., Hillard, C.J., Campbell, W.B. *Cancer Res*. 2004, *64*, 8826.
[94] (a) Ligresti, A., Bisogno, T., Matias, I., De Petrocellis, L., Cascio, M. C., Cosenza, V., D'argenio, G., Scaglione, G., Bifulco, M., Sorrentini, I., Di Marzo, V. *Gastroenterology* 2003, *125*, 677. (b) Fowler, C.J., Jonsson, K.O., Andersson, A., Juntunen, J., Järvinen, T., Vandevoorde, S., Lambert, D.M., Jerman, J.C., Smart, D. *Biochem. Pharmacol*. 2003, *66*, 757. (c) Petersen, G., Moesgaard, B., Schmid, P.C., Schmid, H.H.O., Broholm, H., Kosteljanetz, M., Hansen, H.S. *J. Neurochem*. 2005, *93*, 299.
[95] Nomura, D.K., Long, J.Z., Niessen, S., Hoover, H.S., Ng, S.W., Cravatt, B.F. *Cell* 2010, *140*, 49.

MGL in these aggressive cells decreases malignant character of these cells.

Considered together, all the above data have raised the view that the inhibitors of 2-AG degradation may open new possibilities in the treatment of these types of cancer.

1.4.4. Other disorders

The brain reward system constitutes another point of interest for endocannabinoids.[96] This result is in agreement with the proposed upregulation of CB_1 receptors in morphine dependence, and it supports the hypothesis that either activators of endocannabinoid synthesis or inhibitors of its degradation may have a therapeutic potential to treat opiate withdrawal symptoms. The profound changes that the ECS undergoes during the different phases of sensitization to morphine in rats provide a possible neurochemical basis for this cross-sensitization between opiates and cannabinoids.[97]

Moreover, 2-AG could play a role in alcohol addiction and in other drug addictions like marijuana, nicotine and cocaine by activation of the same or related reward pathways.[98]

It is known that cannabinoid receptor agonists induce analgesia, although their psychoactive side effects avoid their therapeutic development. Alternatively, inhibiting FAAH and MGL reduce nociception in a variety of nociceptive assays with no or minimal behavioural effects.[99]

Another aspect of interest is the presence of CB_1 receptor and both AEA and 2-AG in ocular tissues. Cannabinoids have shown capacity to reduce the ocular hypertension and, in particular, topical application of AEA was shown to decrease the intraocular pressure in normotensive rabbits. Moreover, topical administration of 2-AG and noladin ether also decreased intraocular pressure in rabbits, reduction that has been attributed to the CB_1 receptor.[100] These effects could be of direct application in glaucoma, disorder characterized by a pathological enhancement of the intraocular pressure. In this regard, the levels of 2-AG and PEA have been found to be significantly decreased in the ciliary body in eyes from patients with glaucoma,[101] further supporting the role of these endogenous compounds in the regulation of intraocular pressure. Finally, it is of note the role of 2-AG in the immune system and in particular its effect on the motility of human natural killer cells. 2-AG induces the migration of KHYG-1 cells (a natural killer leukemia cell line) and human peripheral blood natural killer cells. This migration can be blocked by the presence of the CB_2 antagonist SR144528, and interestingly it does not occur in the case of AEA or THC. Accordingly, it has been suggested that 2-AG could contribute to the host-defense mechanism against infectious viruses and tumour cells.[102]

In this context, the development of new potent and selective inhibitors for MGL constitutes an important part of the study, validation and exploitation of this enzyme as therapeutic target. It is paramount to

[96] Navarrete, M., Araque, A. *Neuron* 2008, *57*, 883.
[97] Viganò, D., Valenti, M., Cascio, M.G., Di Marzo, V., Parolaro, D., Rubino, T. *Eur. J. Neurosci*. 2004, *20*, 1849.
[98] Schlosburg, J.E., Carlson, B.L., Ramesh, D., Abdullah, R.A., Long, J.Z., Cravatt, B.F., Lichtman, A.H. *AAPS J*. 2009, *11*, 342.
[99] (a) Naidu, P.S., Kinsey, S.G., Guo, T., Cravatt, B.F., Lichtman, A.H. *J. Pharmacol. Exp. Ther*. 2010, *334*, 182. (b) Kinsey, S.G., Long, J.Z., O'Neal, S.T., Abdullah, R.A., Poklis, J.L., Boger, D.L., Cravatt, B.F., Lichtman, A.H. *J. Pharmacol. Exp. Ther*. 2009, *330*, 902.

[100] (a) Laine, K., Jarvinen, K., Mechoulam, R., Breuer, A., Jarvinen, T. *Invest. Ophthalmol. Vis. Sci.* 2002, *43*, 3216. (b) Nucci, C., Bari, M., Spanò, A., Corasaniti, M., Bagetta, G., Maccarrone, M., Morrone, L.A. *Prog. Brain Res*. 2008, *173*, 451.
[101] Chen, J., Matias, I., Dinh, T., Lu, T., Venezia, S., Nieves, A., Woodward, D. F., Di Marzo, V. *Biochem. Biophys. Res. Commun*. 2005, *330*, 1062.
[102] (a) Kishimoto, S., Muramatsu, M., Gokoh, M., Oka, S., Waku, K., Sugiura, T. *J. Biochem. (Tokyo)* 2005, *137*, 217. (b) Pandey, R., Mousawy, K., Nagarkatti, M., Nagarkatti, P. *Pharmacol. Res*. 2009, *60*, 85.

establish whether these enzyme(s) are susceptible of inhibition without compromising the activity of other enzymes closely related. Additionally, it should be necessary to ascertain, if more than one MGL activity exits, whether the inhibition of only one would be therapeutically relevant for increasing 2-AG levels. Finally it is important to study the importance of simultaneously increase AEA and 2-AG levels with dual inhibitors.

2. OBJECTIVES

At the beginning of this project, information about MGL was very scarce and almost no inhibitors had been identified. In this context, our main objective was to unravel the structural requirements involved in the recognition of substrates for MGL. This systematic SAR study should aid the development of new inhibitors that enable validation of MGL as a therapeutic target.

The achievement of this goal involves the following steps:

1. Design of new MGL inhibitors.
2. Synthesis of new derivatives with general structure **I**, which comprises derivatives of fatty acids **Ia** and aromatic compounds **Ib-d**.
3. Determination of the ability of compounds **Ia-d** to inhibit 2-AG and AEA hydrolysis.
4. SAR study.
5. Study of the different 2-AG hydrolyzing activities in distinct brain cell types using selected inhibitors.
6. Determination of the neuroprotective effect of selected inhibitors in order to confirm the interest of MGL as therapeutic target.
7. Study the inhibition mechanism of optimal compounds.

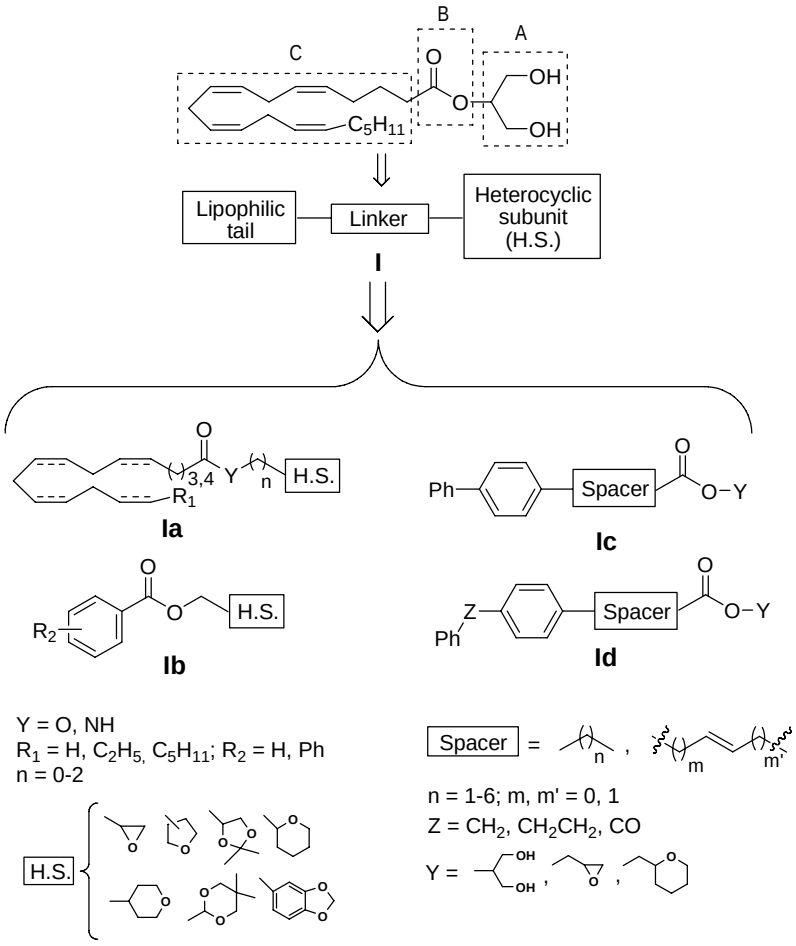

3. RESULTS AND DISCUSSION

In the inception of this project, information about MGL was very scarce. Its 3D structure had not been elucidated, no potent and/or specific MGL inhibitors were known and no systematic SAR studies had been carried out. In this context, we based our initial design on the endogenous substrate of MGL, the endocannabinoid 2-AG. The synthesis of the designed compounds and their biological evaluation in terms of ability to inhibit 2-AG hydrolysis (as well as to block FAAH activity) allowed us to carry out the first systematic SAR study in order to unravel the structural requirements involved in 2-AG hydrolysis inhibition.[103]

Further modification of the initial hits identified in this work using iterative SAR studies and docking models based on the recently described MGL 3D structure[59,60] has enabled us to optimize the initial series and to identify structurally new inhibitors of 2-AG hydrolysis with IC_{50} values in the submicromolar range.[104] One interesting question arising from these studies was to establish whether the ability of the compounds to inhibit 2-AG hydrolysis was due to their capacity to inhibit directly MGL or was related with the inhibition of other 2-AG hydrolyzing activities. This discrimination is relevant because although the 85% of brain membrane 2-AG hydrolyzing activity has been ascribed to MGL,[50] other hydrolases also exist and their importance in different cells or tissues is yet to be determined. Therefore, those compounds with the best profiles to inhibit cytosolic 2-AG degradation have been selected and further assessed for their ability to block 2-AG hydrolysis in brain membrane fractions and in neurons as well as for their capacity to directly target the human recombinant MGL (hrMGL). Interestingly, a variety of *in vitro* profiles have been obtained. Therefore, this subset of compounds constitutes a good toolbox to identify other 2-AG hydrolyzing activities and to start to validate MGL as a therapeutic target. In this context, the synthesized inhibitors[103,104] have allowed us to identify a new MGL activity expressed in microglia[105] and to study 2-AG hydrolysis in neurons.[106] Finally, preliminary *in vitro* neuroprotection experiments have suggested that MGL inhibitors are neuroprotective. This result supports the therapeutic validation of MGL and led us to initiate a series of mechanistical studies with the most promising compound in order to obtain deeper insights about its inhibition mode.[104] This information is critical to establish the potential of this inhibitor for its use as a tool in *in vitro* models.

3.1. Design and synthesis of compounds of general structure Ia,b

As indicated above, in the absence of any potent inhibitor of 2-AG hydrolysis that could be used as initial hit and without the 3D structure of MGL, we took as the starting point the structure of its endogenous substrate, 2-AG. Accordingly, we designed a series of compounds Ia,b wherein the glycerol moiety was substituted by different heterocyclic subunits with the objective of introducing structural variations that mimicked the glycerol fragment (A). Additionally, we have studied the effect of modifications in the fatty acid chain (C) as well as in the ester group (B) (Figure 7, page 30).

[103] Cisneros, J.A., Vandevoorde, S., Ortega-Gutiérrez, S., Paris, C., Fowler, C.J., López-Rodríguez, M.L. *J. Med. Chem.* 2007, *50*, 5012.
[104] Cisneros, J.A. *et al. J. Med. Chem*. In preparation.
[105] Muccioli, G.G., Xu, C., Odah, E., Cudaback, E., Cisneros, J.A., Lambert, D.M., López-Rodríguez, M.L., Bajjalieh, S., Stella, N. *J. Neurosci.* 2007, *27*, 2883.
[106] Marrs, W.R., Horne, E.A., Ortega-Gutiérrez, S., Cisneros, J.A., Xu, C., Lin, Y.H., Muccioli, G.G., López-Rodríguez, M.L., Stella, N. *J. Biol. Chem.* 2010, submitted.

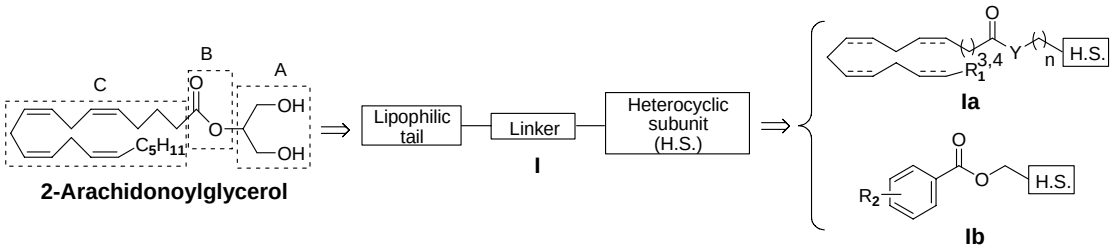

Figure 7.

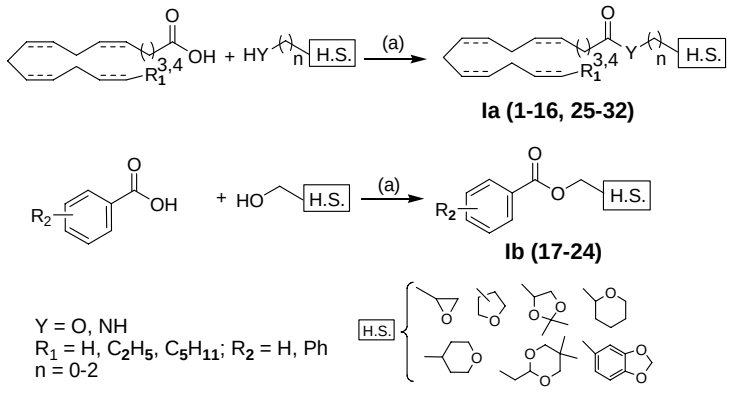

Reagents and conditions: (a) DCC, DMAP, CH_2Cl_2, Ar, rt

Scheme 1.

The synthesis of esters and amides Ia,b is indicated in Scheme 1. These compounds were prepared by condensation between the adequate carboxylic acid and the corresponding alcohol or amine, in the presence of dicyclohexylcarbodiimide (DCC) and catalytic amounts of *N*,*N*-dimethyl-4-aminopyridine (DMAP).

3.2. SAR study for monoacylglycerol hydrolysis inhibition for compounds Ia,b

The synthesized compounds have been assessed for their ability to inhibit the hydrolysis of 2-AG in cytosolic fractions, using 2-OG as a surrogate. Effects upon the FAAH-catalysed hydrolysis of AEA by the membrane fractions were also determined in order to identify compounds that could selectively block monoacylglycerol hydrolysis by the brain without concomitant effects upon AEA hydrolysis. For consistency of notation, throughout the tables, IC_{50} and pI_{50} values for 2-OG or AEA hydrolysis inhibition are denoted as 2-OG and AEA, respectively. However, in some cases 100% inhibition was not seen at the highest dose tested. This type of situation is indicated throughout the tables by adding the percentage of maximum inhibition value obtained for the highest concentration tested (100 μM).

3.2.1. Influence of the heterocyclic moiety (1-8)

Compounds 1-8 (Table 1) are able to inhibit the cytosolic 2-OG hydrolysing activity with IC_{50} values in the low micromolar range (4.5-45 μM; Table 1, page 31). The best profiles were obtained for compounds 1 and 5. Oxiran-2-ylmethyl (5*Z*,8*Z*,11*Z*,14*Z*)-icosa-

5,8,11,14-tetraenoate (1) resulted the most potent derivative towards 2-OG hydrolysis [IC_{50} (1) = 4.5 μM] whilst tetrahydro-2*H*-pyran-2-ylmethyl (5*Z*,8*Z*,11*Z*,14*Z*)-icosa-5,8,11,14-tetraenoate (5), with IC_{50} (2-OG) = 5.6 μM, was the most selective compound *vs* FAAH with almost ten fold selectivity [IC_{50} (FAAH) = 51 μM]. Interestingly, for 1-8, loss of affinity towards the 2-OG hydrolytic activity correlates with relative increases in FAAH affinity, as occurs with 3 [IC_{50} (2-OG) = 43 μM and IC_{50} (FAAH) = 11 μM] and 6 [IC_{50} (2-OG) = 30 μM and IC_{50} (FAAH) = 5.3 μM]. Finally, the decrease in potency observed for compound 8 in both assays suggests the negative influence of increasing the size of the heterocyclic moiety.

Table 1. Influence of the heterocyclic subunit (H.S.)

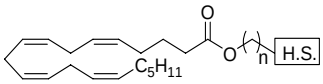

Cpd	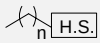	Hydrolysis inhibition pI_{50} [IC_{50}, μM][a,b]	
		2-OG	AEA
1		5.35±0.05 [4.5]	4.91±0.05 [12]
2		4.67±0.04 [21]	4.48±0.06 [33]
3		4.37±0.06 [43]	4.98±0.08 [11, 78%][a]
4		4.3±0.1 [45]	4.0±0.1 [98]
5		5.26±0.04 [5.6]	4.30±0.06 [51]
6		4.5±0.1 [30, 62%][a]	5.3±0.2 [5.3, 63%][a]
7	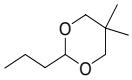	4.57±0.07 [27]	4.68±0.05 [21]
8	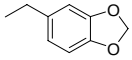	4.35±0.07 [45]	4.0±0.2 [91]

Throughout the Tables, the pI_{50} values (-log[IC_{50}]) are expressed as mean ± s.e.m. The IC_{50} values derived from the mean pI_{50} values are given in brackets. [a]When the data was better fitted to an inhibition curve with a residual activity, the maximum inhibition is given and the data expressed as [IC_{50}, percentage of maximum inhibition]. [b]When the inhibitable component was less than 50%, at the highest concentration tested (100 μM), the pI_{50} values have been indicated as <4 (i.e. IC_{50} value >100 μM), and the percentage of inhibition attained at 100 μM has been indicated between parentheses as mean ± s.e.m.

3.2.2. Modifications on the lipophilic moiety (9-24)

For the compounds with the best profiles of potency and selectivity (1 and 5), we replaced the arachidonic acid moiety for different fatty acid chains keeping constant the heterocyclic subunit (Table 2, compounds 9-16). However, none of the modifications yielded any appreciable improvement either in potency or selectivity. With respect to the oxirane derivatives 9-11, decrease in the number of double bonds involves a concomitant reduction in the potency as inhibitors of 2-OG hydrolysis, ranging from the initial value of 4.5 μM of the arachidonic acid derivative 1 to no inhibition at 100 μM for compound 11, the oleic acid analog.

Table 2. Influence of the fatty acid chain

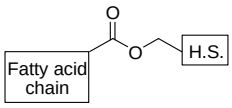

Cpd	Fatty acid chain	H.S.	Hydrolysis inhibition pI_{50} [IC_{50}, μM]	
			2-OG	AEA
1	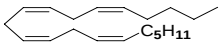		5.35±0.05 [4.5]	4.91±0.05 [12]
9	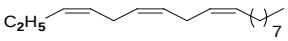		4.97±0.05 [11]	5.80±0.05 [1.6]
10	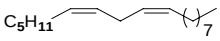		4.64±0.05 [23]	5.00±0.03 [10, 94%][a]
11	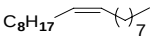		<4 (6±4%)[b]	4.96±0.05 [11]
12	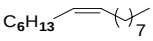		4.87±0.08 [13, 84%][a]	5.09±0.07 [8.2]
5			5.26±0.04 [5.6]	4.30±0.06 [51]
13	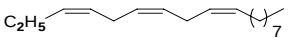		4.64±0.03 [23]	4.73±0.02 [19]
14	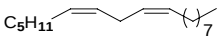		4.1±0.1 [73]	5.13±0.04 [7.5]
15	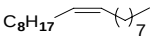		<4 (12±7%)[b]	4.53±0.05 [29]
16	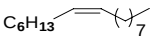		<4 (42±6%)[b]	5.0±0.1 [10, 82%][a]

[a,b] For explanation of data, see footnote for Table 1.

The same tendency is observed for the tetrahydropyran derivatives, where the progressive elimination of unsaturations brings about a parallel decrease in inhibitory potency towards 2-OG hydrolysis, as seen for compounds **13**-**15** (Table 2), which IC_{50} values range from 23 μM for compound **13** to a lack of activity of compound **15** (12% inhibition at 100 μM). In both cases, for oxirane and tetrahydropyran derivatives, FAAH inhibition is less sensitive to the variations in the fatty acid chain, showing even slight increases in potency. With respect to chain length of the monounsaturated compounds, shortening of the chain from the oleic acid (C-18) derivatives **11** and **15** to their corresponding palmitoleic (C-16) derivatives **12** and **16** improved the affinity of the compounds towards 2-OG hydrolysis. Thus, **12** inhibited 2-OG hydrolysis with an IC_{50} value of 13 μM whereas **11** was inactive. Similarly, in the tetyrahydropyran series the maximum observed inhibition values were 42% (**16**) *vs* 12% (for **15**). Since none of the acyl side chains gave better results than arachidonic acid, next we tried to restrict the flexible conformation of this chain with the isosteric but more rigid core of biphenyl group. Thus, we synthesized compounds **17**-**22** (Table 3). Unfortunately, none of the relative orientations tested (*ortho*, *meta* or *para*-positions) resulted in any appreciable inhibition of 2-OG hydrolytic activitiy, showing very low maximum inhibition values between 29%-43% at 100 μM concentration. To rule out the existence of steric factors that could hinder the binding in the pocket of the enzyme(s), we eliminated one of the phenyl rings (compounds **23** and **24**). Nonetheless, the inhibitory potency remained low, with little or no inhibition being found for compound **23**, and a partial, albeit potent, inhibition of 2-OG hydrolysis for the tetrahydropyran derivative **24**.

Table 3. Influence of phenyl and biphenyl groups

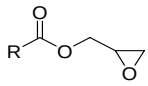

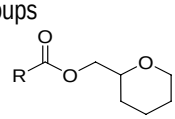

Cpd	R	Hydrolysis inhibition pI_{50} [IC_{50}, μM]		Cpd	R	Hydrolysis inhibition pI_{50} [IC_{50}, μM]	
		2-OG	AEA			2-OG	AEA
17	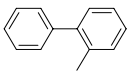	<4 (29±3%)[b]	<4 (5±7%)[b]	20	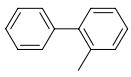	<4 (38±3%)[b]	4.37±0.09 [43]
18	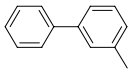	<4 (40±1%)[b]	4.22±0.04 [61]	21	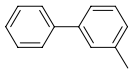	<4 (36±3%)[b]	4.75±0.04 [18]
19	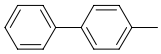	<4 (43±2%)[b]	4.45±0.04 [35]	22	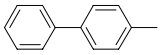	<4 (43±7%)[b]	4.49±0.04 [32]
23		<4 (14±5%)[b]	<4 (19±4%)[b]	24		5.5±0.2 [3, 53%][a]	4.28±0.05 [53]

[a,b] For explanation of data, see footnote for Table 1.

3.2.3. Influence of the ester group (25, 26)

Next, we have studied the influence of the ester linkage by substitution for an isosteric amide group (Table 4). In general, substitution of ester group by the amide did not improve neither potency nor selectivity in any consistent manner. Thus, whilst there was no remarkable difference in the potencies for the compounds 25 and 2 (IC_{50} values of 34 and 21 μM, respectively), amide 26 was slightly more potent as an inhibitor of 2-OG hydrolysis compared to its corresponding ester 4 [IC_{50} values of 15 μM (albeit not with complete inhibition) and 45 μM, respectively]. No large changes in potency for FAAH inhibition were seen.

3.2.4. Influence of the stereogenic center (27-32)

We have also studied the influence of the stereogenic center in the heterocyclic subunit for some of the representative compounds (Table 5, page 35). The stereogenic center does not exert a great influence on inhibition of 2-OG hydrolysis, as seen in compounds 27 and 28, with IC_{50} values of 4.5 μM (racemic 1), 6.3 μM (*R*-enantiomer 27) and 8.0 μM (*S*-enantiomer 28). Additional examples with larger oxygenated cycles (29-32) did not suggest any consistent trend. For example, the *R*-enantiomer 29 is more potent than its *S*-counterpart 30 [IC_{50} (29) = 60 μM and maximal inhibition of 100% *vs* IC_{50} (30) >100 μM and maximal inhibition of 46%] whereas the *S* enantiomer 32 is more potent than the *R*-derivative 31 [IC_{50} (32) = 25 μM and a maximum inhibition of 100% *vs* IC_{50} (31) = 3.5 μM corresponding to a maximum inhibition value of 59%].

Table 4. Influence of the ester group

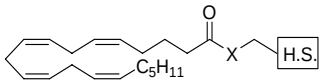

Cpd	H.S.	X	Hydrolysis inhibition pI_{50} [IC_{50}, μM] 2-OG	AEA	Cpd	H.S.	X	Hydrolysis inhibition pI_{50} [IC_{50}, μM] 2-OG	AEA
2		O	4.67±0.04 [21]	4.48±0.06 [33]	4		O	4.3±0.1 [45]	4.0±0.1 [98]
25		NH	4.47±0.06 [34]	4.25±0.04 [56]	26		NH	4.8±0.1 [15, 71%][a]	4.05±0.05 [90]

[a] For explanation of data, see footnote for Table 1.

Table 5. Influence of the stereogenic center

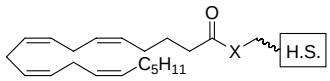

Cpd	H. S.	X	Hydrolysis inhibition pI_{50} [IC_{50}, μM] 2-OG	AEA	Cpd	H. S.	X	Hydrolysis inhibition pI_{50} [IC_{50}, μM] 2-OG	AEA
1		O	5.35±0.05 [4.5]	4.91±0.05 [12]	25		NH	4.47±0.06 [34]	4.25±0.04 [56]
27			5.2±0.1 [6.3, 68%][a]	5.22±0.04 [6.0]					
28			5.1±0.1 [8, 69%][a]	4.93±0.04 [12]	31			5.5±0.2 [3.5, 59%][a]	4.16±0.02 [69]
4			4.3±0.1 [45]	4.0±0.1 [98]					
29		O	4.22±0.09 [60]	4.55±0.06 [28]	32			4.59±0.05 [25]	4.01±0.06 [99]
30			<4 (46±3%)[b]	4.76±0.05 [17]					

[a,b] For explanation of data, see footnote for Table 1.

3.3. Design and synthesis of compounds of general structure Ic,d

The best compounds identified in this first series are the derivatives 1 and 5 with an IC_{50} value for 2-OG hydrolysis inhibition of 4.5 μM and 5.6 μM, respectively. These two derivatives still conserve the arachidonic acid chain as hydrophobic group. However, this fatty acid moiety could be prone to oxidation. In addition, the presence of arachidonic acid can decrease the selectivity of the compounds for a given target since arachidonic acid is a key metabolite in several pathways and therefore can be recognized by different enzymes, including an assortment of lipases and cyclooxygenases.[107] Hence, we sought to replace the arachidonic acid moiety with a suitable bioisostere. Optimally, the selected group should be more stable than the fatty acid and chemically versatile to enable structure exploration. The biphenyl group has been suggested[108] as an isostere of arachidonic acid, but our previous attempts of introducing this moiety (series Ib, compounds 17-22) were not successful. However, taking a closer look to the arachidonic acid structure, there are three methylenic units between its carbonyl

[107] Needleman, P., Turk, J., Jakschik, B.A., Morrison, A.R., Lefkowith, J.B. *Annu. Rev. Biochem*. 1986, *55*, 69.
[108] Tarzia, G., Duranti, A., Tontini, A., Piersanti, G., Mor, M., Rivara, S., Plazzi, P.V., Park, C., Kathuria, S., Piomelli, D. *J. Med. Chem.* 2003, *46*, 2352.

group and the first insaturation. This spacer was not present in compounds 17-22, so we envisioned the possibility of introducing spacers between the carbonyl and the biphenyl groups or between the two benzene rings. In order to support this hypothesis, and taking advantage of the 3D structure of MGL, recently released,[59,60] we carried out docking studies of compound 19 in complex with MGL. Models were constructed using the crystal structure of the human MGL (PDB code 3JW8[60]) and the GLIDE software. Figure 8A shows the computational model of the complex between inactive compound 19 and MGL. In this model the biphenyl ring cannot interact simultaneously with two important zones in the enzyme: the catalytic triad (S132, H279 and D249) and the hydrophobic pocket defined by the side chains of residues A174, L186 and L224. The incorporation of a spacer with five methylenic units between the carbonyl group and the first benzene ring (Figure 8B) or one methylene between the two benzene rings and a spacer of three methylenes between the carbonyl group and the first phenyl ring (Figure 8C) allows for the favorable hydrophobic interactions of the aromatic rings of the compounds and the hydrophobic pocket while keeping the carbonyl group at the adequate distance and orientation to be attacked by the catalytic serine. Accordingly to this computational model, we designed two new series of derivatives Ic and Id where the lipophilic moiety has been substituted by biphenyl, 4-benzylphenyl (Z = CH_2), 4-phenylethylphenyl (Z = CH_2CH_2) and 4-benzoylphenyl (Z = CO) groups (Figure 9, page 37).

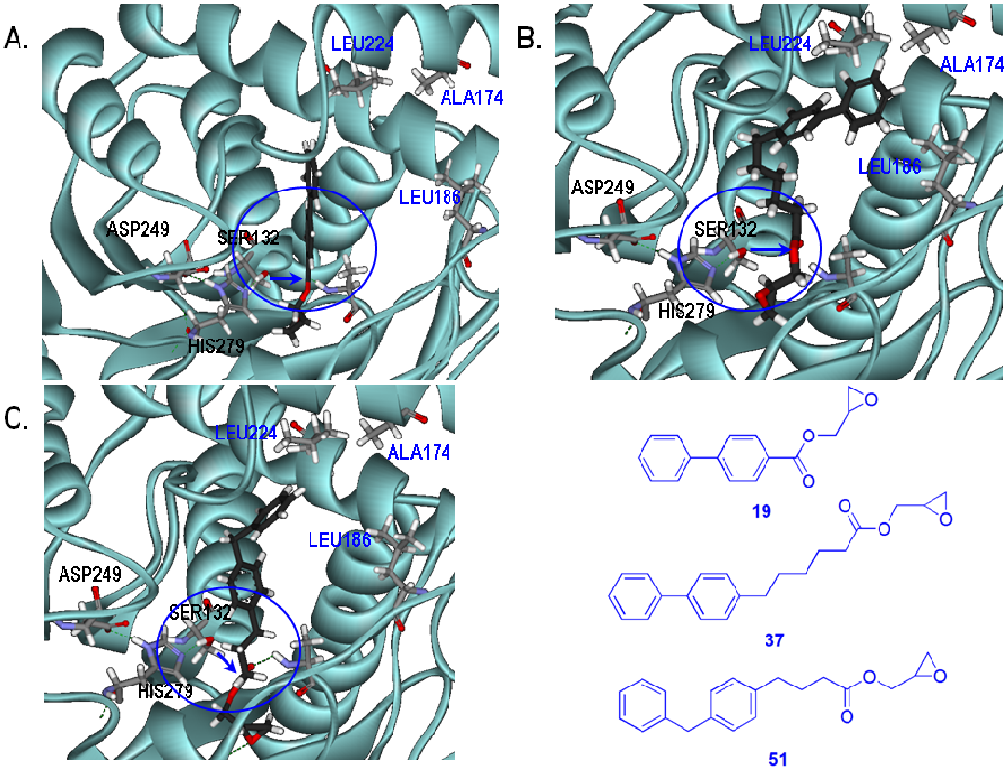

Figure 8. Computational models of the complexes between compounds 19 (A), 37 (B), and 51 (C) and MGL (PDB code 3JW8)

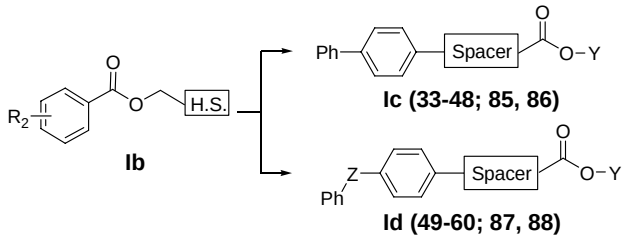

Figure 9.

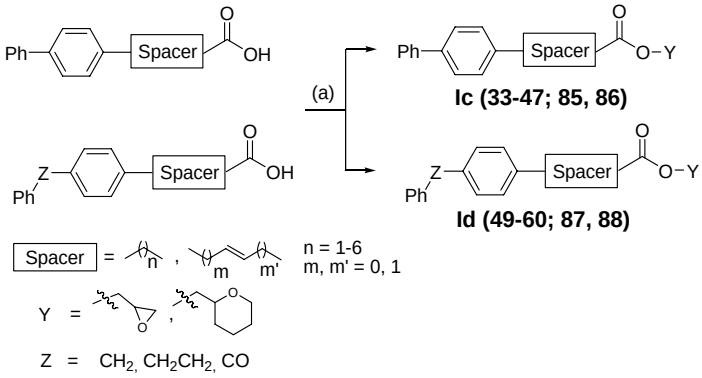

Reagents and conditions: (a) HO−Y, DCC, DMAP, CH_2Cl_2, Ar, rt

Scheme 2.

Compounds 33-60 and 85-88 have been synthesized through the condensation between the adequate carboxylic acid and the corresponding alcohol in the presence of DCC and catalytic amounts of DMAP (Scheme 2) except for compound 48, which has been prepared by Wittig reaction between tetrahydro-2*H*-pyran-2-ylmethyl (triphenylphosphoranylidene)acetate and (1,1'-biphenyl-4-yl)acetaldehyde (Scheme 8, page 39).

This general route envisioned for compounds Ic,d made necessary the previous preparation of the non-commercial 1,1'-biphenyl-4-yl-, 4-benzoylphenyl- and 4-benzylphenyl carboxylic acids.

3.3.1. Synthesis of 1,1'-biphenyl-4-yl carboxylic acids 61-66

Intermediates 61-65 were obtained either by catalytic hydrogenation of the corresponding precursor (carboxylic acid 61) or Friedel-Crafts acylation (compounds 62-65) between biphenyl and the corresponding anhydride, followed by reduction with $Zn/HgCl_2$ (Scheme 3).

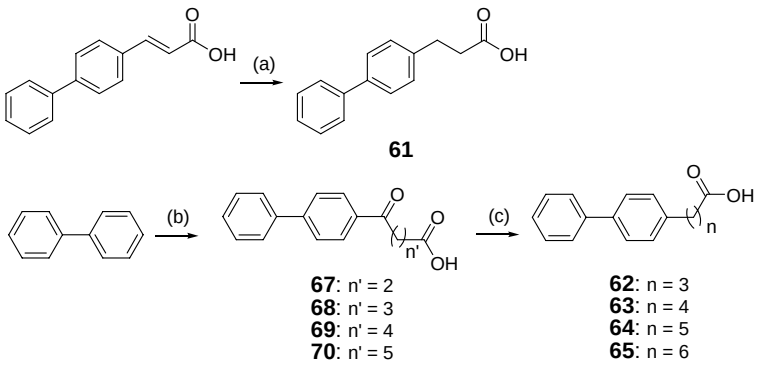

Reagents and conditions: (a) H_2, Pd/C, rt, 2h; (b)  , $AlCl_3$, nitrobenzene, rt, 16h; (c) $Zn/HgCl_2$, H_2O, HCl, Δ, 24h

Scheme 3.

Anhydrides of hexanedioic (71) and heptanedioic (72) carboxylic acids were prepared by refluxing them in acetic anhydride (Scheme 4).

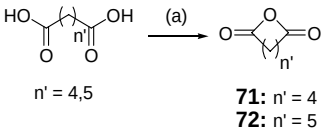

Reagents and conditions: (a) $(CH_3CO)_2O$, Δ, 2h

Scheme 4.

Finally, unsaturated acid 66 was synthesized through the sequence of reactions indicated in Scheme 5. Methyl esterification of (1,1'-biphenyl-4-yl)acetic acid followed by reduction with diisobutylaluminium hydride (DIBALH) yielded the corresponding aldehyde, which, through Wittig reaction with methyl (triphenylphosphoranylidene)acetate afforded acid 66 after hydrolysis of the ester group and isomerization of the double bond promoted by base treatment.

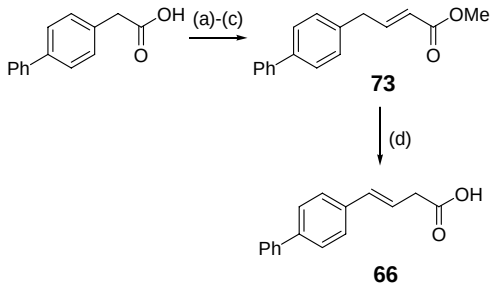

Reagents and conditions: (a) MeOH, $SOCl_2$, Δ, 2h; (b) DIBALH, -78 ºC, 2h; (c) $Ph_3P{=}CHCOOCH_3$, toluene, Δ, 1h; (d) 2M aq NaOH, 60 ºC, 1h

Scheme 5.

3.3.2. Synthesis of 4-benzoylphenyl carboxylic acids 74 and 75

Intermediate (4-benzoylphenyl)acetic acid 74 was prepared following the sequence of reactions previously described[109] starting form *p*-methylbenzophenone. Bromination of the benzylic methyl group with *N*-bromosuccinimide (NBS) followed by substitution with sodium cyanide and basic hydrolysis of the resulting nitrile afforded the acid 74 in good yield (Scheme 6, page 39). 3-(4-Benzoylphenyl)propanoic acid 75 was prepared by Friedel-Crafts acylation of 3-

[109] Zderic, J., Kubitschek, M.M, Bonner, W. *J. Org. Chem.* 1961, *26*, 1635.

phenylpropanoic acid methyl ester with benzoyl chloride in the presence of aluminium trichloride and subsequent saponification of the methyl ester.

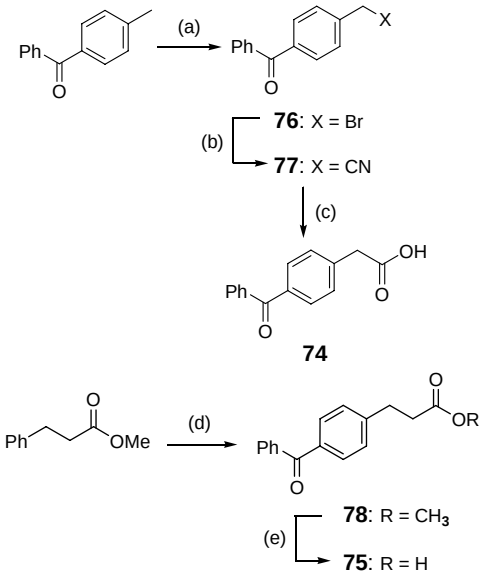

Reagents and conditions: (a) NBS, CCl_4, Δ, 4h; (b) NaCN, dioxane/H_2O, Δ, 2h; (c) 40% NaOH/EtOH, Δ, 2h; (d) PhCOCl, $AlCl_3$, nitrobenzene, rt, 16h; (e) 6M aq NaOH, Δ, 4h

Scheme 6.

3.3.3. Synthesis of 4-benzylphenyl carboxylic acids 79-81

(4-Benzylphenyl)acetic and -propanoic acids (79 and 80, respectively) were obtained by reduction of their corresponding 4-benzoylphenyl carboxylic acids 74 and 75, previously synthesized, in presence of potassium hydroxide and hydrazine (Scheme 7), whereas Friedel-Crafts acylation of benzylbenzene with succinic anhydride followed by reduction of the carbonyl group of the intermediate 82 yielded 4-(4-benzylphenyl)butanoic acid 81.

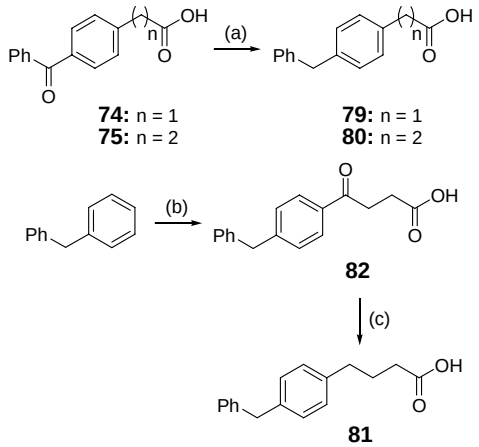

Reagents and conditions: (a) KOH, NH_2NH_2, ethylenglycol, 110ºC, 2h → 180ºC, 20h; (b) Succinic anhydride, $AlCl_3$, nitrobenzene, rt, 16h; (c) $Zn/HgCl_2$, H_2O, Δ, 24h

Scheme 7.

3.3.4. Synthesis of derivative 48

Final compound 48 has been prepared through Wittig reaction between the adequate (triphenylphosphoranylidene)acetate (83) previously synthesized and (1,1'-biphenyl-4-yl)acetaldehyde (Scheme 8).

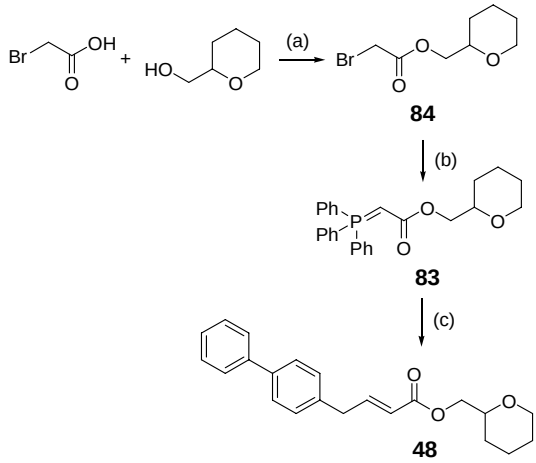

Reagents and conditions: (a) DCC, DMAP, CH_2Cl_2, Ar, rt, 6h; (b) PPh_3, CH_2Cl_2, rt, 3h; (c) (1,1'-biphenyl-4-yl)acetaldehyde, toluene, Δ, 30 min

Scheme 8.

3.4. SAR study for monoacylglycerol hydrolysis inhibition for compounds Ic,d

All synthesized final compounds have been assessed for their ability to inhibit 2-AG and AEA hydrolysis under the same conditions as those previously indicated for series Ia,b (see 3.2., page 30).

3.4.1. Influence of the spacer in the biphenyl derivatives (33-48)

First, we analyzed the effect of increasing the length of the spacer in the biphenyl derivatives (Table 6). For the oxirane esters 33-38, increasing the length of the methylenic spacer enhances the inhibitory activity of the compounds, from IC_{50} values greater than 100 μM (compounds 33-35) to values of 7.9 and 4.5 μM for spacers of 4 and 5 methylenic units, respectively (compounds 36 and 37). Further elongation decreases inhibition of 2-OG hydrolysis, as shown by derivative 38 (IC_{50} > 100 μM). However, regarding FAAH, the trend is the opposite, being the shortest spacers (n = 1-3, compounds 33-35) the ones that yielded the lowest IC_{50} values (0.59, 1.2 and 0.94 μM, respectively).

When the heterocyclic subunit is a tetrahydropyran ring, no significant inhibition values of 2-OG hydrolysis blockade were observed for any of the synthesized compounds [39-44, IC_{50} (2-OG) > 100 μM]. These derivatives, nonetheless, show a moderate potency as FAAH inhibitors, with IC_{50} values ranging from 3.9 μM (compound 44) to 20 μM (compound 42).

Table 6. Influence of the length of the spacer

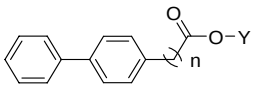

Cpd	Y	n	Hydrolysis inhibition pI_{50} [IC_{50}, μM]		Cpd	Y	n	Hydrolysis inhibition pI_{50} [IC_{50}, μM]	
			2-OG	AEA				2-OG	AEA
33		1	<4 (44±3%)[b]	6.23±0.02 [0.59]	39		1	<4 (33±2%)[b]	4.80±0.05 [16]
34		2	<4 (25±2%)[b]	5.94±0.03 [1.2]	40		2	<4 (50±2%)[b]	4.82±0.04 [15]
35		3	<4 (46±3%)[b]	6.03±0.03 [0.94]	41		3	<4 (9±3%)[b]	4.94±0.04 [12]
36		4	5.10±0.10 [7.9]	5.33±0.03 [4.6]	42		4	<4 (13±7%)[b]	4.70±0.05 [20, 95%][a]
37		5	5.35±0.05 [4.5]	5.29±0.03 [5.1]	43		5	<4 (27±2%)[b]	4.94±0.05 [12]
38		6	<4 (14±4%)[b]	5.50±0.03 [3.2]	44		6	<4 (53±2%)[b]	5.41±0.07 [3.9]

[a,b] For explanation of data, see footnote for Table 1.

Next, we studied whether the presence of one insaturation in the spacer could be favorable for the inhibition of 2-AG and AEA hydrolysis (Table 7). However, none of the synthesized compounds (45-48) regardless the presence of oxirane or tetrahydropyran as heterocyclic subunit showed any significant capacity to block 2-OG hydrolysis. Only derivative 45 showed a moderate activity towards FAAH inhibition with an IC_{50} value of 3.8 μM. Therefore, among all these derivatives 33-48, compounds 36 and 37 are the most potent inhibitors of the series, deserving special attention derivative 37, which is as potent as initial 1 to inhibit 2-OG hydrolysis (IC_{50} = 4.5 μM) but lacks the arachidonic acid chain in its structure.

3.4.2. Modifications in the biphenyl moiety (49-60)

Taking into account the previous results, we also studied the possibility of replacing the biphenyl moiety for two benzene rings separated by different spacers (one or two methylenic units or a carbonyl group) and decreasing the length chain that separates the hydrophobic moiety and the heterocyclic subunit. The introduction of flexibility between the two benzene rings could favor the interaction with the enzyme since docking studies indicated that this type of compounds was able to recognize MGL (Figure 8, page 36). Therefore, we studied the influence of different spacers between the two benzene rings and between the lipophilic moiety and the heterocyclic subunit (Table 8, page 42) in compounds 49-56. For oxirane derivatives, the presence of one methylenic unit between both benzene rings allowed to obtain good inhibition values for monoacylglycerol hydrolysis with IC_{50} values between 8 and 19 μM for compounds 49, 50 and 51, being the best inhibitor the derivative with one methylenic unit between both rings and one methylenic unit between the lipophilic moiety and the carbonyl group [compound 49, IC_{50} (2-OG) = 8 μM].

Table 7. Influence of unsaturation in the spacer

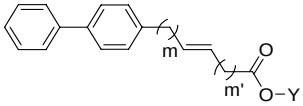

Cpd	m	m'	Y	Hydrolysis inhibition pI_{50} [IC_{50}, μM]	
				2-OG	AEA
45	0	0		<4 (4±1%)[b]	5.42±0.12 [3.8, 92%][a]
46	0	0		<4 (6±2%)[b]	<4 (39±5%)[b]
47	0	1		<4 (34±7%)[b]	<4 (72±3%)[b]
48	1	0		<4 (19±9%)[b]	<4 (57±5%)[b]

[a,b] For explanation of data, see footnote for Table 1.

The increase of the length of the linker between the two benzene rings to two methylenic units abolished all activity, as shown by compound **52**, where only 18% inhibition at the maximal concentration tested was observed. Regarding the tetrahydropyran derivatives, none of the modifications yielded significant inhibition values for 2-OG hydrolysis.

With respect to FAAH inhibition, in general, all these compounds were able to inhibit AEA hydrolysis with moderate IC_{50} values between 2.3 and 37 μM with the exception of **55**, which turned out to be inactive (IC_{50} > 100 μM).

Given that the best results have been obtained when one methylenic unit separates the two benzene rings, we have studied the effect of replacing it by a carbonyl group (Table 9, page 43), which imposes a coplanar orientation of the aromatic rings. We considered as spacers one or two methylenic units since they gave good results in inhibitors **49** and **50** with IC_{50} values for 2-OG hydrolysis inhibition of 8 and 19 μM, respectively. Compounds **57-60** inhibited FAAH (IC_{50} values between 1.4 and 22 μM), but none of them showed any effect on the 2-OG hydrolyzing activity. As occurred in the corresponding analogs with one methylenic unit between the two benzene rings (Table 8), the compounds where the heterocyclic subunit is the oxirane fragment exhibited higher inhibition towards the AEA hydrolyzing activity than the corresponding tetrahydropyran derivatives (compounds **57** *vs* **59** and **58** *vs* **60**).

Table 8. Influence of the 4-benzylphenyl and 4-phenylethylphenyl moieties

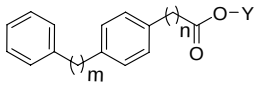

Cpd	m	n	Y	Hydrolysis inhibition pI_{50} [IC_{50}, μM]		Cpd	m	n	Y	Hydrolysis inhibition pI_{50} [IC_{50}, μM]	
				2-OG	AEA					2-OG	AEA
49	1	1		5.00±0.02 [8]	5.01±0.04 [9.8, 92%][a]	**53**	1	1		<4 (25±4%)[b]	4.73±0.04 [18, 91%][a]
50	1	2		4.73±0.05 [19]	5.63±0.03 [2.3]	**54**	1	2		<4 (41±1%)[b]	5.40±0.11 [4.0]
51	1	3		5.10±0.05 [10]	4.99±0.09 [10]	**55**	1	3		<4 (13±1%)[b]	<4 (47±1%)[b]
52	2	0		<4 (18±2%)[b]	4.44±0.04 [37]	**56**	2	0		<4 (8±2%)[b]	4.78±0.06 [17]

[a,b] For explanation of data, see footnote for Table 1.

Table 9. Influence of the benzoyl group

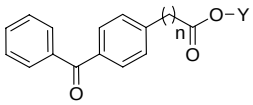

Cpd	n	Y	Hydrolysis inhibition pI50 [IC50, μM] 2-OG	AEA	Cpd	n	Y	Hydrolysis inhibition pI50 [IC50, μM] 2-OG	AEA
57	1		<4 (5±1%)[b]	5.85±0.02 [1.4]	59	1		<4 (5±2%)[b]	4.77±0.07 [17]
58	2		<4 (33±3%)[b]	5.41±0.03 [3.9]	60	2		<4 (27±2%)[b]	4.65±0.09 [22, 90%][a]

[a,b] For explanation of data, see footnote for Table 1.

3.4.3. Influence of the stereogenic center (85-88)

In summary, from all synthesized compounds **1c,d** the ones with the best inhibitory profile towards 2-OG hydrolysis were the biphenyl derivative **37** (IC_{50} = 4.5 μM) and the benzylphenyl derivative **49** (IC_{50} = 8 μM). Since both of them contain a stereogenic center, we next studied its influence by synthesizing the two enantiomers of **37** (derivatives **85** and **86**) and **49** (**87** and **88**). The results compiled in Table 10 indicated that the stereogenic center does not exert a great influence in the inhibitory ability of compounds **85** and **86**, with IC_{50} values for 2-OG hydrolysis of 4.5 μM (racemic **37**), 4.9 μM (*R*-enantiomer **85**) and 5.1 μM (*S*-enantiomer **86**).

Table 10. Influence of the stereogenic center

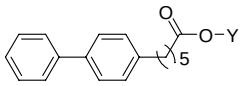

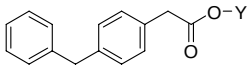

Cpd	Y	Hydrolysis inhibition pI50 [IC50, μM] 2-OG	AEA	Cpd	Y	Hydrolysis inhibition pI50 [IC50, μM] 2-OG	AEA
37		5.35±0.05 [4.5]	5.29±0.03 [5.1]	49		5.00±0.02 [8]	5.01±0.04 [9.8, 92%][a]
85		5.31±0.03 [4.9]	5.41±0.01 [3.9]	87		6.17±0.03 [0.68]	6.54±0.01 [0.29]
86		5.29±0.03 [5.1]	5.35±0.02 [4.5]	88		4.15±0.09 [70]	6.47±0.01 [0.34]

[a] For explanation of data, see footnote for Table 1.

With respect to the benzylphenyl derivative 49, we can observe a significant difference between both enantiomers. While *S*-enantiomer 88 showed a low inhibitory capacity [IC_{50} (2-OG) = 70 μM] compared with the racemic 49 [IC_{50} (2-OG) = 8 μM], its *R*-counterpart 87 behaves as a potent inhibitor of 2-OG hydrolysis with an IC_{50} value in the submicromolar range (0.68 μM).

3.4.4. Replacement of the oxirane group with the 2-glycerol moiety (89, 90)

Finally, and in an attempt to further optimize the potency of 37 and 49 to inhibit 2-OG hydrolysis, we have replaced their oxirane ring with the 2-glycerol moiety, present in 2-AG. The synthesis of derivatives 89 and 90 has been carried out through esterification of their corresponding carboxylic acids 64 and 79 with 1,3-dibenzyloxypropan-2-ol followed by deprotection of the hydroxyl groups by catalytic hydrogenation in presence of palladium hydroxide (Scheme 9).

The activity assays showed that this modification smoothly improved the inhibitory ability of 89 when compared with its analog 37, with IC_{50} values for 2-OG hydrolysis of 1.5 and 4.5 μM, respectively (Table 11). On the contrary, the same modification basically abolished the inhibitory ability of the parent compound 49 (90 showed only a 49% inhibition at 100 μM, whereas 49 had an IC_{50} value of 8 μM). Regarding AEA hydrolysis inhibition, both derivatives 89 and 90 improved the potency of their respective analogs [IC_{50} (37, AEA) = 5.1 μM *vs* IC_{50} (89, AEA) = 1.9 μM and IC_{50} (49, AEA) = 9.8 μM *vs* IC_{50} (90, AEA) = 0.7 μM].

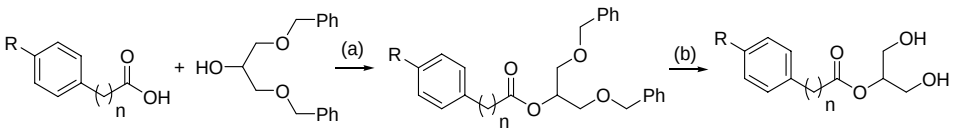

64: R = Ph, n = 5
79: R = $PhCH_2$, n = 1

91: R = Ph, n = 5
92: R = $PhCH_2$, n = 1

89: R = Ph, n = 5
90: R = $PhCH_2$, n = 1

Reagents and conditions: (a) DCC, DMAP, CH_2Cl_2, rt, 16h; (b) $Pd(OH)_2$, CH_2Cl_2/EtOH, rt, 3h

Scheme 9.

Table 11. Influence of the introduction of the glycerol moiety

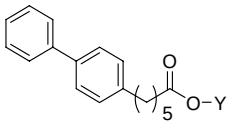

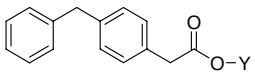

Cpd	Y	Hydrolysis inhibition pI_{50} [IC_{50}, μM]		Cpd	Y	Hydrolysis inhibition pI_{50} [IC_{50}, μM]	
		2-OG	AEA			2-OG	AEA
37		5.35±0.05 [4.5]	5.29±0.03 [5.1]	49		5.00±0.02 [8]	5.01±0.04 [9.8, 92%][a]
89		5.81±0.07 [1.5]	5.73±0.02 [1.9]	90		<4 (49±2%)[b]	6.15±0.02 [0.70]

[a,b] For explanation of data, see footnote for Table 1.

In summary, modifications of the initial hits guided by SAR studies and computational models have enabled us to optimize the initial series and to identify structurally new 2-AG hydrolysis inhibitors with IC_{50} values in the submicromolar range.

3.5. Study of different 2-AG hydrolyzing activities

One of the most important questions is the characterization of the diverse MGL activities expressed in different brain cell types and subcellular fractions. Thus, it has been reported the differential contribution of several serine hydrolases to 2-AG hydrolysis in brain membrane fractions such as MGL, ABHD-6 and ABHD-12.[50] Furthermore, very recently, this new characterized hydrolase (ABHD-6) has been found to be expressed in neurons in primary culture and its inhibition led to activity-dependent accumulation of 2-AG.[110] Thus, the most potent compounds ($IC_{50} \leq 15$ μM for 2-OG hydrolysis inhibition, 2-OG cyt, and maximum inhibition ≥ 70%) have been selected and assessed for their ability to inhibit 2-OG hydrolysis in rat brain membrane fractions (2-OG memb) as well as to block hrMGL, in order to study whether the inhibitory action of the compounds is due to a direct effect on the enzyme. In addition, and in collaboration with the group of Professor Nephi Stella (University of Washington, USA) some of these compounds have been tested in neuron homogenates in order to study whether they could affect the 2-AG hydrolysis in these cells.

As shown in Table 12 (page 46), the analyzed compounds exhibit different inhibitory profiles, which suggests that they target different enzymes involved in 2-AG hydrolysis. Those compounds which conserve a fatty acid chain as hydrophobic subunit (derivatives 1, 5, 9, 12 and 26) showed, in general, a decrease of their activity when assessed in membrane fractions. However, since 85% of the 2-AG hydrolytic activity in membrane is due to MGL,[50] these results suggest that the main effect of these compounds is due to the inhibition of other enzymatic activity different from the MGL molecularly characterized. In support of this, some of these compounds were tested against hrMGL and showed IC_{50} values ranging from low [IC_{50} (1, hrMGL) = 50 μM] to inactive [IC_{50} (5 and 12, hrMGL) > 100 μM].

Taking into account these results, the rest of the selected compounds were tested directly against hrMGL. In general, all biphenyl (36, 37, 85, 86 and 89) and benzylphenyl (49, 51 and 87) derivatives showed closer IC_{50} values for these two assays. These data suggest that compounds of general structure Ic,d are better suited to target hrMGL than the initial series Ia.

Finally, some compounds with different structures were selected to perform a preliminary screening on their effect to inhibit 2-AG hydrolysis in neurons in primary culture. Up to this moment, 12 and 36 have turned out as the most interesting compounds with IC_{50} values in neurons of 1.2 and 0.5 μM, respectively (Table 12). In particular, derivative 12 stands out as the most selective towards an enzyme which hydrolyzes 2-AG in neurons [IC_{50} (12, 2-OG cyt) = 13 μM; IC_{50} (12, 2-OG memb) = 28 μM; IC_{50} (12, neurons) = 1.2 μM; IC_{50} (12, hrMGL) > 100 μM]. Additional experiments have identified this activity as ABHD-6, enzyme that is the main target of derivative 12.[106]

[110] Marrs, W.R., Blankman, J.L., Horne, E.A., Thomazeau, A., Lin, Y.H., Coy, J., Bodor, A.L., Muccioli, G.G., Hu, S.S., Woodruff, G., Fung, S., Lafourcade, M., Alexander, J.P., Long, J.Z., Li, W., Xu, C., Möller, T., Mackie, K., Manzoni, O.J., Cravatt, B.F., Stella, N. *Nat. Neurosci.* 2010, *13*, 951.

Table 12. Study of different 2-AG hydrolyzing activities

Cpd	Structure	Hydrolysis inhibition IC_{50} (μM)[a]			
		2-OG cyt	2-OG memb	hrMGL[b]	Neuron[c]
1	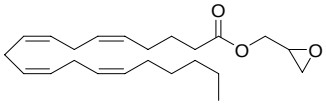	4.5	29	50	ND[d]
5	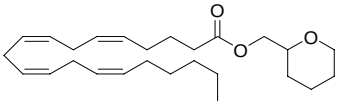	5.6	26	>100	10
9	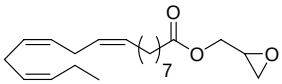	11	51	ND	1.7
12	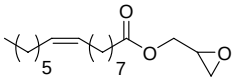	13	28	>100	1.2
26	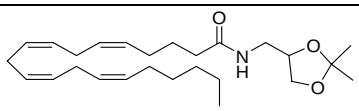	15	100	ND	ND
36	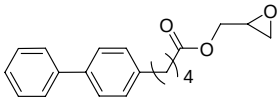	7.9	ND	6.2	0.5
37	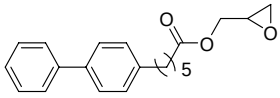	4.5	ND	4.1	1.4
49	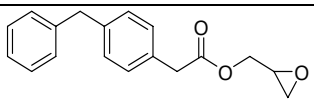	8	ND	9.8	ND
51	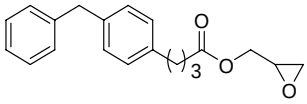	10	ND	16	ND
85	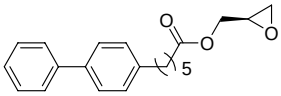	4.9	ND	21	ND
86	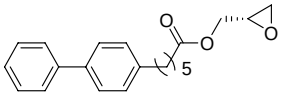	5.1	ND	10	ND

Table 12. (Continuation)

Cpd	Structure	Hydrolysis inhibition IC_{50} (μM)[a]			
		2-OG cyt	2-OG memb	hrMGL[b]	Neuron[c]
87	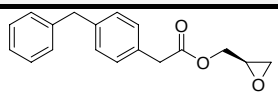	0.68	ND	2.4	ND
89	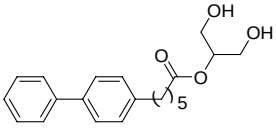	1.5	ND	7.5	ND

[a]The IC_{50} values are the mean of at least two independent experiments performed in duplicate. Assay substrates: [b]4-Nitrophenyl acetate, [c][^{3}H]-2-AG. [d]ND, Not determined.

In summary, taken together, all this data confirm the fact that 2-AG degradation is a complex process that involves multiple enzymes and that compounds I can differentially target these different enzyme activities. Hence, they represent a suitable toolbox for attempting the identification of new 2-AG hydrolyzing activities. As a proof of principle, we have addressed this possibility in microglial cells in collaboration with the research group of Professor Nephi Stella.

3.6. Identification of a novel MGL activity in microglia

Considering the relevance of microglia in CNS disorders such as Alzheimer's disease and MS, compounds targeting the ECS expressed in microglial cells might represent pharmacological tools therapeutically useful for these pathologies. Microglia is strongly involved in the response to neuronal cell damage, in which it changes their "resting" phenotype to an "activated" state, process called "microglial cell activation". Damaged cells release molecules which are recognized by receptors located in microglial cell membranes, including CB receptors. The activation of such receptors and the subsequent expression of specific genes produce the change in the phenotype of these cells which become pro-inflammatory or anti-inflammatory.[111] Moreover, it has been reported that microglial cells in culture produce 20-fold more endocannabinoids than neurons and astrocytes and that these cells are able to inactivate both AEA and 2-AG.[112] In spite of this capacity, retrotranscriptase-polymerase chain reaction (RT-PCR) failed to detect any MGL expression in BV-2 microglia cell line although these cells were able to hydrolyze [^{3}H]-2-AG with a specific activity of 1.2 pmol/min/mg protein.[105] It could be argued that 2-AG might be hydrolyzed by other enzymes such as LOXs and COXs in the same way that reported for AEA,[27,28] but the use of specific inhibitors of these activities did not affect [^{3}H]-2-AG hydrolysis in BV-2 cells, clearly ruling out their involvement. Finally, the contribution of FAAH was also analyzed using the potent FAAH inhibitor URB597 [IC_{50} (FAAH) = 4.6 nM[113]]. As expected, this inhibitor completely blocked

[111] Garden, G.A., Möller, T. *J. Neuroimmune Pharmacol*. 2006, *1*, 127.
[112] Walter, L., Franklin, A., Witting, A., Wade, C., Xie, Y., Kunos, G., Mackie, K., Stella, N. *J. Neurosci*. 2003, *23*, 1398.
[113] Kathuria, S., Gaetani, S., Fegley, D., Valiño, F., Duranti, A., Tontini, A., Mor, M., Tarzia, G., La Rana, G., Calignano, A., Giustino, A., Tattoli, M., Palmery, M., Cuomo, V., Piomelli, D. *Nat. Med*. 2003, *9*, 76.

AEA hydrolysis as well as about one half of the 2-AG hydrolysis in neurons (Figure 10).

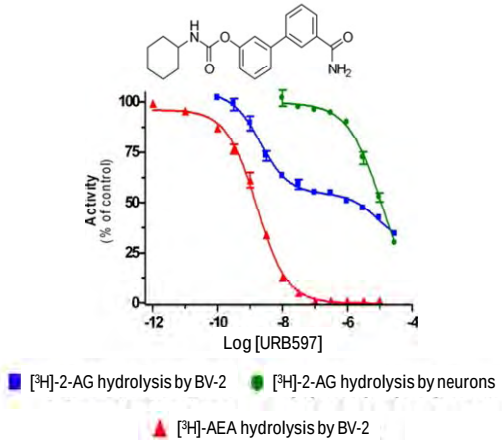

Figure 10. Effect of increasing concentrations of the FAAH inhibitor URB597 on [^{3}H]-2-AG hydrolysis by BV-2 ([^{3}H]-2-AG by BV-2; blue) and primary neurons ([^{3}H]-2-AG by neurons; green) homogenates and on [^{3}H]-AEA hydrolysis by BV-2 ([^{3}H]-AEA by BV-2; red) homogenates.

These results are consistent with the fact that FAAH inactivates AEA and that MGL hydrolyzes 2-AG in these cells. Since URB597 is a much weaker inhibitor of MGL (no inhibition at 30 μM)[113] than of FAAH, this curve did not reach the point of complete activity inhibition (i.e. 0% at the maximum concentration of the inhibitor) and showed a remarkable right-shift. Nonetheless, URB597 inhibited 2-AG hydrolysis in BV-2 cells in a biphasic manner. This result indicated the existence of at least two distinct 2-AG hydrolytic activities in these cells, FAAH, which accounts for the upper part of the curve, and another hydrolytic enzyme responsible for the bottom part of the curve.

Given the different *in vitro* activity profiles of compounds of series I (Table 12), it is conceivable that if exists an additional 2-AG hydrolyzing activity, the compounds would show different inhibition curves for 2-AG and AEA hydrolysis in neurons and in BV-2 cells. Therefore, a library of several compounds was screened in order to identify inhibitors capable of discriminating between MGL, FAAH and the "novel MGL".

Figure 11 shows two representative results obtained for compounds 5, which exhibits a comparable capacity to inhibit the three enzymatic activities with similar IC_{50} values (7-12 μM), and 16, which was characterized as inhibitor of FAAH and of the novel MGL expressed by BV-2 cells with a weak effect on MGL expressed in neurons.

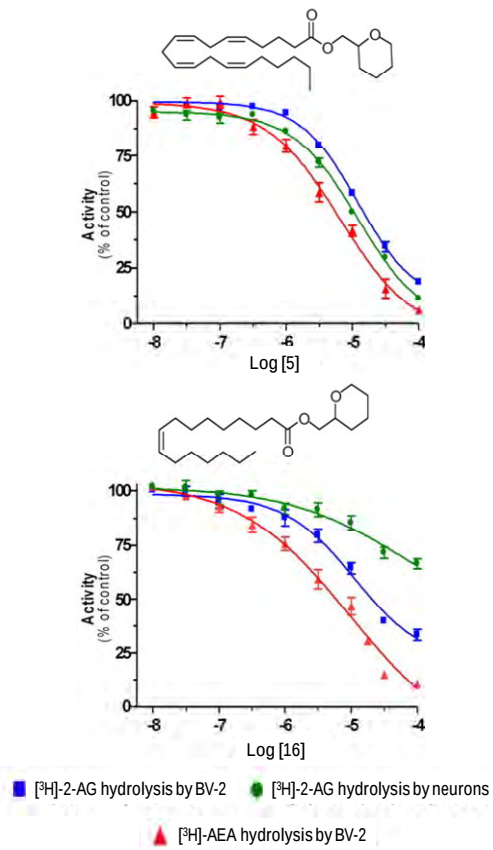

Figure 11. Pharmacological distinction of the novel MGL, MGL, and FAAH. Effect of increasing concentrations of the derivatives 5 and 16.

Taken together, these results clearly support that in BV-2 cells it exists at least one 2-AG hydrolyzing activity different from MGL.[105] Concomitant in-depth

molecular characterization of this enzyme together with identification of its physiological functions aided by the use of inhibitor 16, should help to clarify the 2-AG role in microglia and validate the increase of its levels as a useful therapeutic approach for different disorders where microglia plays a pivotal role.

3.7. Neuroprotective role of derivatives 1 and 5

One of the most interesting features of endocannabinoids is their neuroprotective properties in different *in vivo* and *in vitro* models. They can protect neurons from hypoxic injury, and may represent endogenous neuroprotective molecules in cerebral ischemia.[82] In order to start to validate MGL as a therapeutic target of interest for the treatment of excitotoxicity-associated pathologies, we have initiated the *in vitro* evaluation of some selected compounds to study their capacity to protect cells from glutamate-induced excitotoxicty, an established *in vitro* model to screen neuroprotective molecules. Most studies of this type have been performed in the HT-22 cell line, which is an immortalized mouse hippocampal cell line that lacks ionotropic glutamate receptors.[114] HT-22 cells are similar to undifferentiated neural stem cells. They express neuron-specific enolase and neurofilament proteins, but because of their fast division and the lack of ionotropic glutamate receptors, they do not exhibit the normal morphology of neurons. HT-22 cells are sensitive to glutamate-induced toxicity because extracellular glutamate inhibits glutathione synthesis causing depletion of glutathione, increased reactive oxygen species production, calcium influx, and subsequent cell death.[115] Therefore, we used glutamate-induced toxicity in HT-22 cells as our *in vitro* model.

[114] Maher, P., Davis, J.B. *J. Neurosci.* 1996, *16*, 6394.
[115] Tan, S., Schubert, D., Maher, P. *Curr. Top. Med. Chem.* 2001, *1*, 497.

These experiments were set up during a predoctoral stay in the Laboratory of Professor Beat Lutz (Johannes Gutenberg University, Mainz, Germany) using the best inhibitors developed up to that moment, which were derivatives 1 and 5, with IC_{50} values to inhibit 2-OG hydrolysis of 4.5 and 5.6 μM, respectively (Table 1, page 31). First, we checked the expression of the proteins of the ECS CB_1, CB_2, FAAH and MGL in HT-22 cells. RT-PCR experiments showed the expression of the hydrolytic enzymes FAAH and MGL and the lack of CB receptors (Figure 12).

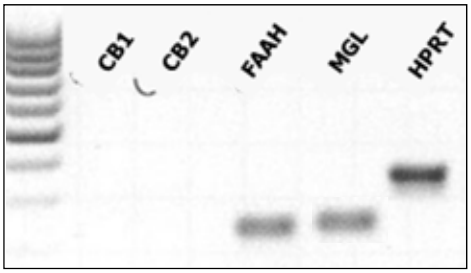

Figure 12. RT-PCR from HT-22 mRNA was performed with primers recognizing mouse CB_1, CB_2, FAAH and MGL. Hypoxanthine guanine phosphoribosyltransferase (HPRT) was used as positive control.

Since the neuroprotective effects of endocannabinoids have been previously described as a CB_1-mediated effect,[84] we carried out these experiments in HT-22 cells previously transfected with the CB_1 receptor and its expression was confirmed by immunocytochemistry and fluorescence microscopy (Figure 13, page 50).

Accordingly, excitotoxicity in CB_1-transfected HT-22 cells was induced with 10 mM glutamate and cells were incubated with different concentration of compounds 1 and 5. After 48 hours, cell viability was quantified through MTT [3-(4,5-dimethylthiazol-2-yl)-2,5-diphenyltetrazolium bromide] assay (Figure 14, page 50).

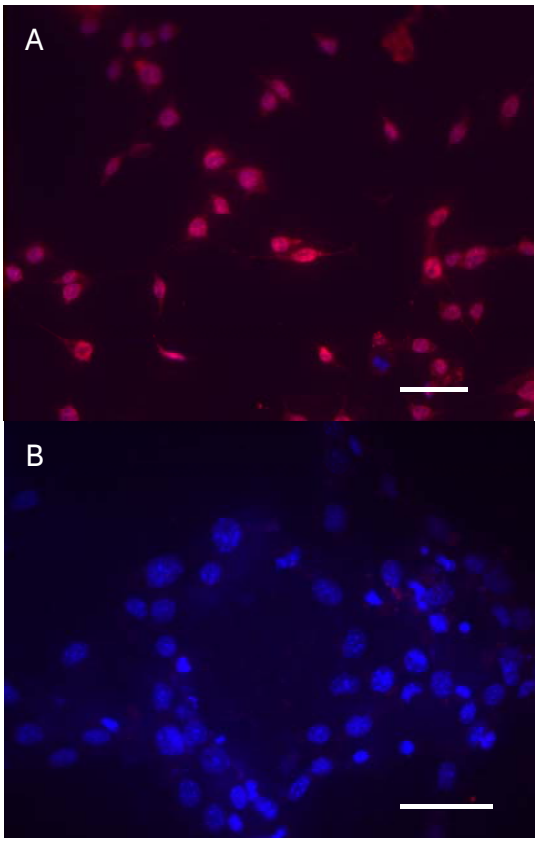

Figure 13. Fluorescence immunocytochemistry showing CB_1 expression (red) in transfected HT-22 cells (A) and non-transfected cells (B). Nuclei were stained with Höchst 33258. Scale: bars, 200 μm

Both compounds are able to protect, in a significant manner, HT-22 cells from glutamate-induced death. Inhibitors 1 and 5 increased cell viability to 54% and 56%, respectively, at 10 μM. These results suggest that inhibitors of 2-AG hydrolysis can induce neuroprotection at least in *in vitro* cellular models. Further studies with the new optimized MGL inhibitors will be carried out in due course and should confirm whether this effect is due to a direct effect on MGL inhibition and mediated by an increase in the endogenous levels of 2-AG, therefore aiding the definitive validation of this enzyme as a suitable therapeutic target for excitotoxicity-related disorders.

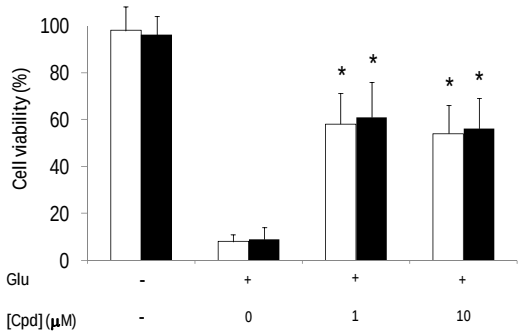

Figure 14. Cell viability after 48h incubation with 10 mM glutamate (Glu) in absence and presence of compounds 1 (white bars) and 5 (black bars). * $P < 0.05$ *vs* untreated cells

3.8. Insights into the inhibition mechanism

In the search of new MGL inhibitors it is of importance not only to determine their ability to inhibit 2-AG hydrolysis but also to establish whether they are reversible or irreversible inhibitors as well as the binding mode towards the enzyme. This is relevant when considering their potential for further drug development as well as for optimization processes. In particular, leads such 37 or 87 (active enantiomer of 49) identified in the present work would be amenable of optimization in terms of potency towards MGL and selectivity for this enzyme *vs* FAAH. One possible manner of optimization relies on the use of ^{15}N-labelled protein and NMR studies to determine the binding site of the compound in the protein. Then, computational studies using the 3D crystal structure of the protein could guide the design and synthesis of new structures. Within this aim, we have started to study the mechanism of inhibition of 37 and 87, the two best inhibitors identified so far. Our results indicate that inhibitor 37 acts as a reversible and competitive inhibitor (Figure 15, page 51) with a K_i value of 8 ± 2 μM.

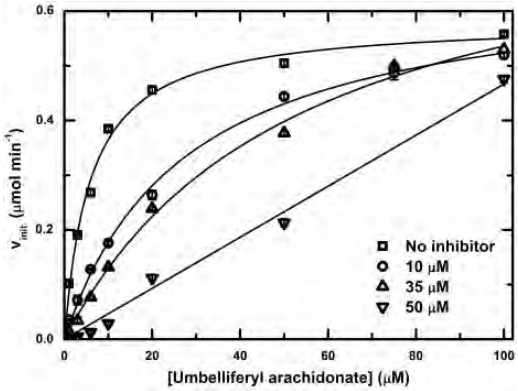

Figure 15. Competitive nature of derivative 37 for inhibition of MGL. Effects of increasing concentration of 37 on umbelliferyl arachidonate hydrolysis saturation curve.

In order to confirm that 37 binds MGL, we have carried out saturation transfer difference (STD) experiments. However, STD effect is not observed and instead, the hydrolysis of 37 by MGL over the time is the predominating feature in the NMR spectra. This result is in agreement with the competitive character of 37 but precludes the usefulness of this inhibitor for NMR experiments with the ^{15}N-labelled protein. Analogous experiments with 87 as well as the synthesis of different structures based on 37 and 87 scaffolds that should exhibit better stabilities in the presence of the enzyme are under way at this moment.

In summary, these results reveal useful information about the structural requirements involved in the 2-AG hydrolysis inhibition by different enzymatic activities and support the interest of MGL as a therapeutic target.

4. EXPERIMENTAL SECTION

4.1. Chemistry

Melting points (mp, uncorrected) were determined on a Stuart Scientific electrothermal apparatus for all solid compounds. Those compounds for which mp was not determined were oils. Infrared (IR) spectra were measured on a Perkin-Elmer 781, Shimadzu-8300 infrared spectrophotometer, or a Bruker Tensor 27 instrument equipped with a Specac ATR accessory of 5200-650 cm^{-1} transmission range; frequencies (ν) are expressed in cm^{-1}. Optical rotation [α] was measured using a Perkin-Elmer 781 polarimeter. ^{1}H and ^{13}C NMR spectra have been obtained at the UCM's NMR core facility and were recorded on a Varian VXR-300S, Bruker Avance 300-AM or Bruker 200-AC instrument at room temperature (rt) unless stated otherwise. Chemical shifts (δ) are expressed in parts per million relative to internal tetramethylsilane; coupling constants (*J*) are in hertz (Hz). The following abbreviations are used to describe peak patterns when appropriate: s (singlet), d (doublet), t (triplet), q (quartet), qt (quintuplet), sept (septuplet), m (multiplet), br (broad), app (apparent). For the sake of clarity in the NMR assignation, all fatty acid chains have been numbered starting in the carbonyl group as position 1. For all final compounds, purity was determined either by elemental analyses or high-performance liquid chromatography coupled to mass spectrometry (HPLC-MS) and high-resolution mass spectrometry (HRMS) (Tables 13 and 14, pages 89 and 90). Elemental analyses (C, H, N) were performed on a LECO CHNS-932 apparatus at the UCM's analysis services and were within 0.5% of the theoretical values, confirming a purity of at least 95%. In the case of HPLC-MS, satisfactory chromatograms (purity > 95%) were obtained. HPLC-MS analysis was performed using an Agilent 1200LC-MSD VL instrument. LC separation was achieved with an Eclipse XDB-C18 column (5 μm, 4.6 mm x 150 mm) together with a guard column (5 μm, 4.6 mm x 12.5 mm). The gradient mobile phases consisted of A (95:5 water/acetonitrile or water/methanol) and B (5:95 water/acetonitrile or water/methanol) with 0.1% ammonium hydroxide and 0.1% formic acid as the solvent modifiers. The gradient started at 0% B (for 5 min) and increased linearly to 100% B over the course of 20 min, with a flow rate of 0.5 mL/min, and it was followed by an isocratic gradient of 100% B for 5 min before equilibrating for 5 min at 0% B. MS analysis was performed with an electrospray ionization (ESI) source. The capillary voltage was set to 3.0 kV, and the fragmentor voltage was set at 70 eV. The drying gas temperature was 350 ºC, the drying gas flow was 10 L/min, and the nebulizer pressure was 20 psi. HRMS was carried out on a FTMS Bruker APEX Q IV spectrometer in ESI mode at UCM's mass spectrometry core facility. Thin-layer chromatography (TLC) was run on Merck silica gel type 60 F-254 plates. For normal pressure chromatography, Merck silica gel type (size 70-230) was used. Unless stated otherwise, starting materials used were high-grade commercial products from Sigma-Aldrich, Acros, Fluka, Merck or Panreac. Arachidonic acid (90% of purity) was purchased from Sigma. Methylene chloride was used freshly distilled over CaH_2.

4.1.1. General procedure for the synthesis of final compounds 1-47, 49-60 and 85-88

To a stirred solution of 1 equivalent of carboxylic acid in dry dichloromethane (0.82 mL/mmol) and the appropriate alcohol or amine (5 equiv) in dry dichloromethane (0.27 mL/mmol) in ice bath under argon, a solution of DCC (1 equiv) and DMAP (0.068 equiv) in dry dichloromethane (1.9 mL/mmol) was added dropwise. The mixture was stirred for 5 min at this temperature and then removed from the cooling bath and stirred at room temperature (3-6h) until no further evolution was observed by TLC. The dicyclohexylurea was filtered off, and the filtrate washed with saturated

$NaHCO_3$ and, in the case of amides, with 0.5 M HCl. The organic extracts were dried over anhydrous Na_2SO_4. Then, the solvent was evaporated under reduced pressure and the product purified by column chromatography on silica gel using the appropriate eluent. Compounds 2, 3 and 25 showed spectroscopic data identical to those reported previously in the literature.[116]

(±)-Oxiran-2-ylmethyl (5*Z*,8*Z*,11*Z*,14*Z*)-icosa-5,8,11,14-tetraenoate (1)

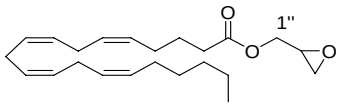

Yield: 42%.
Rf: 0.7 (hexane/chloroform, 3:7).
IR ($CHCl_3$, cm^{-1}): 1377, 1418, 1456, 1738, 2860, 2930, 2955, 3014.
^{1}H-NMR ($CDCl_3$, δ): 0.88 (t, *J* = 6.8 Hz, 3H, H_{20}); 1.18-1.43 (m, 6H, H_{17}, H_{18}, H_{19}); 1.72 (qt, *J* = 7.1 Hz, 2H, H_3); 2.00-2.17 (m, 4H, H_4, H_{16}); 2.37 (t, *J* = 7.6 Hz, 2H, H_2); 2.64 (dd, *J* = 4.9; 2.7 Hz, 1H, 1H oxirane); 2.78-2.86 (m, 7H, H_7, H_{10}, H_{13}, 1H oxirane); 3.16-3.24 (m, 1H, 1H oxirane); 3.91 (dd, *J* = 12.2; 6.3 Hz, 1H, $1H_{1''}$); 4.41 (dd, *J* = 12.2; 2.9 Hz, 1H, $1H_{1''}$); 5.26-5.47 (m, 8H, vinylic-H).
^{13}C-NMR ($CDCl_3$, δ): 14.2 (CH_3), 22.7, 24.8 ($2CH_2$), 25.7 ($3CH_2$), 26.6, 27.3, 29.4, 31.6, 33.5 ($5CH_2$), 44.8 (CH_2 oxirane), 49.4 (CH oxirane), 64.9 ($C_{1''}$), 127.5, 127.8, 128.1, 128.2, 128.6, 128.8, 129.0, 130.5 (8CH), 173.4 (CO).
Chromatography: hexane/chloroform, 1:9.
Anal.: ($C_{23}H_{36}O_3$) C, H, N.

(±)-2-Tetrahydrofur-2-ylmethyl (5*Z*,8*Z*,11*Z*,14*Z*)-icosa-5,8,11,14-tetraenoate (2)[116]

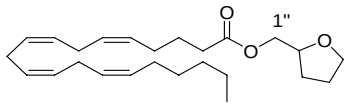

Yield: 48%.
^{1}H-NMR ($CDCl_3$, δ): 0.86 (t, *J* = 6.9 Hz, 3H, $3H_{20}$), 1.22−1.38 (m, 6H, $2H_{17}$, $2H_{18}$, $2H_{19}$), 1.53−1.63 (m, 2H, 2H tetrahydrofuran), 1.70 (qt, *J* = 7.5 Hz, 2H, $2H_3$), 1.83−1.95 (m, 2H, 2H tetrahydrofuran), 1.98−2.12 (m, 4H, $2H_4$, $2H_{16}$), 2.33 (t, *J* = 7.6 Hz, 2H, $2H_2$), 2.76−2.82 (m, 6H, $2H_7$, $2H_{10}$, $2H_{13}$), 3.71−3.78 (m, 1H, 1H tetrahydrofuran), 3.81−3.89 (m, 1H, 1H tetrahydrofuran), 3.91−3.99 (m, 1H, 1H tetrahydrofuran), 4.05−4.20 (m, 2H, $2H_{1''}$), 5.32−5.35 (m, 8H, vinylic-H).
Anal.: ($C_{25}H_{40}O_3$) C, H, N.

(±)-Tetrahydrofur-3-ylmethyl (5*Z*,8*Z*,11*Z*,14*Z*)-icosa-5,8,11,14-tetraenoate (3)[116]

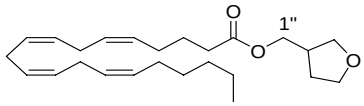

Yield: 38%.
^{1}H-NMR ($CDCl_3$, δ): 0.88 (t, *J* = 6.8 Hz, 3H, $3H_{20}$), 1.19−1.32 (m, 6H, $2H_{17}$, $2H_{18}$, $2H_{19}$), 1.54−1.77 (m, 3H, $2H_3$, 1H tetrahydrofuran), 1.95−2.16 (m, 5H, 1H tetrahydrofuran, $2H_4$, $2H_{16}$), 2.32 (t, *J* = 7.8 Hz, 2H, $2H_2$), 2.50−2.64 (m, 1H, 1H tetrahydrofuran), 2.78−2.86 (m, 6H, $2H_7$, $2H_{10}$, $2H_{13}$), 3.56 (dd, *J* = 8.8; 5.6 Hz, 1H, 1H tetrahydrofuran), 3.69−4.13 (m, 5H, $2H_{1''}$, 3H tetrahydrofuran), 5.26−5.41 (m, 8H, vinylic-H).
Anal.: ($C_{25}H_{40}O_3$) C, H, N.

[116] López-Rodríguez, M.L., Viso, A., Ortega-Gutiérrez, S., Fowler, C.J., Tiger, G., de Lago, E., Fernández-Ruiz, J., Ramos, J.A. *J. Med. Chem.* 2003, *46*, 1512.

(±)-2,2-Dimethyl-1,3-dioxolan-4-ylmethyl (5*Z*,8*Z*,11*Z*,14*Z*)-icosa-5,8,11,14-tetraenoate (4)

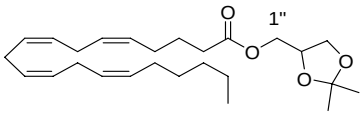

Yield: 60%.
Rf: 0.4 (chloroform).
IR ($CHCl_3$, cm^{-1}): 1030, 1113, 1416, 1450, 1735, 2833, 2945.
^{1}H-NMR ($CDCl_3$, δ): 0.88 (t, *J* = 6.8 Hz, 3H, H_{20}); 1.26-1.32 (m, 6H, H_{17}, H_{18}, H_{19}); 1.37 (s, 3H, CH_3); 1.43 (s, 3H, CH_3); 1.71 (qt, *J* = 7.3 Hz, 2H, H_3); 2.00-2.16 (m, 4H, H_4, H_{16}); 2.36 (t, *J* = 7.3 Hz, 2H, H_2); 2.78-2.86 (m, 6H, H_7, H_{10}, H_{13}); 3.73 (dd, *J* = 8.3; 6.1 Hz, 1H, 1H dioxolane); 4.04-4.15 (m, 3H, $1H_{1''}$, 2H dioxolane); 4.19-4.37 (m, 1H, $1H_{1''}$); 5.23-5.40 (m, 8H, vinylic-H).
^{13}C-NMR ($CDCl_3$, δ): 14.1 (CH_3), 22.5, 24.7, 25.4 ($3CH_2$), 25.6 ($3CH_2$), 26.5, 26.7 ($2CH_3$ dioxolane), 27.2, 29.3, 31.5, 33.4 ($4CH_2$), 64.6 ($C_{1''}$), 66.4 (CH_2 dioxolane), 73.7 (CH dioxolane), 109.8 (C dioxolane), 127.5, 127.8, 128.1, 128.2, 128.6, 128.8, 128.9, 130.5 (8CH), 173.4 (CO).
Chromatography: hexane/chloroform, 3:7.
Anal.: ($C_{26}H_{42}O_4$) C, H, N.

(±)-Tetrahydro-2*H*-pyran-2-ylmethyl (5*Z*,8*Z*,11*Z*,14*Z*)-icosa-5,8,11,14-tetraenoate (5)

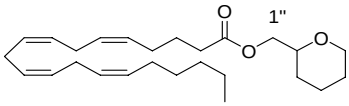

Yield: 29%.
Rf: 0.5 (chloroform).
IR ($CHCl_3$, cm^{-1}): 1558, 1653, 1684, 1718, 2934, 3018.
^{1}H-NMR ($CDCl_3$, δ): 0.89 (t, *J* = 6.6 Hz, 3H, H_{20}); 1.25-1.40 (m, 6H, H_{17}, H_{18}, H_{19}); 1.49-1.58 (m, 5H, 5H tetrahydropyran); 1.71 (qt, *J* = 7.3 Hz, 2H, H_3); 1.82-1.90 (m, 1H, 1H tetrahydropyran); 2.01-2.16 (m, 4H, H_4, H_{16}); 2.37 (t, *J* = 7.5 Hz, 2H, H_2); 2.78-2.86 (m, 6H, H_7, H_{10}, H_{13}); 3.37-3.59 (m, 2H, 2H tetrahydropyran); 3.96-4.13 (m, 3H, $2H_{1''}$, 1H tetrahydropyran); 5.23-5.37 (m, 8H, vinylic-H).
^{13}C-NMR ($CDCl_3$, δ): 14.0 (CH_3), 22.6, 23.0, 24.8 ($3CH_2$), 25.6 ($3CH_2$), 25.7, 26.6, 27.2, 27.9, 29.3, 31.5, 33.6 ($7CH_2$), 67.3 ($C_{1''}$), 68.4 (OCH_2 tetrahydropyran), 75.5 (OCH tetrahydropyran), 127.5, 127.9, 128.2, 128.6 (4CH), 128.8 (2CH), 129.0, 130.5 (2CH), 173.5 (CO).
Chromatography: hexane/ethyl acetate, 9:1.
Anal.: ($C_{26}H_{42}O_3$) C, H, N.

Tetrahydro-2*H*-pyran-4-yl (5*Z*,8*Z*,11*Z*,14*Z*)-icosa-5,8,11,14-tetraenoate (6)

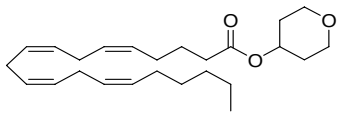

Yield: 23%.
Rf: 0.5 (chloroform).
IR ($CHCl_3$, cm^{-1}): 1362, 1456, 1558, 1653, 1684, 1716, 2933, 3018.
^{1}H-NMR ($CDCl_3$, δ): 0.89 (t, *J* = 6.6 Hz, 3H, H_{20}); 1.22-1.39 (m, 6H, H_{17}, H_{18}, H_{19}); 1.57-1.78 (m, 4H, H_3, 2H tetrahydropyran); 1.85-1.95 (m, 2H, 2H tetrahydropyran); 2.00-2.17 (m, 4H, H_4, H_{16}); 2.32 (t, *J* = 7.5 Hz, 2H, H_2); 2.78-2.86 (m, 6H, H_7, H_{10}, H_{13}); 3.47-3.59 (m, 2H, 2H tetrahydropyran); 3.86-3.96 (m, 2H, 2H tetrahydropyran); 4.95 (sept, *J* = 4.3 Hz, 1H, 1H tetrahydropyran); 5.27-5.47 (m, 8H, vinylic-H).
^{13}C-NMR ($CDCl_3$, δ): 14.2 (CH_3), 22.7, 25.0 ($2CH_2$), 25.8 ($3CH_2$), 26.7, 27.4, 29.5, 31.7 ($4CH_2$), 32.0 ($2CH_2$), 34.1 (CH tetrahydropyran), 65.5, 69.1 ($2CH_2O$ tetrahydropyran), 76.5 (CH tetraydropyran), 127.7, 128.0, 128.3, 128.4, 128.7 (5CH), 129.0 (2CH), 130.7 (CH), 173.4 (CO).
Chromatography: hexane/ethyl acetate, 9:1.
Anal.: ($C_{25}H_{40}O_3$) C, H, N.

2-(5,5-Dimethyl-1,3-dioxan-2-yl)ethyl (5*Z*,8*Z*,11*Z*,14*Z*)-icosa-5,8,11,14-tetraenoate (7)

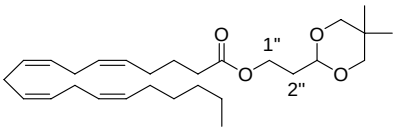

Yield: 41 %.
Rf: 0.4 (chloroform).
IR ($CHCl_3$, cm^{-1}): 1094, 1456, 1472, 1732.
^{1}H-NMR ($CDCl_3$, δ): 0.72 (s, 3H, CH_3); 0.89 (t, *J* = 6.8 Hz, 3H, H_{20}); 1.18 (s, 3H, CH_3); 1.23-1.43 (m, 6H, H_{17}, H_{18}, H_{19}); 1.70 (qt, *J* = 7.3 Hz, 2H, H_3); 1.96 (q, 2H, *J* = 6.6 Hz, $2H_{2''}$); 2.04-2.17 (m, 4H, H_4, H_{16}); 2.31 (t, *J* = 7.3 Hz, 2H, H_2); 2.78-2.86 (m, 6H, H_7, H_{10}, H_{13}); 3.41 (d, *J* = 10.5 Hz, 2H, 2H dioxane); 3.60 (d, *J* = 11.0 Hz, 2H, 2H dioxane); 4.20 (t, *J* = 6.6 Hz, 2H, $2H_{1''}$); 4.53 (t, *J* = 5.1 Hz, 1H, 1H dioxane); 5.26-5.46 (m, 8H, vinylic-H).
^{13}C-NMR ($CDCl_3$, δ): 14.0 (CH_3), 21.8 (CH_3 dioxane), 22.6 (CH_2), 22.9 (CH_3 dioxane), 24.8 (CH_2), 25.6 ($3CH_2$), 26.6, 27.2, 29.3 ($3CH_2$), 30.1 (C dioxane), 31.5, 33.7 ($2CH_2$), 34.1 ($C_{2''}$), 60.0 ($C_{1''}$), 77.2 ($2CH_2$ dioxane), 99.4 (CH dioxane), 127.5, 127.9, 128.1, 128.2, 128.6, 128.8, 129.0, 130.5 (8CH), 173.4 (CO).
Chromatography: chloroform.
Anal.: ($C_{28}H_{46}O_4$) C, H, N.

1,3-Benzodioxol-5-ylmethyl (5*Z*,8*Z*,11*Z*,14*Z*)-icosa-5,8,11,14-tetraenoate (8)

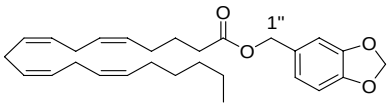

Yield: 74%.
Rf: 0.3 (hexane/dichloromethane, 1:1).
IR ($CHCl_3$, cm^{-1}): 1447, 1491, 1504, 1728, 2930, 2959, 3016.
^{1}H-NMR ($CDCl_3$, δ): 0.81 (t, *J* = 6.6 Hz, 3H, H_{20}); 1.18-1.32 (m, 6H, H_{17}, H_{18}, H_{19}); 1.64 (qt, *J* = 7.4 Hz, 2H, H_3); 1.93-2.08 (m, 4H, H_4, H_{16}); 2.28 (t, *J* = 7.5 Hz, 2H, H_2); 2.68-2.76 (m, 6H, H_7, H_{10}, H_{13}); 4.94 (s, 2H, $2H_{1''}$); 5.20-5.37 (m, 8H, vinylic-H); 5.89 (s, 2H, OCH_2O); 6.68-6.78 (m, $3H_{Ar}$).
^{13}C-NMR ($CDCl_3$, δ): 14.5 (CH_3), 23.0 (CH_2), 25.2 ($2CH_2$), 26.0, 27.0, 27.6, 29.4, 29.7, 31.9, 34.1 ($7CH_2$), 66.5 ($C_{1''}$), 101.6 (CH_2 benzodioxol), 108.6, 109.4, 122.7 ($3CH_{Ar}$), 127.9, 128.3, 128.5, 128.6, 129.0 (5CH), 129.3 (2CH), 130.2 (CH), 130.9 (C_{Ar}), 148.0, 148.2 ($2C_{Ar}$), 173.8 (CO).
Chromatography: hexane/dichloromethane, 1:1.
Anal.: ($C_{28}H_{38}O_4$) C, H, N.

(±)-Oxiran-2-ylmethyl (9*Z*,12*Z*,15*Z*)-octadeca-9,12,15-trienoate (9)

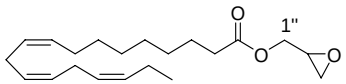

Yield: 19%.
Rf: 0.7 (chloroform).
IR ($CHCl_3$, cm^{-1}): 1653, 1732, 2858, 2933, 3020.
^{1}H-NMR ($CDCl_3$, δ): 0.98 (t, *J* = 7.5 Hz, 3H, H_{18}); 1.25-1.31 (m, 8H, H_4, H_5, H_6, H_7); 1.60-1.67 (m, 2H, H_3); 2.01-2.21 (m, 4H, H_8, H_{17}); 2.36 (t, *J* = 7.6 Hz, 2H, H_2); 2.58 (dd, *J* = 4.9; 2.6 Hz, 1H, 1H oxirane); 2.78-2.87 (m, 5H, H_{11}, H_{14}, 1H oxirane); 3.17-3.26 (m, 1H, 1H oxirane); 3.91 (dd, *J* = 12.2; 5.8 Hz, 1H, $1H_{1''}$); 4.42 (dd, *J* = 12.2; 2.9 Hz, 1H, $1H_{1''}$); 5.25-5.46 (m, 6H, vinylic-H).
^{13}C-NMR ($CDCl_3$, δ): 14.3 (CH_3), 20.6, 24.9, 25.5 ($3CH_2$), 25.6 ($2CH_2$), 27.2, 29.1, 29.2, 29.6, 34.1 ($5CH_2$), 44.7 (CH_2 oxirane), 49.4 (CH oxirane), 64.8 ($C_{1''}$), 127.1, 127.8 (2CH), 128.3 (2CH), 130.3, 132.0 (2CH), 183.0 (CO).
Chromatography: hexane/dichloromethane, 2:8.
Anal.: ($C_{21}H_{34}O_3$) C, H, N.

(±)-Oxiran-2-ylmethyl (9*Z*,12*Z*)-octadeca-9,12-dienoate (10)

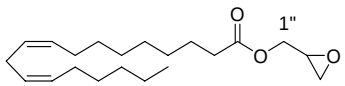

Yield: 36%.
Rf: 0.3 (dichloromethane).
IR ($CHCl_3$, cm^{-1}): 1379, 1437, 1460, 1732, 2858, 2932.
^{1}H-NMR ($CDCl_3$, δ): 0.88 (t, *J* = 6.5 Hz, 3H, H_{18}); 1.18-1.35 (m, 14H, H_{4-7}, H_{15-17}); 1.60-1.67 (m, 2H, H_3); 2.00-2.06 (m, 4H, H_8, H_{14}); 2.35 (t, *J* = 7.3 Hz, 2H, H_2); 2.65 (dd, *J* = 4.9; 2.6 Hz, 1H, 1H oxirane); 2.77 (t, *J* = 5.7 Hz, 2H, H_{11}); 2.82-2.87 (m, 1H, 1H oxirane); 3.17-3.25 (m, 1H, 1H oxirane); 3.90 (dd, *J* = 12.3; 6.3 Hz, 1H, $1H_{1''}$); 4.41 (dd, *J* = 12.3; 3.0 Hz, 1H, $1H_{1''}$); 5.25-5.45 (m, 4H, vinylic-H).
^{13}C-NMR ($CDCl_3$, δ): 14.2 (CH_3), 22.7, 24.9, 25.7 ($3CH_2$), 27.3 ($2CH_2$), 29.2 ($3CH_2$), 29.4, 29.7, 31.6, 34.2 ($4CH_2$), 44.7 (CH_2 oxirane), 49.5 (CH oxirane), 64.8 ($C_{1''}$), 128.0, 128.1, 130.1, 130.3 (4CH), 173.6 (CO).
Chromatography: hexane/dichloromethane, 2:8.
Anal.: ($C_{21}H_{36}O_3$) C, H, N.

(±)-Oxiran-2-ylmethyl (9*Z*)-octadec-9-enoate (11)

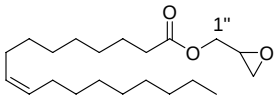

Yield: 33%.
Rf: 0.5 (chloroform).
IR ($CHCl_3$, cm^{-1}): 1456, 1558, 1653, 1734, 2856, 2928, 3018.
^{1}H-NMR ($CDCl_3$, δ): 0.81 (t, *J* = 6.7 Hz, 3H, H_{18}); 1.15-1.24 (m, 20H, H_{4-7}, H_{12-17}); 1.53-1.57 (m, 2H, H_3); 1.89-1.96 (m, 4H, H_8, H_{11}); 2.28 (t, *J* = 7.3 Hz, 2H, H_2); 2.58 (dd, *J* = 4.9; 2.6 Hz, 1H, 1H oxirane); 2.78 (t, *J* = 4.9 Hz, 1H, 1H oxirane); 3.12-3.15 (m, 1H, 1H oxirane); 3.84 (dd, *J* = 12.3; 6.3 Hz, 1H, $1H_{1''}$); 4.35 (dd, *J* = 12.3; 3.0 Hz, 1H, $1H_{1''}$); 5.25-5.31 (m, 2H, vinylic-H).
^{13}C-NMR ($CDCl_3$, δ): 14.1 (CH_3), 22.6, 24.8, 27.1, 27.2 ($4CH_2$), 29.1 ($3CH_2$), 29.3 ($2CH_2$), 29.5, 29.6, 29.7, 31.9, 34.0 ($5CH_2$), 44.6 (CH_2 oxirane), 49.3 (CH oxirane), 64.7 ($C_{1''}$), 129.7, 130.0 (2CH), 173.1 (CO).
Chromatography: hexane/ethyl acetate, 9:1.
Anal.: ($C_{21}H_{38}O_3$) C, H, N.

(±)-Oxiran-2-ylmethyl (9*Z*)-hexadec-9-enoate (12)

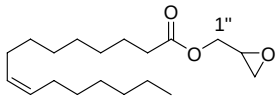

Yield: 25%.
Rf: 0.5 (chloroform).
IR ($CHCl_3$, cm^{-1}): 1551, 1743, 2856, 2928.
^{1}H-NMR ($CDCl_3$, δ): 0.88 (t, *J* = 6.8 Hz, 3H, H_{16}); 1.28-1.30 (m, 16H, H_{4-7}, H_{12-15}); 1.59-1.67 (m, 2H, H_3); 1.99-2.02 (m, 4H, H_8, H_{11}); 2.35 (t, *J* = 7.1 Hz, 2H, H_2); 2.63 (dd, *J* = 4.9; 2.4 Hz, 1H, 1H oxirane); 2.84 (dd, *J* = 4.9; 4.2 Hz, 1H, 1H oxirane); 3.16-3.24 (m, 1H, 1H oxirane); 3.90 (dd, *J* = 12.2; 6.3 Hz, 1H, $1H_{1''}$); 4.41 (dd, *J* = 12.3; 3.2 Hz, 1H, $1H_{1''}$); 5.26-5.37 (m, 2H, vinylic-H).
^{13}C-NMR ($CDCl_3$, δ): 14.0 (CH_3), 22.6, 24.8, 27.1, 27.2, 28.9 ($5CH_2$), 29.0 ($2CH_2$), 29.1, 29.6, 29.7, 31.7, 34.0, ($5CH_2$) 44.6 (CH_2 oxirane), 49.3 (CH oxirane), 64.7 ($C_{1''}$), 129.7, 130.0 (2CH), 173.5 (CO).
Chromatography: hexane/chloroform, 2:8.
Anal.: ($C_{19}H_{34}O_3$) C, H, N.

(±)-Tetrahydro-*2H*-pyran-2-ylmethyl (9*Z*,12*Z*,15*Z*)-octadeca-9,12,15-trienoate (13)

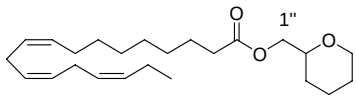

Yield: 55%.

Rf: 0.2 (hexane/chloroform, 2:8).
IR ($CHCl_3$, cm^{-1}): 1558, 1732, 2856, 2935, 3016.
^{1}H-NMR ($CDCl_3$, δ): 0.90 (t, J = 7.5 Hz, 3H, H_{18}); 1.23-1.42 (m, 10H, H_{4-7}, 2H tetrahydropyran); 1.46-1.67 (m, 5H, H_3, 3H tetrahydropyran); 1.80-1.91 (m, 1H, 1H tetrahydropyran); 1.94-2.08 (m, 4H, H_8, H_{17}); 2.28 (t, J = 7.5 Hz, 2H, H_2); 2.71-2.76 (m, 4H, H_{11}, H_{14}); 3.31-3.49 (m, 2H, 2H tetrahydropyran); 3.88-4.06 (m, 3H, $2H_{1''}$, 1H tetrahydropyran); 5.18-5.39 (m, 6H, vinylic-H).
^{13}C-NMR ($CDCl_3$, δ): 14.3 (CH_3), 20.6, 23.0, 25.0, 25.5, 25.6, 25.8, 27.2, 27.9 ($8CH_2$), 29.1 ($2CH_2$), 29.2, 29.6, 34.2 ($3CH_2$), 67.3 ($C_{1''}$), 68.4 (OCH_2 tetrahydropyran), 75.5 (OCH tetrahydropyran), 127.1, 127.7 (2CH), 128.3 (2CH), 130.3, 132.0 (2CH), 173.9 (CO).
Chromatography: hexane/chloroform, 2:8.
Anal.: ($C_{24}H_{40}O_3$) C, H, N.

(±)-Tetrahydro-*2H*-pyran-2-ylmethyl (9*Z*,12*Z*)-octadeca-9,12-dienoate (14)

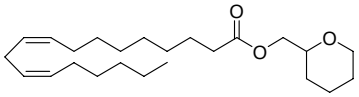

Yield: 44%.
Rf: 0.1 (hexane/chloroform, 1:1).
IR ($CHCl_3$, cm^{-1}): 1558, 1653, 1734, 2856, 2930, 3018.
^{1}H-NMR ($CDCl_3$, δ): 0.82 (t, J = 6.7 Hz, 3H, H_{18}); 1.09-1.32 (m, 16H, H_{4-7}, H_{15-17}, 2H tetrahydropyran); 1.40-1.61 (m, 5H, H_3, 3H tetrahydropyran); 1.77-1.82 (m, 1H, 1H tetrahydropyran); 1.93-1.99 (m, 4H, H_8, H_{14}); 2.28 (t, J = 7.3 Hz, 2H, H_2); 2.70 (t, J = 5.7 Hz, 2H, H_{11}); 3.31-3.49 (m, 2H, 2H tetrahydropyran); 3.88-4.06 (m, 3H, $2H_{1''}$, 1H tetrahydropyran); 5.19-5.31 (m, 4H, vinylic-H).
^{13}C-NMR ($CDCl_3$, δ): 14.0 (CH_3), 22.5, 23.0, 24.9, 25.6, 25.7 ($5CH_2$), 27.2 ($2CH_2$), 27.8 (CH_2), 29.1 ($2CH_2$), 29.2, 29.3, 29.6, 31.5, 34.2 ($5CH_2$), 67.2 ($C_{1''}$), 68.4 (OCH_2 tetrahydropyran), 75.5 (OCH tetrahydropyran), 127.9, 128.0, 130.0, 130.2 (4CH), 173.8 (CO).
Chromatography: hexane/chloroform, 1:1.
Anal.: ($C_{24}H_{42}O_3$) C, H, N.

(±)-Tetrahydro-*2H*-pyran-2-ylmethyl (9*Z*)-octadec-9-enoate (15)

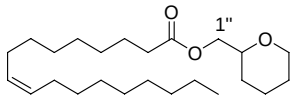

Yield: 91%.
Rf: 0.1 (hexane/chloroform, 1:1).
IR ($CHCl_3$, cm^{-1}): 1558, 1734, 2928, 3018.
^{1}H-NMR ($CDCl_3$, δ): 0.81 (t, J = 6.7 Hz, 3H, H_{18}); 1.18-1.24 (m, 22H, H_{4-7}, H_{12-17}, 2H tetrahydropyran); 1.39-1.55 (m, 5H, H_3, 3H tetrahydropyran); 1.77-1.82 (m, 1H, 1H tetrahydropyran); 1.92-1.98 (m, 4H, H_8, H_{11}); 2.28 (t, J = 7.3 Hz, 2H, H_2); 3.31-3.49 (m, 2H, 2H tetrahydropyran); 3.88-4.06 (m, 3H, $2H_{1''}$, 1H tetrahydropyran); 5.20-5.36 (m, 2H, vinylic-H).
^{13}C-NMR ($CDCl_3$, δ): 14.2 (CH_3), 22.8, 23.1, 25.0, 25.9, 27.3, 27.4, 28.0 ($7CH_2$), 29.2 ($2CH_2$), 29.3 ($2CH_2$), 29.4, 29.7, 29.8, 29.9, 32.0, 34.3 ($6CH_2$), 67.4 ($C_{1''}$), 68.5 (OCH_2 tetrahydropyran), 75.6 (OCH tetrahydropyran), 129.9, 130.1 (2CH), 174.0 (CO).
Chromatography: hexane/chloroform, 1:1.
Anal.: ($C_{24}H_{44}O_3$) C, H, N.

(±)-Tetrahydro-*2H*-pyran-2-ylmethyl (9*Z*)-hexadec-9-enoate (16)

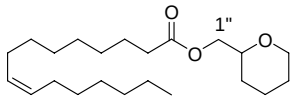

Yield: 69%.
Rf: 0.1 (hexane/chloroform, 1:1).
IR ($CHCl_3$, cm^{-1}): 1558, 1734, 2930, 3018.
^{1}H-NMR ($CDCl_3$, δ): 0.81 (t, J = 6.7 Hz, 3H, H_{16}); 1.18-1.34 (m, 18H, H_{4-7}, H_{12-15}, 2H tetrahydropyran); 1.40-1.58 (m, 5H, H_3, 3H tetrahydropyran); 1.77-1.82 (m, 1H, 1H tetrahydropyran); 1.85-2.03 (m, 4H, H_8, H_{11}); 2.28 (t,

J = 7.3 Hz, 2H, H_2); 3.31-3.52 (m, 2H, 2H tetrahydropyran); 3.88-4.06 (m, 3H, $2H_{1''}$, 1H tetrahydropyran); 5.19-5.35 (m, 2H, vinylic-H).
^{13}C-NMR ($CDCl_3$, δ): 14.1 (CH_3), 22.6, 23.0, 25.0, 25.8 ($4CH_2$), 27.2 ($2CH_2$), 27.9, 29.0 ($2CH_2$), 29.1 ($2CH_2$), 29.2, 29.7, 29.8, 31.8, 34.2 ($5CH_2$), 67.3 ($C_{1''}$), 68.4 (OCH_2 tetrahydropyran), 75.5 (OCH tetrahydropyran), 129.8, 130.0 (2CH), 173.9 (CO).
Chromatography: hexane/chloroform, 1:1.
Anal.: ($C_{22}H_{40}O_3$) C, H, N.

(±)-Oxiran-2-ylmethyl 1,1'-biphenyl-2-carboxylate (17)

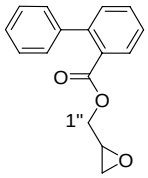

Yield: 27%.
Rf: 0.3 (chloroform).
IR ($CHCl_3$, cm^{-1}): 1344, 1418, 1452, 1506, 1720, 2932, 2974.
^{1}H-NMR ($CDCl_3$, δ): 2.32 (dd, *J* = 4.9; 2.6 Hz, 1H, 1H oxirane); 2.60 (app t, *J* = 4.8 Hz, 1H, 1H oxirane); 2.78-2.86 (m, 1H, 1H oxirane); 3.89 (dd, *J* = 12.2; 5.8 Hz, 1H, $1H_{1''}$); 4.20 (dd, *J* = 12.2; 3.6 Hz, 1H, $1H_{1''}$); 7.23-7.40 (m, 7H, $7H_{Ar}$); 7.46-7.50 (m, 1H, $1H_{Ar}$); 7.80 (dd, *J* = 7.5; 1.4 Hz, 1H, $1H_{Ar}$).
^{13}C-NMR ($CDCl_3$, δ): 44.5 (CH_2 oxirane), 48.7 (CH oxirane), 65.2 ($C_{1''}$), 127.0, 127.1 ($2CH_{Ar}$), 127.9 ($2CH_{Ar}$), 128.2 ($2CH_{Ar}$), 129.9, 130.2, 130.6 ($3CH_{Ar}$), 131.4, 141.3, 142.6 ($3C_{Ar}$), 168.2 (CO).
Chromatography: chloroform.
Anal.: ($C_{16}H_{14}O_3$) C, H, N.

(±)-Oxiran-2-ylmethyl 1,1'-biphenyl-3-carboxylate (18)

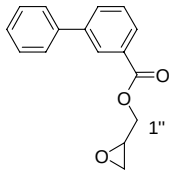

Yield: 24%.
Rf: 0.4 (hexane/dichloromethane, 1:9).
IR ($CHCl_3$, cm^{-1}): 1304, 1346, 1587, 1601, 1717, 3020.
^{1}H-NMR ($CDCl_3$, δ): 2.67 (dd, *J* = 4.8; 2.6 Hz, 1H, 1H oxirane); 2.84 (app t, *J* = 4.7 Hz, 1H, 1H oxirane); 3.26-3.34 (m, 1H, 1H oxirane); 4.13 (dd, *J* = 12.3; 6.3 Hz, 1H, $1H_{1''}$); 4.62 (dd, *J* = 12.3; 3.1 Hz, 1H, $1H_{1''}$); 7.30-7.38 (m, 6H, $6H_{Ar}$); 7.70-7.75 (m, 1H, $1H_{Ar}$); 7.95-7.99 (m, 1H, $1H_{Ar}$); 8.21-8.25 (m, 1H, $1H_{Ar}$).
^{13}C-NMR ($CDCl_3$, δ): 44.7 (CH_2 oxirane), 49.4 (CH oxirane), 65.5 ($C_{1''}$), 127.1 ($2CH_{Ar}$), 127.7, 128.3, 128.4 ($3CH_{Ar}$), 128.8 ($3CH_{Ar}$), 130.1 (CH_{Ar}), 131.8, 140.0, 141.5 ($3C_{Ar}$), 166.2 (CO).
Chromatography: hexane/dichloromethane, 1:9.
Anal.: ($C_{16}H_{14}O_3$) C, H, N.

(±)-Oxiran-2-ylmethyl 1,1'-biphenyl-4-carboxylate (19)

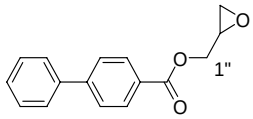

Yield: 35%.
Rf: 0.3 (chloroform).
IR ($CHCl_3$, cm^{-1}): 1312, 1448, 1609, 1717, 3018.
^{1}H-NMR ($CDCl_3$, δ): 2.69 (dd, *J* = 4.8; 2.6 Hz, 1H, 1H oxirane); 2.85 (app t, *J* = 4.6 Hz, 1H, 1H oxirane); 3.26-3.34 (m, 1H, 1H oxirane); 4.12 (dd, *J* = 12.3; 6.3 Hz, 1H, $1H_{1''}$); 4.62 (dd, *J* = 12.3; 3.0 Hz, 1H, $1H_{1''}$); 7.30-7.46

(m, 3H, $3H_{Ar}$); 7.55-7.63 (m, 4H, $4H_{Ar}$); 8.08 (d, *J* = 8.3 Hz, 2H, $2H_{Ar}$).
^{13}C-NMR ($CDCl_3$, δ): 44.6 (CH_2 oxirane), 49.4 (CH oxirane), 65.3 ($C_{1''}$), 127.0 ($2CH_{Ar}$), 127.2 ($2CH_{Ar}$), 128.1, 128.3 ($2CH_{Ar}$), 128.8 ($2CH_{Ar}$), 130.2 (CH_{Ar}, C_{Ar}), 139.8, 145.8 ($2C_{Ar}$), 166.0 (CO).
Chromatography: chloroform.
Anal.: ($C_{16}H_{14}O_3$) C, H, N.

(±)-Tetrahydro-*2H*-pyran-2-ylmethyl 1,1'-biphenyl-2-carboxylate (20)

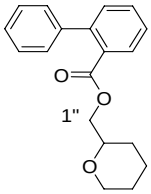

Yield: 61%.
Rf: 0.4 (chloroform).
IR ($CHCl_3$, cm^{-1}): 1452, 1724, 2939.
^{1}H-NMR ($CDCl_3$, δ): 0.94-1.08 (m, 1H, 1H tetrahydropyran); 1.18-1.29 (m, 1H, 1H tetrahydropyran); 1.32-1.43 (m, 3H, 3H tetrahydropyran); 1.52-1.67 (m, 1H, 1H tetrahydropyran); 3.06-3.30 (m, 2H, 2H tetrahydropyran); 3.81-3.96 (m, 3H, $2H_{1''}$, 1H tetrahydropyran); 7.24-7.49 (m, 8H, $8H_{Ar}$); 7.77 (dd, *J* = 7.7; 1.4 Hz, 1H, $1H_{Ar}$).
^{13}C-NMR ($CDCl_3$, δ): 23.0, 25.8, 27.9 ($3CH_2$ tetrahydropyran), 68.0 ($C_{1''}$), 68.4 (OCH_2 tetrahydropyran), 75.2 (OCH tetrahydropyran), 127.2 ($2CH_{Ar}$), 128.2 ($2CH_{Ar}$), 128.6 ($2CH_{Ar}$), 130.1, 130.8, 131.1 ($3CH_{Ar}$), 131.3, 141.7, 142.6 ($3C_{Ar}$), 168.8 (CO).
Chromatography: hexane/chloroform, 2:8.
Anal.: ($C_{19}H_{20}O_3$) C, H, N.

(±)-Tetrahydro-*2H*-pyran-2-ylmethyl 1,1'-biphenyl-3-carboxylate (21)

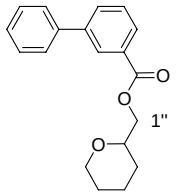

Yield: 45%.
Rf: 0.4 (chloroform).
IR ($CHCl_3$, cm^{-1}): 1049, 1310, 1423, 1716, 2943.
^{1}H-NMR ($CDCl_3$, δ): 1.35-1.66 (m, 5H, 5H tetrahydropyran); 1.89-1.92 (m, 1H, 1H tetrahydropyran); 3.42-3.54 (m, 1H, 1H tetrahydropyran); 3.66-3.76 (m, 1H, 1H tetrahydropyran); 3.91-4.15 (m, 1H, 1H tetrahydropyran); 4.32-4.38 (m, 2H, $2H_{1''}$); 7.34-7.65 (m, 6H, $6H_{Ar}$); 7.78 (dt, *J* = 7.7; 1.8 Hz, 1H, $1H_{Ar}$); 8.05 (dt, *J* = 7.7; 1.8 Hz, 1H, $1H_{Ar}$); 8.30 (t, *J* = 1.8 Hz, 1H, $1H_{Ar}$).
^{13}C-NMR ($CDCl_3$, δ): 23.0, 25.8, 28.1 ($3CH_2$ tetrahydropyran), 68.0 ($C_{1''}$), 68.4 (OCH_2 tetrahydropyran), 75.5 (OCH tetrahydropyran), 127.2 ($2CH_{Ar}$), 127.7, 128.4, 128.5, 128.8 ($4CH_{Ar}$), 128.9 ($2CH_{Ar}$), 130.7 (CH_{Ar}), 131.6, 140.2, 141.4 ($3C_{Ar}$), 166.5 (CO).
Chromatography: dichloromethane.
Anal.: ($C_{19}H_{20}O_3$) C, H, N.

(±)-Tetrahydro-*2H*-pyran-2-ylmethyl 1,1'-biphenyl-4-carboxylate (22)

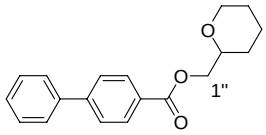

Yield: 61%.
Rf: 0.4 (hexane/chloroform, 2:8).
IR ($CHCl_3$, cm^{-1}): 1610, 1711, 2943.

^{1}H-NMR ($CDCl_3$, δ): 1.36-1.71 (m, 5H, 5H tetrahydropyran); 1.90-1.93 (m, 1H, 1H tetrahydropyran); 3.35-3.48 (m, 1H, 1H tetrahydropyran); 3.66-3.76 (m, 1H, 1H tetrahydropyran); 4.01-4.09 (m, 1H, 1H tetrahydropyran); 4.25-4.40 (m, 2H, $2H_{1''}$); 7.36-7.52 (m, 3H, $3H_{Ar}$); 7.59-7.69 (m, 4H, $4H_{Ar}$); 8.14 (dt, *J* = 8.6; 1.9 Hz, 2H, $2H_{Ar}$).
^{13}C-NMR ($CDCl_3$, δ): 23.0, 25.8, 28.1 ($3CH_2$ tetrahydropyran), 67.9 ($C_{1''}$), 68.5 (OCH_2 tetrahydropyran), 75.6 (OCH tetrahydropyran), 127.0 ($2CH_{Ar}$), 127.3 ($2CH_{Ar}$), 128.1 ($2CH_{Ar}$), 128.9 ($2CH_{Ar}$), 130.3 (CH_{Ar}, C_{Ar}), 140.0, 145.7 ($2C_{Ar}$), 166.5 (CO).
Chromatography: hexane/chloroform, 2:8.
Anal.: ($C_{19}H_{20}O_3$) C, H, N.

(±)-Oxiran-2-ylmethyl benzoate (23)

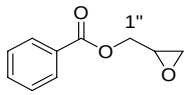

Yield: 14%.
Rf: 0.3 (chloroform).
IR ($CHCl_3$, cm^{-1}): 1344, 1719, 2964.
^{1}H-NMR ($CDCl_3$, δ): 2.74 (dd, *J* = 4.9; 2.6 Hz, 1H, 1H oxirane); 2.91 (app t, *J* = 4.5 Hz, 1H, 1H oxirane); 3.32-3.40 (m, 1H, 1H oxirane); 4.11 (dd, *J* = 12.3; 6.2 Hz, 1H, $1H_{1''}$); 4.60 (dd, *J* = 12.3; 3.0 Hz, 1H, $1H_{1''}$); 7.36-7.62 (m, 3H, $3H_{Ar}$); 8.02-8.07 (m, 2H, $2H_{Ar}$).
^{13}C-NMR ($CDCl_3$, δ): 43.7 (CH_2 oxirane), 48.5 (CH oxirane), 64.4 ($C_{1''}$), 127.4 ($2CH_{Ar}$), 128.6 (CH_{Ar}), 128.7 ($2CH_{Ar}$), 132.2 (C_{Ar}), 165.5 (CO).
Chromatography: chloroform.
Anal.: ($C_{10}H_{10}O_3$) C, H, N.

(±)-Tetrahydro-*2H*-pyran-2-ylmethyl benzoate (24)

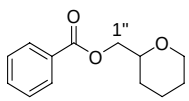

Yield: 44%.
Rf: 0.3 (hexane/chloroform, 2:8).
IR ($CHCl_3$, cm^{-1}): 1275, 1450, 1720, 2939, 3063.
^{1}H-NMR ($CDCl_3$, δ): 1.33-1.62 (m, 5H, 5H tetrahydropyran); 1.81-1.84 (m, 1H, 1H tetrahydropyran); 3.34-3.47 (m, 1H, 1H tetrahydropyran); 3.57-3.67 (m, 1H, 1H tetrahydropyran); 3.93-4.00 (m, 1H, 1H tetrahydropyran); 4.21-4.30 (m, 2H, $2H_{1''}$); 7.33- 7.54 (m, 3H, $3H_{Ar}$); 7.98-8.04 (m, 2H, $2H_{Ar}$).
^{13}C-NMR ($CDCl_3$, δ): 22.9, 25.7, 28.0 ($3CH_2$ tetrahydropyran), 67.7 ($C_{1''}$), 68.3 (OCH_2 tetrahydropyran), 75.4 (OCH tetrahydropyran), 128.2 ($2CH_{Ar}$), 129.6 ($2CH_{Ar}$), 130.1 (CH_{Ar}), 132.8 (C_{Ar}), 166.5 (CO).
Chromatography: hexane/chloroform, 2:8.
Anal.: ($C_{13}H_{16}O_3$) C, H, N.

(±)-(5*Z*,8*Z*,11*Z*,14*Z*)-*N*-(Tetrahydrofur-2-ylmethyl)icosa-5,8,11,14-tetraenamide (25)[116]

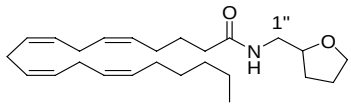

Yield: 83%.
^{1}H-NMR ($CDCl_3$, δ): 0.85 (t, *J* = 6.0 Hz, 3H, $3H_{20}$), 1.22−1.35 (m, 6H, $2H_{17}$, $2H_{18}$, $2H_{19}$), 1.46−1.55 (m, 1H, 1H tetrahydrofuran), 1.71 (qt, *J* = 7.8 Hz, 2H, $2H_3$), 1.81−1.91 (m, 4H, $2H_4$, $2H_{16}$), 1.97−2.11 (m, 3H, 3H tetrahydrofuran), 2.16 (t, *J* = 7.2 Hz, 2H, $2H_2$), 2.76−2.82 (m, 6H, $2H_7$, $2H_{10}$, $2H_{13}$), 3.07 (ddd, *J* = 13.5; 7.5; 4.5 Hz, 1H, $1H_{1''}$), 3.57 (ddd, *J* = 13.8; 6.6; 3.3 Hz, 1H, $1H_{1''}$), 3.70 (q, *J* = 6.9 Hz, 1H, 1H tetrahydrofuran), 3.81 (q, *J* = 6.6 Hz, 1H, 1H tetrahydrofuran), 3.91 (qd, *J* = 7.5; 3.3 Hz, 1H, 1H tetrahydrofuran), 5.26−5.39 (m, 8H, vinylic-H), 5.81 (br s, 1H, NH).
Anal.: ($C_{25}H_{41}NO_2$) C, H, N.

(±)-(5*Z*,8*Z*,11*Z*,14*Z*)-*N*-((2,2-dimethyl-1,3-dioxolan-4-yl)methyl)icosa-5,8,11,14-tetraenamide (26)

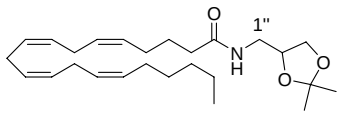

Yield: 43%.
Rf: 0.3 (hexane/ethyl acetate, 6:4).
IR ($CHCl_3$, cm^{-1}): 1375, 1522, 1653, 1718, 2934.
^{1}H-NMR ($CDCl_3$, δ): 0.82 (t, *J* = 6.6 Hz, 3H, H_{20}); 1.18-1.23 (m, 6H, H_{17}, H_{18}, H_{19}); 1.28 (s, 3H, CH_3); 1.36 (s, 3H, CH_3); 1.65 (qt, *J* = 7.5 Hz, 2H, H_3); 1.94-2.05 (m, 4H, H_4, H_{16}); 2.02-2.14 (m, 2H, H_2); 2.71-2.79 (m, 6H, H_7, H_{10}, H_{13}); 3.17-3.27 (m, 1H, $1H_{1''}$); 3.45-3.49 (m, 1H, $1H_{1''}$); 3.55 (dd, *J* = 8.2; 1.9 Hz, 1H, 1H dioxolane); 3.97 (dd, *J* = 8.3; 1.8 Hz, 1H, 1H dioxolane); 4.10-4.18 (m, 1H, 1H dioxolane); 5.22-5.40 (m, 8H, vinylic-H); 5.74 (br s, 1H, NH).
^{13}C-NMR ($CDCl_3$, δ): 13.9 (CH_3), 22.4, 25.0, 25.4 ($3CH_2$), 25.5 ($2CH_2$), 26.6, 26.7 ($2CH_3$), 27.1, 29.2, 31.4, 33.8, 35.9 ($5CH_2$), 41.4 ($C_{1''}$), 66.6 (CH_2 dioxolane), 74.6 (CH dioxolane), 109.2 (C dioxolane), 122.7, 127.4, 128.0, 128.1, 128.5, 128.7, 128.9, 130.4 (8CH), 172.9 (CO).
Chromatography: hexane/ethyl acetate, 6:4.
Anal.: ($C_{26}H_{43}NO_3$) C, H, N.

(2*R*)-(-)-Oxiran-2-ylmethyl (5*Z*,8*Z*,11*Z*,14*Z*)-icosa-5,8,11,14-tetraenoate (27)

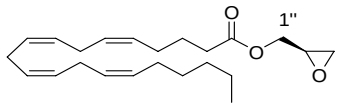

Data of (-)-27 were identical to those recorded for the racemic material 1 except for the optical rotation. (-)-27: $[\alpha]_D^{20}$ -9.1 (*c* = 1.5, ethanol).
Anal.: ($C_{23}H_{36}O_3$) C, H, N.

(2*S*)-(+)-Oxiran-2-ylmethyl (5*Z*,8*Z*,11*Z*,14*Z*)-icosa-5,8,11,14-tetraenoate (28)

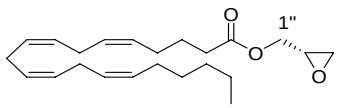

Data of (+)-28 were identical to those recorded for the racemic material 1 except for the optical rotation. (+)-28: $[\alpha]_D^{20}$ +9.2 (*c* = 1.5, ethanol).
Anal.: ($C_{23}H_{36}O_3$) C, H, N.

(4*R*)-(-)-2,2-Dimethyl-1,3-dioxolan-4-ylmethyl (5*Z*,8*Z*,11*Z*,14*Z*)-icosa-5,8,11,14-tetraenoate (29)

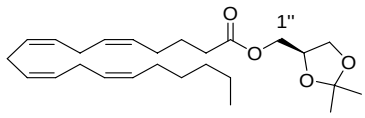

Data of (-)-29 were identical to those recorded for the racemic material 4 except for the optical rotation. (-)-29: $[\alpha]_D^{20}$ -0.7 (*c* = 2, ethanol).
Anal.: ($C_{26}H_{42}O_4$) C, H, N.

(4*S*)-(+)-2,2-Dimethyl-1,3-dioxolan-4-ylmethyl (5*Z*,8*Z*,11*Z*,14*Z*)-icosa-5,8,11,14-tetraenoate (30)

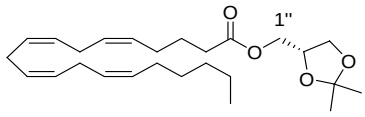

Data of (+)-30 were identical to those recorded for the racemic material 4 except for the optical rotation. (+)-30: $[\alpha]_D^{20}$ +0.8 (*c* = 2, ethanol).
Anal.: ($C_{26}H_{42}O_4$) C, H, N.

(-)-(5*Z*,8*Z*,11*Z*,14*Z*)-*N*-(2*R*)-(Tetrahydrofur-2-ylmethyl)icosa-5,8,11,14-tetraenamide (31)

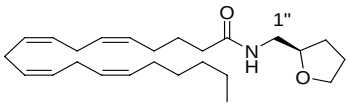

Data of (-)-31 were identical to those recorded for the racemic material 25 except for the optical rotation.
(-)-31: $[\alpha]_D^{20}$ -9.4 (*c* = 2, ethanol).
Anal.: ($C_{25}H_{41}NO_2$) C, H, N.

(+)-(5*Z*,8*Z*,11*Z*,14*Z*)-*N*-(2*S*)-(Tetrahydrofur-2-ylmethyl)icosa-5,8,11,14-tetraenamide (32)

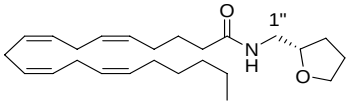

Data of (+)-32 were identical to those recorded for the racemic material 25 except for the optical rotation.
(+)-32: $[\alpha]_D^{20}$ +10.9 (*c* = 2, ethanol).
Anal.: ($C_{25}H_{41}NO_2$) C, H, N.

(±)-Oxiran-2-ylmethyl (1,1'-biphenyl-4-yl)acetate (33)

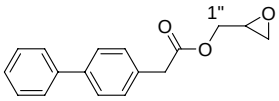

Yield: 55%.
Rf: 0.3 (dichloromethane).
mp: 55-57 ºC.
IR (CH_2Cl_2, cm^{-1}): 2922, 2854, 1740, 1462, 1248, 1152, 1009, 856.
^{1}H-NMR ($CDCl_3$, δ): 2.63 (dd, *J* = 4.9; 2.6 Hz, 1H, 1H oxirane); 2.82-2.86 (m, 1H, 1H oxirane); 3.19-3.27 (m, 1H, 1H oxirane); 3.72 (s, 2H, CH_2CO); 3.96 (dd, *J* = 12.3 Hz, 6.2 Hz, 1H, $1H_{1''}$); 4.47 (dd, *J* = 12.3; 3.0 Hz, 1H, $1H_{1''}$); 7.31-7.48 (m, 5H, $5H_{Ar}$); 7.54-7.61 (m, 4H, $4H_{Ar}$).
^{13}C-NMR ($CDCl_3$, δ): 40.5 ($\underline{C}H_2CO$), 44.4 (CH_2 oxirane), 49.1 (CH oxirane), 65.1 ($C_{1''}$), 126.9 ($2CH_{Ar}$), 127.1 (CH_{Ar}), 127.2 ($2CH_{Ar}$), 128.5 ($2CH_{Ar}$), 129.5 ($2CH_{Ar}$), 132.5, 140.3, 140.8 ($3C_{Ar}$), 171.3 (CO).
Chromatography: dichloromethane.
HRMS (ESI): calcd for $(M+Na)^+$: 291.0997. Found: 291.0986.
Anal.: ($C_{17}H_{16}O_3$) C, H, N.

(±)-Oxiran-2-ylmethyl 3-(1,1'-biphenyl-4-yl)propanoate (34)

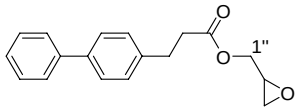

Yield: 59%.
Rf: 0.4 (dichloromethane).
IR (CH_2Cl_2, cm^{-1}): 2925, 2856, 1737, 1520, 1289, 1158, 840, 763.
^{1}H-NMR ($CDCl_3$, δ): 2.54 (dd, *J* = 4.9; 2.6 Hz, 1H, 1H oxirane); 2.65 (t, *J* = 7.4 Hz, 2H, CH_2CO); 2.75 (app t, *J* = 4.5 Hz, 1H, 1H oxirane); 2.94 (t, *J* = 7.7 Hz, 2H, $ArCH_2$); 3.07-3.15 (m, 1H, 1H oxirane); 3.86 (dd, *J* = 12.3; 6.3 Hz, 1H, $1H_{1''}$); 4.35 (dd, *J* = 12.3; 3.0 Hz, 1H, $1H_{1''}$); 7.19-7.53 (m, 9H, $9H_{Ar}$).
^{13}C-NMR ($CDCl_3$, δ): 30.4, 35.5 ($ArCH_2$, $\underline{C}H_2CO$), 44.5 (CH_2 oxirane), 49.2 (CH oxirane), 64.9 ($C_{1''}$), 126.9 ($2CH_{Ar}$), 127.0 (CH_{Ar}), 127.1 ($2CH_{Ar}$), 128.6 ($4CH_{Ar}$), 139.2, 139.3, 140.8 ($3C_{Ar}$), 172.4 (CO).
Chromatography: dichloromethane.
HRMS (ESI): calcd for $(M+Na)^+$: 305.1154. Found: 305.1149.
HPLC-MS: > 95%.

(±)-Oxiran-2-ylmethyl 4-(1,1'-biphenyl-4-yl)butanoate (35)

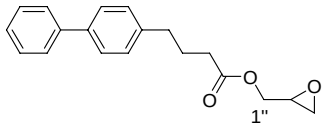

Yield: 41%.
Rf: 0.3 (chloroform).
IR (CH_2Cl_2, cm^{-1}): 2928, 2855, 2118, 1737, 1524, 1246, 1178, 1144, 846, 759.
^{1}H-NMR ($CDCl_3$, δ): 1.94 (qt, *J* = 7.4 Hz, 2H, $CH_2CH_2CH_2$); 2.35 (t, *J* = 7.4 Hz, 2H, CH_2CO); 2.56-2.67 (m, 3H, $ArCH_2$, 1H oxirane); 2.77 (app t, *J* = 4.5 Hz, 1H, 1H oxirane); 3.09-3.17 (m, 1H, 1H oxirane); 3.84 (dd, *J* = 12.3; 6.4 Hz, 1H, $1H_{1''}$); 4.36 (dd, *J* = 12.3; 3.0 Hz, 1H, $1H_{1''}$); 7.16-7.53 (m, 9H, $9H_{Ar}$).
^{13}C-NMR ($CDCl_3$, δ): 26.4 ($CH_2CH_2CH_2$), 33.4, 34.7 ($ArCH_2$, CH_2CO), 44.7 (CH_2 oxirane), 49.4 (CH oxirane), 64.9 ($C_{1''}$), 127.0 ($2CH_{Ar}$), 127.1 (CH_{Ar}), 127.2 ($2CH_{Ar}$), 128.8 ($2CH_{Ar}$), 129.0 ($2CH_{Ar}$), 139.1, 140.4, 141.0 ($3C_{Ar}$), 173.2 (CO).
Chromatography: dichloromethane.
HRMS (ESI): calcd for $(M+Na)^+$: 319.1310. Found: 319.1305.
HPLC-MS: > 95%.

(±)-Oxiran-2-ylmethyl 5-(1,1'-biphenyl-4-yl)pentanoate (36)

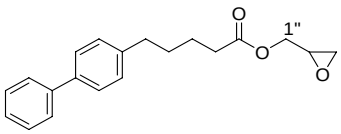

Yield: 56%.
Rf: 0.4 (chloroform).
IR (CH_2Cl_2, cm^{-1}): 2921, 2853, 1737, 1484, 1256, 1175, 758.
^{1}H-NMR ($CDCl_3$, δ): 1.57-1.71 (m, 4H, $(CH_2)_2CH_2CO$); 2.33 (t, *J* = 7.1 Hz, 2H, CH_2CO); 2.49-2.63 (m, 3H, $ArCH_2$, 1H oxirane); 2.76 (app t, *J* = 4.5 Hz, 1H, 1H oxirane); 3.10-3.16 (m, 1H, 1H oxirane); 3.84 (dd, *J* = 12.3; 6.3 Hz, 1H, $1H_{1''}$); 4.35 (dd, *J* = 12.3; 3.0 Hz, 1H, $1H_{1''}$); 7.16-7.19 (m, 2H, $2H_{Ar}$); 7.22-7.28 (m, 1H, $1H_{Ar}$); 7.33-7.38 (m, 2H, $2H_{Ar}$); 7.42-7.45 (m, 2H, $2H_{Ar}$); 7.48-7.52 (m, 2H, $2H_{Ar}$).
^{13}C-NMR ($CDCl_3$, δ): 24.5, 30.9 ($2CH_2$), 34.0, 35.2 ($ArCH_2$, CH_2CO), 44.7 (CH_2 oxirane), 49.4 (CH oxirane), 64.9 ($C_{1''}$), 127.0 ($2CH_{Ar}$), 127.1 (CH_{Ar}), 127.3 ($2CH_{Ar}$), 128.7 ($2CH_{Ar}$), 128.8 ($2CH_{Ar}$), 138.8, 141.1, 141.2 ($3C_{Ar}$), 173.3 (CO).
Chromatography: chloroform.
HRMS (ESI): calcd for $(M+Na)^+$: 333.1467. Found: 333.1466.
HPLC-MS: > 95%.

(±)-Oxiran-2-ylmethyl 6-(1,1'-biphenyl-4-yl)hexanoate (37)

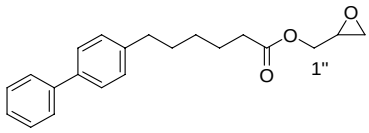

Yield: 53%.
Rf: 0.2 (hexane/dichloromethane, 1:9).
mp: 64-65 ºC.
IR (CH_2Cl_2, cm^{-1}): 2923, 2854, 2119, 1737, 1485, 1257, 1174, 1013, 759.
^{1}H-NMR ($CDCl_3$, δ): 1.26-1.38 (m, 2H, $CH_2(CH_2)_2CO$); 1.56-1.68 (m, 4H, $2CH_2$); 2.30 (t, *J* = 7.5 Hz, 2H, CH_2CO); 2.56-2.61 (m, 3H, $ArCH_2$, 1H oxirane); 2.76 (app t, *J* = 4.5 Hz, 1H, 1H oxirane); 3.10-3.15 (m, 1H, 1H oxirane); 3.83 (dd, *J* = 12.3; 6.3 Hz, 1H, $1H_{1''}$); 4.35 (dd, *J* = 12.3; 3.0 Hz, 1H, $1H_{1''}$); 7.16-7.53 (m, 9H, $9H_{Ar}$).
^{13}C-NMR ($CDCl_3$, δ): 24.8, 28.8, 31.1 ($3CH_2$), 34.0, 35.4 ($ArCH_2$, CH_2CO), 44.7 (CH_2 oxirane), 49.4 (CH oxirane), 64.8 ($C_{1''}$), 127.0 ($3CH_{Ar}$), 127.1 ($2CH_{Ar}$), 128.7 ($2CH_{Ar}$), 128.8 ($2CH_{Ar}$), 138.7, 141.1, 141.6 ($3C_{Ar}$), 173.5 (CO).

Chromatography: hexane/dichloromethane, 1:9.
HRMS (ESI): calcd for $(M+Na)^+$: 347.1623. Found: 347.1621.
Anal.: ($C_{21}H_{24}O_3$) C, H, N.

(±)-Oxiran-2-ylmethyl 7-(1,1'-biphenyl-4-yl)heptanoate (38)

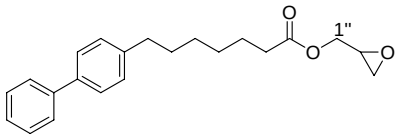

Yield: 27%.
Rf: 0.3 (dichloromethane).
mp: 67 ºC
IR (CH_2Cl_2, cm^{-1}): 3026, 2929, 2856, 1737, 1519, 1255, 1174, 846, 760.
^{1}H-NMR ($CDCl_3$, δ): 1.30 (qt, *J* = 3.6 Hz, 4H, $(C\underline{H_2})_2$-$(CH_2)_2$-CO); 1.53-1.65 (m, 4H, $2CH_2$); 2.28 (t, *J* = 7.5 Hz, 2H, CH_2CO); 2.54-2.60 (m, 3H, $ArCH_2$, 1H oxirane); 2.76 (app t, *J* = 4.5 Hz, 1H, 1H oxirane); 3.10-3.15 (m, 1H, 1H oxirane); 3.83 (dd, *J* = 12.3; 6.3 Hz, 1H, $1H_{1''}$); 4.34 (dd, *J* = 12.3; 3.0 Hz, 1H, $1H_{1''}$); 7.16-7.18 (m, 2H, $2H_{Ar}$); 7.21-7.27 (m, 1H, $1H_{Ar}$); 7.32-7.37 (m, 2H, $2H_{Ar}$); 7.42-7.45 (m, 2H, $2H_{Ar}$); 7.48-7.53 (m, 2H, $2H_{Ar}$).
^{13}C-NMR ($CDCl_3$, δ): 24.8, 28.9, 29.0, 31.3 ($4CH_2$), 34.1, 35.5 ($ArCH_2$, $\underline{C}H_2CO$), 44.7 (CH_2 oxirane), 49.4 (CH oxirane), 64.8 ($C_{1''}$), 127.0 ($3CH_{Ar}$), 127.1 ($2CH_{Ar}$), 128.7 ($2CH_{Ar}$), 128.8 ($2CH_{Ar}$), 138.6, 141.2, 141.8 ($3C_{Ar}$), 173.5 (CO).
Chromatography: dichloromethane.
HRMS (ESI): calcd for $(M+Na)^+$: 361.1780. Found: 361.1778.
Anal.: ($C_{22}H_{26}O_3$) C, H, N.

(±)-Tetrahydro-*2H*-pyran-2-ylmethyl (1,1'-biphenyl-4-yl)acetate (39)

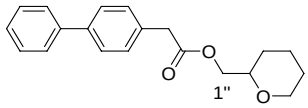

Yield: 58%.
Rf: 0.3 (chloroform).
mp: 37 ºC.
IR (CH_2Cl_2, cm^{-1}): 2935, 2853, 1736, 1152, 1088, 1048, 1007, 752.
^{1}H-NMR ($CDCl_3$, δ): 1.49-1.53 (m, 5H, 5H tetrahydropyran); 1.75-1.82 (m, 1H, 1H tetrahydropyran); 3.31-3.54 (m, 2H, 2H tetrahydropyran); 3.64 (s, 2H, CH_2CO); 3.91-4.04 (m, 3H, 1H tetrahydropyran, $2H_{1''}$); 7.29-7.48 (m, 5H, $5H_{Ar}$); 7.52-7.61 (m, 4H, $4H_{Ar}$).
^{13}C-NMR ($CDCl_3$, δ): 22.8, 25.5, 27.6 ($3CH_2$ tetrahydropyran), 40.6 ($\underline{C}H_2CO$), 67.7 ($C_{1''}$), 68.2 (OCH_2 tetrahydropyran), 75.2 (OCH tetrahydropyran), 126.8 ($2CH_{Ar}$), 127.0 (CH_{Ar}), 127.1 ($2CH_{Ar}$), 128.5 ($2CH_{Ar}$), 129.5 ($2CH_{Ar}$), 132.9, 139.8, 140.7 ($3C_{Ar}$), 171.4 (CO).
Chromatography: chloroform.
HRMS (ESI): calcd for $(M+Na)^+$: 333.1467. Found: 333.1461.
Anal.: ($C_{20}H_{22}O_3$) C, H, N.

(±)-Tetrahydro-*2H*-pyran-2-ylmethyl 3-(1,1'-biphenyl-4-yl)propanoate (40)

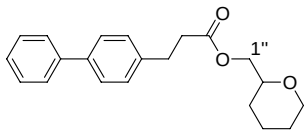

Yield: 49%.
Rf: 0.4 (dichloromethane).
mp: 45 ºC.
IR (CH_2Cl_2, cm^{-1}): 2926, 2851, 1735, 1175, 1089, 1049,

835, 698.
^{1}H-NMR ($CDCl_3$, δ): 1.40-1.50 (m, 5H, 5H tetrahydropyran); 1.73-1.78 (m, 1H, 1H tetrahydropyran); 2.64 (t, *J* = 7.9 Hz, 2H, CH_2CO); 2.93 (t, *J* = 7.6 Hz, 2H, $ArCH_2$); 3.30-3.45 (m, 2H, 2H tetrahydropyran); 3.90-4.07 (m, 3H, 1H tetrahydropyran, $2H_{1''}$); 7.30-7.60 (m, 7H, $7H_{Ar}$); 7.54-7.60 (m, 2H, $2H_{Ar}$).
^{13}C-NMR ($CDCl_3$, δ): 22.9, 25.7, 27.8 ($3CH_2$ tetrahydropyran), 30.5, 35.6 ($\underline{C}H_2CO$, $ArCH_2$), 67.5 ($C_{1''}$), 68.4 (OCH_2 tetrahydropyran), 75.4 (OCH tetrahydropyran), 126.9 ($2CH_{Ar}$), 127.1 (CH_{Ar}), 127.2 ($2CH_{Ar}$), 128.7 ($2CH_{Ar}$), 128.8 ($2CH_{Ar}$), 139.2, 139.6, 140.9 ($3C_{Ar}$), 172.9 (CO).
Chromatography: dichloromethane.
HRMS (ESI): calcd for $(M+Na)^+$: 347.1623. Found: 347.1632.
Anal.: ($C_{21}H_{24}O_3$) C, H, N.

(±)-Tetrahydro-*2H*-pyran-2-ylmethyl 4-(1,1'-biphenyl-4-yl)butanoate (41)

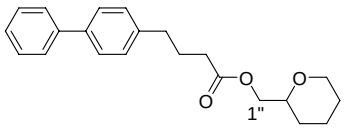

Yield: 71%.
Rf: 0.2 (hexane/chloroform, 1:9).
mp: 51 ºC.
IR (CH_2Cl_2, cm^{-1}): 2938, 2852, 1734, 1179, 1089, 844, 756, 699.
^{1}H-NMR ($CDCl_3$, δ): 1.40-1.49 (m, 5H, 5H tetrahydropyran); 1.78-1.82 (m, 1H, 1H tetrahydropyran); 1.92 (qt, *J* = 7.5 Hz, 2H, $CH_2C\underline{H_2}CH_2$); 2.34 (t, *J* = 7.4 Hz, 2H, CH_2CO); 2.63 (t, *J* = 7.6 Hz, 2H, $ArCH_2$); 3.31-3.49 (m, 2H, 2H tetrahydropyran); 3.90-4.07 (m, 3H, 1H tetrahydropyran, $2H_{1''}$); 7.16-7.18 (m, 2H, $2H_{Ar}$); 7.21-7.27 (m, 1H, $1H_{Ar}$); 7.32-7.38 (m, 2H, $2H_{Ar}$); 7.42-7.45 (m, 2H, $2H_{Ar}$); 7.47-7.51 (m, 2H, $2H_{Ar}$).
^{13}C-NMR ($CDCl_3$, δ): 23.0 (CH_2 tetrahydropyran), 25.8 ($CH_2\underline{C}H_2CH_2$), 26.5, 28.0 ($2CH_2$ tetrahydropyran), 33.6, 34.8 ($ArCH_2$, $\underline{C}H_2CO$), 67.4 ($C_{1''}$), 68.4 (OCH_2 tetrahydropyran), 75.6 (OCH tetrahydropyran), 127.0 ($2CH_{Ar}$), 127.1 (CH_{Ar}), 127.2 ($2CH_{Ar}$), 128.8 ($2CH_{Ar}$), 129.0 ($2CH_{Ar}$), 139.0, 140.6, 141.1 ($3C_{Ar}$), 173.5 (CO).
Chromatography: hexane/chloroform, 1:9.
HRMS (ESI): calcd for $(M+Na)^+$: 361.1780. Found: 361.1777.
Anal.: ($C_{22}H_{26}O_3$) C, H, N.

(±)-Tetrahydro-*2H*-pyran-2-ylmethyl 5-(1,1'-biphenyl-4-yl)pentanoate (42)

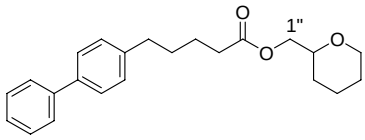

Yield: 54%.
Rf: 0.3 (dichloromethane).
IR (CH_2Cl_2, cm^{-1}): 3028, 2933, 2853, 1735, 1519, 1487, 1177, 1088, 1050, 760, 698.
^{1}H-NMR ($CDCl_3$, δ): 1.35-1.50 (m, 5H, 5H tetrahydropyran); 1.61-1.68 (m, 4H, $(C\underline{H_2})_2CH_2CO$); 1.76-1.81 (m, 1H, 1H tetrahydropyran); 2.33 (t, *J* = 7.1 Hz, 2H, CH_2CO); 2.60 (t, *J* = 7.1 Hz, 2H, $ArCH_2$); 3.32-3.50 (m, 2H, 2H tetrahydropyran); 3.91-4.05 (m, 3H, 1H tetrahydropyran, $2H_{1''}$); 7.16-7.19 (m, 2H, $2H_{Ar}$); 7.23-7.28 (m, 1H, $1H_{Ar}$); 7.32-7.40 (m, 2H, $2H_{Ar}$); 7.42-7.45 (m, 2H, $2H_{Ar}$); 7.48-7.53 (m, 2H, $2H_{Ar}$).
^{13}C-NMR ($CDCl_3$, δ): 23.0 (CH_2 tetrahydropyran), 24.6 (CH_2), 25.8, 27.9 ($2CH_2$ tetrahydropyran), 30.9 (CH_2), 34.1, 35.2 ($ArCH_2$, $\underline{C}H_2CO$), 67.4 ($C_{1''}$), 68.5 (OCH_2 tetrahydropyran), 75.5 (OCH tetrahydropyran), 127.0 ($3CH_{Ar}$), 127.1 ($2CH_{Ar}$), 128.7 ($2CH_{Ar}$), 128.8 ($2CH_{Ar}$), 138.9, 141.3, 141.7 ($3C_{Ar}$), 173.7 (CO).
Chromatography: dichloromethane.
HRMS (ESI): calcd for $(M+Na)^+$: 375.1936. Found: 375.1941.
HPLC-MS: > 95%.

(±)-Tetrahydro-*2H*-pyran-2-ylmethyl 6-(1,1'-biphenyl-4-yl)hexanoate (43)

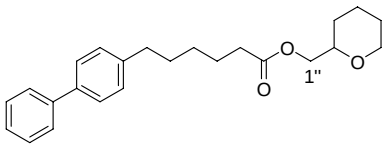

Yield: 29%.
Rf: 0.2 (dichloromethane).
IR (CH_2Cl_2, cm^{-1}): 3029, 2929, 2854, 1733, 1453, 1272, 1180, 1089, 756, 698.
^{1}H-NMR ($CDCl_3$, δ): 1.20-1.66 (m, 11H, $3CH_2$, 5H tetrahydropyran); 1.77-1.80 (m, 1H, 1H tetrahydropyran); 2.29 (t, *J* = 7.5 Hz, 2H, CH_2CO); 2.58 (t, *J* = 7.7 Hz, 2H, $ArCH_2$); 3.32-3.48 (m, 2H, 2H tetrahydropyran); 3.90-4.04 (m, 3H, $2H_{1''}$, 1H tetrahydropyran); 7.15-7.18 (m, 2H, $2H_{Ar}$); 7.22-7.27 (m, 1H, $1H_{Ar}$); 7.32-7.40 (m, 2H, $2H_{Ar}$); 7.42-7.45 (m, 2H, $2H_{Ar}$); 7.48-7.60 (m, 2H, $2H_{Ar}$).
^{13}C-NMR ($CDCl_3$, δ): 23.0 (CH_2 tetrahydropyran), 24.8 (CH_2), 25.8, 27.9 ($2CH_2$ tetrahydropyran), 28.8, 31.1 ($2CH_2$), 34.1, 35.4 ($ArCH_2$, $\underline{C}H_2CO$), 67.4 ($C_{1''}$), 68.5 (OCH_2 tetrahydropyran), 75.5 (OCH tetrahydropyran), 127.0 ($3CH_{Ar}$), 127.1 ($2CH_{Ar}$), 128.7 ($2CH_{Ar}$), 128.8 ($2CH_{Ar}$), 138.7, 141.2, 141.7 ($3C_{Ar}$), 173.9 (CO).
Chromatography: dichloromethane.
HRMS (ESI): calcd for $(M+Na)^+$: 389.2093. Found: 389.2091.
HPLC-MS: > 95%.

(±)-Tetrahydro-*2H*-pyran-2-ylmethyl 7-(1,1'-biphenyl-4-yl)heptanoate (44)

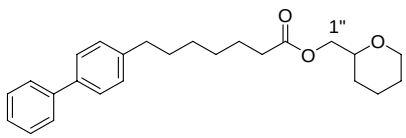

Yield: 32%.
Rf: 0.2 (hexane/ethyl acetate, 9:1).
IR (CH_2Cl_2, cm^{-1}): 3028, 2930, 2853, 1735, 1519, 1177, 1088, 760, 733.
^{1}H-NMR ($CDCl_3$, δ): 1.18-1.41 (m, 6H, $3CH_2$); 1.43-1.66 (m, 7H, CH_2, 5H tetrahydropyran); 1.75-1.80 (m, 1H, 1H tetrahydropyran); 2.28 (t, *J* = 7.5 Hz, 2H, CH_2CO); 2.56 (t, *J* = 7.7 Hz, 2H, $ArCH_2$); 3.32-3.49 (m, 2H, 2H tetrahydropyran); 3.90-4.04 (m, 3H, $2H_{1''}$, 1H tetrahydropyran); 7.15-7.18 (m, 2H, $2H_{Ar}$); 7.21-7.27 (m, 1H, $1H_{Ar}$); 7.32-7.39 (m, 2H, $2H_{Ar}$); 7.41-7.45 (m, 2H, $2H_{Ar}$); 7.47-7.53 (m, 2H, $2H_{Ar}$).
^{13}C-NMR ($CDCl_3$, δ): 23.0 (CH_2 tetrahydropyran), 24.9 (CH_2), 25.8, 27.8 ($2CH_2$ tetrahydropyran), 28.9, 29.0, 31.3 ($3CH_2$), 34.2, 35.5 ($ArCH_2$, $\underline{C}H_2CO$), 67.3 ($C_{1''}$), 68.5 (OCH_2 tetrahydropyran), 75.5 (OCH tetrahydropyran), 126.9 ($2CH_{Ar}$), 127.0 ($3CH_{Ar}$), 128.7 ($2CH_{Ar}$), 128.8 ($2CH_{Ar}$), 138.6, 141.2, 141.9 ($3C_{Ar}$), 173.9 (CO).
Chromatography: hexane/ethyl acetate, 9:1.
HRMS (ESI): calcd for $(M+Na)^+$: 403.2249. Found: 403.2253.
HPLC-MS: > 95%.

(±)-Oxiran-2-ylmethyl (2*E*)-3-(1,1'-biphenyl-4-yl)acrilate (45)

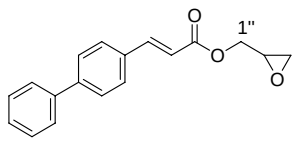

Yield: 41%.
Rf: 0.3 (dichloromethane).
mp: 99 ºC.
IR (CH_2Cl_2, cm^{-1}): 2925, 2852, 1713, 1636, 1450, 1349, 1266, 1187, 1177, 985, 852, 768.
^{1}H-NMR ($CDCl_3$, δ): 2.72 (dd, *J* = 4.9; 2.6 Hz, 1H, 1H oxirane); 2.88-2.92 (m, 1H, 1H oxirane); 3.27-3.35 (m, 1H, 1H oxirane); 4.06 (dd, *J* = 12.3; 6.3 Hz, 1H, $1H_{1''}$); 4.57 (dd, *J* = 12.3; 3.0 Hz, 1H, $1H_{1''}$); 6.51 (d, *J* = 16.0

Hz, 1H, CH-CO); 7.34-7.51 (m, 3H, $3H_{Ar}$); 7.59-7.67 (m, 6H, $6H_{Ar}$); 7.77 (d, *J* = 16.0 Hz, 1H, ArCH).
^{13}C-NMR ($CDCl_3$, δ): 44.8 (CH_2 oxirane), 49.5 (CH oxirane), 65.1 ($C_{1''}$), 117.2 (CHCO), 127.1 ($2CH_{Ar}$), 127.6 (CH_{Ar}), 127.9 ($2CH_{Ar}$), 128.7 ($2CH_{Ar}$), 128.9 ($2CH_{Ar}$), 133.2, 140.1, 143.3 ($3C_{Ar}$), 145.2 (ArCH), 166.7 (CO).
Chromatography: dichloromethane.
HRMS (ESI): calcd for $(M+Na)^+$: 303.0997. Found: 303.0998.
Anal.: ($C_{18}H_{16}O_3$) C, H, N.

(±)-Tetrahydro-*2H*-pyran-2-ylmethyl (2*E*)-3-(1,1'-biphenyl-4-yl)acrilate (46)

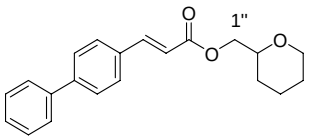

Yield: 60%.
Rf: 0.2 (dichloromethane).
mp: 113-115 ºC.
IR (CH_2Cl_2, cm^{-1}): 2940, 2850, 1712, 1636, 1317, 1175, 1085, 1048, 867, 801.
^{1}H-NMR ($CDCl_3$, δ): 1.30-1.59 (m, 5H, 5H tetrahydropyran); 1.79-1.90 (m, 1H, 1H tetrahydropyran); 3.35-3.46 (m, 1H, 1H tetrahydropyran); 3.49-3.57 (m, 1H, 1H tetrahydropyran); 4.09-4.22 (m, 3H, 1H tetrahydropyran, $2H_{1''}$); 6.48 (d, *J* = 16.0 Hz, 1H, CHCO); 7.26-7.43 (m, 3H, $3H_{Ar}$), 7.52-7.57 (m, 6H, $6H_{Ar}$); 7.68 (d, *J* = 16.0 Hz, 1H, ArCH).
^{13}C-NMR ($CDCl_3$, δ): 23.0, 25.8, 27.9 ($3CH_2$ tetrahydropyran), 67.6 ($C_{1''}$), 68.5 (OCH_2 tetrahydropyran), 75.6 (OCH tetrahydropyran), 117.8 (CHCO), 127.0 ($2CH_{Ar}$), 127.5 ($2CH_{Ar}$), 127.8 (CH_{Ar}), 128.6 ($2CH_{Ar}$), 128.9 ($2CH_{Ar}$), 133.4, 140.2, 143.1 ($3C_{Ar}$), 144.6 (ArCH), 167.1 (CO).
Chromatography: dichloromethane.
HRMS (ESI): calcd for $(M+Na)^+$: 345.1467. Found: 345.1469.
Anal.: ($C_{21}H_{22}O_3$) C, H, N.

(±)-Tetrahydro-2*H*-pyran-2-ylmethyl (3*E*)-4-(1,1'-biphenyl-4-yl)but-3-enoate (47)

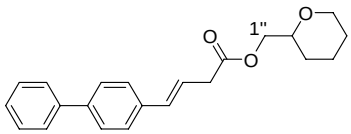

Yield: 69%.
Rf: 0.2 (hexane/dichloromethane, 2:8).
mp: 92-94 ºC.
IR (CH_2Cl_2, cm^{-1}): 3032, 2938, 2852, 1734, 1262, 1162, 1090, 759.
^{1}H-NMR ($CDCl_3$, δ): 1.22-1.56 (m, 5H, 5H tetrahydropyran); 1.77-1.82 (m, 1H, 1H tetrahydropyran); 3.25 (dd, *J* = 6.9; 1.1 Hz, 2H, CH_2CO); 3.34-3.47 (m, 2H, 2H tetrahydropyran), 3.98-4.09 (m, 3H, $2H_{1''}$, 1H tetrahydropyran); 6.28 (dt, *J* = 15.9; 7.0 Hz, 1H, $CHCH_2$); 6.46 (d, *J* = 15.9 Hz, 1H, ArCH), 7.26-7.38 (m, 5H, $5H_{Ar}$), 7.46-7.54 (m, 4H, $4H_{Ar}$).
^{13}C-NMR ($CDCl_3$, δ): 23.0, 25.8, 27.9 ($3CH_2$ tetrahydropyran), 38.3 (CH_2CO), 67.8 ($C_{1''}$), 68.5 (OCH_2 tetrahydropyran), 75.4 (OCH tetrahydropyran), 121.9 ($CHCH_2$), 126.7 ($2CH_{Ar}$), 126.9 ($2CH_{Ar}$), 127.2 ($2CH_{Ar}$), 127.3 (CH_{Ar}), 128.8 ($2CH_{Ar}$), 133.0 (ArCH), 136.3, 140.3, 140.7 ($3C_{Ar}$), 171.6 (CO).
Chromatography: hexane/dichloromethane, 2:8.
HRMS (ESI): calcd for $(M+Na)^+$: 359.1623. Found: 359.1622.
Anal.: ($C_{22}H_{24}O_3$) C, H, N.

(±)-Oxiran-2-ylmethyl (4-benzylphenyl)acetate (49)

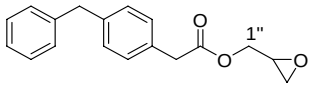

Yield: 71%.
Rf: 0.3 (dichloromethane).
IR (CH_2Cl_2, cm^{-1}): 2922, 2853, 1738, 1147, 1011, 854.
^{1}H-NMR ($CDCl_3$, δ): 2.61 (dd, *J* = 4.8; 2.6 Hz, 1H, 1H oxirane), 2.80-2.84 (m, 1H, 1H oxirane), 3.16-3.24 (m, 1H, 1H oxirane), 3.64 (s, 2H, $ArCH_2CO$), 3.89-3.97 (m, 3H, $ArCH_2Ar$, $1H_{1''}$), 4.43 (dd, *J* = 12.3; 3.0 Hz, 1H, $1H_{1''}$), 7.05-7.25 (m, 9H, $9H_{Ar}$).
^{13}C-NMR ($CDCl_3$, δ): 40.6 ($ArCH_2CO$), 41.5 ($ArCH_2Ar$), 44.6 (OCH_2 oxirane), 49.3 (OCH oxirane), 65.2 ($C_{1''}$), 126.1 (CH_{Ar}), 128.4 ($2CH_{Ar}$), 128.9 ($2CH_{Ar}$), 129.2 ($2CH_{Ar}$), 129.4 ($2CH_{Ar}$), 131.5, 140.1, 141.5 ($3C_{Ar}$), 171.5 (CO).
Chromatography: dichloromethane.
HRMS (ESI): calcd for $(M+Na)^+$: 305.1154. Found: 305.1150.
HPLC-MS: > 95%.

(±)-Oxiran-2-ylmethyl 3-(4-benzylphenyl)propanoate (50)

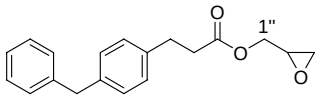

Yield: 75%.
Rf: 0.2 (hexane/dichloromethane, 3:7).
IR (CH_2Cl_2, cm^{-1}): 3020, 2926, 2855, 1737, 1156, 907, 848.
^{1}H-NMR ($CDCl_3$, δ): 2.58-2.70 (m, 3H, 1H oxirane, CH_2CO); 2.79-2.83 (m, 1H, 1H oxirane); 2.90-2.98 (m, 2H, $ArCH_2CH_2$); 3.13-3.21 (m, 1H, 1H oxirane); 3.84-3.95 (m, 3H, $ArCH_2Ar$, $1H_{1''}$); 4.40 (dd, *J* = 12.3; 3.1 Hz, 1H, $1H_{1''}$); 7.07-7.35 (m, 9H, $9H_{Ar}$).
^{13}C-NMR ($CDCl_3$, δ): 30.5, 35.7 (CH_2CO, $ArCH_2CH_2$), 41.6 ($ArCH_2Ar$), 44.7 (CH_2 oxirane), 49.3 (CH oxirane), 65.0 ($C_{1''}$), 126.1 (CH_{Ar}), 128.4 ($2CH_{Ar}$), 128.5 ($2CH_{Ar}$), 128.9 ($2CH_{Ar}$), 129.1 ($2CH_{Ar}$), 138.0, 139.2, 141.2 ($3C_{Ar}$), 172.6 (CO).
Chromatography: hexane/dichloromethane, 3:7.
HRMS (ESI): calcd for $(M+Na)^+$: 319.1310. Found: 319.1302.
HPLC-MS: > 95%.

(±)-Oxiran-2-ylmethyl 4-(4-benzylphenyl)butanoate (51).

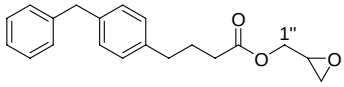

Yield: 76%.
Rf: 0.3 (dichloromethane).
IR (CH_2Cl_2, cm^{-1}): 3019, 2924, 2854, 1737, 1504, 1449, 1177, 1143, 850.
^{1}H-NMR ($CDCl_3$, δ): 1.85 (qt, *J* = 7.3 Hz, 2H, $CH_2CH_2CH_2$); 2.27 (t, *J* = 7.5 Hz, 2H, CH_2CO); 2.49-2.56 (m, 3H, $ArCH_2CH_2$, 1H oxirane); 2.74 (app t, *J* = 6.0 Hz, 1H, 1H oxirane); 3.05-3.13 (m, 1H, 1H oxirane); 3.74-3.89 (m, 3H, $ArCH_2Ar$, $1H_{1''}$); 4.30 (dd, *J* = 12.3; 3.0 Hz, 1H, $1H_{1''}$); 7.07-7.23 (m, 9H, $9H_{Ar}$).
^{13}C-NMR ($CDCl_3$, δ): 26.4 ($CH_2CH_2CH_2$), 33.4, 34.7 (CH_2CO, $ArCH_2$), 41.5 ($ArCH_2Ar$), 44.6 (CH_2 oxirane), 49.3 (CH oxirane), 64.8 ($C_{1''}$), 126.0 (CH_{Ar}), 128.4 ($2CH_{Ar}$), 128.6 ($2CH_{Ar}$), 128.8 ($2CH_{Ar}$), 128.9 ($2CH_{Ar}$), 138.9, 139.0, 141.3 ($3C_{Ar}$), 173.2 (CO).
Chromatography: dichloromethane.
HRMS (ESI): calcd for $(M+Na)^+$: 333.1467. Found: 333.1461.
HPLC-MS: > 95%.

(±)-Oxiran-2-ylmethyl 4-(2-phenylethyl)benzoate (52)

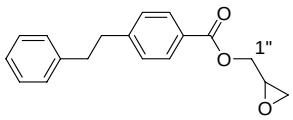

Yield: 75%.
Rf: 0.3 (dichloromethane).

IR (CH_2Cl_2, cm^{-1}): 2921, 2853, 1720, 1458, 1179, 1106, 843.
^{1}H-NMR ($CDCl_3$, δ): 2.65 (dd, *J* = 4.8; 2.6 Hz, 1H, 1H oxirane); 2.79-2.94 (m, 5H, 1H oxirane, $Ar(CH_2)_2Ar$); 3.22-3.30 (m, 1H, 1H oxirane); 4.08 (dd, *J* = 12.3; 6.2 Hz, 1H, $H_{1''}$); 4.57 (dd, *J* = 12.3; 3.0 Hz, 1H, $1H_{1''}$); 7.05-7.23 (m, 7H, $7H_{Ar}$); 7.89 (d, *J* = 8.2 Hz, 2H, $2H_{Ar}$).
^{13}C-NMR ($CDCl_3$, δ): 37.3, 37.7 ($2CH_2Ar$), 44.6 (CH_2 oxirane), 49.4 (CH oxirane), 65.1 ($C_{1''}$), 125.9 (CH_{Ar}), 127.3 (C_{Ar}), 128.2 ($2CH_{Ar}$), 128.3 ($2CH_{Ar}$), 128.5 ($2CH_{Ar}$), 129.7 ($2CH_{Ar}$), 140.9, 147.4 ($2C_{Ar}$), 166.1 (CO).
Chromatography: dichloromethane.
HRMS (ESI): calcd for $(M+Na)^+$: 305.1154. Found: 305.1146.
HPLC-MS: > 95%.

(±)-Tetrahydro-2*H*-pyran-2-ylmethyl (4-benzylphenyl)acetate (53)

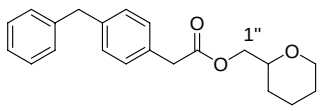

Yield: 69%.
Rf: 0.2 (chloroform).
mp: 65 ºC.
IR (CH_2Cl_2, cm^{-1}): 3026, 2937, 2850, 1736, 1147, 1089, 1012.
^{1}H-NMR ($CDCl_3$, δ): 1.21-1.56 (m, 5H, 5H tetrahydropyran); 1.81-1.86 (m, 1H, 1H tetrahydropyran); 3.36-3.58 (m, 2H, 2H tetrahydropyran); 3.64 (s, 2H, $ArCH_2CO$); 3.96 (s, 2H, $ArCH_2Ar$); 3.98-4.09 (m, 3H, $2H_{1''}$, 1H tetrahydropyran); 7.12-7.33 (m, 9H, $9H_{Ar}$).
^{13}C-NMR ($CDCl_3$, δ): 23.0, 25.8, 27.8 ($3CH_2$ tetrahydropyran), 40.8 ($ArCH_2CO$), 41.6 ($ArCH_2Ar$), 67.8 ($C_{1''}$), 68.4 (OCH_2 tetrahydropyran), 75.4 (OCH tetrahydropyran), 126.1 (CH_{Ar}), 128.5 ($2CH_{Ar}$), 128.9 ($2CH_{Ar}$), 129.1 ($2CH_{Ar}$), 129.4 ($2CH_{Ar}$), 131.8, 139.9, 141.1 ($3C_{Ar}$), 171.8 (CO).
Chromatography: chloroform.
HRMS (ESI): calcd for $(M+Na)^+$: 347.1623. Found: 347.1626.
Anal.: ($C_{21}H_{24}O_3$) C, H, N.

(±)-Tetrahydro-2*H*-pyran-2-ylmethyl 3-(4-benzylphenyl)propanoate (54)

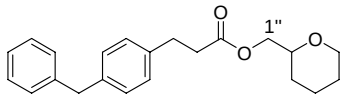

Yield: 76%.
Rf: 0.2 (hexane/dichloromethane, 2:8).
IR (CH_2Cl_2, cm^{-1}): 3023, 2925, 2852, 1735, 1447, 1174, 1090, 855.
^{1}H-NMR ($CDCl_3$, δ): 1.26-1.61 (m, 5H, 5H tetrahydropyran); 1.81-1.86 (m, 1H, 1H tetrahydropyran); 2.62-2.70 (m, 2H, CH_2CO); 2.89-2.96 (m, 2H, $ArCH_2CH_2$); 3.36-3.53 (m, 2H, 2H tetrahydropyran); 3.95-4.13 (m, 5H, $ArCH_2Ar$, 1H tetrahydropyran, $2H_{1''}$); 7.12-7.35 (m, 9H, $9H_{Ar}$).
^{13}C-NMR ($CDCl_3$, δ): 23.0, 25.8, 27.8 ($3CH_2$ tetrahydropyran), 30.5, 35.8 (CH_2CO, $ArCH_2CH_2$), 41.6 ($ArCH_2Ar$), 67.5 ($C_{1''}$), 68.4 (OCH_2 tetrahydropyran), 75.5 (OCH tetrahydropyran), 126.1 (CH_{Ar}), 128.4 ($2CH_{Ar}$), 128.5 ($2CH_{Ar}$), 128.9 ($2CH_{Ar}$), 129.0 ($2CH_{Ar}$), 138.2, 139.1, 141.2 ($3C_{Ar}$), 173.0 (CO).
Chromatography: hexane/dichloromethane, 2:8.
HRMS (ESI): calcd for $(M+Na)^+$: 361.1780. Found: 361.1769.
HPLC-MS: > 95%.

(±)-Tetrahydro-2*H*-pyran-2-ylmethyl 4-(4-benzylphenyl)butanoate (55)

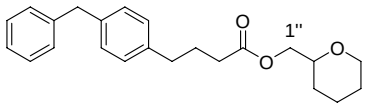

Yield: 75%.
Rf: 0.2 (hexane/ethyl acetate, 8:2).
IR (CH_2Cl_2, cm^{-1}): 3023, 2938, 2851, 1734, 1447, 1089, 772.
^{1}H-NMR ($CDCl_3$, δ): 1.23-1.59 (m, 5H, 5H tetrahydropyran); 1.81-1.96 (m, 3H, 1H tetrahydropyran, $CH_2CH_2CH_2$); 2.34 (t, *J* = 7.4 Hz, 2H, CH_2CO); 2.58 (t, *J* = 7.6 Hz, 2H, $ArCH_2CH_2$); 3.36-3.54 (m, 2H, 2H tetrahydropyran); 3.89-4.08 (m, 5H, 1H tetrahydropyran, $2H_{1''}$, $ArCH_2Ar$); 7.07-7.28 (m, 9H, $9H_{Ar}$).
^{13}C-NMR ($CDCl_3$, δ): 23.0 (CH_2 tetrahydropyran), 25.8 (CH_2), 26.6, 27.9 ($2CH_2$ tetrahydropyran), 33.6, 34.7 (CH_2CO, $ArCH_2CH_2$), 41.6 ($ArCH_2Ar$), 67.4 ($C_{1''}$), 68.4 (OCH_2 tetrahydropyran), 75.5 (OCH tetrahydropyran), 126.0 (CH_{Ar}), 128.5 ($2CH_{Ar}$), 128.6 ($2CH_{Ar}$), 128.9 ($4CH_{Ar}$), 138.8, 139.2, 141.3 ($3C_{Ar}$), 173.6 (CO).
Chromatography: hexane/ethyl acetate, 8:2.
HRMS (ESI): calcd for $(M+Na)^+$: 375.1936. Found: 375.1925.
HPLC-MS: > 95%.

(±)-Tetrahydro-2*H*-pyran-2-ylmethyl 4-(2-phenylethyl)benzoate (56)

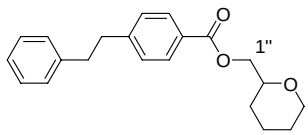

Yield: 74%.
Rf: 0.2 (dichloromethane).
IR (CH_2Cl_2, cm^{-1}): 3029, 2933, 2853, 1718, 1091.
^{1}H-NMR ($CDCl_3$, δ): 1.37-1.61 (m, 5H, 5H tetrahydropyran); 1.81-1.84 (m, 1H, 1H tetrahydropyran); 2.79-2.96 (m, 4H, $Ar(CH_2)_2Ar$); 3.33-3.46 (m, 1H, 1H tetrahydropyran); 3.55-3.66 (m, 1H, 1H tetrahydropyran); 3.93-4.13 (m, 1H, 1H tetrahydropyran); 4.19-4.28 (m, 2H, $2H_{1''}$,); 7.05-7.25 (m, 7H, $7H_{Ar}$); 7.90 (dd, *J* = 6.6; 1.7 Hz, 2H, $2H_{Ar}$).
^{13}C-NMR ($CDCl_3$, δ): 22.9, 25.7, 28.0 ($3CH_2$ tetrahydropyran), 37.3, 37.7 ($2CH_2Ar$), 67.6 ($C_{1''}$), 68.3 (OCH_2 tetrahydropyran), 75.4 (OCH tetrahydropyran), 125.9 (CH_{Ar}), 127.8 (C_{Ar}), 128.2 ($2CH_{Ar}$), 128.3 ($2CH_{Ar}$), 128.4 ($2CH_{Ar}$), 129.7 ($2CH_{Ar}$), 141.0, 147.0 ($2C_{Ar}$), 166.4 (CO).
Chromatography: dichloromethane.
HRMS (ESI): calcd for $(M+Na)^+$: 347.1623. Found: 347.1617.
HPLC-MS: > 95%.

(±)-Oxiran-2-ylmethyl (4-benzoylphenyl)acetate (57)

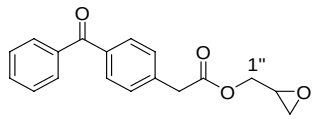

Yield: 72%.
Rf: 0.2 (hexane/ethyl acetate, 7:3).
mp: 76 ºC.
IR (CH_2Cl_2, cm^{-1}): 3059, 2932, 2856, 1739, 1657, 1277, 1155, 928.
^{1}H-NMR ($CDCl_3$, δ): 2.56 (dd, *J* = 4.9; 2.6 Hz, 1H, 1H oxirane); 2.76-2.79 (m, 1H, 1H oxirane); 3.12-3.18 (m, 1H, 1H oxirane); 3.70 (s, 2H, CH_2CO), 3.88 (dd, *J* = 12.3; 6.4 Hz, 1H, $1H_{1''}$); 4.41 (dd, *J* = 12.3; 2.9 Hz, 1H, $1H_{1''}$); 7.33-7.55 (m, 4H, $4H_{Ar}$); 7.68-7.74 (m, 5H, $5H_{Ar}$).
^{13}C-NMR ($CDCl_3$, δ): 41.0 (CH_2CO), 44.6 (CH_2 oxirane), 49.2 (CH oxirane), 65.6 ($C_{1''}$), 128.3 ($2CH_{Ar}$), 129.3 ($2CH_{Ar}$), 130.0 ($2CH_{Ar}$), 130.5 ($2CH_{Ar}$), 132.4 (CH_{Ar}), 136.6, 137.6, 138.3 ($3C_{Ar}$), 170.6 (CO), 196.3 (ArCOAr).
Chromatography: hexane/ethyl acetate, 8:2.
HRMS (ESI): calcd for $(M+Na)^+$: 319.0946. Found: 319.0937.
Anal.: ($C_{18}H_{16}O_3$) C, H, N.

(±)-Oxiran-2-ylmethyl 3-(4-benzoylphenyl)propanoate (58)

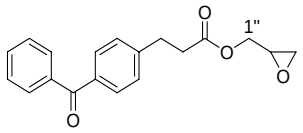

Yield: 78%.
Rf: 0.2 (hexane/ethyl acetate, 7:3).
IR (CH_2Cl_2, cm^{-1}): 3058, 2930, 2858, 1737, 1656, 1604, 1446, 1417, 1176, 928.
^{1}H-NMR ($CDCl_3$, δ): 2.56 (dd, *J* = 4.8; 2.6 Hz, 1H, 1H oxirane); 2.67 (t, *J* = 7.6 Hz, 2H, CH_2CO); 2.76-2.79 (m, 1H, 1H oxirane); 2.99 (t, *J* = 7.6 Hz, 2H, $ArCH_2$); 3.01-3.15 (m, 1H, 1H oxirane); 3.84 (dd, *J* = 12.3; 6.4 Hz, 1H, $1H_{1''}$); 4.38 (dd, *J* = 12.2; 2.9 Hz, 1H, $1H_{1''}$); 7.24-7.73 (m, 9H, $9H_{Ar}$).
^{13}C-NMR ($CDCl_3$, δ): 30.8, 35.2 (CH_2CO, $ArCH_2$), 44.6 (CH_2 oxirane), 49.3 (CH oxirane), 65.2 ($C_{1''}$), 128.3 ($4CH_{Ar}$), 130.0 ($2CH_{Ar}$), 130.5 ($2CH_{Ar}$), 132.3 (CH_{Ar}), 135.8, 137.8, 138.6 ($3C_{Ar}$) 172.4 (CO), 196.9 (ArCOAr).
Chromatography: hexane/ethyl acetate, 7:3.
HRMS (ESI): calcd for $(M+Na)^+$: 333.1103. Found: 333.1093.
HPLC-MS: > 95%.

(±)-Tetrahydro-2*H*-pyran-2-ylmethyl (4-benzoylphenyl)acetate (59)

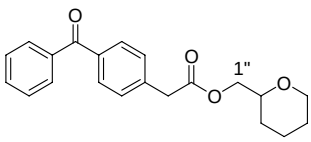

Yield: 68%.
Rf: 0.3 (hexane/ethyl acetate, 7:3).
IR (CH_2Cl_2, cm^{-1}): 3058, 2940, 2851, 1737, 1658, 1154, 1088, 930.
^{1}H-NMR ($CDCl_3$, δ): 1.22-1.56 (m, 5H, 5H tetrahydropyran); 1.83-1.88 (m, 1H, 1H tetrahydropyran); 3.38-3.58 (m, 2H, 2H tetrahydropyran); 3.76 (s, 2H, CH_2CO); 3.99-4.18 (3H, 1H tetrahydropyran, $2H_{1''}$); 7.39-7.63 (m, 5H, $5H_{Ar}$), 7.75-7.81 (m, 4H, $4H_{Ar}$).
^{13}C-NMR ($CDCl_3$, δ): 23.0, 25.7, 27.8 ($3CH_2$ tetrahydropyran), 41.1 (CH_2CO), 68.0 ($C_{1''}$), 68.4 (OCH_2 tetrahydropyran), 75.4 (OCH tetrahydropyran), 128.3 ($2CH_{Ar}$), 129.3 ($2CH_{Ar}$), 130.0 ($2CH_{Ar}$), 130.4 ($2CH_{Ar}$), 132.4 (CH_{Ar}), 136.4, 137.7, 138.7 ($3C_{Ar}$), 170.9 (CO), 196.3 (ArCOAr).
Chromatography: hexane/ethyl acetate, 7:3.
HRMS (ESI): calcd for $(M+Na)^+$: 361.1416. Found: 361.1410.
HPLC-MS: > 95%.

(±)-Tetrahydro-2*H*-pyran-2-ylmethyl 3-(4-benzoylphenylpropanoate (60)

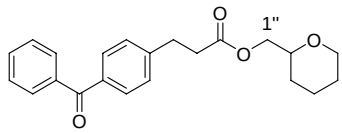

Yield: 62%.
Rf: 0.3 (hexane/ethyl acetate, 7:3).
IR (CH_2Cl_2, cm^{-1}): 3057, 2937, 2852, 1734, 1657, 1604, 1445, 1178, 1088, 930.
^{1}H-NMR ($CDCl_3$, δ): 1.21-1.57 (m, 5H, 5H tetrahydropyran); 1.76-2.02 (m, 1H, 1H tetrahydropyran); 2.66 (t, *J* = 7.6 Hz, 2H, CH_2CO); 2.98 (t, *J* = 7.6 Hz, 2H, $ArCH_2$); 3.32-3.47 (m, 2H, 2H tetrahydropyran); 3.91-4.06 (m, 3H, 1H tetrahydropyran, $2H_{1''}$); 7.19-7.73 (m, 9H, $9H_{Ar}$).
^{13}C-NMR ($CDCl_3$, δ): 22.9, 25.7, 27.8 ($3CH_2$ tetrahydropyran), 30.9, 35.2 (CH_2CO, $ArCH_2$), 67.6 ($C_{1''}$), 68.4 (OCH_2 tetrahydropyran), 75.4 (OCH tetrahydropyran), 128.2 ($2CH_{Ar}$), 128.3 ($2CH_{Ar}$), 130.0 ($2CH_{Ar}$), 130.5 ($2CH_{Ar}$), 132.3 (CH_{Ar}), 135.7, 137.8, 145.6 ($3C_{Ar}$), 172.6 (CO), 196.4 (ArCOAr).
Chromatography: hexane/ethyl acetate, 7:3.

HRMS (ESI): calcd for $(M+Na)^+$: 375.1572. Found: 375.1564.
HPLC-MS: > 95%.

(2*R*)-(-)-Oxiran-2-ylmethyl 6-(1,1´-biphenyl-4-yl)hexanoate (85)

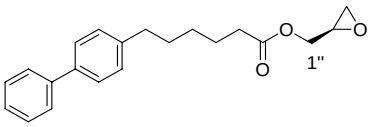

Data of (-)-85 were identical to those recorded for the racemic material 37 except for the optical rotation.
(-)-85: $[\alpha]_D^{20}$ -15.5 (*c* = 1.9, ethanol).
Anal.: ($C_{21}H_{24}O_3$) C, H, N.

(2*S*)-(+)-Oxiran-2-ylmethyl 6-(1,1´-biphenyl-4-yl)hexanoate (86)

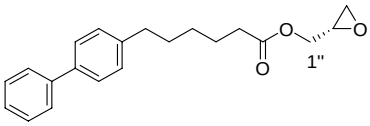

Data of (+)-86 were identical to those recorded for the racemic material 37 except for the optical rotation.
(+)-86: $[\alpha]_D^{20}$ +16.3. (*c* = 1.9, ethanol).
Anal.: ($C_{21}H_{24}O_3$) C, H, N.

(2*R*)-(-)-Oxiran-2-ylmethyl(4-benzylphenyl)acetate (87)

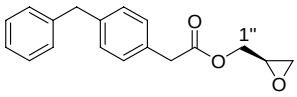

Data of (-)-87 were identical to those recorded for the racemic material 49 except for the optical rotation.
(-)-87: $[\alpha]_D^{20}$ -9.1 (*c* = 1.5, ethanol).
HPLC-MS: > 95%.

(2*S*)-(+)-Oxiran-2-ylmethyl(4-benzylphenyl)acetate (88)

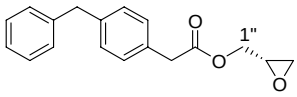

Data of (+)-88 were identical to those recorded for the racemic material 49 except for the optical rotation.
(+)-88: $[\alpha]_D^{20}$ +9.0 (*c* = 1.5, ethanol).
HPLC-MS: > 95%.

4.1.2. Synthesis of final compound 48

(±)-Tetrahydro-2*H*-pyran-2-ylmethyl bromoacetate (84)

Compound 84 was synthesized according to the general procedure described in 4.1.1. (page 55) starting form bromoacetic acid and (±)-tetrahydro-2*H*-pyran-2-ylmethanol.

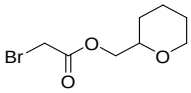

Yield: 78%.
Rf: 0.3 (dichloromethane).
IR (CH_2Cl_2, cm^{-1}): 1733, 1418, 1105, 882.
^{1}H-NMR ($CDCl_3$, δ): 1.48-1.53 (m, 5H, 5H tetrahydropyran); 1.79-1.84 (m, 1H, 1H tetrahydropyran); 3.34-3.52 (m, 2H, 2H tetrahydropyran); 3.82 (s, 2H, $BrCH_2$); 3.92-4.13 (3H, $2H_{1''}$, 1H tetrahydropyran).
^{13}C-NMR ($CDCl_3$, δ): 22.9 (CH_2 tetrahydropyran), 25.7 ($BrCH_2$), 25.9, 27.7 ($2CH_2$ tetrahydropyran), 68.4 ($C_{1''}$), 69.0 (OCH_2 tetrahydropyran), 75.2 (OCH tetrahydropyran), 167.3 (CO).
Chromatography: dichloromethane.
ESI $(M+H)^+$: 237.0, 239.0.

(±)-Tetrahydro-2*H*-pyran-2-ylmethyl (triphenylphosphoranilyden)acetate (83)

A solution of triphenylphosphine (2.3 mmol, 1 equiv) and 84 (1 equiv) in dry dichloromethane (7 mL/mmol) was stirred at rt for 4h. The resulting precipitate was filtered off and washed with diethyl ether. Then, the solid was resuspended in an aqueous solution of 0.5 M NaOH (20 mL/mmol) and stirred for 1h to eliminate HBr. Intermediate 83 was isolated by filtration and used without further purification.

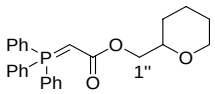

Yield: 45%.
mp: 133-136 ºC.
IR (CH_2Cl_2, cm^{-1}): 3957, 1620, 1332, 1103, 888, 752.
^{1}H-NMR ($CDCl_3$, δ): 1.18-1.44 (m, 5H, 5H tetrahydropyran); 1.68-1.74 (m, 1H, 1H tetrahydropyran); 2.91-3.42 (m, 3H, 2H tetrahydropyran, CHCO); 3.78-3.89 (m, 3H, 1H tetrahydropyran, $2H_{1''}$); 7.34-7.64 (m, 15H, $15H_{Ar}$).
^{13}C-NMR ($CDCl_3$, δ): 23.1, 25.9, 28.1 ($3CH_2$ tetrahydropyran), 30.2 (d, *J* = 125.1 Hz, P=CH), 65.5 ($C_{1''}$), 68.3 (OCH_2 tetrahydropyran), 76.6 (OCH tetrahydropyran), 128.7 (d, *J* = 12.2 Hz, $6CH_{Ar}$), 131.9 (d, *J* = 2.7 Hz, $3CH_{Ar}$), 132.1 (d, *J* = 9.8 Hz, $3C_{Ar}$), 133.0 (d, *J* = 10.1 Hz, $6CH_{Ar}$), 171.3 (d, *J* = 12.9 Hz, CO).
ESI $(M+H)^+$: 419.2.

(±)-Tetrahydro-2*H*-pyran-2-ylmethyl (2*E*)-4-(1,1'-biphenyl-4-yl)but-2-enoate (48)

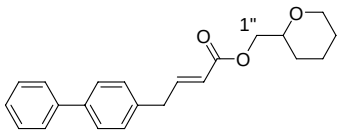

To a solution of (1,1'-biphenyl-4-yl)acetaldehyde (1.0 mmol, 1 equiv) in anhydrous toluene (12 mL/mmol) was added intermediate 83 (1 equiv). The reaction mixture was stirred at reflux for 30 min. The solvent was evaporated under reduced pressure and the product purified by column chromatography on silica gel.

Yield: 67%.
Rf: 0.2 (hexane/dichloromethane, 2:8).
mp: 71 ºC.
IR (CH_2Cl_2, cm^{-1}): 3029, 2936, 2850, 1718, 1653, 1269, 1087, 763.
^{1}H-NMR ($CDCl_3$, δ): 1.18-1.55 (m, 5H, 5H tetrahydropyran); 1.76-1.81 (m, 1H, 1H tetrahydropyran); 3.32-3.53 (m, 4H, $ArCH_2$, 2H tetrahydropyran); 3.91-4.10 (m, 3H, $2H_{1''}$, 1H tetrahydropyran); 5.83 (dt, *J* = 15.6; 1.6 Hz, 1H, CH_2CH=CH); 7.10 (dt, *J* = 15.6; 6.7 Hz, 1H, CHCO); 7.19-7.39 (m, 5H, $5H_{Ar}$); 7.46-7.53 (m, 4H, $4H_{Ar}$).
^{13}C-NMR ($CDCl_3$, δ): 23.0, 25.8, 27.9 ($3CH_2$ tetrahydropyran), 38.1 ($ArCH_2$), 67.4 ($C_{1''}$), 68.4 (OCH_2 tetrahydropyran), 75.5 (OCH tetrahydropyran), 122.2 (CH_2CH=CH), 127.1 ($2CH_{Ar}$), 127.2 (CH_{Ar}), 127.5 ($2CH_{Ar}$), 128.8 ($2CH_{Ar}$), 129.3 ($2CH_{Ar}$), 136.7, 139.7, 140.9 ($3C_{Ar}$), 147.7 (CHCO), 166.5 (CO).
Chromatography: hexane/dichloromethane, 2:8.
HRMS (ESI): calcd for $(M+Na)^+$: 359.1623. Found: 359.1616.
Anal.: ($C_{22}H_{24}O_3$) C, H, N.

4.1.3. General procedure for the synthesis of final compounds 89 and 90

4.1.3.1. Synthesis of intermediates 91 and 92

Intermediates 91 and 92 were synthesized according to general procedure described in 4.1.1. (page 55) starting from the corresponding carboxylic acid (64 or 79, respectively) and 1,3-dibenzyloxypropan-2-ol.

2-(Benzyloxy)-1-[(benzyloxy)methyl]ethyl 6-(1,1'-biphenyl-4-yl)hexanoate (91)

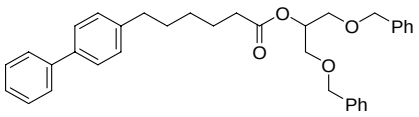

Yield: 30%.
Rf: 0.2 (dichloromethane/hexane, 9:1).
IR (CH_2Cl_2, cm^{-1}): 2921, 2853, 1735, 738, 698.
^{1}H-NMR ($CDCl_3$, δ): 1.27-1.37 (m, 2H, $CH_2(CH_2)_2CO$); 1.53-1.66 (m, 4H, $2CH_2$); 2.27 (t, *J* = 7.5 Hz, 2H, CH_2CO); 2.55 (t, *J* = 7.7 Hz, 2H, $ArCH_2$); 3.57 (d, *J* = 5.1 Hz, 4H, $2CH_2O$); 4.44 (s, 2H, OBn); 4.46 (s, 2H, OBn); 5.14-5.19 (m, 1H, CHO); 7.13-7.51 (m, 19H, $19H_{Ar}$).
^{13}C-NMR ($CDCl_3$, δ): 24.9, 28.8, 31.1 ($3CH_2$), 34.4, 35.4 (Ar-CH_2, CH_2-CO), 68.8 ($2CH_2OBn$), 71.3 (CH), 73.3 ($2OCH_2Ph$), 127.0 ($3CH_{Ar}$), 127.1 ($2CH_{Ar}$), 127.6 ($4CH_{Ar}$), 127.7 ($2CH_{Ar}$), 128.4 ($4CH_{Ar}$), 128.7 ($2CH_{Ar}$), 128.8 ($2CH_{Ar}$), 138.0 ($2C_{Ar}$), 138.7, 141.2, 141.7 ($3C_{Ar}$), 173.4 (CO).
Chromatography: dichloromethane/hexane, 9:1.
ESI $(M+H)^+$: 523.3.

2-(Benzyloxy)-1-[(benzyloxy)methyl]ethyl (4-benzylphenyl)acetate (92)

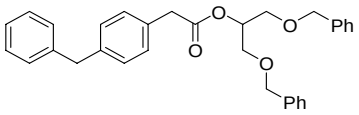

Yield: 40%.
Rf: 0.3 (dichloromethane).
IR (CH_2Cl_2, cm^{-1}): 3029, 2862, 1736, 1149, 735, 699.
^{1}H-NMR ($CDCl_3$, δ): 3.54-3.57 (m, 6H, CH_2CO, 2CH-CH_2O); 3.86 (s, 2H, $ArCH_2Ar$); 4.39 (s, 2H, OBn); 4.41 (s, 2H, OBn); 5.12-5.17 (m, 1H, CHO); 7.01-7.27 (m, 19H, $19H_{Ar}$).
^{13}C-NMR ($CDCl_3$, δ): 41.0 (CH_2CO), 41.6 ($ArCH_2Ar$), 68.7 ($2CHCH_2O$), 72.1 (CH), 73.3 ($2OCH_2Ar$), 126.1 (CH_{Ar}), 127.6 ($4CH_{Ar}$), 127.7 ($2CH_{Ar}$), 128.4 ($4CH_{Ar}$), 128.5 ($2CH_{Ar}$), 129.0 ($2CH_{Ar}$), 129.1 ($2CH_{Ar}$), 129.4 ($2CH_{Ar}$), 131.7 (C_{Ar}), 138.0 ($2C_{Ar}$), 140.0, 141.0 ($2C_{Ar}$), 171.2 (CO).
Chromatography: dichloromethane.
ESI $(M+H)^+$: 481.2.

4.1.3.2. Synthesis of final compounds 89 and 90

To a solution of 1.0 mmol of 91 or 92 in a mixture of dry dichloromethane/absolute ethanol (3:1; 115 mL/mmol), 327 mg/mmol of $Pd(OH)_2$ were added and the mixture was hydrogenated during 3h at rt. The catalyst was filtered off over celite and the solvent evaporated under reduced pressure. The resulting final compounds were purified by column chromatography on silica gel.

2-Hydroxy-1-(hydroxymethyl)ethyl 6-(1,1'-biphenyl-4-yl)hexanoate (89)

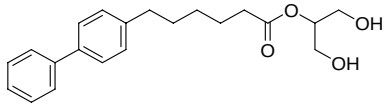

Yield: 28%.
Rf: 0.1 (dichloromethane/ethanol, 9.6:0.4).
IR (CH_2Cl_2, cm^{-1}): 3369, 2924, 2855, 1735, 1176, 744.
^{1}H-NMR ($CDCl_3$, δ): 1.35-1.45 (m, 2H, $CH_2(CH_2)_2CO$); 1.62-1.74 (m, 4H, $2CH_2$); 2.36 (t, *J* = 7.5 Hz, 2H, CH_2CO); 2.65 (t, *J* = 7.6 Hz, 2H, $ArCH_2$); 3.54-3.70 (m, 2H, $2CH_{2a}OH$); 3.80-3.94 (m, 1H, CHO); 4.11-4.22 (m, 2H, $2CH_{2b}OH$); 7.22-7.59 (m, 9H, $9H_{Ar}$).
^{13}C-NMR ($CDCl_3$, δ): 24.8, 28.7, 31.0 ($3CH_2$), 34.1, 35.3 ($ArCH_2$, CH_2CO), 63.4, 65.2 ($2CH_2OH$), 70.3 (CH), 127.0 ($2CH_{Ar}$), 127.1 ($3CH_{Ar}$), 128.7 ($2CH_{Ar}$), 128.8 ($2CH_{Ar}$), 138.7, 141.1, 141.6 ($3C_{Ar}$), 174.2 (CO).
Chromatography: Dichloromethane/ethanol (9.6:0.4).
HRMS (ESI): calcd for $(M+Na)^+$: 365.1729. Found: 365.1709.
HPLC-MS: > 95%

2-Hydroxy-1-(hydroxymethyl)ethyl (4-benzylphenyl)acetate (90)

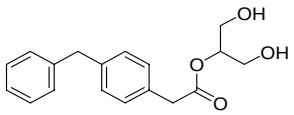

Yield: 70%.
Rf: 0.3 (dichloromethane/ethanol, 9.7:0.3).
mp: 82 ºC.
IR (CH_2Cl_2, cm^{-1}): 3404, 2924, 1732, 1157, 726, 699.
^{1}H-NMR ($CDCl_3$, δ): 2.15 (br s, 2H, 2OH), 3.51-3.93 (m, 5H, $2CH_{2a}OH$, CH_2CO, CH), 3.98 (s, 2H, $ArCH_2Ar$), 4.13-4.24 (m, 2H, $2CH_{2b}OH$), 7.15-7.28 (m, 9H, $9H_{Ar}$).
^{13}C-NMR ($CDCl_3$, δ): 41.2 (CH_2CO), 41.9 ($ArCH_2Ar$), 63.6, 66.1 ($2CH_2OH$), 70.5 (CH), 126.5 (CH_{Ar}), 128.9 ($2CH_{Ar}$), 129.3 ($2CH_{Ar}$), 129.6 ($2CH_{Ar}$), 129.7 ($2CH_{Ar}$), 131.7, 140.7, 141.3 ($3C_{Ar}$), 172.5 (CO).
Chromatography: dichloromethane/ethanol, 9.8:0.2.
HRMS (ESI): calcd for $(M+Na)^+$: 300.1362. Found: 300.1365.
Anal.: ($C_{18}H_{20}O_4$) C, H, N.

4.1.4. Synthesis of 1,1'-biphenyl-4-yl carboxylic acids 61-66

4.1.4.1. Synthesis of 3-(1,1'-Biphenyl-4-yl)propanoic acid (61)

To a solution of 9.0 mmol of (2*E*)-3-(1,1'-biphenyl-4-yl)acrylic acid in anhydrous acetone (6 mL/mmol), 20 mg/mmol of palladium on carbon were added, and the mixture was hydrogenated during 2h at rt. The catalyst was removed by filtration over celite and washed with acetone. The solvent was evaporated under reduced pressure to afford the product as a white solid which was used without further purification.

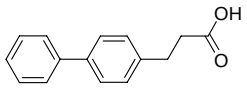

The ^{1}H- and ^{13}C-NMR data correspond with those previously reported.[117]
Yield: 76%.
Rf: 0.3 (dichloromethane/ ethanol, 95:5).
mp: 150 ºC (lit.[117] 147-149 ºC)
IR (CH_2Cl_2, cm^{-1}): 3027, 2923, 1697, 1220, 1176, 756.
^{1}H-NMR ($CDCl_3$, δ): 2.65 (t, 2H, *J* = 7.5 Hz, CH_2-COOH); 2.94 (t, 2H, *J* = 7.5 Hz, Ar-CH_2); 7.18-7.53 (m, 9H, $9H_{Ar}$)
ESI $(M+H)^+$: 327.1.

4.1.4.2. General procedure for the synthesis of carboxylic acids 62-65

General procedure for the synthesis of anhydrides 71 and 72

Under argon atmosphere, a solution of hexanedioic acid or heptanedioic acid (13.6 mmol) in acetic anhydride (2.5 mL/mmol) was stirred at reflux during 4h to yield the corresponding anhydride (71 and 72, respectively). The solvent was evaporated under reduced pressure and the resulting solid used in the next step without further purification.

Oxepane-2,7-dione (71)

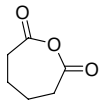

Yield: 77%.
Rf: 0.1 (dichloromethane).
mp: 64 ºC.
^{1}H-NMR ($CDCl_3$, δ): 1.73-1.80 (m, 4H, $2CH_2$); 2.50-2.57 (m, 4H, $2CH_2CO$).

[117] Hardouin, C. Kelso, M.J., Romero, F.A., Rayl, T.J., Leung, D., Hwang, I., Cravatt, B.F., Boger, D.L. *J. Med. Chem.* 2007, *50*, 3359.

Oxocane-2,8-dione (72)

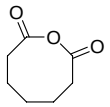

Yield: 71%.
Rf: 0.1 (dichloromethane).
mp: 59 ºC.
^{1}H-NMR ($CDCl_3$, δ): 1.29-1.43 (m, 2H, $(CH_2)_2CH_2(CH_2)_2$), 1.62 (qt, *J* = 7.4 Hz, 4H, 2 $COCH_2CH_2$); 2.40 (t, *J* = 7.2 Hz, 4H, $2COCH_2$).

General procedure for the synthesis of oxocarboxylic acids 67-70

The procedure previously described for the synthesis of 67[118] was used for preparation of all oxocarboxylic acids 67-70. Briefly, to a 100 mL round-bottom flask containing 32 mmol (1 equiv) of the corresponding anhydride and biphenyl (1 equiv), nitrobenzene (1 mL/mmol) was added. The mixture was heated until a clear solution was obtained and then cooled to rt. Afterwards, 2 equiv of powdered anhydrous aluminum trichloride were added slowly while the mixture was being stirred (aprox. 5 min). After stirring was continued for 24h at rt with a HCl trap, the reaction was stopped by adding 5 mL of concentrated HCl. The precipitate was filtered, dried under vacuum, and washed thoroughly with diethylether. The crude product was purified by column chromatography on silica gel.

4-(1,1'-Biphenyl-4-yl)-4-oxobutanoic acid (67)

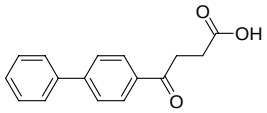

The ^{1}H- and ^{13}C-NMR data correspond with those previously reported.[118,119]
Yield: 32%.
Rf: 0.2 (chloroform/acetone, 2:1).
mp: 183-184 ºC (lit.[119] 185-187 ºC).
IR (CH_2Cl_2, cm^{-1}): 3014, 2923, 1708; 1678, 1267, 1242, 1173.
^{1}H-NMR (DMSO-d^6, δ): 2.63 (t, *J* = 6.4 Hz, 2H, CH_2-COOH); 3.31 (t, *J* = 6.4 Hz, 2H, $COCH_2$); 7.43-7.56 (m, 3H, $3H_{Ar}$), 7.76-7.87 (m, 4H, $4H_{Ar}$), 8.09 (d, *J* = 8.4 Hz, 2H, $2H_{Ar}$); 12.17 (s, OH).
Chromatography: chloroform/ acetone, 2:1.
ESI $(M+H)^+$: 255.1.

5-(1,1'-Biphenyl-4-yl)-5-oxopentanoic acid (68)

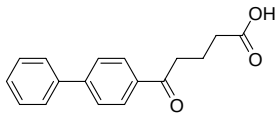

Yield: 31%.
Rf: 0.2 (dichloromethane/acetone, 3:1).
mp: 153 ºC. (lit.[120] 157-158 ºC)
IR (CH_2Cl_2, cm^{-1}): 3059, 2929, 1703, 1674, 1446, 1290, 1192.
^{1}H-NMR ($CDCl_3$, δ): 2.23 (qt, *J* = 7.2 Hz, 2H, $CH_2CH_2CH_2$); 2.65 (t, *J* = 7.1 Hz, 2H, CH_2COOH); 3.23 (t, *J* = 7.1 Hz, 2H, $COCH_2$); 7.47-7.63 (m, 3H, $3H_{Ar}$), 7.72-7.82 (m, 4H, $4H_{Ar}$), 8.15 (d, *J* = 8.6 Hz, 2H, $2H_{Ar}$).
^{13}C-NMR ($CDCl_3$, δ): 19.1 ($CH_2CH_2CH_2$), 33.0, 37.4 (CH_2COOH, $COCH_2$), 127.3 ($4CH_{Ar}$), 128.3 (CH_{Ar}), 128.7 ($2CH_{Ar}$), 129.0 ($2CH_{Ar}$), 139.3, 139.4, 140.9 ($3C_{Ar}$), 178.7 (COOH), 198.9 (ArCO).
Chromatography: dichloromethane/acetone, 3:1.
ESI $(M+H)^+$: 369.1.

[118] Tan, C., Fung, B.M., Cho, G. *J. Am. Chem. Soc*. 2002, *24*, 11827.

[119] Gang, L., Franzén R., Zhang, Q, Xu, Y. *Tetrahedron Lett.* 2005, *46*, 4255.

[120] Bonnler, J.M. *Bull. Soc. Chim. Fr*. 1967, *11*, 4067.

6-(1,1'-Biphenyl-4-yl)-6-oxohexanoic acid (69)

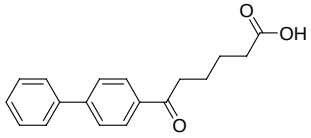

^{1}H-NMR spectroscopic data correspond with those previously reported.[121]
Yield: 23%.
Rf: 0.1 (dichloromethane/ethanol, 9.8:0.2)
mp: 159-162 ºC.
IR (CH_2Cl_2, cm^{-1}): 3057, 2943, 1705, 1679, 1280.
^{1}H-NMR ($CDCl_3$, δ): 1.63-1.74 (m, 4H, $CH_2(CH_2)_2CH_2$); 2.38 (t, *J* = 6.9 Hz, 2H, CH_2COOH); 2.97 (t, *J* = 6.8 Hz, 2H, $COCH_2$); 7.29-7.45 (m, 3H, $3H_{Ar}$); 7.54-7.63 (m, 4H, $4H_{Ar}$); 7.96 (dd, *J* = 6.7; 1.9 Hz, 2H, $2H_{Ar}$).
^{13}C-NMR ($CDCl_3$, δ): 23.6, 24.3 ($COCH_2(CH_2)_2CH_2COOH$), 33.8 ($COCH_2$), 38.1 (CH_2COOH), 127.3 ($4CH_{Ar}$), 128.2 (CH_{Ar}), 128.7 ($2CH_{Ar}$), 129.0 ($2CH_{Ar}$), 135.7, 139.9, 145.7 ($3C_{Ar}$), 179.0 (COOH), 199.4 (ArCO).
Chromatography: Dichloromethane/ethanol, 9.8:0.2
ESI $(M+H)^+$: 383.1.

7-(1,1'-Biphenyl-4-yl)-7-oxoheptanoic acid (70)

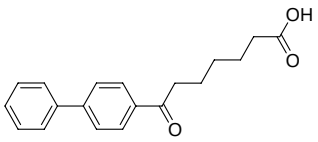

Yield: 20 %.
Rf: 0.4 (dichloromethane/ methanol, 95:5).
mp: 153 ºC.
IR (CH_2Cl_2, cm^{-1}): 3042, 2940, 1698, 1226, 1137.
^{1}H-NMR ($CDCl_3$, δ): 1.49-1.71 (m, 6H, $3CH_2$), 2.38 (t, *J* = 7.0 Hz, 2H, CH_2COOH); 2.95 (t, *J* = 7.6 Hz, 2H, $COCH_2$); 7.15-7.57 (m, 9H, $9H_{Ar}$).
^{13}C-NMR ($CDCl_3$, δ): 24.1, 28.1, 28.7 ($3CH_2$), 33.7 (CH_2COOH), 38.3 ($COCH_2$), 127.2 ($4CH_{Ar}$), 128.1 (CH_{Ar}), 128.6 ($2CH_{Ar}$), 128.9 ($2CH_{Ar}$), 135.4, 138.4, 144.2 ($3C_{Ar}$), 179.6 (COOH), 199.5 (ArCO).
Chromatography: dichloromethane/methanol, 95:5.
ESI $(M+H)^+$: 397.1.

General procedure for the synthesis of carboxylic acids 62-65

The procedure previously described for the synthesis of carboxylic acid 62[118] was used for the preparation of all carboxylic acids 62-65. Amalgamated zinc was prepared from zinc powder contained in a 100 mL round flask: a mixture of 1.3 g of zinc powder, 0.1 g of mercury (II) chloride, 0.06 mL of concentrated HCl and 1.5 mL of water was stirred for 5 min and the liquid was decanted as completely as possible. Then 0.8 mL of water, 2 mL of concentrated HCl, 2 mL of pure toluene and 1 mmol of the corresponding oxocarboxylic acid 67-70 were added consecutively. The reaction mixture was boiled vigorously for 24 hours. During the reflux period, three 0.4 mL of portions of concentrated HCl were added at approximately 6h intervals to maintain the acid concentration. The mixture was allowed to cool to rt to separate into two layers. The aqueous portion was diluted with 10 mL H_2O and extracted several times with diethyl ether. The combined extracts were dried over Na_2SO_4 and the solvent removed under reduced pressure to give the crude product, which was purified by column chromatography on silica gel.

4-(1,1'-Biphenyl-4-yl)butanoic acid (62)

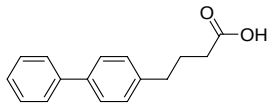

The ^{1}H- and ^{13}C-NMR data correspond with those

[121] U.S. Pat. Appl. Publ. 2005154022, 2005.

previously reported.[118,122]
Yield: 63%.
Rf: 0.1 (dichloromethane/ethanol, 9.8:0.2).
mp: 162 ºC.
IR (CH_2Cl_2, cm^{-1}): 3027, 2949, 1694, 1277, 1210.
^{1}H-NMR ($CDCl_3$, δ): 1.93 (qt, 2H, *J* = 7.5 Hz, $CH_2CH_2CH_2$); 2.34 (t, 2H, *J* = 7.4 Hz, CH_2COOH); 2.65 (t, 2H, *J* = 7.5 Hz, $ArCH_2$); 7.16-7.52 (m, 9H, $9H_{Ar}$).
Chromatography: Dichloromethane/ethanol, 9.8:0.2.
ESI $(M+H)^+$: 241.1.

5-(1,1'-Biphenyl-4-yl)pentanoic acid (63)

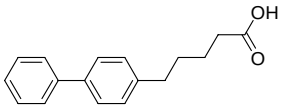

Yield: 64%.
Rf: 0.3 (dichloromethane/acetone, 9:1).
mp: 128 ºC.
IR (CH_2Cl_2, cm^{-1}): 3030, 2934, 1706, 1260, 1191.
^{1}H-NMR ($CDCl_3$, δ): 1.65 (qt, *J* = 3.5 Hz, 4H, $CH_2(CH_2)_2CH_2$), 2.31 (t, 2H, *J* = 6.8 Hz, CH_2COOH); 2.61 (t, 2H, *J* = 6.8 Hz, $ArCH_2$); 7.18-7.53 (m, 9H, $9H_{Ar}$).
^{13}C-NMR ($CDCl_3$, δ): 24.3; 30.8 ($2CH_2$); 33.8; 35.2 (CH_2COOH, $ArCH_2$); 127.0 ($2CH_{Ar}$); 127.1 (CH_{Ar}); 127.3 ($2CH_{Ar}$); 128.7 ($2CH_{Ar}$); 128.8 ($2CH_{Ar}$); 138.9; 141.0, 141.2 ($3C_{Ar}$); 179.2 (COOH).
Chromatography: dichloromethane/acetone, 9:1.
ESI $(M+H)^+$: 255.1.

6-(1,1'-Biphenyl-4-yl)hexanoic acid (64)

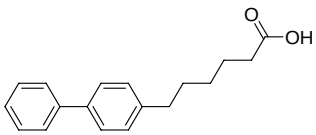

The ^{1}H-NMR data correspond with those previously reported.[121]
Yield: 41%.
Rf: 0.2 (dichloromethane/ethanol, 9.8:0.2)
mp: 103-105 ºC.
IR (CH_2Cl_2, cm^{-1}): 3030, 2933, 1703, 1287.
^{1}H-NMR ($CDCl_3$, δ): 1.30-1.40 (m, 2H, $(CH_2)_2CH_2(CH_2)_2$); 1.56-1.67 (m, 4H, CH_2CH_2COOH, Ar-CH_2-CH_2); 2.29 (t, *J* = 7.5 Hz, 2H, CH_2COOH); 2.59 (t, *J* = 7.6 Hz, 2H, $ArCH_2$); 7.15-7.64 (m, 9H, $9H_{Ar}$).
^{13}C-NMR ($CDCl_3$, δ): 24.5, 28.6, 31.0 ($3CH_2$), 33.8, 35.2 (CH_2CO, $ArCH_2$), 126.9 ($2CH_{Ar}$), 127.0 (CH_{Ar}), 127.2 ($2CH_{Ar}$), 128.6 ($2CH_{Ar}$), 128.7 ($2CH_{Ar}$), 138.7, 141.3, 141.5 ($3C_{Ar}$), 178.1 (COOH).
Chromatography: dichloromethane/ethanol, 9.8:0.2.
ESI $(M+H)^+$: 269.1.

7-(1,1'-Biphenyl-4-yl)heptanoic acid (65)

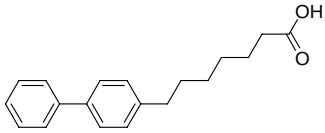

Yield: 68%.
Rf: 0.1 (dichloromethane/ethanol, 99:1).
mp: 69-70 ºC.
IR (CH_2Cl_2, cm^{-1}): 3033, 2926, 1701, 1232, 1130.
^{1}H-NMR ($CDCl_3$, δ): 1.25-1.41 (m, 4H, $2CH_2$); 1.49-1.71 (m, 4H, $2CH_2$), 2.28 (t, *J* = 7.4 Hz, 2H, CH_2COOH); 2.57 (t, 2H, *J* = 7.6 Hz, $ArCH_2$); 7.15-7.57 (m, 9H, $9H_{Ar}$).
^{13}C-NMR ($CDCl_3$, δ): 24.3, 24.6, 28.9, 31.2 ($4CH_2$), 33.9, 35.5 (CH_2COOH, $ArCH_2$), 126.7 (CH_{Ar}), 127.0 ($2CH_{Ar}$), 127.1 ($2CH_{Ar}$), 128.7 ($2CH_{Ar}$), 128.8 ($2CH_{Ar}$), 138.6, 141.2, 141.8 ($3C_{Ar}$), 179.6 (COOH).
Chromatography: dichloromethane/ethanol, 99:1.
ESI $(M+H)^+$: 283.1.

[122] Garfunkle, J., Ezzili, C., Rayl, T.J., Hochstatter, D.G., Hwang, I., Boger, D.L. *J. Med. Chem*. 2008, *51*, 4392.

4.1.4.3. Synthesis of carboxylic acid 66

Methyl 1,1'-biphenyl-4-ylacetate

4-Biphenylacetic acid (9.4 mmol, 1 equiv) was dissolved in methanol (0.25 mL/mmol), and thionyl chloride (2 equiv) was added at 0 °C. The solution was heated at reflux for 2h. The excess of thionyl chloride was removed under vacuum and the resulting residue diluted with ethyl acetate, washed with saturated $NaHCO_3$ and brine and dried over Na_2SO_4. Finally, the solvent was removed under reduced pressure to afford the methyl ester as an oil, which was purified by column chromatography in silica gel.

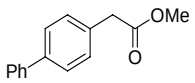

The ^{1}H- and ^{13}C-NMR data correspond with those previously reported.[123]

Yield: 91%.

Rf: 0.6 (dichloromethane).

IR (CH_2Cl_2, cm^{-1}): 3031, 2952, 1737, 1255, 1162, 754.

^{1}H-NMR ($CDCl_3$, δ): 3.72 (s, 2H, CH_2CO); 3.76 (s, 3H, OCH_3); 7.36-7.50 (m, 5H, $5H_{Ar}$); 7.59-7.64 (m, 4H, $4H_{Ar}$).

Chromatography: hexane/dichloromethane, 1:1.

ESI $(M+H)^+$: 227.1.

1,1'-Biphenyl-4-ylacetaldehyde

To a solution of methyl 1,1'-biphenyl-4-ylacetate (9.4 mmol, 1 equiv) in anhydrous toluene (2 mL/mmol) cooled at -78 ºC, a solution of 1.7 M of DIBALH in toluene (1.2 equiv) was added dropwise. The reaction was stirred for 2h at -78ºC and quenched by addition of cold methanol (0.4 mL/mmol). Then, the solution was poured into 50 mL 1M HCl. The mixture was additionally stirred for 15 min and washed with ethyl acetate. The organic layer was dried over anhydrous Na_2SO_4 and the solvent removed under reduced pressure to yield the title compound as an oil which was purified by column chromatography on silica gel.

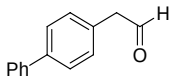

The ^{1}H- and ^{13}C-NMR data correspond with those previously reported.[124]

Yield: 30%.

Rf: 0.4 (dichloromethane).

IR (CH_2Cl_2, cm^{-1}): 3031, 2923, 1718, 1128, 834.

^{1}H-NMR ($CDCl_3$, δ): 3.78 (s, 2H, CH_2), 7.30-7.52 (m, 5H, $5H_{Ar}$), 7.60-7.64 (m, 4H, $4H_{Ar}$), 9.84 (t, J = 2.2 Hz, 1H, CHO).

Chromatography: hexane/dichloromethane, 1:1.

ESI $(M+H)^+$: 197.0.

Methyl (2*E*)-4-(1,1'-biphenyl-4-yl)but-2-enoate (73)

To a solution of 2.5 mmol (1 equiv) of 1,1'-biphenyl-4-ylacetaldehyde in anhydrous toluene (10 mL/mmol), 1 equiv of methyl (triphenylphosphoranylidene)acetate were added and the reaction stirred at reflux for one hour. Then, the reaction was cooled and the solvent removed under reduced pressure to afford the desired ester as a solid which was used in the next step without further purification.

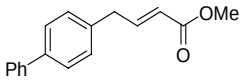

Yield: 90%.

Rf: 0.2 (hexane/dichloromethane, 1:1).

mp: 49-52 ºC.

[123] Schulz, J., Císařová, I., Štěpnička, P. *J. Organomet. Chem*. 2009, *694*, 2519.

[124] Grolla, A.A., Podestà, V., Chini, M.G., Di Micco, S., Vallario, A., Genazzani, A.A., Canonico, P.L., Bifulco, G., Tron, G.C., Sorba, G., Pirali, T. *J. Med. Chem*. 2009, *52*, 2776.

IR (CH_2Cl_2, cm^{-1}): 3028, 2950, 1721, 1654, 1273, 985.
^{1}H-NMR ($CDCl_3$, δ): 3.61 (d, *J* = 6.7 Hz, 2H, CH_2); 3.77 (s, 3H, OCH_3); 5.90 (dt, *J* = 15.6; 1.5 Hz, 1H, CHCO); 7.18 (dt, *J* = 15.5; 6.8 Hz, 1H, CH_2CH); 7.36-7.41 (m, 3H, $3H_{Ar}$), 7.46-7.50 (m, 2H, $2H_{Ar}$); 7.58-7.64 (m, 4H, $4H_{Ar}$).
^{13}C-NMR ($CDCl_3$, δ): 38.1 (CH_2), 51.6 (CH_3), 122.1 (CHCO), 127.1 ($2CH_{Ar}$), 127.3 (CH_{Ar}), 127.5 ($2CH_{Ar}$), 128.8 ($2CH_{Ar}$), 129.2 ($2CH_{Ar}$), 136.7, 139.8, 140.8 ($3C_{Ar}$), 147.5 (CH_2CH), 166.9 (CO).
Chromatography: hexane/dichloromethane, 1:1.
ESI $(M+H)^+$: 253.1.

(3*E*)-4-(1,1'-biphenyl-4-yl)but-3-enoic acid (66)

To a solution of ester 73 (2.2 mmol, 1 equiv) in a mixture of dichloromethane/methanol (9:1, 10 mL/mmol) was added 2M NaOH (1 mL/mmol) and the reaction was stirred at 60 ºC for one hour, when a precipitate appeared. The solvent was removed under reduced pressure and the crude dissolved in water. The solution was washed with diethyl ether. The aqueous phase was acidulated with concentrated HCl and extracted with ethyl acetate. The combined organic phases were dried over Na_2SO_4 and the solvent removed under reduced pressure to obtain the title compound as a solid which was purified by column chromatography on silica gel.

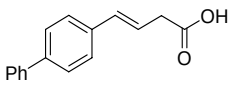

Yield: 83%.
Rf: 0.2 (dichloromethane:ethanol, 95:5).
mp: 183-185 ºC.
IR (CH_2Cl_2, cm^{-1}): 3034, 1703, 1418, 1242.
^{1}H-NMR (CD_3OD, δ): 3.15 (dd, *J* = 7.0; 1.2 Hz, 2H, CH_2CO); 6.28 (dt, *J* = 15.9; 7.0 Hz, 1H, $CHCH_2$); 6.45 (d, *J* = 15.9 Hz, 1H, ArCH); 7.18-7.38 (m, 5H, $5H_{Ar}$), 7.43-7.48 (m, 4H, $4H_{Ar}$).
^{13}C-NMR (CD_3OD, δ): 39.0 (CH_2), 123.6 ($CHCH_2$), 127.8 ($4CH_{Ar}$), 128.1 ($2CH_{Ar}$), 128.3 (ArCH), 129.9 ($2CH_{Ar}$), 133.6 (CH_{Ar}), 137.6, 141.5, 142.0 ($3C_{Ar}$), 175.7 (COOH).
Chromatography: dichloromethane/ethanol, 95:5.
ESI $(M+H)^+$: 239.1.

4.1.5. Synthesis of carboxylic acid 74
[4-(Bromomethyl)phenyl](phenyl)methanone (76)

A solution of (4-methylphenyl)(phenyl)methanone (15.3 mmol, 1 equiv), NBS (1 equiv), and a catalytic amount of benzoyl peroxide (2 mg/mmol) in anhydrous CCl_4 (4 mL/mmol) was stirred at rt for 10 min and then heated under reflux for 4h. Succinimide was filtered off and washed with CCl_4. The combined organic phases were washed with a small amount of water and dried over Na_2SO_4. The solvent was evaporated under reduced pressure and the compound was purified by column chromatography on silica gel.

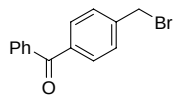

The ^{1}H- and ^{13}C-NMR data correspond with those previously reported.[125]
Yield: 81%.
Rf: 0.3 (hexane/ethyl acetate, 95:5).
mp: 113 ºC (lit.[125] 117 ºC).
IR (CH_2Cl_2, cm^{-1}): 3058, 1657, 744.
^{1}H-NMR ($CDCl_3$, δ): 4.47 (s, 2H, CH_2Br); 7.37-7.63 (m, 5H, $5H_{Ar}$); 7.69-7.75 (m, 4H, $4H_{Ar}$).
Chromatography: hexane/ethyl acetate, 95:5.
ESI $(M+H)^+$: 275.0, 277.0

[125] Podgoršek, A., Stavber, S., Zupan, M, Iskra, J. *Tetrahedron* 2009, *65*, 4429.

(4-Benzoylphenyl)acetonitrile (77)

To a solution of NaCN (10.8 mmol, 2 equiv) in H_2O (3 mL/mmol) was added 76 (1 equiv), dissolved in 1,4-dioxane (6 mL/mmol). The resulting mixture was heated under reflux for 2h. After cooling to rt, the solution was acidified cautiously with 20 mL 1M HCl and extracted four times with ethyl acetate. The combined organic layers were washed with 5% aqueous $NaHCO_3$ solution and brine. After drying over Na_2SO_4 and solvent removal under reduced pressure, the title compound was purified by column chromatography on silica gel.

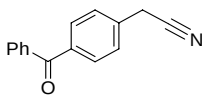

The ^{1}H- and ^{13}C-NMR data correspond with those previously reported.[126]
Yield: 72%.
Rf: 0.3 (dichloromethane).
mp: 72-74 ºC (lit.[109] 64 ºC).
IR (CH_2Cl_2, cm^{-1}): 3052, 2252, 1655.
^{1}H-NMR ($CDCl_3$, δ): 3.78 (s, 2H, CH_2CN); 7.37-7.58 (m, 5H, $5H_{Ar}$); 7.67-7.77 (m, 4H, $4H_{Ar}$).
Chromatography: dichloromethane.
ESI $(M+H)^+$: 222.1.

(4-Benzoylphenyl)acetic acid (74)

A mixture of 77 (4.2 mmol, 1 equiv), 40% aqueous NaOH solution (7 mL/mmol), and absolute ethanol (6 mL/mmol) was heated under reflux for 2h. After cooling to room temperature, the mixture was acidified with concentrated HCl (30 mL) and extracted three times with ethyl acetate. The combined organic layers were washed with water and brine and dried over Na_2SO_4. After removal of the solvent under reduced pressure, the compound was purified by column chromatography on silica gel.

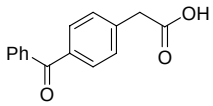

Yield: 83%.
Rf: 0.1 (hexane/ethyl acetate, 1:1).
mp: 113 ºC (lit.[109] 111 ºC).
IR (CH_2Cl_2, cm^{-1}): 3060, 1710, 1655.
^{1}H-NMR ($CDCl_3$, δ): 3.68 (s, 2H, CH_2); 7.32-7.56 (m, 5H, $5H_{Ar}$), 7.69-7.74 (m, 4H, $4H_{Ar}$).
^{13}C-NMR ($CDCl_3$, δ): 40.9 (CH_2), 128.3 ($2CH_{Ar}$), 129.4 ($2CH_{Ar}$), 130.0 ($2CH_{Ar}$), 130.5 ($2CH_{Ar}$), 132.5 (CH_{Ar}), 136.7, 137.5, 137.9 ($3C_{Ar}$), 178.0 (COOH), 196.3 (ArCOAr).
Chromatography: hexane/ethyl acetate, 95:5.
ESI $(M+H)^+$: 241.1.

4.1.6. Synthesis of carboxylic acid 75

Methyl 3-(4-benzoylphenyl)propanoate (78)

Ester 78 was obtained through Friedel-Crafts acylation between benzoyl chloride and methyl 3-(phenyl)propanoate according to the procedure carried out for intermediates 67-70 (page 79) using dichloromethane as solvent.

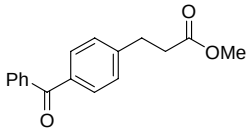

The ^{1}H- and ^{13}C-NMR data correspond with those previously reported.[127]
Yield: 35%.
Rf: 0.3 (dichloromethane).

[126] Wu, L., Hartwig, J.F. *J. Am. Chem. Soc.* 2005, 127, 15824.

[127] de Kort, M., Luijendijk, J., van der Marel, G.A., van Boom, J.H. *Eur. J. Org. Chem.* 2000, 17, 3085.

IR (CH_2Cl_2, cm^{-1}): 3058, 1730, 1657.
^{1}H-NMR ($CDCl_3$, δ): 2.61 (t, *J* = 7.7 Hz, 2H, CH_2CO); 2.96 (t, *J* = 7.6 Hz, 2H, $ArCH_2$); 3.61 (s, 3H, OCH_3); 7.14-7.58 (m, 5H, $5H_{Ar}$); 7.65-7.73 (m, 4H, $4H_{Ar}$).
ESI $(M+H)^+$: 269.1.

3-(4-Benzoylphenyl)propanoic acid (75)

A solution of 2.1 mmol (1 equiv) of ester 78 in 1.5 mL 6M aqueous NaOH was stirred at reflux during 4h. Then, the reaction was cooled with ice and acidulated with 6M HCl in a dropwise manner. Then resulting viscous solid was isolated by filtration and extracted by exhaustive washes with dichloromethane. This organic phase was washed with water, dried with anhydrous Na_2SO_4 and the solvent evaporated under reduced pressure to obtain acid 75 which was used in the next step without further purification.

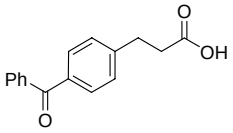

The ^{1}H- and ^{13}C-NMR data correspond with those previously reported.[127]
Yield: 83%.
Rf: 0.1 (hexane/ethyl acetate, 1:1).
IR (CH_2Cl_2, cm^{-1}): 3025, 1705, 1654.
^{1}H-NMR ($CDCl_3$, δ): 2.68 (t, *J* = 7.5 Hz, 2H, CH_2COOH); 2.99 (t, *J* = 7.6 Hz, 2H, $ArCH_2$); 7.25-7.60 (m, 5H, $5H_{Ar}$), 7.67-7.74 (m, 4H, $4H_{Ar}$).
ESI $(M+H)^+$: 255.1.

4.1.7. General procedure for synthesis of carboxylic acids 79 and 80

(4-Benzoylphenyl)acetic (74) or (4-benzoylphenyl)propanoic (75) acids (1 equiv) and KOH (3 equiv) were dissolved in hydrazine monohydrate (0.2 mL/mmol) and ethylenglycol (3 mL/mmol). The reaction was heated to 110 ºC during 2h, followed by 20h at 180 ºC. Then, it was cooled at rt and H_2O was added until only a unique phase is observed. Then, this phase was washed with diethyl ether and concentrated HCl was added (0.7 mL/mmol) and extracted with dichloromethane. The combined organic layers were dried over anhydrous Na_2SO_4, the solvent evaporated under reduced pressure and the resulting product purified by column chromatography on silica gel.

(4-Benzylphenyl)acetic acid (79)

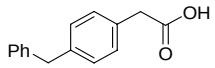

Yield: 58%.
Rf: 0.1 (hexane/ethyl acetate, 1:1).
mp: 123 ºC.
IR (CH_2Cl_2, cm^{-1}): 3060, 1710, 1655.
^{1}H-NMR ($CDCl_3$, δ): 3.54 (s, 2H, CH_2COOH); 3.89 (s, 2H, $ArCH_2Ar$); 7.05-7.25 (m, 9H, $9H_{Ar}$)
^{13}C-NMR ($CDCl_3$, δ): 40.6 (CH_2CO), 41.6 ($ArCH_2Ar$), 126.2 (CH_{Ar}), 128.5 ($2CH_{Ar}$), 128.9 ($2CH_{Ar}$), 129.2 ($2CH_{Ar}$), 129.5 ($2CH_{Ar}$), 130.1, 140.3, 140.9 ($3C_{Ar}$), 177.8 (COOH).
Chromatography: hexane/ethyl acetate, 95:5.
ESI $(M+H)^+$: 227.1.

3-(4-Benzylphenyl)propanoic acid (80)

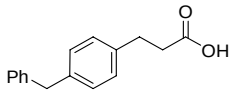

The ^{1}H- and ^{13}C-NMR data correspond with those previously reported.[117]
Yield: 66%.
Rf: 0.1 (hexane/ethyl acetate, 1:1).
mp: 72-75 ºC.
IR (CH_2Cl_2, cm^{-1}): 3027, 2920, 1693, 1438.
^{1}H-NMR ($CDCl_3$, δ): 2.58 (t, *J* = 7.8 Hz, 2H, CH_2COOH);

2.85 (t, *J* = 7.6 Hz, 2H, $ArCH_2$); 3.88 (s, 2H, $ArCH_2Ar$); 6.98-7.25 (m, 9H, $9H_{Ar}$)
Chromatography: hexane/ethyl acetate, 95:5.
ESI $(M+H)^+$: 241.1.

4.1.8. Synthesis of carboxylic acid 81
4-(4-Benzylphenyl)-4-oxobutanoic acid (82)

Intermediate 82 was synthesized through Friedel-Crafts acylation between diphenylmethane and succinic anhydride as described previously for intermediates 67-70 (page 79).

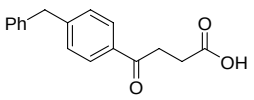

The ^{1}H- and ^{13}C-NMR data correspond with those previously reported.[128]
Yield: 53%.
Rf: 0.4 (dichloromethane/ethanol, 95:5).
mp: 120 ºC (lit.[128] 123 ºC).
IR (CH_2Cl_2, cm^{-1}): 3029, 2920, 1683, 1604, 1238.
^{1}H-NMR ($CDCl_3$, δ): 2.80 (t, *J* = 6.5 Hz, 2H, CH_2COOH); 3.28 (t, *J* = 6.5 Hz, 2H, $COCH_2$); 4.04 (s, 2H, $ArCH_2Ar$); 7.10-7.35 (m, 7H, $7H_{Ar}$); 7.91 (d, *J* = 8.3 Hz, 2H, $2H_{Ar}$).
Chromatography: dichloromethane/ethanol, 95:5.
ESI $(M+H)^+$: 269.1.

4-(4-Benzylphenyl)butanoic acid (81)

Acid 81 was synthesized through reduction of its precursor 82 as described previously for intermediates 62-65 (see page 80).

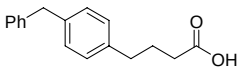

Yield: 71%.
Rf: 0.3 (hexane/ethyl acetate, 1:1).
mp: 88-92 ºC.
IR (CH_2Cl_2, cm^{-1}): 3026, 2946, 1695, 1277.
^{1}H-NMR ($CDCl_3$, δ): 1.87 (qt, *J* = 7.4 Hz, 2H, $CH_2CH_2CH_2$); 2.29 (t, *J* = 7.4 Hz, 2H, CH_2COOH); 2.56 (t, *J* = 7.8 Hz, 2H, $ArCH_2$); 3.87 (s, 2H, $ArCH_2Ar$); 7.03-7.24 (m, 9H, $9H_{Ar}$).
^{13}C-NMR ($CDCl_3$, δ): 26.2 ($CH_2CH_2CH_2$), 33.3, 34.6 ($ArCH_2$, CH_2COOH), 41.6 ($ArCH_2Ar$), 126.1 (CH_{Ar}), 128.5 ($2CH_{Ar}$), 128.6 ($2CH_{Ar}$), 128.9 ($2CH_{Ar}$), 129.0 ($2CH_{Ar}$), 138.8, 138.9, 141.3 ($3C_{Ar}$), 179.4 (CO).
Chromatography: hexane/ethyl acetate, 1:1.
ESI $(M+H)^+$: 255.1.

4.2. Enzyme inhibition assays in brain membrane and soluble fractions

All final compounds were tested for their ability to inhibit 2-OG and AEA hydrolysis using a substrate concentration of 2 μM and the assay procedures described previously.[73] FAAH and MGL assays were undertaken using membrane and cytosolic fractions of rat cerebella. Briefly, cerebella that had been obtained previously and stored frozen were thawed and homogenized in 0.32 M sucrose containing 50 mM sodium phosphate, pH 8.0. Following homogenization, the samples were centrifuged at 100000*g* for 60 min at 4 °C and the supernatants ("cytosolic fractions") were collected. The pellets were resuspended in 50 mM sodium phosphate, pH 8.0 ("membrane fractions") and the fractions were stored frozen in aliquots until used for assay. Protein concentrations for the assays were in the range 1-3 μg/assay, the fractions being diluted with 10 mM Tris-HCl, 1 mM ethylenediaminetetraacetic acid (EDTA), pH 7.2. Each assay consisted of the fraction to be tested, test compound, substrate ([^{3}H]-2-OG or [^{3}H]-AEA labeled in its glycerol or ethanolamine moiety, respectively, final concentration 2 μM), and, when appropriate (for 2-OG-m) 3 μM URB597, in an assay

[128] Høg, S., Wellendorph, P., Nielsen, B., Frydenvang, K., Dahl, I.F., Bräuner-Osborne, H., Brehm, L., Frølund, B., Clausen, R.P. *J. Med. Chem.* 2008, *51*, 8088.

volume of 200 μL. The radiolabeled substrates were obtained from American Radiolabeled Chemicals, St Louis, MO, USA. URB597 was obtained from Cayman Chemical, Ann Arbor, MI, USA. The substrate solution contained fatty acid-free bovine serum albumin (BSA), to give an assay concentration of 0.125% w/v. After incubation for 10 min at 37 °C, reactions were stopped by the addition of 400 μL of chloroform:methanol (1:1 v/v). The tubes were capped, vortex mixed and the phases were separated by centrifugation in a bench centrifuge. Aliquots (200 μL) of the upper phase were taken and tritium content was determined by liquid scintillation spectrometry with quench collection. Results were expressed as % of the activity of controls containing the same volume of solvent carrier.

4.3. hrMGL inhibition assay

This assay was undertaken as described in 4.2. using hrMGL (catalog number 10007812, Cayman Europe) and 0.25 mM 4-nitrophenyl acetate as substrate.

4.4. Measurement of [^{3}H]-2-AG and [^{3}H]-AEA hydrolysis in neurons and microglia homogenates

2-AG was from Cayman Chemical (Ann Arbor, MI, USA). [^{3}H]-2-AG and [^{3}H]-AEA (radiolabeled on their glycerol and ethanolamine moieties, respectively) were from American Radiolabeled Chemicals (St. Louis, MO, USA) and the National Institute on Drug Abuse drug supply system.

BV-2 cells (8 x 10^6) or 2 x 10^6 neurons (in 100 mm dishes) were rinsed once with phosphate buffered saline (PBS), lysed in 1 mL of ice-cold HEPES (250 mM)–sucrose (10 mM) buffer, pH 7.4, and homogenized on ice using a Dounce tissue homogenizer. Homogenates [20 μg of proteins in 400 μL of Tris-HCl (100 mM, pH 7.4)] were added to silanized glass tubes containing either 0.5 μL of drug in DMSO or DMSO alone (0.1%, control). Hydrolysis was initiated by adding 100 μL of [^{3}H]-2-AG (1.25 nM, ≈ 55,000 disintegrations per minute, dpm) or [^{3}H]-AEA (0.8 nM, ≈ 50,000 dpm) in Tris-HCl containing 0.1% fatty acid-free BSA. All additions were done using silanized pipette tips. Tubes were incubated in a shaking water bath at 37 °C. Tubes containing buffer only were used as control for chemical hydrolysis (blank) and this value was systematically subtracted. Reactions were stopped by adding 2 mL of ice-cold chloroform:methanol (1:1 v/v) and the hydrophilic products of the hydrolysis extracted by vigorous mixing and subsequent centrifugation at 800*g* for 10 min. One milliliter of the upper layer was recovered and mixed with Ecoscint (4 mL), and radioactivity was determined by liquid scintillation counting.

4.5. HT-22 cell culture

All reagents were from Gibco. HT-22 cells were grown in Dulbecco's modified Eagle medium (DMEM) supplemented with 10% fetal bovine serum (FBS), 1% non-essential aminoacids, 1% sodium pyruvate, 100 U/mL penicillin and 100 μg/mL streptomycin in a 5% CO_2 humidified atmosphere at 37 ºC. For passage, cells were rinsed with PBS and incubated with 0.125% trypsin, 0.02% EDTA solution for 2 min at 37 ºC. Detached cells were resuspended in DMEM, counted if necessary and splitted onto fresh dishes.

4.6. RT-PCR

RT-PCR was performed using superscript first-strand synthesis kit (Invitrogen). PCR was performed using the adequate forward and reverse primers for CB_1, CB_2, MGL, FAAH and HPRT. Amplicons were separated on agarose gels and visualized using ethidium bromide. Absence of RT-PCR product in the "no RT-PCR" reaction was systematically verified to confirm the lack of genomic DNA in samples.

4.7. Cell transfection

Cells were transfected with plasmid pcDNA 3.1-mouse CB_1 using Escort IV transfection reagent (Sigma Aldrich) following the manufacturer's instructions. Briefly, cells at 50% confluence in 24-well plates were washed twice with 0.5 mL serum- and antibiotic free DMEM and 0.4 mL serum- and antibiotic free DMEM was added. On the meantime, a DNA/liposome (Escort IV) complex solution was prepared to achieve a final concentration of 1 μg DNA/well. 100 mL of the prepared DNA/liposome complex solution were added to each well in a dropwise manner, and cells were cultured for additional 6h under standard culture conditions. Subsequently, 0.5 mL of DMEM containing 20% FBS, 2% non-essential aminoacids, 2% sodium pyruvate, 200 U/mL penicillin and 200 μg/mL streptomycin were added and cells were incubated overnight under standard culture conditions. After that, medium was aspirated and replaced with fresh complete medium. Cells were assayed 48h post-transfection.

4.8. Immunocytochemistry

For immunocytochemistry, cells were washed with 0.5 mL PBS and fixed with 300 μL 2%-paraformaldehyde by incubation for 15 min at rt. Cells were then washed twice with 0.5 mL PBS-T (PBS with 0.1% Triton X-100) and treated with polyclonal rabbit anti-CB_1 (1:1000, ABR, Rockford, IL, USA) in PBS containing 4% FBS for 1h at rt. Then, cells were washed twice with PBS-T and treated with anti-rabbit Alexa Fluor 633 (1:1000, Invitrogen) in PBS containing 1% FBS for 1 hour at rt. Samples were rinsed again 3 times with Tris-buffered solution containing 0.1% Triton X-100, and then, nuclei were stained with bis-benzimide (Höchst 33258, 5 μg/mL in PBS for 15 min at rt). Finally, cells were washed 3 times with PBS, and mounted on glass slides with Immuno-mount (Thermo Scientific, Pittsburgh, PA). Fluorescence images were acquired using Metamorph-Offline 6.2 software (Universal Imaging) in a Zeiss Axioplan 2 microscope with the 40x and 63x (oil inmersion) objectives.

4.9. Excitotoxocity assay

For cell viability assay, cells were passaged onto 96 well-plates (5 x 10^3 cells/100 μL/well) and incubated under standard conditions for 24h. Excitotoxicity was induced by addition of 50 μL of a 20 mM sodium glutamate solution in PBS. Immediately, 50 μL of the solutions containing different concentrations of the compounds under study were added. After 48h, 10 μL of a solution of MTT (5 mg/mL in Hank's buffered salt solution) were added to each well and incubated for 4h. Finally, 100 μL solubilization solution (0.1 M HCl in isopropanol) were added. The plate was shaken and absorbance measured in a microplate reader.

Table 13. Elemental analyses

Cpd	Molecular formula	Calculated			Found		
		C	H	N	C	H	N
1	$C_{23}H_{36}O_3$	76.62	10.06		76.51	9.94	
2	$C_{25}H_{40}O_3$	77.27	10.38		77.17	10.49	
3	$C_{25}H_{40}O_3$	77.27	10.38		77.06	10.21	
4	$C_{26}H_{42}O_4$	74.60	10.11		74.48	10.01	
5	$C_{26}H_{42}O3$	77.56	10.51		77.82	10.67	
6	$C_{25}H_{40}O_3$	77.27	10.38		77.45	10.51	
7	$C_{28}H_{46}O_4$	75.29	10.38		75.31	10.56	
8	$C_{28}H_{38}O_4$	76.68	8.73		76.49	8.74	
9	$C_{21}H_{34}O_3$	75.41	10.25		75.38	10.32	
10	$C_{21}H_{36}O_3$	74.95	10.78		75.07	10.65	
11	$C_{21}H_{38}O_3$	74.51	11.31		74.41	11.47	
12	$C_{19}H_{34}O_3$	73.50	11.04		73.42	11.26	
13	$C_{24}H_{40}O_3$	76.55	10.71		76.29	10.85	
14	$C_{24}H_{42}O_3$	76.14	11.18		76.29	11.35	
15	$C_{24}H_{44}O_3$	75.74	11.65		75.85	11.73	
16	$C_{22}H_{40}O_3$	74.95	11.44		75.06	11.31	
17	$C_{16}H_{14}O_3$	75.57	5.55		75.73	5.39	
18	$C_{16}H_{14}O_3$	75.57	5.55		75.41	5.63	
19	$C_{16}H_{14}O_3$	75.57	5.55		75.52	5.46	
20	$C_{19}H_{20}O_3$	77.00	6.80		77.29	6.69	
21	$C_{19}H_{20}O_3$	77.00	6.80		76.92	6.95	
22	$C_{19}H_{20}O_3$	77.00	6.80		77.32	6.79	
23	$C_{10}H_{10}O_3$	67.41	5.66		67.35	5.74	
24	$C_{13}H_{16}O_3$	70.89	7.32		70.98	7.45	
25	$C_{25}H_{41}NO_2$	77.47	10.66	3.61	77.63	10.58	3.54
26	$C_{26}H_{43}NO_3$	74.77	10.38	3.35	74.64	10.21	3.31
27	$C_{23}H_{36}O_3$	76.62	10.06		76.48	10.11	
28	$C_{23}H_{36}O_3$	76.62	10.06		76.76	9.98	
29	$C_{26}H_{42}O_4$	74.60	10.11		74.56	10.18	
30	$C_{26}H_{42}O_4$	74.60	10.11		74.73	10.01	
31	$C_{25}H_{41}NO_2$	77.47	10.66	3.61	77.58	10.73	3.64
32	$C_{25}H_{41}NO_2$	77.47	10.66	3.61	77.57	10.59	3.59
33	$C_{17}H_{16}O_3$	76.10	6.01		75.10	6.79	
37	$C_{21}H_{24}O_3$	77.75	7.46		78.16	7.56	
38	$C_{22}H_{26}O_3$	78.07	7.74		77.92	7.66	

Table 13. (Continuation)

Cpd	Molecular formula	Calculated			Found		
		C	H	N	C	H	N
39	$C_{20}H_{22}O_3$	77.39	7.14		77.46	7.20	
40	$C_{21}H_{24}O_3$	77.75	7.46		77.61	7.49	
41	$C_{22}H_{26}O_3$	78.07	7.74		77.73	7.58	
45	$C_{18}H_{16}O_3$	77.12	5.75		76.89	6.17	
46	$C_{21}H_{22}O_3$	78.23	6.88		78.19	7.19	
47	$C_{22}H_{24}O_3$	78.54	7.19		78.35	7.22	
48	$C_{22}H_{24}O_3$	70.94	7.58		71.49	6.97	
53	$C_{21}H_{24}O_3$	77.75	7.46		77.69	7.30	
57	$C_{18}H_{16}O_3$	72.96	5.44		72.76	5.51	
85	$C_{21}H_{24}O_3$	77.75	7.46		78.13	7.58	
86	$C_{21}H_{24}O_3$	77.75	7.46		78.09	7.60	
90	$C_{18}H_{20}O_4$	71.98	6.71		71.89	7.02	

Table 14. HPLC-MS analysis of purity

Cpd	Molecular formula	Retention time (min)	MS (ESI) ($[M+H]^+$, m/z)	System
34	$C_{18}H_{18}O_3$	22.7	283.1	Methanol/water
35	$C_{19}H_{20}O_3$	23.7	297.1	Acetonitrile/water
36	$C_{20}H_{22}O_3$	24.6	311.2	Methanol/water
42	$C_{23}H_{28}O_3$	27.0	353.2	Methanol/water
43	$C_{24}H_{30}O_3$	25.2	367.2	Acetonitrile/water
44	$C_{25}H_{32}O_3$	28.9	381.2	Methanol/water
49	$C_{18}H_{18}O_3$	21.4	283.1	Methanol/water
50	$C_{19}H_{20}O_3$	22.7	297.1	Methanol/water
51	$C_{20}H_{22}O_3$	23.5	311.2	Methanol/water
52	$C_{18}H_{18}O_3$	23.6	283.1	Methanol/water
54	$C_{22}H_{26}O_3$	25.3	339.2	Acetonitrile/water
55	$C_{23}H_{28}O_3$	26.3	353.2	Acetonitrile/water
56	$C_{21}H_{26}O_4$	26.1	325.2	Methanol/water
58	$C_{19}H_{18}O_4$	19.1	311.1	Acetonitrile/water
59	$C_{21}H_{22}O_4$	21.4	339.2	Methanol/water
60	$C_{22}H_{24}O_4$	22.6	353.2	Methanol/water
87	$C_{18}H_{18}O_3$	21.4	283.1	Methanol/water
88	$C_{18}H_{18}O_3$	21.4	283.1	Methanol/water
89	$C_{21}H_{26}O_4$	20.6	343.2	Methanol/water

5. CONCLUSIONS

1. In the present work we have designed and synthesized new MGL inhibitors of general structure **Ia-d**.
2. All the synthesized compounds have been assessed for their ability to inhibit 2-AG and AEA hydrolysis.
3. These data have enabled us to perform the first series of systematic SAR studies aimed at the elucidation of the structural requirements involved in the MGL inhibition.
4. The use of some of the synthesized inhibitors, selected among those with the best *in vitro* profile, has confirmed that 2-AG degradation is a complex process which involves multiple enzymes that can be differentially targeted by compounds I. In addition, these compounds have allowed us to identify a novel MGL activity expressed in microglial cells.
5. The neuroprotective effect of selected inhibitors in a glutamate-induced model of excitotoxicity supports the interest of MGL as a therapeutic target for excitotoxicity-associated disorders.
6. Among all the synthesized compounds deserve special attention compounds **37**, **87** and **89**. In particular, derivatives **87** and **89** are dual MGL/FAAH inhibitors and **37** acts as a potent reversible and competitive MGL inhibitor. Therefore, they represent promising lead compounds for further optimization aimed at increasing potency at MGL and selectivity *vs* FAAH, research that it is ongoing in our laboratory.

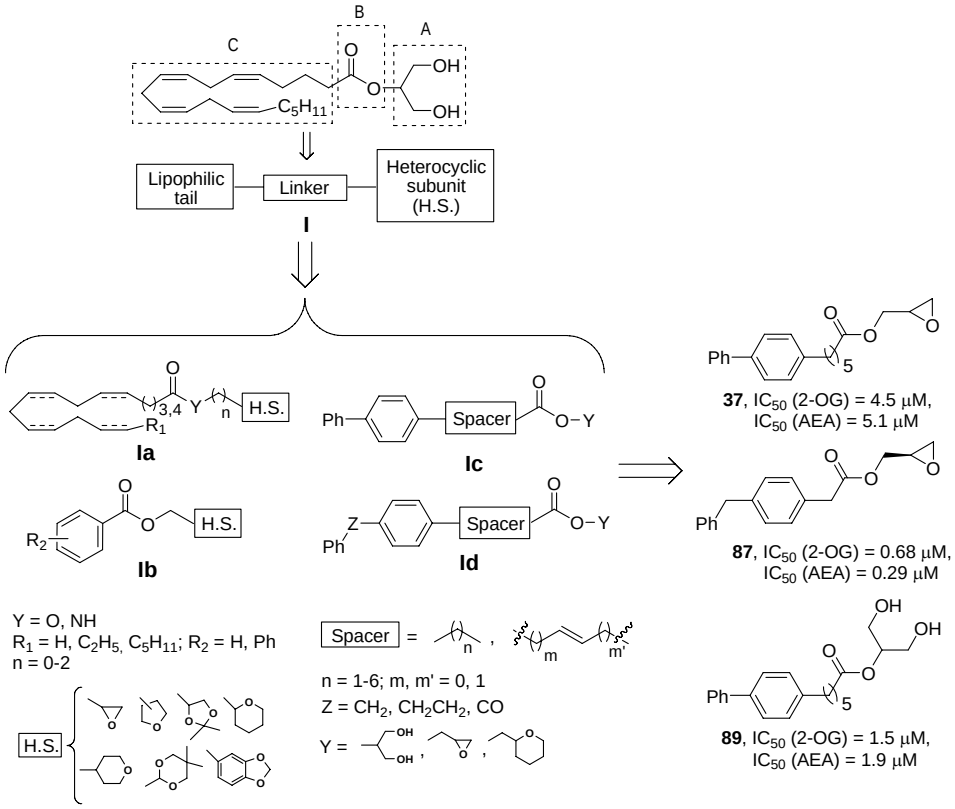

UNIVERSIDAD COMPLUTENSE DE MADRID

FACULTAD DE CIENCIAS QUÍMICAS

Departamento de Química Orgánica I

DESARROLLO DE NUEVOS INHIBIDORES

DE LA ENZIMA LIPASA DE MONOACILGLICÉRIDOS (MGL)

Memoria que para optar al
TÍTULO DE DOCTOR
presenta

José Antonio Cisneros Trigo

Directoras:
Prof. Dra. María Luz López Rodríguez
Dra. Silvia Ortega Gutiérrez

MADRID, 2011

1. INTRODUCCIÓN

1.1. El sistema cannabinoide endógeno (SCE)

La planta *Cannabis sativa* contiene más de 60 fitocannabinoides, tres de los cuales son bioactivos debido a su capacidad para interaccionar con receptores específicos denominados receptores de cannabinoides (CBRs): (-)-Δ^9-tetrahidrocannabinol (THC), cannabinol (CBN) y cannabidiol (CBD). THC es el más conocido ya que es el principal mediador de las propiedades psicotrópicas y adictivas de los cannabinoides, además de modificar procesos fisiológicos esenciales mediante la activación de los CBRs.[1] Sin embargo, esta sustancia también provoca otros efectos no psicotrópicos tales como analgesia, hipotensión, modulación de la respuesta inflamatoria así como influencia en el comportamiento sexual.[1,2]

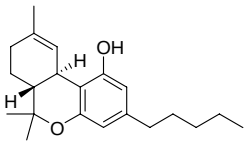

(-)-Δ^9-Tetrahidrocannabinol (THC)

El aislamiento del THC en 1964 por el grupo del profesor Mechoulam[3] representó el primer paso en la investigación sobre cannabinoides, la cual continuó con la descripción de su síntesis total.[4]

Por otro lado, las propiedades antiinflamatorias de *C. sativa* han sido atribuidas a la presencia de CBN y CBD. Por tanto, estos cannabinoides constituyen prometedores cabezas de serie en el desarrollo de fármacos antiinflamatorios de base cannabinoide.[5]

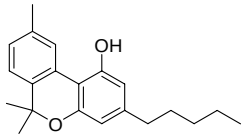

Cannabinol (CBN)

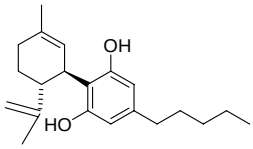

Cannabidiol (CBD)

Durante la última década, la investigación en el área de los cannabinoides se ha dirigido hacia la elucidación de los mecanismos moleculares que median la acción de los cannabinoides en tipos celulares específicos. Así, se han desarrollado potentes herramientas genéticas y farmacológicas que actúan sobre el sistema cannabinoide endógeno (SCE) y que han servido para profundizar en la implicación de este sistema en numerosos procesos patológicos y funciones fisiológicas.[6]

Actualmente, se han descrito cinco CBRs: los molecularmente caracterizados CB_1 y CB_2, el recientemente propuesto GPR55, y otros dos receptores que no han sido caracterizados molecularmente aún.[7]

Ambos receptores CB_1 y CB_2 se encuentran localizados en la membrana plasmática y pertenecen a la superfamilia de receptores de siete segmentos transmembrana acoplados a proteínas G (GPCRs), aunque presentan patrones de expresión diferentes.[8] CB_1 se expresa principalmente en neuronas, mientras que CB_2 se encuentra fundamentalmente en células del sistema inmune (células B, células NK, macrófagos y neutrófilos),[9] aunque experimentos recientes han puesto

---

[1] Howlett, A.C., Barth, F., Bonner, T.I., Cabral, G., Casellas, P., Devane, W.A., Felder, C.C., Herkenham, M., Mackie, K., Martin, B.R., Mechoulam, R., Pertwee, R.G. *Pharmacol. Rev.* 2002, *54*, 161.
[2] (a) Stella, N. *Proc. Natl. Acad. Sci. USA* 2001, *98*, 793. (b) Elmes, S.J.R., Winyard, L.A., Medhurst, S.J., Clayton, N.M., Wilson, A.W., Kendall, D.A., Chapman, V. *Pain* 2005, *118*, 327.
[3] Gaoni, Y., Mechoulam, R. *J. Am. Chem. Soc*. 1964, *86*, 1646.
[4] Mechoulam, R., Gaoni, Y. *J. Am. Chem. Soc*. 1965, *87*, 3273.
[5] (a) Malfait, A.M., Gallily, R., Sumariwalla, P.F., Malik, A.S., Andreakos, E., Mechoulam, R., Feldmann, M. *Proc. Natl. Acad. Sci. USA* 2000, *97*, 9561. (b) Kozela, E., Pietr, M., Juknat, A., Rimmerman, N., Levy, R., Vogel, Z. *J. Biol. Chem*. 2010, *285*, 1616.
[6] Di Marzo, V. *Pharmacol. Res*. 2009, *60*, 77.
[7] Stella, N. *Neuropharmacology* 2009, *56*, 244.
[8] (a) Matsuda, L.A., Lolait, S.J., Brownstein, M.J., Young, A.C., Bonner, T.I. *Nature* 1990, *346*, 561. (b) Munro, S., Thomas, K.L., Abu-Shaar, M. *Nature* 1993, *365*, 61.
[9] Cabral, G.A., Griffin-Thomas, L. *Expert Rev. Mol. Med*. 2009, *11*, e3.

de manifiesto su localización en determinadas regiones del cerebro.[10] Por otro lado, investigaciones recientes apuntan al receptor huérfano GPR55 como un posible CB_3[11] y diversos laboratorios, mediante el uso de ratones *knockout* CB_1, han sugerido la existencia de otro subtipo adicional de CBR. Este receptor no modifica la actividad adenilato ciclasa[12] y es activado por agonistas de cannabinoides. El último grupo de receptores de cannabinoides está formado por los receptores de abnormal-cannabidiol (abn-CBD). Éstos se expresan en células endoteliales de los vasos sanguíneos y se activan por abn-CBD siendo inactivados por CBD y O-1918. Están acoplados a proteínas $G_{i/o}$ e implicados en el incremento de la producción de monofosfato de guanosina cíclico (cGMP), lo que influye en la regulación de la presión sanguínea.[13]

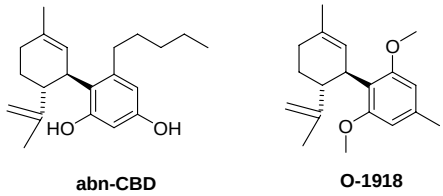

El conocimiento de estos receptores y sus efectos biológicos asociados sugirió la existencia de ligandos endógenos que interaccionaran específicamente con ellos. En 1992 el grupo del profesor Mechoulam identificó el primer endocannabinoide, la *N*-araquidonoiletanolamina, también denominada anandamida (AEA), que se une con elevada afinidad a los receptores CB_1.[14] AEA es considerada un endocannabinoide puesto que: (i) es producida por las células de manera dependiente de actividad, (ii) activa específicamente CBRs, y (iii) experimenta biosíntesis y degradación regulada por enzimas. Así, se ha propuesto la síntesis de este endocannabinoide desde su precursor *N*-araquidonoilfosfatidiletanolamina (NAPE) por una NAPE fosfolipasa D,[15] aunque también se han descrito rutas biosintéticas alternativas.[16]

La AEA ejerce sus efectos en la sinapsis, desde donde es transportada al citosol mediante un proceso de recaptación[17] para ser hidrolizada a ácido araquidónico y etanolamina (Figura 1).

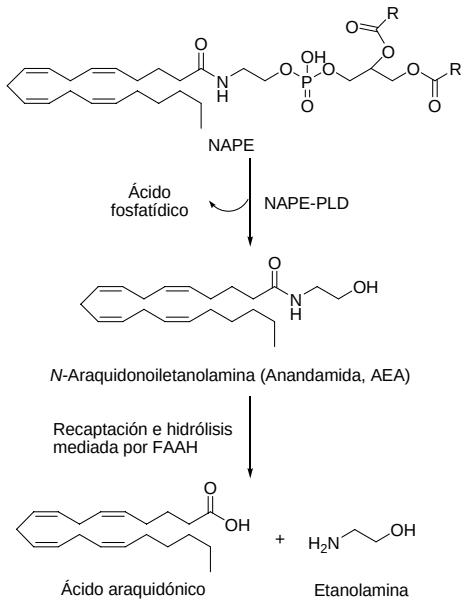

Figura 1. Biosíntesis y degradación de AEA

[10] Van Sickle, M.D., Duncan, M., Kingsley, P.J., Mouihate, A., Urbani, P., Mackie, K., Stella, N., Makriyannis, A., Piomelli, D., Davison, J.S., Marnett, L.J., Di Marzo, V., Pittman, Q.J., Patel, K.D., Sharkey, K.A. *Science* 2005, *310*, 329.

[11] Ross, R.A. *Trends Pharmacol. Sci*. 2009, *30*, 156.

[12] (a) Hoffman, A.F., Macgill, A.M., Smith, D., Oz, M., Lupica, C.R. *Eur. J. Neurosci*. 2005, *22*, 2387. (b) Monory, K., Tzavara, E.T., Leximе, J., Ledent, C., Parmentier, M., Borsodi, A., Hanoune, J. *Biochem. Biophys. Res. Commun*. 2002, *292*, 231.

[13] Begg, M., Mo, F.-M, Offertáler, L., Bátkai, S., Pacher, P., Razdan, R.K., Lovinger, D.M., Kunos, G. *J. Biol. Chem.* 2003, *278*, 46188.

[14] Devane, W.A., Hanus, L., Breuer, A., Pertwee, R.G., Stevenson, L.A., Griffin, G., Gibson, D., Mandelbaum, A., Etinger, A., Mechoulam, R. *Science* 1992, *258*, 1946.

[15] (a) Okamoto, Y., Morishita, J., Tsuboi, K., Tonai, T., Ueda, N. *J. Biol. Chem*. 2004, *279*, 5298. (b) Simon, G.M., Cravatt, B.F. *J. Biol. Chem*. 2008, *283*, 9341.

[16] Ahn, K., McKinney, M.K., Cravatt, B.F. *Chem. Rev*. 2008, *108*, 1687.

[17] Piomelli, D. *Prostaglandins Other Lipid Mediat*. 2005, *77*, 223.

Este paso está mediado principalmente por la enzima amido hidrolasa de ácidos grasos (FAAH),[18] aunque también se han descrito otras rutas que involucran a diferentes enzimas.[19]

En 1995 se identificó el segundo ligando endógeno de los CBRs, 2-araquidonoilglicerol (2-AG, Figura 2), el cual es cerca de cien veces más abundante en cerebro que AEA.[20]

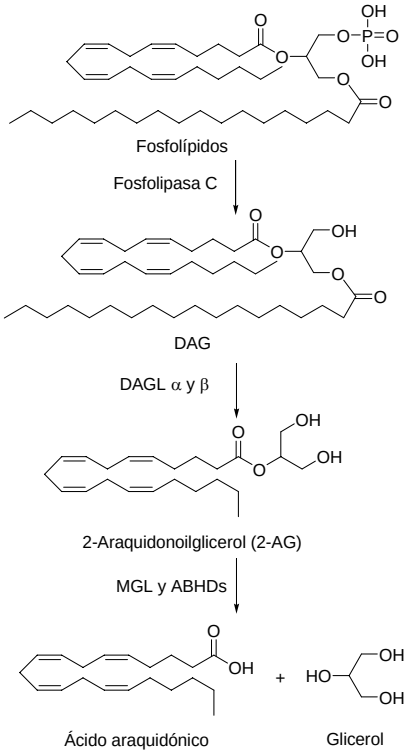

Figura 2. Biosíntesis y degradación de 2-AG

2-AG se biosintetiza fundamentalmente a partir de diacilglicerol (DAG) por la acción de dos diacilglicerol lipasas (DAGL) denominadas α y β. Sin embargo, también han sido descritas rutas alternativas para la biosíntesis de 2-AG.[21]

A diferencia de AEA, 2-AG se une a los receptores CB_1 y CB_2 como agonista total, pero con menor afinidad,[21] comportándose como agonista total sobre los receptores abn-CBD.[7] 2-AG se produce en células postsinápticas, es liberado al espacio sináptico e internalizado al citoplasma de la célula presináptica. La inactivación de este endocannabinoide se puede llevar a cabo mediante tres mecanismos: (i) hidrólisis a ácido araquidónico y glicerol, (ii) oxidación a una serie de derivados oxigenados, y (iii) metabolismo anabólico.[22] De todos ellos, la hidrólisis constituye el mecanismo fundamental, siendo la enzima lipasa de monoacilglicéridos (MGL) la principal responsable.

Adicionalmente se ha propuesto la existencia de otras tres sustancias como endocannabinoides:[23] (i) virodamina, (ii) 2-araquidil gliceril éter (noladin éter) y (iii) *N*-palmitoiletanolamina (PEA).[24]

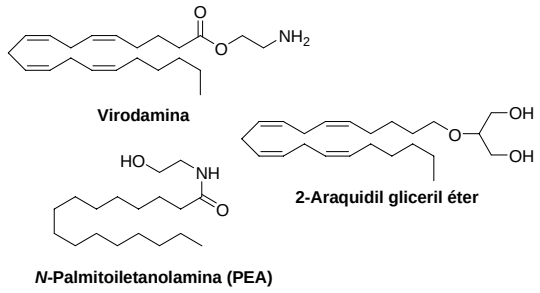

[18] (a) Cravatt, B.F., Demarest, K., Patricelli, M.P., Bracey, M.H., Giang, D.K., Martin, B.R., Lichtman, A.H. *Proc. Natl. Acad. Sci. USA* 2001, *98*, 9371. (b) Cravatt, B.F., Giang, D.K., Mayfield, S.P., Boger, D.L., Lerner, R.A., Gilula, N.B. *Nature* 1996, *384*, 83.

[19] (a) Kim, J., Alger, B.E. *Nat. Neurosci*. 2004, *7*, 697. (b) Starowicz, K., Nigam, S., Di Marzo, V. *Pharmacol. Ther*. 2007, *114*, 13. (c) Snider, N.T., Kornilov, A.M., Kent, U.M., Hollenberg, P.F. *J. Pharmacol. Exp. Ther.* 2007, *321*, 590.

[20] (a) Mechoulam, R., Ben-Shabat, S., Hanus, L., Ligumsky, M., Kaminski, N.E., Schatz, A.R., Gopher, A., Almog, S., Martin, B.R., Compton, D.R., Pertwee, R.G., Griffin, G., Bayewitch, M., Barg, J., Vogel, Z. *Biochem. Pharmacol*. 1995, *50*, 83. (b) Sugiura, T., Kondo, S., Sukagawa, A., Nakane, S., Shinoda, A., Itoh, K., Yamashita, A., Waku, K. *Biochem. Biophys. Res. Commun*. 1995, *215*, 89.

[21] Sugiura, T., Kishimoto, S., Oka, S., Gokoh, M. *Prog. Lipid Res*. 2006, *45*, 405.

[22] Astarita, G., Geaga, J., Ahmed, F., Piomelli, D. *Int. Rev. Neurobiol*. 2009, *85*, 35.

[23] Petrosino, S., Ligresti, A., Di Marzo, V. *Curr. Opin. Chem. Biol*. 2009, *13*, 309.

[24] (a) Hanus, L., Abu-Lafi, S., Fride, E., Breuer, A., Vogel, Z., Shalev, D.E., Kustanovich, I., Mechoulam, R. *Proc. Natl. Acad. Sci. USA* 2001, *98*, 3662. (b) Porter, A.C., Sauer, J.M., Knierman, M.D., Becker, G.W., Berna, M.J., Bao, J., Nomikos, G.G., Carter, P., Bymaster, F.P., Leese, A.B., Felder, C.C. *J. Pharmacol. Exp. Ther*. 2002, *301*, 1020. (c) Mackie, K., Stella, N. *AAPS J*. 2006, *8*, E298.

Todos estos componentes incluyendo receptores, ligandos endógenos y enzimas responsables de su metabolismo constituyen el SCE (Figura 3).

En este contexto, la explotación terapéutica de los CBRs como dianas terapéuticas no resulta sencilla, puesto que se presentan dos problemas principales: (i) los efectos psicotrópicos asociados a la activación de estos receptores, y (ii) la amplia expresión del sistema, de manera que cualquier intervención exógena podría modificar la respuesta de manera indeseada. Esos dos problemas podrían solventarse mediante la regulación de la maquinaria metabólica de los endocannabinoides.

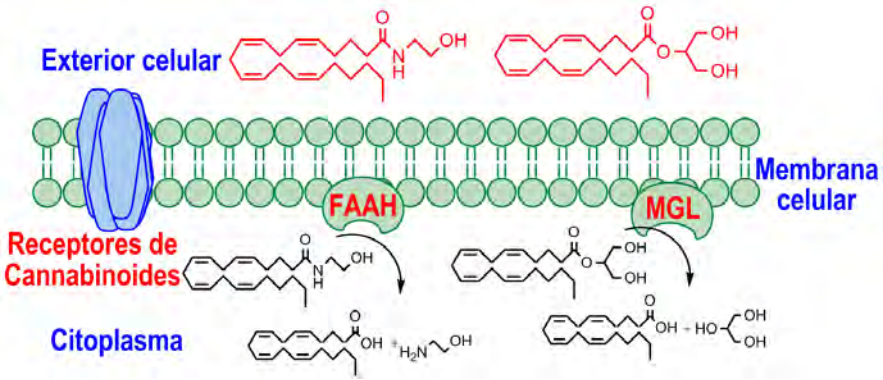

Figura 3. Sistema Cannabinoide Endógeno (SCE)

Así, el incremento en los niveles de AEA ha demostrado relevancia terapéutica en el tratamiento de la nocicepción, daño neuronal, inflamación y síntomas motores asociados a neurodegeneración.[25]

Respecto al 2-AG, en un principio se sugirió la posibilidad de que la enzima FAAH fuera la responsable de la degradación de 2-AG *in vitro*,[26] aunque experimentos posteriores llevados a cabo en ratones FAAH *knockout* descartaron la posibilidad de que esta enzima hidrolizara 2-AG *in vivo*.[27] Diversas evidencias sugieren que la enzima MGL es la principal responsable de esta desactivación biológica del 2-AG: (i) la expresión recombinante de MGL reduce la acumulación de 2-AG en neuronas corticales, (ii) la eliminación por inmunoprecipitación de MGL disminuye la actividad hidrolítica de 2-AG en cerebro de rata a un 50%, y (iii) la técnica de análisis de proteínas basada en actividad (*activity-based protein profiling*, ABPP) ha permitido asignar un 85% de la actividad hidrolítica total de 2-AG en el cerebro a la enzima MGL, estando principalmente localizada en membrana pero también en citosol. La actividad restante se debe principalmente a las hidrolasas α/β-6 (ABHD-6) y α/β-12 (ABHD-12).[28]

Por tanto, aunque el potencial terapéutico de los inhibidores de MGL aún no está definitivamente esclarecido y no se ha dispuesto de modelos *knockout*

[25] (a) Marsicano, G., Goodenough, S., Monory, K., Hermann, H., Eder, M., Cannich, A., Azad, S.C., Cascio, M.G., Ortega-Gutiérrez, S., van der Stelt, M., López-Rodríguez, M.L., Casanova, E., Schütz, G., Zieglgänsberger, W., Di Marzo, V., Behl, C., Lutz, B. *Science* 2003, *302*, 84. (b) Massa, F., Marsicano, G., Hermann, H., Cannich, A., Monory, K., Cravatt, B.F., Ferri, G.L., Sibaev, A., Storr, M., Lutz, B. *J. Clin. Invest*. 2004, *113*, 1202. (c) Lichtman, A.H., Shelton, C.C., Advani, T., Cravatt, B.F. *Pain* 2004, *109*, 319. (d) Ortega-Gutiérrez, S., Molina-Holgado, E., Arévalo-Martín, A., Correa, F., Viso, A., López-Rodríguez, M.L., Di Marzo, V., Guaza, C. *FASEB J*. 2005, *19*, 1338.

[26] Patricelli, M.P., Cravatt, B.F. *Biochemistry* 1999, *38*, 14125.

[27] Lichtman, A.H., Hawkins, E.G., Griffin, G., Cravatt, B.F. *J. Pharmacol. Exp. Ther*. 2002, *302*, 73.

[28] (a) Dinh, T.P., Carpenter, D., Leslie, F.M., Freund, T.F., Katona, I., Sensi, S.L., Kathuria, S., Piomelli, D. *Proc. Natl. Acad. Sci. USA*. 2002, *99*, 10819. (b) Dinh, T.P., Kathuria, S., Piomelli, D. *Mol. Pharmacol*. 2004, *66*, 1260. (c) Blankman, J.L., Simon, G.M., Cravatt, B.F. *Chem. Biol*. 2007, *14*, 1347.

hasta muy recientemente,[29] el desarrollo de inhibidores potentes y selectivos de MGL podría ayudar a la validación definitiva de esta enzima como diana terapéutica.

1.2. Características estructurales y catalíticas de MGL

Esta enzima pertenece a la familia de hidrolasas con un residuo de serina en su centro activo, caracterizada por la presencia de una tríada catalítica clásica formada por residuos de serina (S122), ácido aspártico (D239) e histidina (H269) que conforman el sitio activo de la enzima.

El diseño racional de inhibidores se apoya sobre el conocimiento mecanístico y estructural de la enzima de interés. En este sentido, la estructura tridimensional de la MGL humana (hMGL) ha sido elucidada muy recientemente.[30,31] La hMGL cristalizada consta de 303 aminoácidos con dos moléculas en la unidad asimétrica (Figura 4).

La MGL posee las características estructurales de las α/β hidrolasas. La lámina β central está constituida por siete hebras paralelas y una antiparalela rodeadas de seis hélices α. Este motivo, denominado plegamiento α/β, ha sido identificado en muchas otras enzimas. Un dominio consistente en una *cobertura* (*lid*) se localiza sobre el centro activo y la lámina β. Este dominio está compuesto por dos largas hebras alrededor de la hélice A4 (residuos 156-190, Figura 4). Un dominio equivalente se ha descrito en la enzima FAAH, el cual podría ser la región de la proteína que interacciona con la membrana. En el caso de la MGL, esta hélice anfipática se orienta con su parte hidrofóbica hacia la membrana, lo que hace suponer que desempeña el mismo papel que en FAAH.[30]

Figura 4. Plegamiento global de hMGL (PDB ID: 3HJU)

Actualmente se ha sugerido la idea de que el 2-AG accede al sitio de unión de la MGL a través de la membrana lipídica, proceso favorecido por la flexibilidad del núcleo del plegamiento α/β, y que es conocido como activación interfacial.

Respecto al mecanismo catalítico de las enzimas lipolíticas, se puede considerar como un proceso en dos fases que incluye un primer paso de unión seguido de la hidrólisis del sustrato. La catálisis se inicia por el ataque nucleófilo del grupo hidroxilo de la serina catalítica sobre el carbono carbonílico del sustrato (Figura 5), originando una especie acil-enzima. La desaparición del aducto tetraédrico supone la expulsión del grupo saliente (correspondiente a la subunidad de alcohol) y la generación de un segundo complejo acil-enzima. Finalmente, el paso de desacilación implica el ataque de una molécula de agua que provoca la salida del segundo grupo saliente (correspondiente al ácido) y la recuperación de la enzima (Figura 5, página S6).

---

[29] Schlosburg, J.E., Blankman, J.L., Long, J.Z., Nomura, D.K., Pan, B., Kinsey, S.G., Nguyen, P.T., Ramesh, D., Booker, L., Burston, J.J., Thomas, E.A., Selley, D.E., Sim-Selley, L.J., Liu, Q.S., Lichtman, A.H., Cravatt, B.F. *Nat. Neurosci*. 2010, *13*, 1113.

[30] Labar, G., Bauvois, C., Borel, F., Ferrer, J.L., Wouters, J., Lambert, D.M. *ChemBioChem* 2010, *11*, 218.

[31] Bertrand, T., Augé, F., Houtmann, J., Rak, A., Vallée, F., Mikol, V., Berne, P.F., Michot, N., Cheuret, D., Hoornaert, C., Mathieu, M. *J. Mol. Biol*. 2010, *396*, 663.

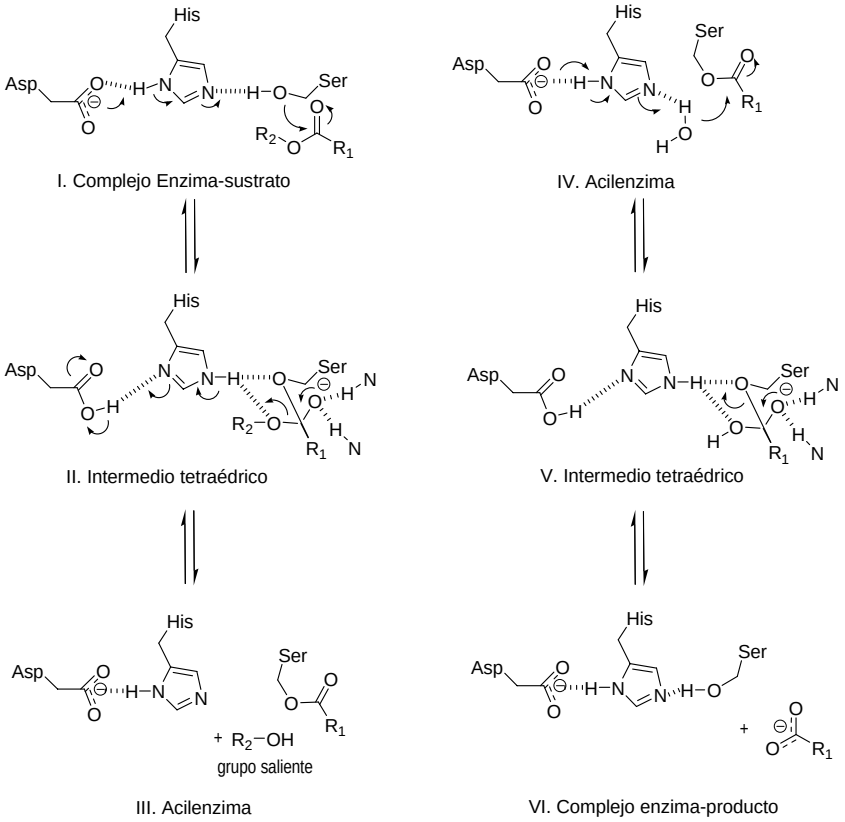

Figura 5. Mecanismo catalítico de MGL

Por otra parte, la homología entre MGL y otras lipasas previamente estudiadas ha facilitado el análisis de la estructura y del mecanismo catalítico de esta enzima. Sin embargo MGL presenta algunas características propias que la diferencian claramente de otras lipasas. Uno de estos aspectos es la especificidad de sustrato. En este sentido, MGL hidroliza 2-monooleolilglicerol con la misma afinidad que 1(3)-monooleoilglicerol, aunque parece presentar preferencia sobre 2-AG respecto a su regioisómero. MGL también hidroliza otros monoésteres diferentes de los de cadena de oleoil- y araquidonoilglicerol.[32] Además, hidroliza preferentemente estos monoésteres frente a AEA, PEA o *N*-oleoiletanolamina, lo cual es consistente con un mejor reconocimiento de 2-monoglicéridos.[33]

1.3. Inhibidores de MGL

A día de hoy se han descrito tan solo unos pocos inhibidores potentes y selectivos. Estos inhibidores se pueden agrupar en tres categorías: inhibidores generales de hidrolasas con serina en su centro activo, análogos del sustrato endógeno, y otras estructuras.

Respecto a los inhibidores generales de hidrolasas con serina en su centro activo podemos distinguir tres grupos reactivos principales: fluorofosfonatos, trifluorometilcetonas y fluoruros de sulfonilo. En general, estos inhibidores, cuyos

[32] (a) Okazaki, T., Sagawa, N., Okita, J.R., Bleasdale, J.E., MacDonald, P.C., Johnston, J.M. *J. Biol. Chem*. 1981, *256*, 7316. (b) Prescott, S.M., Majerus, P.W. *J. Biol. Chem*. 1983, *258*, 764.

[33] Dinh, T.P., Freund, T.F., Piomelli, D. *Chem. Phys. Lipids* 2002, *121*, 149.

compuestos más representativos son araquidonilfluorofosfonato de metilo (MAFP), araquidoniltrifluorometilcetona (ATFMK) y fluoruro de fenilmetanosulfonilo (PMSF) inhiben MGL con valores de CI_{50} de 0.8, 2.5 y 155 μM, respectivamente, pero de forma más débil que FAAH (CI_{50} = 0.0025, 1.9, y 0.9 μM, respectivamente).[34]

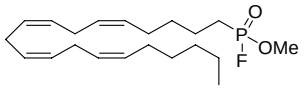

MAFP

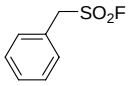

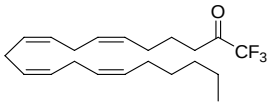

PMSF

ATFMK

Por otra parte, también se ha estudiado la capacidad de distintas series de análogos de 2-AG para inhibir la actividad MGL citosólica. En este sentido, ambos isómeros 2-AG y 1(3)-AG inhiben de forma similar la actividad MGL (CI_{50} = 13 y 17 μM, respectivamente), pero ninguna de las modificaciones posteriores en la cadena de ácido graso ha logrado mejorar ni la potencia ni la selectividad frente a FAAH.[35]

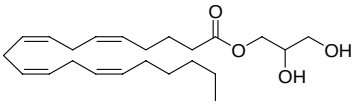

1-Araquidonoilglicerol (1-AG)

Por otro lado, el uso de técnicas de cribado de alto rendimiento (*high throughput screening*, HTS) ha permitido el descubrimiento de inhibidores de MGL cuya estructura no se asemeja a ningún cannabinoide endógeno. URB602 se describió como el primer inhibidor moderado de MGL con selectividad frente a FAAH [CI_{50} (MGL) = 28-75 μM dependiendo de la fuente de enzima, CI_{50} (FAAH) > 100 μM].[36]

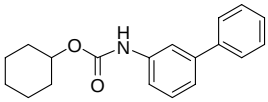

URB602

Basándose en la presencia de grupos tiol libres en el centro activo de la enzima, el grupo de Saario llevó a cabo una aproximación racional para el desarrollo de inhibidores de MGL. Así, se diseñaron varios análogos de maleimida sustituidos en el átomo de nitrógeno con grupos de diferente tamaño y lipofilia.[37] De entre los diferentes compuestos sintetizados destaca *N*-araquidonilmaleimida (NAM, CI_{50} = 140 nM).

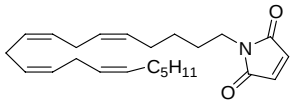

***N*-Araquidonilmaleimida (NAM)**

Asimismo, y con un mecanismo similar de inhibición de MGL, se ha descrito recientemente una nueva clase de inhibidores con estructura de isotiazolona. Entre los compuestos estudiados destacan como inhibidores potentes la octilinona (CI_{50} = 88 nM) y la 2-[(9*Z*)-octadec-9-enil]isotiazol-3(2*H*)-ona (CI_{50} = 43 nM).[38]

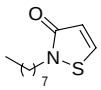

Octilinona

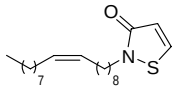

2-[(9*Z*)-octadec-9-enil]isotiazol-3(2*H*)-ona

[34] Viso, A., Cisneros, J.A., Ortega-Gutiérrez, S. *Curr. Top. Med. Chem*. 2008, *8*, 231.
[35] Ghafouri, N., Gunnar, T., Razdan, R.K., Mahadevan, A., Pertwee, R.G., Martin, B.R., Fowler, C.J. *Br. J. Pharmacol.* 2004, *143*, 774.
[36] Hohmann, A.G., Suplita, R.L., Bolton, N.M., Neely, M.H., Fegley, D., Mangieri, R., Krey, J.F., Walker, J.M., Holmes, P.V., Crystal, J.D., Duranti, A., Tontini, A., Mor, M., Tarzia, G., Piomelli, D. *Nature* 2005, *435*, 1108.
[37] Saario, S.M., Salo, O.M.H., Nevalainen, T., Poso, A., Laitinen, J.T., Järvinen, T., Niemi, R. *Chem. Biol.* 2005, *12*, 649.
[38] King, A.R., Lodola, A., Carmi, C., Fu, J., Mor, M., Piomelli, D. *Br. J. Pharmacol.* 2009, *157*, 974.

Más recientemente, JZL184 se ha descrito como un nuevo inhibidor covalente de MGL potente (CI_{50} = 8 nM) y selectivo no sólo frente a FAAH (CI_{50} = 4 μM), sino también frente a un amplio rango de actividades enzimáticas.[39]

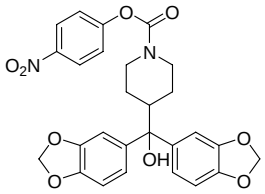

JZL184

Finalmente, estudios farmacológicos han descrito que el bloqueo selectivo de FAAH o MGL puede disociar algunos de los efectos beneficiosos e indeseables de la activación de CB_1.[40] En este campo, el carbamato JZL195 se ha descrito recientemente como un potente inhibidor dual FAAH/MGL (CI_{50} = 2 y 4 nM, respectivamente).[41]

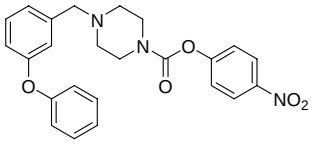

JZL195

1.4. Aplicaciones terapéuticas de los inhibidores de MGL

En los últimos años varios estudios han puesto de manifiesto el importante papel fisiológico del 2-AG. De este modo, el diseño y síntesis de compuestos capaces de inhibir MGL podría ofrecer nuevas perspectivas en la comprensión y el tratamiento de diversas enfermedades. Así, numerosos estudios sugieren que los endocannabinoides son neuroprotectores en diferentes modelos *in vivo* e *in vitro*. Pueden proteger a las neuronas en condiciones de hipoxia, en isquemia cerebral,[42] y también en el modelo de infarto cerebral, donde se encontraron significativamente elevados los niveles de 2-AG, y cuya administración producía una reducción significativa del edema cerebral y el volumen de área infartado.[43] La relación entre 2-AG y epilepsia también se ha estudiado, planteándose la hipótesis de que el 2-AG pudiera inhibir el incremento en el calcio intracelular modulando así varias funciones neuronales.[44] Otro aspecto de interés es la posible implicación del 2-AG en enfermedades neurodegenerativas tales como esclerosis múltiple (EM), donde podría desempeñar un papel importante.[45]

El sistema de recompensa del cerebro constituye otro punto de interés de los endocannabinoides,[46] sugiriéndose que tanto activadores de la síntesis de endocannabinoides como inhibidores de su degradación podrían tener interés para el tratamiento del síndrome de abstinencia de opiáceos.[47] Además, 2-AG podría desempeñar un papel importante en la adicción al alcohol y a otros tipos de sustancias como la

[39] (a) Long, J.Z., Li, W., Booker, L., Burston, J.J., Kinsey, S.G., Schlosburg, J.E., Pavón, F.J., Serrano, A.M., Selley, D.E., Parsons, L.H., Lichtman, A.H., Cravatt, B.F. *Nat. Chem. Biol.* 2008, *5*, 37. (b) Long, J.Z., Nomura, D.K., Cravatt, B.F. *Chem. Biol.* 2009, *16*, 744.

[40] Long, J.Z., Nomura, D.K., Vann, R.E., Walentiny, D.M., Booker, L., Jin, X., Burston, J.J., Sim-Selley, L.J., Lichtman, A.H., Wiley, J.L., Cravatt, B.F. *Proc. Natl. Acad. Sci. USA*. 2009, *106*, 20270.

[41] Long, J.Z., Jin, X., Adibekian, A., Li, W., Cravatt, B.F. *J. Med. Chem.* 2010, *53*, 1830.

[42] Degn, M., Lambertsen, K.L., Petersen, G., Meldgaard, M., Artmann, A., Clausen, B.H., Hansen, S.H., Finsen, B., Hansen, H.S., Lund, T.M. *J. Neurochem.* 2007, *103*, 1907.

[43] Shohami, E., Mechoulam, R. *Proc. Natl. Acad. Sci. USA* 2006, *103*, 6087.

[44] Deshpande, L.S., Blair, R.E., Ziobro, J.M., Sombati, S., Martin, B.R., DeLorenzo, R.J. *Eur. J. Pharmacol.* 2007, *558*, 52.

[45] (a) Baker, D., Pryce, G., Croxford J.L., Brown, P., Pertwee, R.G., Makriyannis, A., Khanolkar, A., Layward, L., Fezza, F., Bisogno, T., Di Marzo, V. *FASEB J.* 2001, *15*, 300. (b) Cabranes, A., Venderova, K., de Lago, E., Fezza, F., Sanchez, A., Mestre, L., Valenti, M., Garcia-Merino, A., Ramos, J. A., Di Marzo, V., Fernandez-Ruiz, J. *Neurobiol. Dis.* 2005, *20*, 207.

[46] Navarrete, M., Araque, A. *Neuron* 2008, *57*, 883.

[47] Viganò, D., Valenti, M., Cascio, M.G., Di Marzo, V., Parolaro, D., Rubino, T. *Eur. J. Neurosci.* 2004, *20*, 1849.

marihuana, nicotina y cocaína mediante la activación de las mismas vías de recompensa.[48]

Por otro lado, los endocannabinoides han sido implicados en el control del balance energético e ingesta alimenticia y sus efectos han sido descritos como mediados principalmente por CB_1.[49] Considerando el papel desempeñado por los endocannabinoides en la red que regula el control alimenticio, la manipulación de sus niveles podría ofrecer aproximaciones útiles en el tratamiento de los desórdenes alimenticios y el síndrome metabólico.[50]

Asimismo, el SCE está implicado en cáncer puesto que juega un papel muy importante en el control de la decisión supervivencia/muerte celular.[51] 2-AG inhibe la proliferación de líneas celulares de cáncer de próstata humano,[52] y recientemente se ha descrito la sobreactivación de MGL en tumores primarios y en líneas tumorales clasificadas como altamente agresivas.[53] Estos datos indican que MGL regula una red de señales lipídicas oncogénicas que promueven la migración celular, invasión, supervivencia y crecimiento tumoral *in vivo*. El bloqueo genético o farmacológico de MGL en estas células agresivas disminuye el carácter maligno de las mismas.

Por otra parte, la inhibición de FAAH y MGL reduce la nocicepción sin inducir alteraciones comportamentales.[54]

Finalmente hay que apuntar el papel de 2-AG en el sistema inmune, y en particular su efecto en la estimulación de la motilidad de las células NK. Esta migración puede ser bloqueada por la presencia de antagonistas de CB_2.[55]

En este contexto, el desarrollo de inhibidores potentes y selectivos de MGL resulta fundamental para el estudio, validación y explotación de esta enzima como diana terapéutica. Es primordial establecer si esta(s) enzima(s) son susceptibles de inhibición sin comprometer la actividad de otras enzimas relacionadas. Adicionalmente, sería necesario determinar si existe más de una actividad MGL, y si éste es el caso, si la inhibición de sólo una de ellas sería terapéuticamente relevante para inducir incrementos significativos en los niveles de 2-AG. Finalmente, otro aspecto importante reside en establecer los efectos del aumento no sólo en los niveles de 2-AG, sino, simultáneamente, en los niveles de ambos endocannabinoides (2-AG y AEA). Por lo tanto, el desarrollo de inhibidores selectivos de MGL y de inhibidores duales MGL/FAAH es un objetivo de gran interés en la actualidad.

---

[48] Schlosburg, J.E., Carlson, B.L., Ramesh, D., Abdullah, R.A., Long, J.Z., Cravatt, B.F., Lichtman, A.H. *AAPS J.* 2009, *11*, 342.

[49] Di Marzo, V., Matias, I. *Nat. Neurosci.* 2005, *8*, 585.

[50] Bellocchio, L., Lafenêtre, P., Cannich, A., Cota, D., Puente, N., Grandes, P., Chaouloff, F., Piazza, P.V., Marsicano, G. *Nat. Neurosci*. 2010, *13*, 281.

[51] (a) López-Rodríguez, M.L., Viso, A., Ortega-Gutiérrez, S., Díaz-Laviada, I. *Mini Rev. Med. Chem*. 2005, *5*, 97. (b) Pisanti, S., Bifulco, M. *Pharmacol. Res*. 2009, *60*, 107.

[52] Endsley, M.P., Aggarwal, N., Isbell, M.A., Wheelock, C.E., Hammock, B.D., Falck, J.R., Campbell, W.B., Nithipatikom, K. *Int. J. Cancer* 2007, *121*, 984.

[53] Nomura, D.K., Long, J.Z., Niessen, S., Hoover, H.S., Ng, S.W., Cravatt, B.F. *Cell* 2010, *140*, 49.

[54] (a) Naidu, P.S., Kinsey, S.G., Guo, T., Cravatt, B.F., Lichtman, A.H. *J. Pharmacol. Exp. Ther*. 2010, *334*, 182. (b) Kinsey, S.G., Long, J.Z., O'Neal, S.T., Abdullah, R.A., Poklis, J.L., Boger, D.L., Cravatt, B.F., Lichtman, A.H. *J. Pharmacol. Exp. Ther*. 2009, *330*, 902.

[55] (a) Kishimoto, S., Muramatsu, M., Gokoh, M., Oka, S., Waku, K., Sugiura, T. *J. Biochem. (Tokyo)* 2005, *137*, 217. (b) Pandey, R., Mousawy, K., Nagarkatti, M., Nagarkatti, P. *Pharmacol. Res*. 2009, *60*, 85.

2. OBJETIVOS

El objetivo principal de este trabajo consiste en la elucidación de los requisitos estructurales implicados en el reconocimiento de los sustratos por la enzima MGL. Este estudio de relación estructura actividad (SAR) ayudaría al desarrollo de nuevos inhibidores que permitirían la validación de MGL como diana terapéutica.

La consecución de este objetivo implica las siguientes etapas:

1. Diseño de nuevos inhibidores de MGL.
2. Síntesis de nuevos compuestos de estructura general I. Éstos comprenden derivados de ácido graso **Ia** y derivados aromáticos **Ib-d**.
3. Determinación de la capacidad de los compuestos **Ia-d** para inhibir la hidrólisis de 2-AG y AEA.
4. Estudio SAR.
5. Estudio de diferentes actividades hidrolíticas de 2-AG en diferentes tipos celulares mediante el uso de inhibidores seleccionados.
6. Determinación del efecto neuroprotector de compuestos seleccionados con el fin de confirmar el interés de la enzima MGL como diana terapéutica.
7. Estudio del mecanismo de inhibición de los inhibidores óptimos.

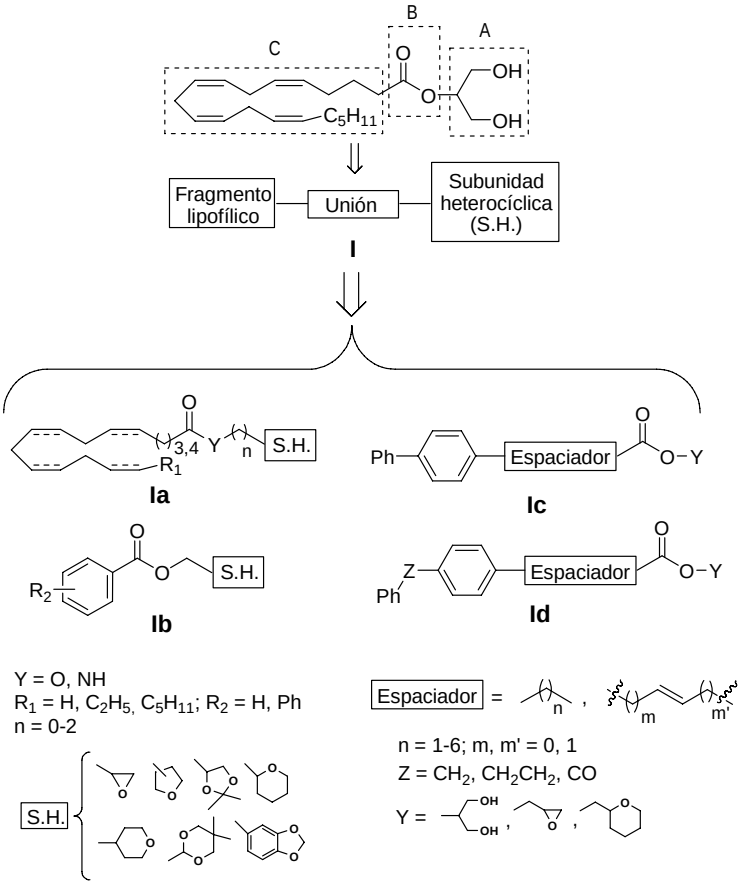

3. RESULTADOS Y DISCUSIÓN

Al inicio de este proyecto, la información sobre la enzima MGL era escasa: no se conocía la estructura tridimensional, no se disponía de inhibidores potentes y selectivos ni se habían realizado estudios SAR sistemáticos. En este contexto basamos nuestro diseño en el sustrato endógeno de la enzima, el endocannabinoide 2-AG. La evaluación biológica de estos compuestos en términos de su capacidad para inhibir la degradación de 2-AG y AEA nos permitió llevar a cabo el primer estudio SAR sistemático con el objetivo de esclarecer los requisitos estructurales involucrados en la inhibición de la hidrólisis de 2-AG.[56]

Posteriores modificaciones de los compuestos óptimos de esta serie y ayudados por modelos de *docking* basados en la estrctura tridimensional de la enzima recientemente elucidada, nos han permitido optimizar los compuestos de la primera serie así como identificar nuevos inhibidores de la hidrólisis de 2-AG con valores de concentración inhibitoria 50 (CI_{50}) en el rango submicromolar.[57] Otra cuestión importante era establecer si la capacidad inhibitoria de los compuestos se debía a la inhibición directa de la enzima o bien a otras actividades hidrolíticas de 2-AG. Este factor es importante puesto que, aunque el 85% de la actividad hidrolítica de 2-AG se atribuye a la enzima MGL,[28] otras hidrolasas están presentes y aún debe ser establecida su importancia en diferentes tipos celulares y/o tejidos. Así, se ha seleccionado un subconjunto de compuestos para el cual se ha estudiado su capacidad para bloquear la hidrólisis de 2-AG en fracciones de membrana y en neuronas, así como para inhibir directamente la enzima MGL humana expresada de forma recombinante (MGLhr). Estos resultados han revelado una variedad de perfiles de inhibición *in vitro* para estos compuestos, lo que los convierte en un conjunto de herramientas útiles para intentar identificar otras actividades hidrolíticas de 2-AG así como para empezar a validar la enzima MGL como una diana terapéutica. Así, en este contexto, los inhibidores sintetizados[56,57] nos han permitido identificar una nueva actividad MGL expresada en microglía,[58] y estudiar la hidrólisis de 2-AG en neuronas.[59] Finalmente, experimentos *in vitro* preliminares en un modelo celular de excitotoxicidad sugieren que estos compuestos son neuroprotectores, resultado que apoya el potencial terapéutico de MGL y nos ha conducido a iniciar una serie de estudios mecanísticos encaminados a obtener datos sobre el tipo de inhibición.[57] Esta información es crítica para establecer el potencial de los inhibidores obtenidos hasta el momento para su uso como herramientas en modelos *in vitro* o bien como fármacos en modelos *in vivo*.

3.1. Diseño y síntesis de compuestos de estructura general I

Tal y como se ha comentado, en ausencia de un *hit* de MGL y de la estructura tridimensional de la enzima, hemos tomado como punto de partida la estructura del 2-AG y hemos diseñado una serie de ésteres y amidas donde la subunidad de glicerol se ha sustituido por diferentes subunidades heterocíclicas con el objetivo de introducir variaciones estructurales que mimeticen el fragmento de glicerol (A). Además, se ha estudiado el efecto de modificaciones en la cadena de ácido graso (C) así como en el enlace éster (B) (Figura 6, página S12).

[56] Cisneros, J.A., Vandevoorde, S., Ortega-Gutiérrez, S., Paris, C., Fowler, C.J., López-Rodríguez, M.L. *J. Med. Chem.* 2007, *50*, 5012.
[57] Cisneros, J.A. *et al. J. Med. Chem.* En preparación.
[58] Muccioli, G.G., Xu, C., Odah, E., Cudaback, E., Cisneros, J.A., Lambert, D.M., López-Rodríguez, M.L., Bajjalieh, S., Stella, N. *J. Neurosci.* 2007, *27*, 2883.
[59] Marrs, W.R., Horne, E.A., Ortega-Gutiérrez, S., Cisneros, J.A., Xu, C., Lin, Y.H., Muccioli, G.G., López-Rodríguez, M.L., Stella, N. *J. Biol. Chem.* 2010, enviado.

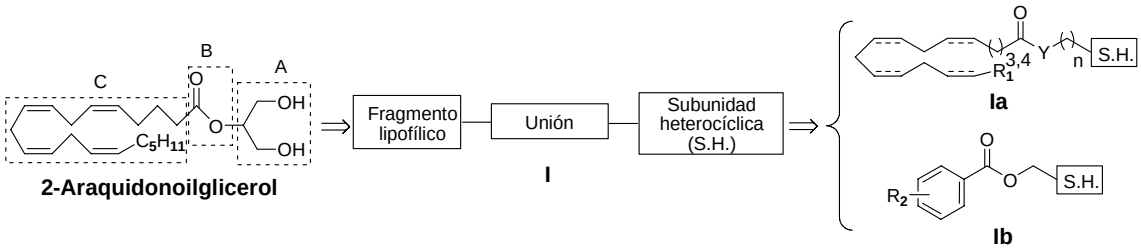

Figura 6.

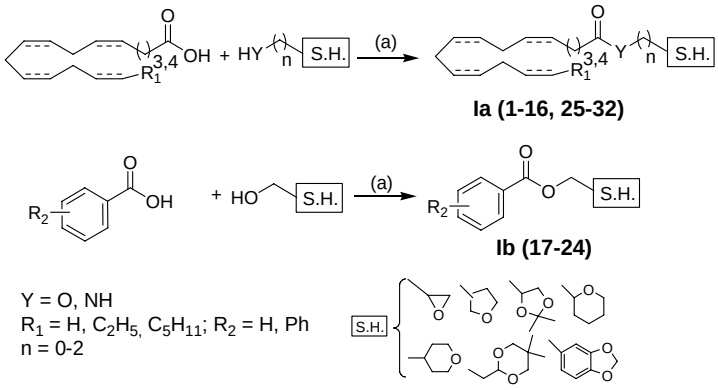

Reactivos y condiciones: (a) DCC, DMAP, CH_2Cl_2, Ar, t.a.

Esquema 1.

La síntesis de ésteres y amidas **Ia,b** se ha llevado a cabo mediante reacción de condensación entre el ácido carboxílico adecuado y el correspondiente alcohol o amina (Esquema 1).

3.2. Estudio SAR de los compuestos Ia,b

Se ha determinado la capacidad de los compuestos **1-32** para inhibir tanto la hidrólisis de 2-AG en fracciones citosólicas utilizando 2-oleoilglicerol (2-OG) marcado con tritio como sustrato así como la hidrólisis de AEA en fracciones de membrana con el objetivo de identificar compuestos que puedan bloquear selectivamente la hidrólisis de monoacilglicerol sin afectar a la de AEA. Los resultados obtenidos se expresan como valores de inhibición a la máxima concentración (100 μM) y valores de CI_{50} calculados a partir de un mínimo de dos o tres experimentos independientes realizados por duplicado.

Los resultados obtenidos en las diferentes modificaciones que se han realizado en los compuestos se recogen en las Tablas 1-5.

Tabla 1. Influencia de la subunidad heterocíclica (S.H.)

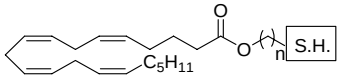

Comp		Inhibición de hidrólisis pI_{50} [CI_{50}, μM]	
		2-OG	AEA
1		5.35±0.05 [4.5]	4.91±0.05 [12]
2		4.67±0.04 [21]	4.48±0.06 [33]
3		4.37±0.06 [43]	4.98±0.08 [11, 78%][a]
4		4.3±0.1 [45]	4.0±0.1 [98]
5		5.26±0.04 [5.6]	4.30±0.06 [51]
6		4.5±0.1 [30, 62%][a]	5.3±0.2 [5.3, 63%][a]
7	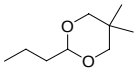	4.57±0.07 [27]	4.68±0.05 [21]
8	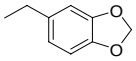	4.35±0.07 [45]	4.0±0.2 [91]

Los valores de pI_{50} (-log[CI_{50}]) se expresan como media ± E.E. Los valores de CI_{50} se indican entre corchetes. [a]Cuando los datos se ajustan a una curva de inhibición con actividad residual, se indica la inhibición máxima y los datos se expresan como [CI_{50}, porcentaje de inhibición máxima]. [b]Cuando la inhibición es menor del 50% a la máxima concentración utilizada (100 μM) el valor de pI_{50} es <4 (i.e. CI_{50} > 100 μM) y el porcentaje de inhibición obtenido a 100 μM se indica entre paréntesis como media ± E.E.

Tabla 2. Influencia de la cadena de ácido graso

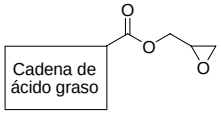

Comp	Cadena de ácido graso	Inhibición de hidrólisis pI_{50} [CI_{50}, μM]	
		2-OG	AEA
1	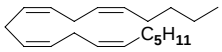	5.35±0.05 [4.5]	4.91±0.05 [12]
9	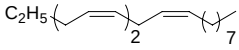	4.97±0.05 [11]	5.80±0.05 [1.6]
10	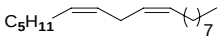	4.64±0.05 [23]	5.00±0.03 [10, 94%][a]
11	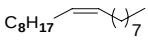	<4 (6±4%)[b]	4.96±0.05 [11]
12	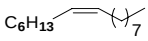	4.87±0.08 [13, 84%][a]	5.09±0.07 [8.2]
	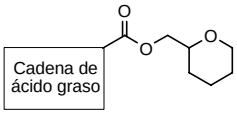		
5	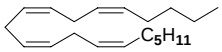	5.26±0.04 [5.6]	4.30±0.06 [51]
13	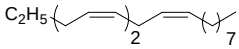	4.64±0.03 [23]	4.73±0.02 [19]
14	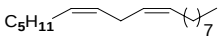	4.1±0.1 [73]	5.13±0.04 [7.5]
15	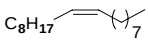	<4 (12±7%)[b]	4.53±0.05 [29]
16	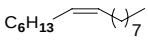	<4 (42±6%)[b]	5.0±0.1 [10, 82%][a]

[a,b] Véase Tabla 1.

Tabla 3. Influencia de los grupos fenilo y bifenilo

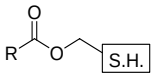

Comp	R	S.H.	Inhibición de hidrólisis pI_{50} [CI_{50}, μM]	
			2-OG	AEA
17	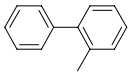		<4 (29±3%)[b]	<4 (5±7%)[b]
18	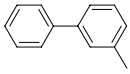		<4 (40±1%)[b]	4.22±0.04 [61]
19	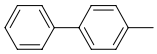		<4 (43±2%)[b]	4.45±0.04 [35]
23			<4 (14±5%)[b]	<4 (19±4%)[b]
20	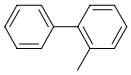		<4 (38±3%)[b]	4.37±0.09 [43]
21	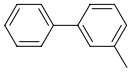		<4 (36±3%)[b]	4.75±0.04 [18]
22	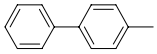		<4 (43±7%)[b]	4.49±0.04 [32]
24			5.5±0.2 [3, 53%][a]	4.28±0.05 [53]

[a,b] Véase Tabla 1.

Tabla 4. Influencia del grupo éster

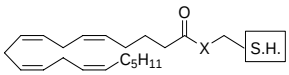

Comp	S.H.	X	Inhibición de hidrólisis pI_{50} [CI_{50}, μM]	
			2-OG	AEA
2		O	4.67±0.04 [21]	4.48±0.06 [33]
25		NH	4.47±0.06 [34]	4.25±0.04 [56]
4		O	4.3±0.1 [45]	4.0±0.1 [98]
26		NH	4.8±0.1 [15, 71%][a]	4.05±0.05 [90]

[a] Véase Tabla 1.

Tabla 5. Influencia del centro estereogénico

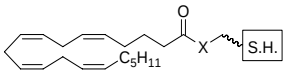

Comp	S.H.	X	Inhibición de hidrólisis pI_{50} [CI_{50}, μM]	
			2-OG	AEA
1		O	5.35±0.05 [4.5]	4.91±0.05 [12]
27			5.2±0.1 [6.3, 68%][a]	5.22±0.04 [6.0]
28			5.1±0.1 [8, 69%][a]	4.93±0.04 [12]
4		O	4.3±0.1 [45]	4.0±0.1 [98]
29			4.22±0.09 [60]	4.55±0.06 [28]
30			<4 (46±3%)[b]	4.76±0.05 [17]
25		NH	4.47±0.06 [34]	4.25±0.04 [56]
31			5.5±0.2 [3.5, 59%][a]	4.16±0.02 [69]
32			4.59±0.05 [25]	4.01±0.06 [99]

[a,b] Véase Tabla 1.

En primer lugar se ha estudiado la influencia de la subunidad heterocíclica (Tabla 1) obteniéndose los mejores resultados para los derivados 1 y 5 (CI_{50} = 4.5 y 5.6 μM, respectivamente) con los sistemas de oxiran-2-ilmetilo y tetrahidro-2*H*-piran-2ilmetilo. Seguidamente, fijando estas estructuras heterocíclicas y un espaciador de una unidad metilénica, se han realizado modificaciones en el fragmento lipofílico introduciendo cadenas de diferentes ácidos grasos así como grupos fenilo y bifenilo (Tablas 2 y 3), aunque no se ha conseguido mejorar los resultados de los compuestos de referencia 1 y 5. Del mismo modo, la sustitución del enlace éster por el grupo amida provoca una pérdida en la potencia inhibitoria (Tabla 4). Finalmente se ha observado que la presencia de un centro estereogénico no influye en la capacidad inhibitoria (Tabla 5). Por tanto, los compuestos con mejor perfil inhibitorio de esta primera serie Ia,b son los derivados 1 y 5. Sin embargo, ambos compuestos conservan la subunidad de ácido araquidónico, fragmento susceptible de sufrir reacciones colaterales en medios biológicos y que podría dificultar la selectividad de los compuestos sintetizados al ser reconocido por otras enzimas. Por tanto, nos planteamos el diseño de una nueva serie de compuestos con el objeto de eliminar este fragmento de ácido graso.

3.3. Diseño y síntesis de los compuestos Ic y Id

Diversos estudios han sugerido la utilidad de un grupo de bifenilo como isóstero de la cadena de ácido araquidónico,[60] por lo que nos planteamos esta posibilidad. Aunque en los derivados de bifenilo 17-22 se obtienen valores de inhibición muy bajos, sin embargo estudios de *docking* llevados a cabo con la estructura tridimensional de la enzima sugieren que la introducción de un espaciador entre el grupo aromático y el carbonilo puede ser favorable para las interacciones del grupo aromático con el bolsillo hidrofóbico (Figura 7, página S16).

De este modo se han diseñado dos nuevas series de derivados Ic y Id que incorporan grupos bifenilo, 4-bencilfenilo (Z = CH_2), 4-feniletilfenilo (Z = CH_2CH_2) y 4-

[60] Tarzia, G., Duranti, A., Tontini, A., Piersanti, G., Mor, M., Rivara, S., Plazzi, P.V., Park, C., Kathuria, S., Piomelli, D. *J. Med. Chem.* 2003, *46*, 2352.

benzoilfenilo (Z = CO) (Figura 8) con los espaciadores adecuados, los cuales son capaces de mantener las interacciones con dos zonas claves de la enzima, el centro catalítico formado por los residuos de S132, H279 y D249 y el bolsillo hidrofóbico constituido por los residuos A174, L186 y L224. Estos nuevos derivados Ic,d han sido sintetizados como se indica en el Esquema 2, excepto el compuesto 48 (Esquema 8, página S18). La obtención de los ácidos carboxílicos no comerciales se ha llevado a cabo mediante las rutas sintéticas representadas en los Esquemas 3-7.

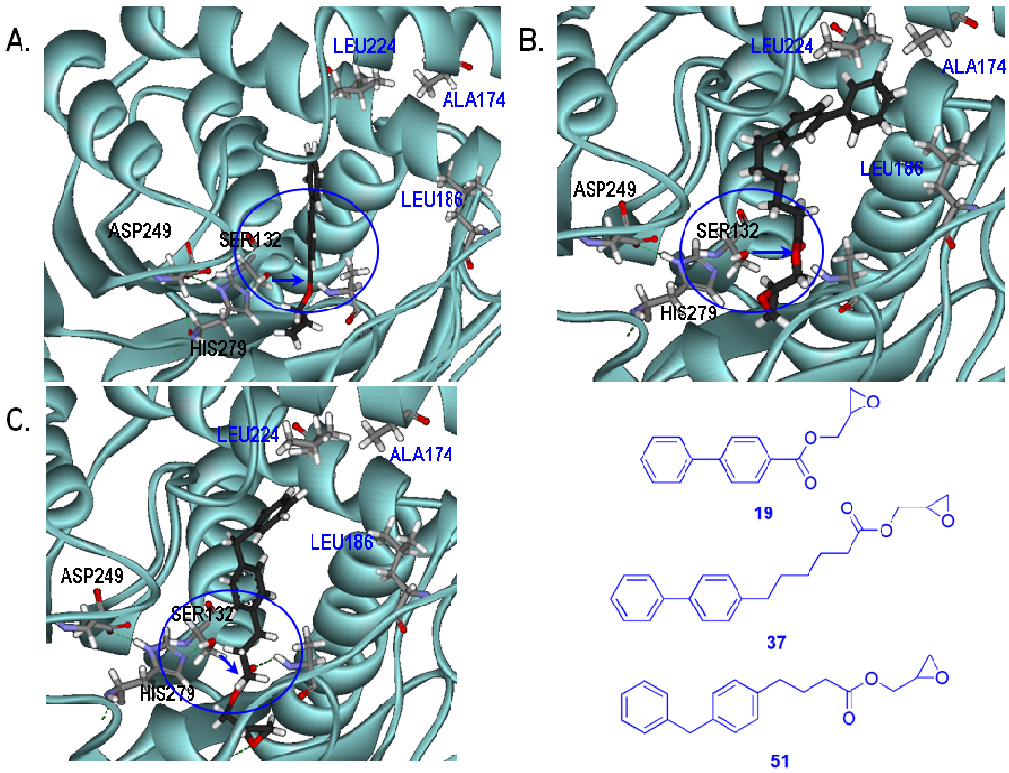

Figura 7. Modelos computacionales de los complejos formados entre los compuestos 19 (A), 37 (B), y 51 (C) y la enzima MGL.

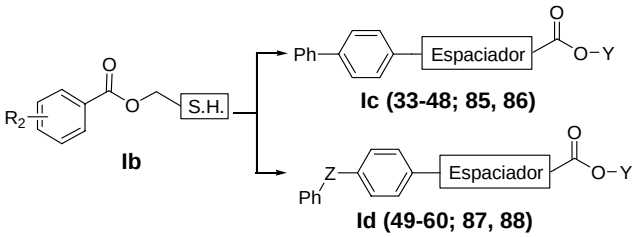

Figura 8.

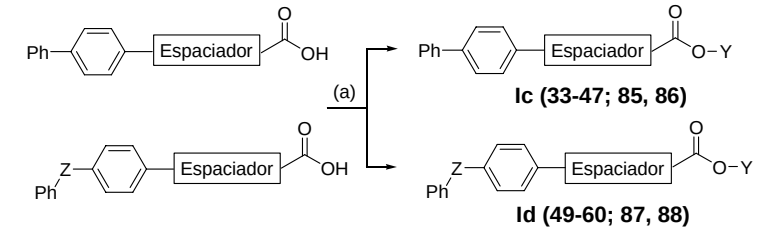

(a) HO−Y, DCC, DMAP, CH_2Cl_2, Ar, t.a.

Espaciador = n , m m' n = 1-6; m, m' = 0,1

Y = O ,

Z = CO, CH_2, CH_2CH_2

Esquema 2.

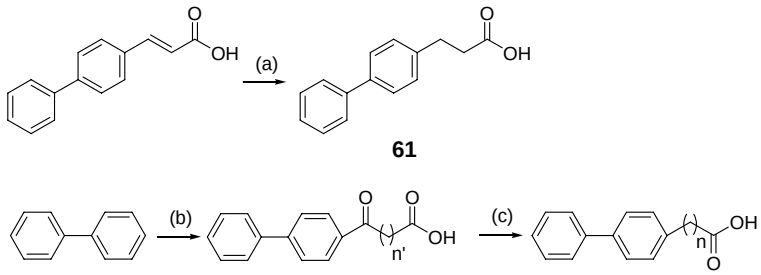

Reactivos y condiciones: (a) H_2, Pd/C, t.a., 2h; (b) o=(CH2)n'=o, $AlCl_3$, nitrobenceno, t.a., 16h; (c) Zn/$HgCl_2$, H_2O, HCl, Δ, 24h

Esquema 3.

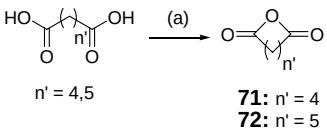

Reactivos y condiciones: (a) $(CH_3CO)_2O$, Δ, 2h

Esquema 4.

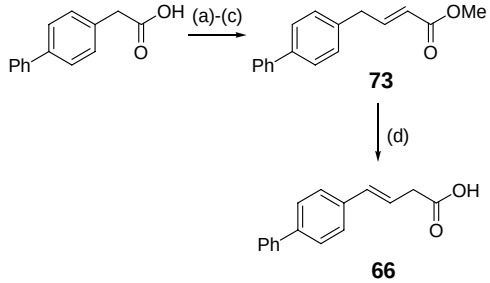

Reactivos y condiciones: (a) MeOH, $SOCl_2$, Δ, 2h; (b) DIBALH, -78 ºC, 2h; (c) Ph_3P=$CHCOOCH_3$, tolueno, Δ, 1h; (d) NaOH 2M ac, 60 ºC, 1h

Esquema 5.

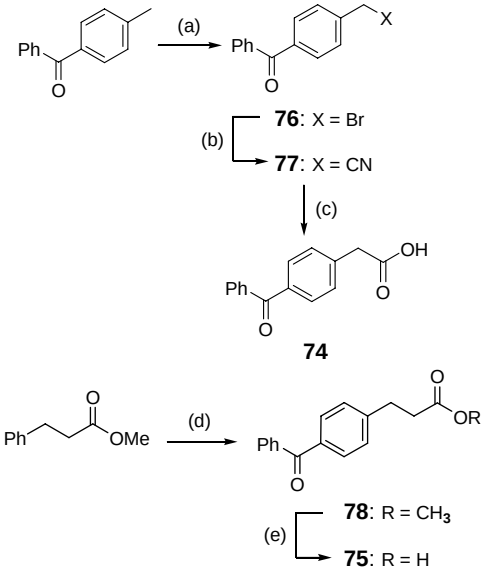

Reactivos y condiciones: (a) NBS, CCl_4, Δ, 4h; (b) NaCN, dioxano/H_2O, Δ, 2h; (c) 40% NaOH/EtOH, Δ, 2h; (d) PhCOCl, $AlCl_3$, nitrobenceno, t.a., 16h; (e) NaOH 6M ac

Esquema 6.

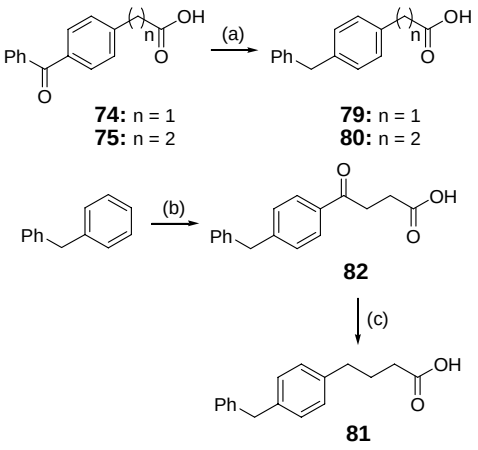

Reactivos y condiciones: (a) KOH, NH_2NH_2, etilenglicol, 110ºC, 2h ⟶ 180ºC, 20h; (b) Anhídrido succínico, $AlCl_3$, nitrobenceno, t.a., 16h; (c) $Zn/HgCl_2$, H_2O, Δ, 24h

Esquema 7.

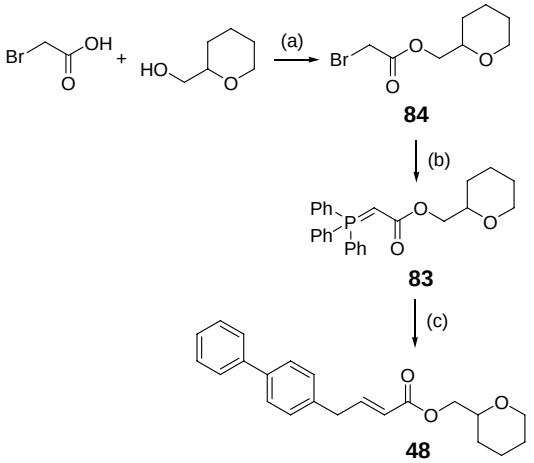

Reactivos y condiciones: (a) DCC, DMAP, Ar, t.a.; (b) PPh_3, CH_2Cl_2, t.a., 3h; (c) (1,1'-bifenil-4-il)acetaldehído, tolueno, Δ, 30 min

Esquema 8.

3.4. Estudio SAR de los compuestos Ic,d

Se ha determinado la capacidad de los compuestos 33-60 para inhibir la hidrólisis de 2-AG y la hidrólisis de AEA en las condiciones indicadas para los compuestos Ia,b (véase 3.2., página S12). Los resultados obtenidos se indican en las Tablas 6-10. En primer lugar se ha estudiado el efecto del espaciador en los derivados de bifenilo (Tabla 6), de donde se concluye que los espaciadores óptimos corresponden a 4 y 5 unidades metilénicas en los derivados de oxirano 36 y 37 (CI_{50} = 7.9 y 4.5 μM, respectivamente). A continuación, el estudio de la presencia de una insaturación en dicho espaciador nos indica que ésta resulta desfavorable en la inhibición (Tabla 7). Seguidamente se han realizado modificaciones en el grupo aromático introduciendo entre los anillos de benceno espaciadores tales como unidades metilénicas o un grupo carbonilo (Tablas 8 y 9). Así, en los derivados de oxirano se obtienen los mejores valores de inhibición para los compuestos 49 y 51, con un sistema de 4-bencilfenilo y espaciadores de 1 y 3 unidades metilénicas, respectivamente (CI_{50} = 8 y 10 μM, Tabla 8).

Tabla 6. Influencia de la longitud del espaciador

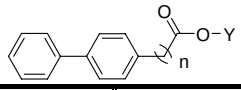

Comp	Y	n	Inhibición de hidrólisis pI_{50} [CI_{50}, μM]		Comp	Y	n	Inhibición de hidrólisis pI_{50} [CI_{50}, μM]	
			2-OG	AEA				2-OG	AEA
33		1	<4 (44±3%)[b]	6.23±0.02 [0.59]	39		1	<4 (33±2%)[b]	4.80±0.05 [16]
34		2	<4 (25±2%)[b]	5.94±0.03 [1.2]	40		2	<4 (50±2%)[b]	4.82±0.04 [15]
35		3	<4 (46±3%)[b]	6.03±0.03 [0.94]	41		3	<4 (9±3%)[b]	4.94±0.04 [12]
36		4	5.10±0.10 [7.9]	5.33±0.03 [4.6]	42		4	<4 (13±7%)[b]	4.70±0.05 [20, 95%][a]
37		5	5.35±0.05 [4.5]	5.29±0.03 [5.1]	43		5	<4 (27±2%)[b]	4.94±0.05 [12]
38		6	<4 (14±4%)[b]	5.50±0.03 [3.2]	44		6	<4 (53±2%)[b]	5.41±0.07 [3.9]

[a,b] Véase Tabla 1.

Tabla 7. Influencia de insaturaciones en el espaciador

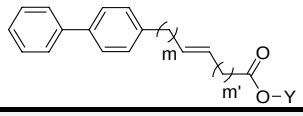

Comp	m	m'	Y	Inhibición de hidrólisis pI_{50} [CI_{50}, μM]	
				2-OG	AEA
45	0	0		<4 (4±1%)[b]	5.42±0.12 [3.8, 92%][a]
46	0	0		<4 (6±2%)[b]	<4 (39±5%)[b]
47	0	1		<4 (34±7%)[b]	<4 (72±3%)[b]
48	1	0		<4 (19±9%)[b]	<4 (57±5%)[b]

[a,b] Véase Tabla 1.

Tabla 8. Influencia de los grupos 4-bencilfenilo y 4-feniletilfenilo

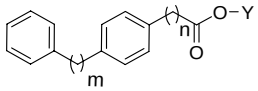

Comp	m	n	Y	Inhibición de hidrólisis pI_{50} [CI_{50}, μM] 2-OG	AEA	Comp	m	n	Y	Inhibición de hidrólisis pI_{50} [CI_{50}, μM] 2-OG	AEA
49	1	1		5.00±0.02 [8]	5.01±0.04 [9.8, 92%][a]	53	1	1		<4 (25±4%)[b]	4.73±0.04 [18, 91%][a]
50	1	2		4.73±0.05 [19]	5.63±0.03 [2.3]	54	1	2		<4 (41±1%)[b]	5.40±0.11 [4.0]
51	1	3		5.10±0.05 [10]	4.99±0.09 [10]	55	1	3		<4 (13±1%)[b]	<4 (47±1%)[b]
52	2	0		<4 (18±2%)[b]	4.44±0.04 [37]	56	2	0		<4 (8±2%)[b]	4.78±0.06 [17]

[a,b] Véase Tabla 1.

Tabla 9. Influencia del grupo benzoilo

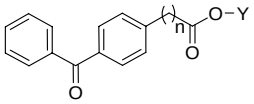

Comp	n	Y	Inhibición de hidrólisis pI_{50} [CI_{50}, μM] 2-OG	AEA
57	1		<4 (5±1%)[b]	5.85±0.02 [1.4]
58	2		<4 (33±3%)[b]	5.41±0.03 [3.9]
59	1		<4 (5±2%)[b]	4.77±0.07 [17]
60	2		<4 (27±2%)[b]	4.65±0.09 [22, 90%][a]

[a,b] Véase Tabla 1.

De todos los compuestos sintetizados, los que presentan un mejor perfil de inhibición son los derivados 37 y 49, con valores de CI_{50} para la inhibición de 2-OG de 4.5 y 8 μM, respectivamente. A continuación hemos procedido a estudiar la influencia del centro estereogénico así como a sustituir el anillo de oxirano por una subunidad de 2-glicerol (Esquema 9), presente en el sustrato endógeno de la enzima. Los resultados obtenidos se recogen en las Tablas 10 y 11.

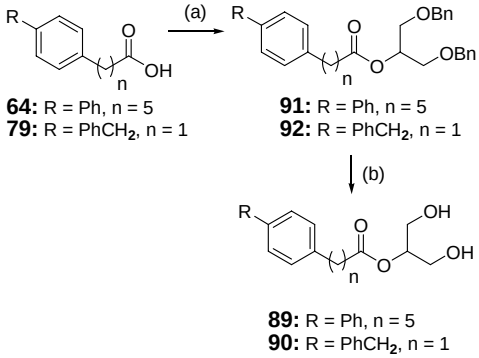

Reactivos y condiciones: (a) 1,3-dibenziloxipropan-2-ol DCC, DMAP, CH_2Cl_2, t.a., 16h; (b) $Pd(OH)_2$, CH_2Cl_2/EtOH, t.a., 3h

Esquema 9

Tabla 10. Influencia del centro estereogénico en 37 y 49

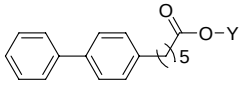

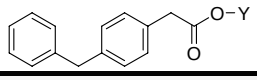

Comp	Y	Inhibición de hidrólisis pI_{50} [CI_{50}, μM]		Comp	Y	Inhibición de hidrólisis pI_{50} [CI_{50}, μM]	
		2-OG	AEA			2-OG	AEA
37		5.35±0.05 [4.5]	5.29±0.03 [5.1]	49		5.00±0.02 [10]	5.01±0.04 [9.8, 92%][a]
85		5.31±0.03 [4.9]	5.41±0.01 [3.9]	87		6.17±0.03 [0.68]	6.54±0.01 [0.29]
86		5.29±0.03 [5.1]	5.35±0.02 [4.5]	88		4.15±0.09 [70]	6.47±0.01 [0.34]

[a] Véase Tabla 1.

Tabla 11. Introducción de un fragmento de 2-glicerol

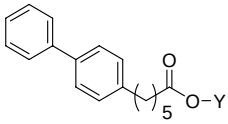

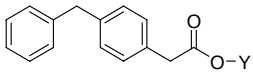

Comp	Y	Inhibición de hidrólisis pI_{50} [CI_{50}, μM]		Comp	Y	Inhibición de hidrólisis pI_{50} [CI_{50}, μM]	
		2-OG	AEA			2-OG	AEA
37		5.35±0.05 [4.5]	5.29±0.03 [5.1]	49		5.00±0.02 [8]	5.01±0.04 [9.8, 92%][a]
89		5.81±0.07 [1.5]	5.73±0.02 [1.9]	90		<4 (49±2%)[b]	6.15±0.02 [0.70]

[a,b] Véase Tabla 1.

De todos los compuestos sintetizados en esta segunda serie, los más prometedores son los derivados 37 y 87 (enantiómero *R* de 49), que presentan unos valores de CI_{50} de 4.5 y 0.68 μM, respectivamente, comportándose además como inhibidores duales MGL/FAAH.

3.6. Estudio de diferentes actividades MGL

Con el objetivo de caracterizar diferentes actividades MGL expresadas en distintas células y fracciones celulares, hemos seleccionado los compuestos más prometedores (valores de CI_{50} < 15 μM), los cuales se han ensayado en fracciones de membrana (2-OG memb) así como directamente sobre la enzima MGLhr. Adicionalmente, también se ha

estudiado la capacidad de algunos de estos compuestos para inhibir la hidrólisis de 2-AG en neuronas.

Los resultados obtenidos se recogen en la Tabla 12. En general, los derivados de ácido graso 1, 5, 9, 12 y 26 se muestran como inhibidores mucho más débiles en la fracción de membrana (2-OG memb) que en la fracción citosólica (2-OG). Puesto que el 85% de la actividad hidrolítica de 2-AG en esta fracción se debe a MGL,[28] estos resultados nos sugieren que los compuestos actúan sobre otra enzima. Este hecho se apoya en los resultados obtenidos para los compuestos 1, 5 y 12 en MGLhr, enzima frente a la cual resultan poco activos (1) o completamente inactivos (5 y 12). Así, el resto de compuestos se ha ensayado directamente sobre la enzima recombinante. Por lo general, los compuestos de bifenilo y bencilfenilo muestran unos resultados más parecidos entre ambos ensayos, lo que indica que los derivados Ic,d son capaces de inhibir directamente la enzima MGL. Finalmente, se ha ensayado la capacidad de algunos compuestos para bloquear la hidrólisis de 2-AG en neuronas. Los resultados más prometedores se han obtenido para los derivados 12 y 36, que presentan unos valores de CI_{50} de 1.2 y 0.5 μM, respectivamente. Ensayos posteriores han identificado que la enzima afectada por la acción del compuesto 12 es la hidrolasa ABHD-6.[59]

Tabla 12. Estudio de diferentes actividades hidrolíticas de 2-AG

Comp	Estructura	Inhibición de hidrólisis CI_{50} (μM)[a]			
		2-OG	2-OG-memb	MGLhr[b]	Neurona[c]
1	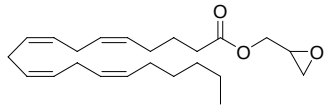	4.5	29	50	ND[d]
5	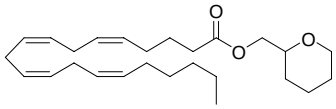	5.6	26	>100	10
9	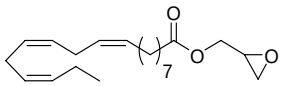	11	51	ND	1.7
12	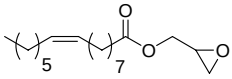	13	28	>100	1.2
26	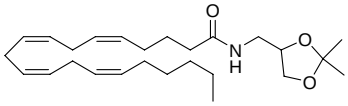	15	100	ND	ND
36	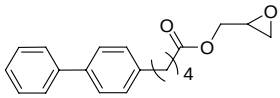	7.9	ND	6.2	0.5

Tabla 12. (Continuación)

Comp	Estructura	Inhibición de hidrólisis CI_{50} (μM)			
		2-OG	2-OG-memb	MGLhr	Neurona
37	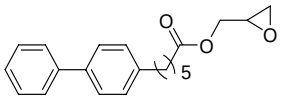	4.5	ND	4.1	1.4
49	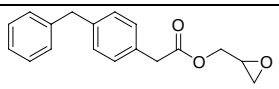	8	ND	9.8	ND
51	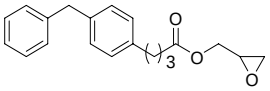	10	ND	16	ND
85	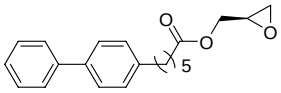	4.9	ND	21	ND
86	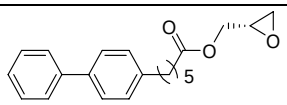	5.1	ND	10	ND
87	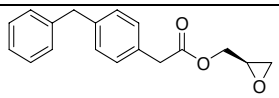	0.68	ND	2.4	ND
89	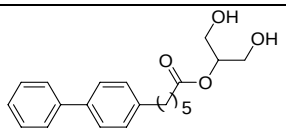	1.5	ND	7.5	ND

[a] Los valores de CI_{50} corresponden a la media de al menos dos experimentos realizados por duplicado. Sustratos de ensayo: [b] Acetato de 4-nitrofenilo, [c][^{3}H]-2-AG. [d]ND, no determinado.

En conjunto, todos estos datos ponen de manifiesto que la hidrólisis de 2-AG es un proceso complejo que involucra a múltiples enzimas y que los compuestos I muestran diferentes perfiles inhibitorios frente a estas distintas actividades. Por tanto, estos compuestos representan unas herramientas apropiadas para identificar diferentes actividades hidrolíticas de 2-AG. Así, hemos aplicado esta idea en células de microglía en colaboración con el grupo del Prof. N. Stella.

3.7. Identificación de una nueva actividad MGL en microglía

Mediante la técnica de la reacción en cadena de la polimerasa reversa (RT-PCR) se ha determinado que la línea celular de microglía BV-2 no expresa niveles de ácido ribonucleico mensajero (ARNm) de MGL, aunque estas células sí poseen capacidad hidrolítica de 2-AG.[58] La implicación de FAAH se ha estudiado mediante el uso de URB597 (Figura 9, página S24), un inhibidor

potente y selectivo de esta enzima (CI_{50} = 4.6 nM[61]). La Figura 9 muestra la gráfica bifásica obtenida para la hidrólisis de 2-AG, lo que sugiere que FAAH es responsable del 50% de la hidrólisis de 2-AG en esta línea celular.

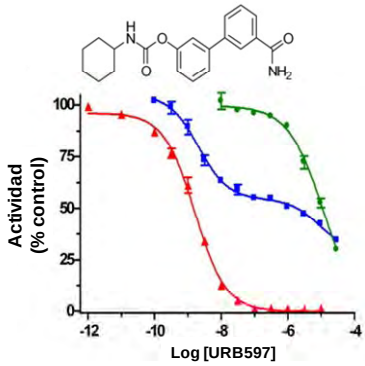

Hidrólisis de [^{3}H]-2-AG en células BV-2 Hidrólisis de [^{3}H]-2-AG en neurona

Hidrólisis de [^{3}H]-AEA en células BV-2

Figura 9. Efecto del incremento de concentraciones de URB597 en la hidrólisis de [^{3}H]-2-AG en células BV-2 (azul), neuronas (verde) y en la hidrólisis de [^{3}H]-AEA en células BV-2 (rojo).

Estos datos indican la existencia de al menos otra enzima responsable de la degradación de 2-AG y distinta de la MGL previamente clonada. Dado que los compuestos I son capaces de discernir entre diferentes actividades hidrolíticas de 2-AG (Tabla 12), se ha llevado a cabo un cribado de varios compuestos capaces de discriminar estas actividades -MGL, FAAH y la "nueva MGL"-. Estos resultados indican que el derivado 5 es igualmente potente frente a las tres actividades, mostrando valores de CI_{50} similares (7-12 μM), mientras que su análogo 16 es más potente en FAAH y la "nueva MGL" que en la MGL de neuronas (Figura 10).

[61] Kathuria, S., Gaetani, S., Fegley, D., Valiño, F., Duranti, A., Tontini, A., Mor, M., Tarzia, G., La Rana, G., Calignano, A., Giustino, A., Tattoli, M., Palmery, M., Cuomo, V., Piomelli, D. *Nat. Med.* 2003, *9*, 76.

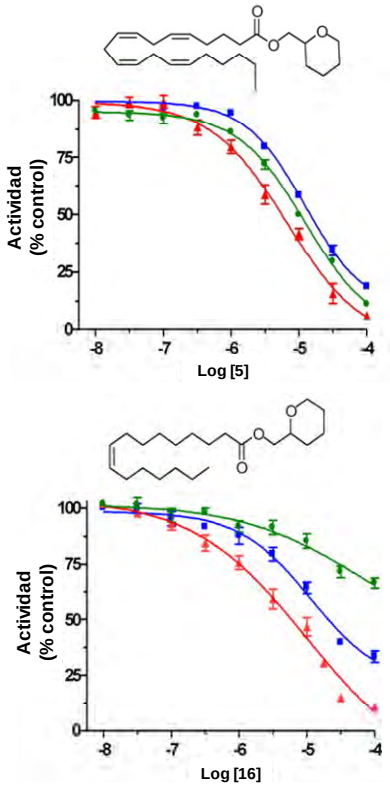

Hidrólisis de [^{3}H]-2-AG en células BV-2 Hidrólisis de [^{3}H]-2-AG en neurona

Hidrólisis de [^{3}H]-AEA en células BV-2

Figura 10. Perfil inhibitorio de la nueva MGL (azul), MGL (verde) y FAAH (rojo). Efecto del incremento de concentraciones de los derivados 5 y 16.

Estos resultados confirman que MGL, FAAH y la "nueva MGL" poseen diferentes perfiles farmacológicos, siendo esta nueva actividad diferente de la actividad hidrolítica de 2-AG molecularmente caracterizada.[58]

3.8. Papel neuroprotector de los derivados 1 y 5

Con el fin de validar la enzima MGL como diana terapéutica, hemos procedido a ensayar los compuestos 1 y 5 en un modelo de excitotoxicidad inducida por glutamato en la línea celular HT-22. Mediante RT-PCR hemos comprobado que estas células expresan ARNm tanto de MGL como de FAAH,

aunque no así el ARNm correspondiente a los receptores CB_1 y CB_2 (Figura 11).

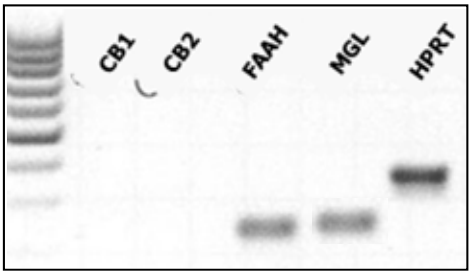

Figura 11. La RT-PCR se ha llevado a cabo con *primers* para CB_1, CB_2, FAAH y MGL de ratón. El ARNm de hipoxantina guanina fosforribosiltransferasa (HPRT) se ha empleado como control positivo.

Puesto que se ha descrito que las propiedades neuroprotectoras de 2-AG están mediadas por CB_1, se ha procedido a transfectar estas células con el plásmido correspondiente, cuya expresión se ha confirmado mediante inmunocitoquímica y microscopía de fluorescencia (Figura 12).

Así, la excitotoxicidad se ha inducido con glutamato (10 mM) y se han incubado las células con diferentes concentraciones de los compuestos 1 y 5. Transcurridas 48 horas, se ha medido la supervivencia celular empleando MTT [bromuro de 3-(4,5-dimetiltiazol-2-il)-2,5-difeniltetrazolio] (Figura 13, página S26). Así, los derivados 1 y 5 protegen de manera significativa a las células de la muerte inducida por glutamato en un 54 y 56%, respectivamente, a una concentración de 10 μM.

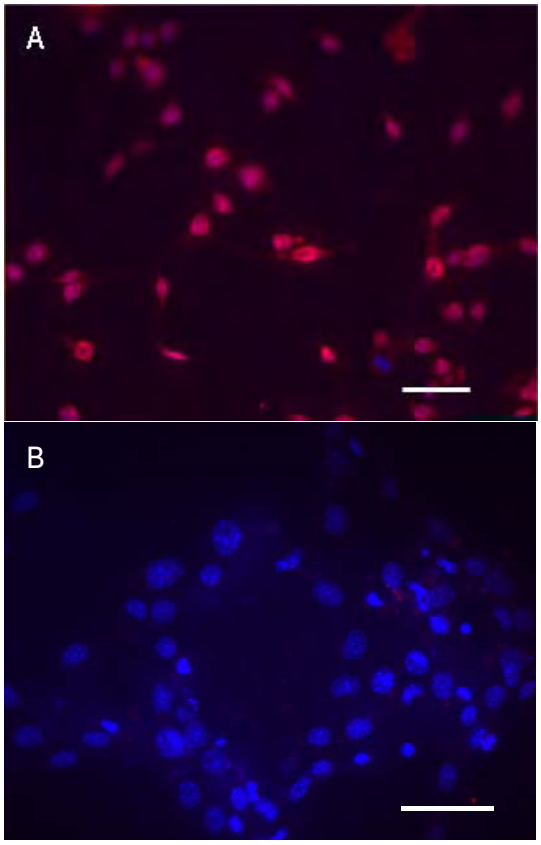

Figura 12. Expresión del receptor CB_1 en células HT-22 transfectadas (A) y sin transfectar (B). Los núcleos se visualizan con Höchst. Escala: 200 μm

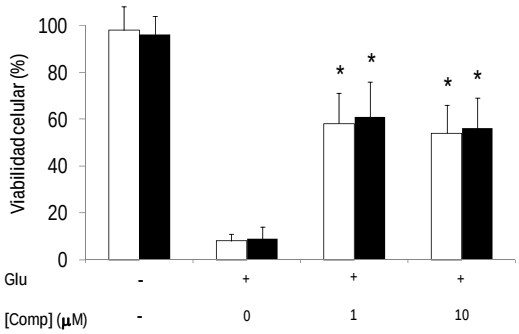

Figura 13. Viabilidad celular después de 48h de incubación con glutamato (Glu) 10 mM en ausencia y presencia de compuesto 1 (barras blancas) y 5 (barras negras). * $P < 0.05$ *vs* células no tratadas

3.9. Mecanismo de inhibición

Finalmente, teniendo en cuenta la relevancia no sólo de la inhibición de la hidrólisis de 2-AG sino también del mecanismo de dicha inhibición así como el modo de unión del inhibidor a la enzima, hemos comenzado a estudiar el mecanismo de los derivados 37 y 87. Los resultados indican que el derivado 37 actúa como un inhibidor competitivo y reversible con un valor de K_i de 8 ± 2 μM (Figura 14). Sin embargo, no se ha podido observar unión del inhibidor a la enzima mediante experimentos de diferencia de transferencia de saturación (*saturation transfer difference*, STD) debido precisamente a que es también sustrato de la enzima.

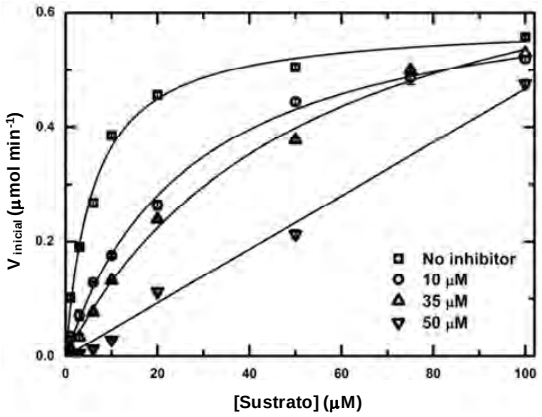

Figura 14. Inhibición competitiva del derivado 37 en la actividad MGLhr. Efecto del incremento de la concentración de 37 en la curva de saturación de hidrólisis de sustrato.

En conjunto, todos los resultados obtenidos hasta este momento han permitido comenzar a elucidar los requisitos estructurales involucrados en la inhibición de la hidrólisis de 2-AG. Asimismo, los compuestos obtenidos pueden ser empleados como herramientas para la caracterización de otras actividades enzimáticas y han permitido comenzar la validación de la enzima MGL como diana para el tratamiento de patologías asociadas a excitotoxicidad neuronal.

5. CONCLUSIONES

1. En el presente trabajo se han diseñado y sintetizado nuevos inhibidores de la enzima MGL con estructura general **Ia-d**.
2. Se ha determinado la capacidad de todos los compuestos sintetizados para inhibir la hidrólisis de 2-AG y AEA.
3. Estos datos nos han permitido llevar a cabo la primera serie de estudios SAR sistemáticos con el fin de elucidar los requisitos estructurales involucrados en la inhibición de MGL.
4. El empleo de inhibidores seleccionados entre aquéllos con mejor perfil *in vitro*, ha confirmado que la degradación de 2-AG es un proceso complejo que implica varias enzimas que pueden verse afectadas de forma diferencial por los compuestos I. Adicionalmente, estos inhibidores han permitido identificar una nueva actividad MGL en células de microglía.
5. El efecto neuroprotector de algunos inhibidores en un modelo de excitotoxicidad inducida por glutamato apoya el interés de MGL como diana terapéutica para enfermedades asociadas a excitotoxicidad.
6. De todos los compuestos sintetizados, merecen especial atención los derivados 37, 87 y 89. En particular, los compuestos 87 y 89 son inhibidores duales MGL/FAAH mientras que 37 actúa como un inhibidor potente y competitivo de MGL. Así, ambos derivados representan unos prometedores compuestos de partida con el fin de obtener inhibidores potentes de MGL y selectivos frente a FAAH, proceso que está siendo llevado a cabo actualmente en nuestro laboratorio.